

**Theoretical investigation on aromaticity, magnetic
exchange coupling and magnetic anisotropy
in
metal based systems**

**A Thesis submitted to the University of North Bengal
For the Award of**

**Doctor of Philosophy
in
Chemistry**

By

Tamal Goswami

GUIDE

Dr. Anirban Misra

**Department of Chemistry
University of North Bengal
August, 2015**

DEDICATION

To my father *Shri Panchanan Goswami*, my mother *Shrimati Ira Goswami* and my aunt *Shrimati Kalpana Goswami* : your unconditional support in every day of my life has made this thesis possible. You have been my source of strength through all the bad times and my source of joy in good times.

DECLARATION

I declare that the thesis entitled “**Theoretical investigation on aromaticity, magnetic exchange coupling and magnetic anisotropy in metal based systems**” has been prepared by me under the guidance of Dr. Anirban Misra, Associate Professor in the Department of Chemistry, University of North Bengal. No part of the thesis has formed the basis for the award of any degree or fellowship previously.

Tamal Goswami

Tamal Goswami

Department of Chemistry,
University of North Bengal,
Raja Rammohunpur,
Siliguri,
Dt. Darjeeling
PIN. 734013

DATE: 11/08/2015

CERTIFICATE

I certify that the thesis entitled “**Theoretical investigation on aromaticity, magnetic exchange coupling and magnetic anisotropy in metal based systems**” has been prepared by Tamal Goswami, for the award of Ph. D. Degree of the University of North Bengal, under my guidance. He has carried out the work in the Department of Chemistry, University of North Bengal.



Dr. Anirban Misra
Associate Professor,
Department of Chemistry,
University of North Bengal,
Raja Rammohunpur,
Siliguri,
Dt. Darjeeling
PIN. 734013

DATE: 11/08/2015

ABSTRACT

The first chapter provides a brief account of the history and significant advances in the fields of aromaticity and magnetism. In this chapter a concise history of the origin and advancement of research in aromaticity is given which correlates the chronological development of the subjects with the evolution of new materials. The current status of the research in aromaticity, with special emphasis on the metal based aromatic molecules, is provided. Magnetism is also discussed according to the chronology of the advancement of the theory and explored materials. The effect of dimension in the magnetic properties is also discussed here. The emergence of new molecules for nanomagnets and the role of the theoretical advancement in designing such materials also discussed in this chapter.

The second chapter presents a concise report of the basic theoretical background related to aromaticity, magnetic exchange coupling constant and magnetic anisotropy. The significance of the quantification of aromaticity has been discussed with special emphasis on the fundamental categories based on which the assessment of aromaticity is performed. A short description of the available methods for quantification of aromaticity, which are of subsequent use in this work, is also presented. A brief background for the estimation of magnetic exchange coupling constant has been provided. Two different methods of determination of the magnetic exchange coupling constant (J) is given, namely, the broken symmetry approach and the spin-flip DFT approach. The theoretical approach behind these two methods are discussed elaborately. A short account of the basic theory behind the quantification of magnetic anisotropy is also provided here. There are two popular methods for the quantification of magnetic anisotropy. The Pederson-Khanna (PK) approach and the Neese method for quantification of zero-field splitting (ZFS) parameter D , in connection to the magnetic anisotropy are discussed with proper emphasis on the estimation of the spin-orbit coupling in spin-systems.

Gradual migration of Na^+ from Mg_3^{2-} brings about fascinating change in aromatic and magnetic behavior of inorganic Mg_3Na_2 cluster, which is addressed at the B3LYP and QCISD levels is discussed in the third chapter. During this process, Na^+ takes away the electron density from Mg_3^{2-} causing a net decrease in aromaticity. A tug-of-war between the Pauli repulsion and the aromaticity is shown to be responsible for the observed stability and aromaticity trends in singlet and triplet states. Implications of a spin crossover vis-à-vis a possible superexchange are also explored.

The fourth chapter is on the magnetism in metallocene based donor-acceptor complexes, which stems from the donor to acceptor charge transfer. Thus, to correlate the exchange coupling constant J and the charge transfer integral, a formalism is developed which enables one to obtain the coupling constant from the value of the charge transfer integral and the spin topology of the system. The variance in the magnetic interaction between donor and acceptor is also investigated along two perpendicular directions in the three dimensional crystal structure of the reference system, decamethylchromocenium ethyl tricyanoethylenecarboxylate $[\text{Cr}(\text{Cp}^*)_2][\text{ETCE}]$. These donor-acceptor pairs (V-pair and H-pair), oriented along vertical and horizontal directions respectively, are found to have different extents of J , which is attributed to the difference in exchange coupling mechanisms, viz., direct exchange and super exchange. Next, V-pair and H-pair are taken together to treat both the intra chain and inter chain magnetic interactions, since this competition is necessary to decipher the overall magnetic ordering in the bulk phase. In fact, this truncated model produces a small positive value of J supporting the weak ferromagnetic nature of the

complex. Lastly, a periodic condition is imposed on the system to comprehend the nature of magnetism in the extended system. Interestingly, the ferromagnetism, prevailing in the aperiodic system, turns into weak antiferromagnetism in the periodic environment. This is explained through the comparison of density of states (DOS) plots in aperiodic and periodic systems. This DOS analysis reveals proximity of the donor and acceptor orbitals, facilitating their mixing in periodic conditions. This mixing causes the antiferromagnetic interaction to prevail over the ferromagnetic one, and imparts an overall antiferromagnetic nature in periodic conditions. This change over in magnetic nature with the imposition of periodicity may be useful to understand the dependence of magnetic behavior with dimensionality in extended systems.

Magnetic anisotropy of a set of octahedral Cr(III) complexes is the key deliberation of chapter five. The magnetic anisotropy is quantified in terms of zero-field splitting (ZFS) parameter D , which appeared sensitive toward ligand substitution. The increased π -donation capacity of the ligand enhances the magnetic anisotropy of the complexes. The axial π -donor ligand of a complex is found to produce an easy-plane type ($D > 0$) magnetic anisotropy, while the replacement of the axial ligands with π -acceptors entails the inversion of magnetic anisotropy into the easy-axis type ($D < 0$). This observation enables one to fabricate a single molecule magnet for which easy-axis type magnetic anisotropy is an indispensable criterion. The equatorial ligands are also found to play a role in tuning the magnetic anisotropy. The magnetic anisotropy property is also correlated with the nonlinear optical (NLO) response. The value of the first hyperpolarizability varies proportionately with the magnitude of the ZFS parameter. Finally, it has also been shown that a rational design of simple octahedral complexes with desired anisotropy characteristics is possible through the proper ligand selection.

In chapter six, the effect of an external electric field on the magnetic anisotropy of a single-molecule magnet has been investigated, with the help of DFT. The magnetic anisotropy of a pseudo-octahedral Co(II) complex namely, $[\text{Co}^{\text{II}}(\text{dmphen})_2(\text{NCS})_2]$, has been investigated in connection to the tunability of the magnetic anisotropy through external electric field. The application of an electric field can alter the magnetic anisotropy from “easy-plane” ($D > 0$) to “easy-axis” ($D < 0$) type. The alteration in the magnetic anisotropy is found due to the change in the Rashba spin-orbit coupling by the external electric field. This variation in the Rashba spin-orbit coupling is further confirmed by the generation of the spin dependent force in the molecule which is later found to manifest separation of α - and β - spins in opposite ends of the molecule. The excitation analysis performed through time-dependent DFT also predicts that the external electric field facilitates metal to π -acceptor ligand charge transfer, leading to uniaxial magnetic anisotropy and concomitant spin Hall effect in a single molecule.

Finally chapter seven presents a general and comprehensive conclusion of all the chapters.

PREFACE

Wiberg once referred aromaticity as a “large fuzzy ball” due to the difficulty in defining the concept precisely. Although aromaticity is popularly considered to be an important concept primarily for organic compounds, but it has been extended to compounds containing transition-metal atoms. Recent findings of aromaticity and antiaromaticity in all-metal clusters have enthused further research in alkaline earth metal clusters referring to their chemical bonding, structures and stability. In this thesis we used the σ -aromatic alkaline earth metal clusters and their alkali metal complexed salts to extended the concept of aromaticity. Motivated by the transformation of σ -aromaticity in free cyclo-[Mg₃]²⁻ to π -aromaticity in the alkali metal salts, we undertake a detailed investigation of the Mg₃Na₂ firstly, to obtain a set of consistent structural data for the species; secondly, to analyze the electronic structure, electron delocalization properties, and aromaticity of these species; and finally, to discuss the changes in aromaticity and emergence of magnetism as a function of the distance from the alkali metal to the center of the Mg₃ ring.

Single molecular magnets have opened an opportunity for the study of physical phenomena at the interface of the microscopic quantum world and the macroscopic classical systems. The field of molecular magnetism has expanded with the discovery of magnetic quantum tunneling in Mn₁₂-acetate molecules. The cornerstone for the rise of present day interest in molecular magnetism owes to the creativity of molecular chemists for designing high and low spin clusters and single chain magnets. There is the vibrant ongoing work on some hole burning phenomenon like molecular spintronics, quantum tunnelling of magnetisation, spin Hall effect etc. The magnetic behaviour in molecules and solids are primarily controlled by exchange interaction. Various microscopic electronic Hamiltonians, spin Hamiltonians have been introduced to solve quantum many body problems and compute magnetic exchange coupling constant. Magnetic anisotropy is responsible for intrinsic ‘easy’ and ‘hard’ directions of the magnetization in some ferromagnetic materials. This magnetic anisotropy is, from both a technological and fundamental viewpoint one of the most important properties of magnetic materials. Owing to the perspective of both fundamental sciences and applications new materials are currently being prepared, named multifunctional molecular materials, which involve interplay or synergy between multiple physical properties like aromaticity and magnetism.

ACKNOWLEDGEMENTS

It is the celebrated 'excitement' of science which led me through the journey with my Ph. D. degree. The five year long voyage through the rough seas of research has come to an end with unforgettable moments of agony and euphoria. Everything moulded into a sense of success and accomplishment. It is a pleasant aspect that I have now the opportunity to express my gratitude for all who made this journey smooth and enjoyable. I would like to start with the person who made the biggest difference in my life, my mentor, Dr. Anirban Misra. He has been there, in front of my eyes for last five years, motivating and inspiring every bit of me towards new possibilities in life. He has been a living role model to me, taking up new challenges every day, tackling them with all his grit and determination and always thriving to come out victorious. It's his vigor and hunger to perform in adverse situation, which has inspired me to thrive for excellence. I have been extremely lucky to have a supervisor who cared so much about my work, and who responded to my questions and queries so promptly. I express my humble gratitude to Ma'm (Mrs. Amrita Misra) and affection to Mithi (Miss Anwita Misra).

I would also like to thank all the faculty members and staff at University of North Bengal who helped me in my supervisor's absence. In particular I would like to thank Prof. B. Basu, Head, Department of Chemistry, Prof. Swapan K. Saha and Dr. Amiya K. Panda for the suggestions they made.

The good advice, support and friendship of my labmates, Dr. Satadal Paul, Dr. Debojit Bhattacharya, Dr. Suranjan Shil, Ms. Sonali Sarkar, Mr. Rakesh Kar, Mr. Manoj Majumder, Ms. Banita Sinha, Miss Prodipta Sarbadhikary and Miss Manoswita Homray have been invaluable on both at academic and personal level, for which I am extremely grateful. I also thank my fellow research scholars of the department for providing the best environment for research in the department.

I have been extremely fortunate in my life to have parents who have shown me unconditional love and support. The relationships and bonds that I have with my parents hold an enormous amount of meaning to me. I admire them for all of their accomplishments in life, for their independence, for their hierarchical role in our family, and for all of the knowledge and wisdom that they have passed on to me over the years. Personally, my parents have played an important role in the development of my identity and shaping the individual that I am today.

TABLE OF CONTENTS

<u>Chapter 1. Aromaticity and magnetism in metal based systems</u>	1 - 15
1.1. Aromaticity	1
1.1.1. History and Key Advances	2
1.1.2. Aromaticity in metal based systems	6
1.2. Magnetism: History and Key Advancements	6
1.2.1. Dimensionality and Magnetic Properties	8
1.2.2. Discrete Molecules	9
1.2.3. The importance of spin-nano magnets	9
1.2.4. The single molecule magnet and the potential of quantum storage	10
1.2.5. The role of theory in developing new magnetic molecules	11
1.3. Objectives of the Thesis	11
1.4. References	12
<u>Chapter 2. Theoretical methods to quantify aromaticity and magnetism</u>	16 - 29
2.1. Quantification of Aromaticity	16
2.1.1. Aromaticity Indices	17
2.2. Estimation of Magnetic Exchange Coupling Constant (<i>J</i>)	20
2.2.1. Broken Symmetry Approach	21
2.2.2. Spin-flip DFT Approach	23
2.3. Quantification of Magnetic Anisotropy	24
2.3.1. Pederson-Khanna (PK) method	24
2.3.2. The Neese technique	26
2.4. References	27
<u>Chapter 3. Concurrent loss of aromaticity and onset of superexchange in Mg₃Na₂ with an increasing Na–Mg₃ distance</u>	30 - 47
3.1. Introduction	30
3.2. Theoretical background and computational details	31
3.3. Results and Discussion	33
3.4. Conclusion	41
3.5. References	42
<u>Chapter 4. Effect of charge transfer and periodicity on the magnetism of [Cr(Cp*)₂][ETCE]</u>	48 - 69
4.1. Introduction	48
4.2. Theoretical framework	50
4.3. Computational details	53

4.4. Results and discussion	55
4.4.1. Competition between exchange mechanisms	59
4.4.2. Effect of periodicity	61
4.5. Conclusion	63
4.6. References	64

Chapter 5. Ligand Effects toward the Modulation of Magnetic Anisotropy and Design of Magnetic Systems with Desired Anisotropy Characteristics **70 - 91**

5.1. Introduction	70
5.2. Theoretical Background	72
5.3. Computational Details	73
5.4. Results and Discussions	74
5.4.1. Role of π -donation from ligand	74
5.4.2. Effect of individual ligands toward the ZFS of a molecule	78
5.4.3. Effect of axial ligand substitution	81
5.4.4. Effect of equatorial ligand substitution	84
5.5. Conclusion	85
5.6. References	86

Chapter 6. On the control of magnetic anisotropy through an external electric field **92 - 103**

6.1 Introduction	92
6.2 Theoretical Background and Method	93
6.3 Results and Discussions	95
6.4 Conclusion	100
6.5 References	101

Chapter 7. Conclusions **104 – 107**

Bibliography **108 – 129**

Index **130 - 131**

LIST OF TABLES

Table	Caption	Page
Table 1.1.	List of the key advances of the concept of aromaticity listed in chronological order.	3
Table 1.2.	List of the key advances in the field of magnetism in the chronological order.	8
Table 3.1.	Energy and geometry comparison of the singlet and triplet states of Mg_3Na_2 , optimized at (a) UB3LYP/6-311+g(d) and (b) QCISD/aug-cc-pVDZ level of theories.	33
Table 3.2.	ΔE and calculated J value on the basis of eqn (3.6).	41
Table 4.1.	Comparison of coupling constant values (J) for the V-pair, obtained through different methodology.	58
Table 5.1.	Experimental (D_{exp}) and calculated (D_{calc}) ZFS parameters for the complexes 1, 2, and 3.	74
Table 5.2.	Individual excitation contribution to the total ZFS parameter D .	76
Table 5.3.	The first hyperpolarizability values of complexes 1, 2, and 3 and corresponding HOMO–LUMO gaps (ΔE_{HL}).	78
Table 5.4.	The values of the total ZFS parameter (D) and after replacement of the halide ligands with point charges of the same magnitude (D_X with $X = Cl, Br, \text{ and } I$).	81
Table 5.5.	Calculated ZFS parameters for complex series $[Cr(dmpe)_2X_2]^+$, with $X = Cl, Br, \text{ and } I$.	82
Table 5.6.	Calculated ZFS parameters for complex series $[Cr(dmpe)_2L_2]^{n+}$, with $L = CN \text{ and } CO$.	83
Table 5.7.	Calculated ZFS parameters for complex Series $[CrX_4(CN)_2]^{3-}$, with $X = Cl, Br, \text{ and } I$.	85
Table 6.1.	A comparison of the experimental magnetic anisotropy energy (MAE) barrier with that computed at the BPW91/TZV level and the individual excitation contributions towards the ZFS parameter in the ground state.	96
Table 6.2.	The ZFS parameters computed at the BPW91/TZV level and the individual excitation contributions towards ZFS under the influence of a finite electric field.	97

Table 6.3. The excitation behavior of $[\text{Co}^{\text{II}}(\text{dmphen})_2(\text{NCS})_2]$ in the ground state and under application of a finite electric field computed at the BPW91/TZV level. 99

LIST OF FIGURES

Figure	Caption	Page
Figure 1.1.	Evolution of resonance structures of benzene and polybenzenoid hydrocarbons from Kekulé to Clar.	1
Figure 1.2.	Most relevant advances of the concept of Aromaticity from 1825 to 1970.	4
Figure 1.3.	Most relevant advances of the concept of Aromaticity from 1970 to 2010.	5
Figure 1.4.	Some early magnetic devices: the ‘South pointer’ used for orientation in China around the beginning of the present era.	7
Figure 1.5.	Diagram of the SMM energy barrier for an $S = 4$ system.	10
Figure 2.1.	The scheme of calculation of NICS and NICS-scan by measuring the magnetic shielding at the ring centre and points above the ring plane.	18
Figure 2.2.	Ferromagnetic (a) and antiferromagnetic (b) coupling of two metal centers via σ -bonding.	20
Figure 2.3.	Spin densities of the broken symmetry solution for the Cu^{II}_2 benchmark system. The two uncoupled spins are in the $d_{x^2-y^2}$ orbitals of the two metal centers. Some spin density is also delocalized over the bridging atoms.	21
Figure 3.1.	Energy (a.u.) profile of Mg_3Na_2 with increasing Na– Mg_3 distance (Å) on the (a) geometry of singlet state optimized at UB3LYP/6-311+g(d) level, (b) geometry of singlet state optimized at QCISD/aug-cc-pvdz level, (c) geometry of singlet and triplet states, both optimized at UB3LYP/6-311+g(d) level, and (d) geometry of singlet and triplet states, both optimized at QCISD/aug-cc-pvdz level of theory.	35
Figure 3.2.	Schematics of the HOMO generated at (a) optimized geometry (b) Na– Mg_3 distance of 4.08 Å where the singlet energy approaches close to the triplet energy, and (c) Na – Mg_3 distance of 5.58 Å.	35
Figure 3.3.	Bonding energy decomposition analysis in the singlet state of the molecule.	36
Figure 3.4.	Plot of (a) NICS(0) and NICS(1) in the singlet and triplet state of Na_2Mg_3 at DFT level. (b) The 26 th MO contributing maximum toward the diamagnetic NICS(0). (c) The average DI and (d) MCI index of	38

aromaticity for the singlet state as a function of increasing Na–Mg₃ distance (Å).

- Figure 3.5.** Plot of Pauli repulsion energy (ΔE_{Pauli}) and $\delta_{\text{NICS}}^{(0)}$ and $\delta_{\text{NICS}}^{(1)}$ with increasing Na–Mg₃ distance (Å) in the singlet state of Na₂Mg₃. 39
- Figure 3.6.** Plot of spin density on Na and Mg₃ in the ground state with increasing Na–Mg₃ distance (Å). 40
- Figure 3.7.** Spin density plot at a Na–Mg₃ separation onward 3.83 Å (green and red color denote up-spin and down-spin density). 41
- Figure 4.1.** (a) Representation of the in registry and out of registry chains (b) blue and brown rectangles in the out of registry chains designate the H-pair and V-pair respectively. 49
- Figure 4.2.** The 133rd α -SOMO in (a) H-pair, and (b) V-pair, solely centered on the acceptor. 56
- Figure 4.3.** The DOS plot of the V-pair. 57
- Figure 4.4.** The 46th α -MO of acceptor unit in both of the V-pair and H-pair. 58
- Figure 4.5.** A qualitative MO diagram of the chosen active space for the CASSCF calculation, containing 10 electrons in 9 orbitals. 59
- Figure 4.6.** The density of states plots of the V-pair in (a) gas phase and (b) under periodic boundary condition. 61
- Figure 5.1.** Structures of the octahedral complexes $[\text{Cr}(\text{dmpe})_2(\text{CN})\text{X}]^+$, (X = Cl, Br, I for complexes 1, 2, and 3, respectively). 71
- Figure 5.2.** The HOMOs and the LUMOs of the octahedral Cr(III) complexes. The equatorial ligands are in tube form for clarity. 77
- Figure 5.3.** Decrease in the HOMO–LUMO gap on going from complex 1 to complex 3, with the increase in π -donation strength from Cl to I. 78
- Figure 5.4.** A qualitative MO diagram of $[\text{Cr}(\text{dmpe})_2(\text{CN})\text{X}]^+$ showing interaction of the metal d -orbitals with π -donor ligands. 80
- Figure 5.5.** Schematic representation of the complexes used in SET-I and SET-II. 81
- Figure 5.6.** A qualitative MO diagram of $[\text{Cr}(\text{dmpe})_2(\text{CN})\text{X}/\text{CN}]^+$ showing interaction of the metal d -orbitals with π -acceptor ligands. 83
- Figure 5.7.** Schematic representation of the designed complexes where equatorial positions are replaced with halides (X = Cl, Br, and I). 84

- Figure 6.1.** Structure of the pseudo-octahedral Co^{II}-complex, [Co^{II}(dmphen)₂(NCS)₂] . 93
- Figure 6.2.** The arrangement of [Co^{II}(dmphen)₂(NCS)₂] complex between two oppositely charged parallel plates. 94
- Figure 6.3.** A plot of the variation in D with external electric field. 97
- Figure 6.4.** The spin-density plots (at an isosurface value of 0.004) of the Co(II) complex in a) the ground state and b) under the applied electric field with a magnitude of 4.0×10³ a.u. The blue color specifies α-spin density and the green color indicates β-spin density. 98

LIST OF APPENDICES

Appendix A: Supplementary Information for Chapter 3

Table A.S1. Computation at UB3LYP/6-311+g(d) level on the singlet state (with optimized wave function) of Mg_3Na_2 with its geometry optimized at QCISD/aug-cc-pVDZ level.

Na-Mg ₃ (Ang)	Energy of Singlet state (au)	$\langle \hat{S}^2 \rangle$	Energy of Triplet state (au)
2.83	-924.917371	0	-924.8748404
3.08	-924.912262	0	-924.8765632
3.33	-924.9036037	0	-924.8764225
3.58	-924.8934524	0	-924.8747282
3.83	-924.8835786	0.293086	-924.8721917
4.08	-924.8760376	0.612094	-924.8693775
4.33	-924.8704624	0.786831	-924.86665
4.58	-924.8663496	0.883578	-924.8642071
4.83	-924.8633201	0.937099	-924.8621331
5.08	-924.8610883	0.966404	-924.8604373
5.33	-924.8594533	0.982391	-924.8591013
5.58	-924.8582648	0.990978	-924.8580755
5.83	-924.857411	0.995495	-924.8573108
6.08	-924.8568134	0.997841	-924.8567602
6.33	-924.8563964	0.999005	-924.8563685
6.58	-924.8561138	0.999566	-924.8560993
6.83	-924.855929	0.999829	-924.8559215
7.08	-924.855803	0.999946	-924.8557991
7.33	-924.8557194	0.999996	-924.8557175
7.58	-924.8556679	1.000014	-924.855667
7.83	-924.8556323	1.000021	-924.855632
8.08	-924.8556065	1.000023	-924.8556064
8.33	-924.8555909	1.000022	-924.8555909
8.58	-924.8555822	1.000021	-924.8555823
8.83	-924.8555752	1.00002	-924.8555753
9.08	-924.8555692	1.00002	-924.8555693
9.33	-924.855565	1.000019	-924.8555651
9.58	-924.8555626	1.000018	-924.8555626
9.83	-924.8555602	1.000018	-924.8555603
10.08	-924.8555575	1.000018	-924.8555575
10.33	-924.855555	1.000018	-924.855555
10.58	-924.8555532	1.000018	-924.8555532
10.83	-924.8555519	1.000018	-924.8555519
11.08	-924.8555503	1.000018	-924.8555503
11.33	-924.8555484	1.000018	-924.8555484
11.58	-924.8555466	1.000018	-924.8555466

11.83	-924.8555451	1.000017	-924.8555451
12.08	-924.8555438	1.000017	-924.8555438
12.33	-924.8555424	1.000017	-924.8555424
12.58	-924.8555406	1.000017	-924.8555406
12.83	-924.8555386	1.000017	-924.8555386
13.08	-924.8555366	1.000017	-924.8555366
13.33	-924.8555348	1.000017	-924.8555348

Table A.S2. Computation at UB3LYP/6-311+g(d) level on the singlet state (with optimized wave function) of Mg₃Na₂ with its geometry optimized at the same DFT level.

Na-Mg ₃ (Ang)	Energy of Singlet state (au)	$\langle \hat{S}^2 \rangle$	Energy of Triplet state (au)
2.74955	-924.9178257	0	-924.87378
2.99955	-924.9146123	0	-924.87617
3.24955	-924.9069096	0	-924.87666
3.49955	-924.8970636	0	-924.8754
3.74955	-924.8867516	0.119752	-924.87306
3.99955	-924.878341	0.520225	-924.87026
4.24955	-924.8721096	0.735886	-924.86745
4.49955	-924.8675079	0.855269	-924.86487
4.74955	-924.8641154	0.92141	-924.86265
4.99955	-924.8616147	0.957805	-924.86081
5.24955	-924.8597764	0.977682	-924.85934
5.49955	-924.8584367	0.988467	-924.8582
5.74955	-924.8574677	0.994174	-924.85734
5.99955	-924.8567834	0.997161	-924.85672
6.24955	-924.8563059	0.998672	-924.85627
6.49955	-924.8559768	0.999407	-924.85596
6.74955	-924.8557605	0.999755	-924.85575
6.99955	-924.8556154	0.999914	-924.85561
7.24955	-924.8555168	0.999982	-924.85551
7.49955	-924.8554551	1.000009	-924.85545
7.74955	-924.8554149	1.000019	-924.85541
7.99955	-924.8553855	1.000022	-924.85539
8.24955	-924.8553662	1.000022	-924.85537
8.49955	-924.8553556	1.000021	-924.85536
8.74955	-924.8553482	1.00002	-924.85535
8.99955	-924.8553417	1.00002	-924.85534
9.24955	-924.8553367	1.000019	-924.85534
9.49955	-924.8553338	1.000019	-924.85533
9.74955	-924.8553315	1.000018	-924.85533
9.99955	-924.8553289	1.000018	-924.85533
10.24955	-924.8553262	1.000018	-924.85533
10.49955	-924.8553242	1.000018	-924.85532
10.74955	-924.8553227	1.000018	-924.85532
10.99955	-924.8553213	1.000018	-924.85532

11.24955	-924.8553195	1.000017	-924.85532
11.49955	-924.8553176	1.000017	-924.85532
11.74955	-924.855316	1.000017	-924.85532
11.99955	-924.8553146	1.000017	-924.85531
12.24955	-924.8553133	1.000017	-924.85531
12.49955	-924.8553117	1.000017	-924.85531
12.74955	-924.8553097	1.000017	-924.85531
12.99955	-924.8553077	1.000017	-924.85531
13.24955	-924.8553058	1.000017	-924.85531

Table A.S3. Description of the orbital, wherefrom and to charge transfer occurs in Na_2Mg_3 with Na – Mg₃ distance of 5.08 Å and corresponding second order energy as obtained from the NBO output.

	Donor NBO with composition	Acceptor NBO with composition	ΔE (kcal/mole)
Within α – spin orbitals	LP* (4) Mg 1 s (0.28%) p 99.99 (99.32%) d 1.42 (0.40%)	LP* (1) Na 4 s (56.69%) p 0.76 (43.30%) d 0.00 (0.01%)	– 0.12
Within β – spin orbitals	LP* (4) Mg 1 s (0.28%) p 99.99 (99.32%) d 1.42 (0.40%)	LP* (1) Na 5 s (56.69%) p 0.76 (43.30%) d 0.00 (0.01%)	– 0.12

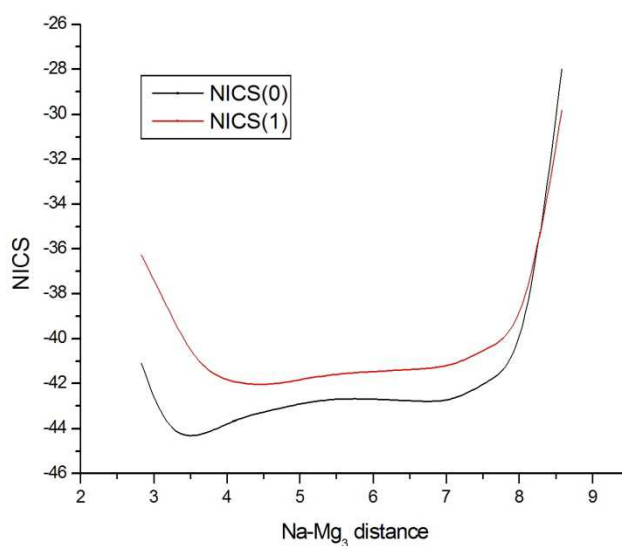


Figure A.S1. Plot of NICS(0) and NICS(1) in the singlet state of Na_2Mg_3 at CCSD/6-311+g(d) level of theory

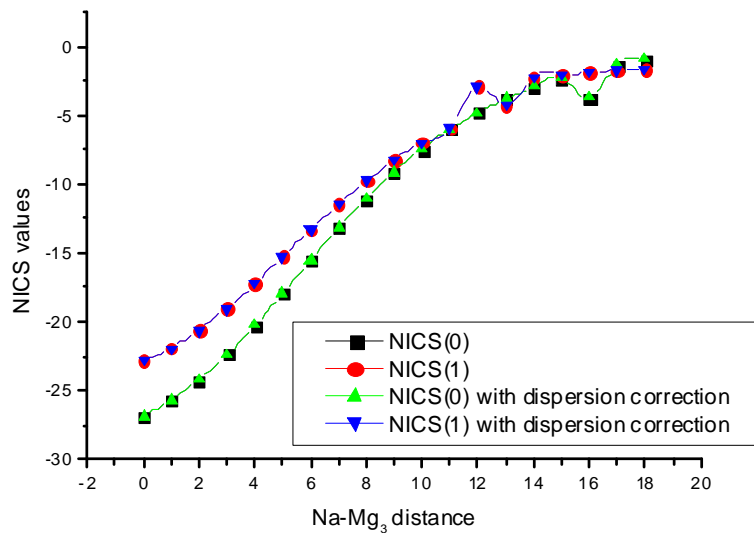


Figure A.S2. Plot of NICS(0) and NICS(1) in the singlet state of Na_2Mg_3 at the DFT level with and without the dispersion correction.

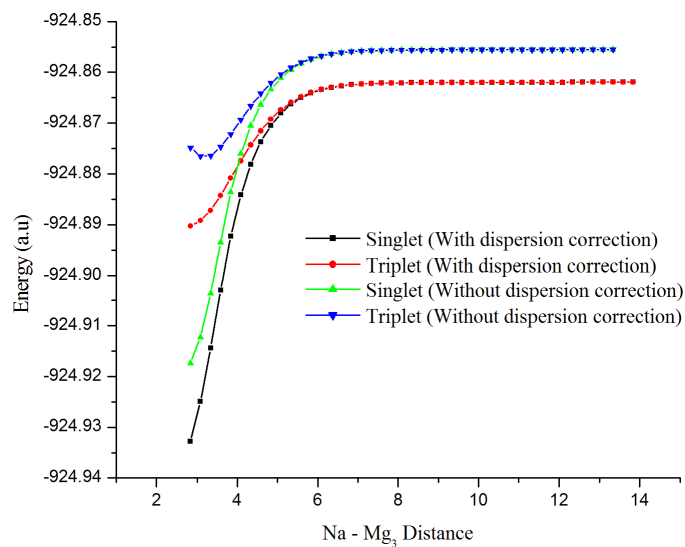
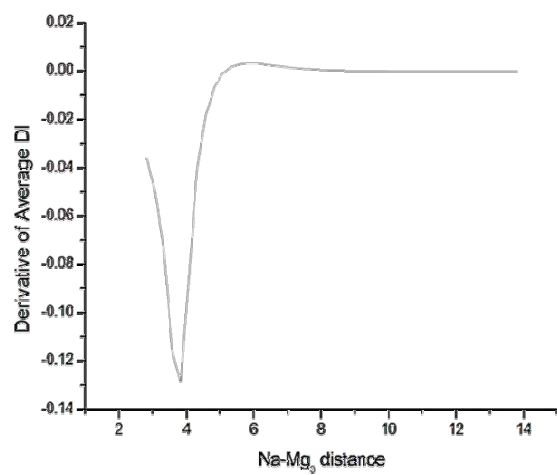
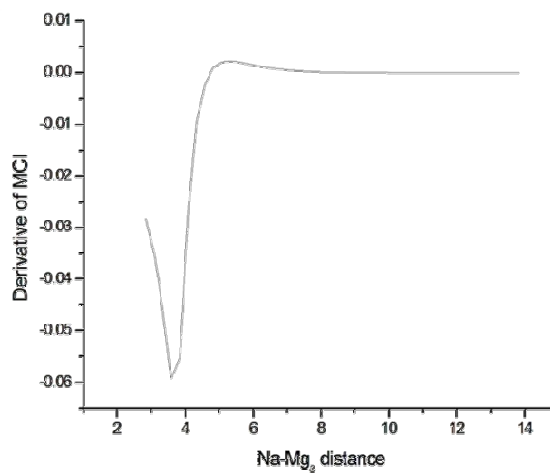


Figure A.S3. Comparison of potential energy curves in Mg_3Na_2 with and without the dispersion correction.



(a)



(b)

Figure A.S4. The derivative plots of (a) Average of DI and (b) MCI indices of aromaticity with increasing Na-Mg₃ separation.

Appendix B: Supplementary Information for Chapter 4

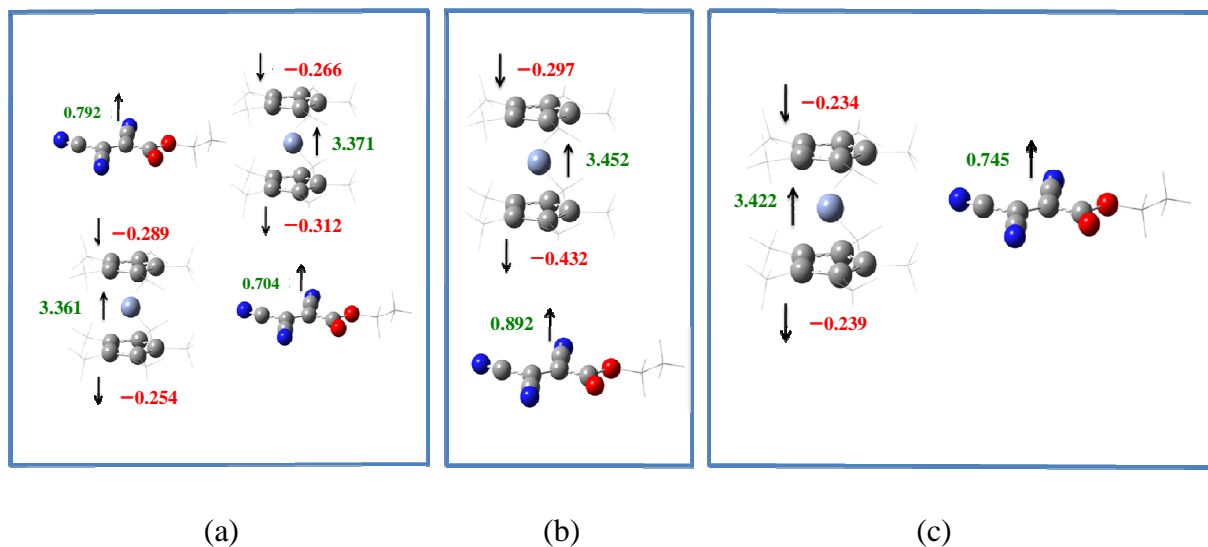
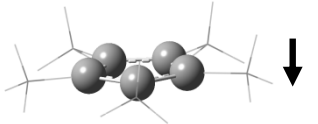

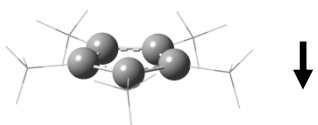
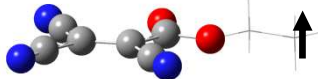


Figure B.S1. Spin populations of the high spin states plotted in (a) two dimensional array (b) V-pair and (c) H-pair of the donor-acceptor complex.

Table B.S1. Energy comparison of triplet and quintet spin states in neutral $[\text{Cr}^{\text{II}}(\text{Cp}^*)_2]$

Level of Theory	Energy difference between the quintet and triplet state in a.u.
UBHandHLYP/6-311++G(d,p) with LANL2DZ as extrabasis on Cr	0.005
CASSCF(6,8)/LANL2DZ	0.003
UBPW91/6-311++G(d,p) with LANL2DZ as extrabasis on Cr	0.042
UB3LYP/6-311++G(d,p) with LANL2DZ as extrabasis on Cr	0.028

Table B.S2. Spin populations at the vertical donor-acceptor stack in different functionals (percentage of HF exchange are given for each functional in the parenthesis)

Functionals	UBHandHLYP	UBPW91	UB3LYP	UPBEPBE	UTPSSH
% of Hartree-Fock Exchange	50 ^{B1}	0 ^{B2}	20 ^{B1}	0 ^{B1}	10 ^{B3}
	-0.297	-0.250	-0.249	-0.255	-0.228
	3.452	3.498	3.423	3.482	3.465
	-0.432	-0.385	-0.373	-0.358	-0.381
	0.892	0.727	0.790	0.706	-0.829
Magnetic exchange coupling constants (J) in cm^{-1}	511	142	137	133	408

B1. Sorkin, A.; Iron, M. A.; Truhlar, D. G. *J. Chem. Theory Comput.*, **2008**, *4*, 307 and references therein.

B2. Kantchev, E. A. B.; Norsten, T. B.; Sullivan, M. B. *Org. Biomol. Chem.*, **2012**, *10*, 6682.

B3. Pantazis, D. A.; Krewald, V.; Orio, M.; Neese, F. *Dalton Trans.*, **2010**, *39*, 4959.

Table B.S3. Variation in spin densities on the magnetic centers $[\text{Cr}(\text{Cp}^*)_2]^+$ (D^+) and $[\text{ETCE}]^-$ (A^-) and coupling constants in the V-pair with nk points ($n = 0, 1, 2$)

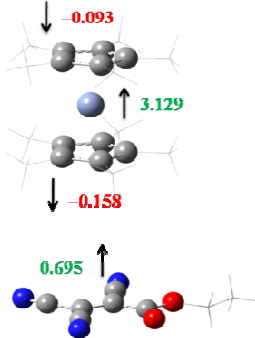
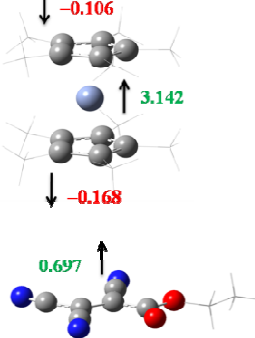
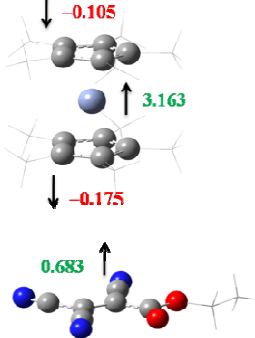
Gamma (Γ) point	n=1	n=2
		
$J = -7.072 \text{ cm}^{-1}$	$J = -7.501 \text{ cm}^{-1}$	$J = -9.297 \text{ cm}^{-1}$

Table B.S4. Estimation of magnetic exchange coupling constant with the hybrid PBE0 functional (at PBE1PBE/LANL2DZ level) at **Gamma (Γ) point** only.

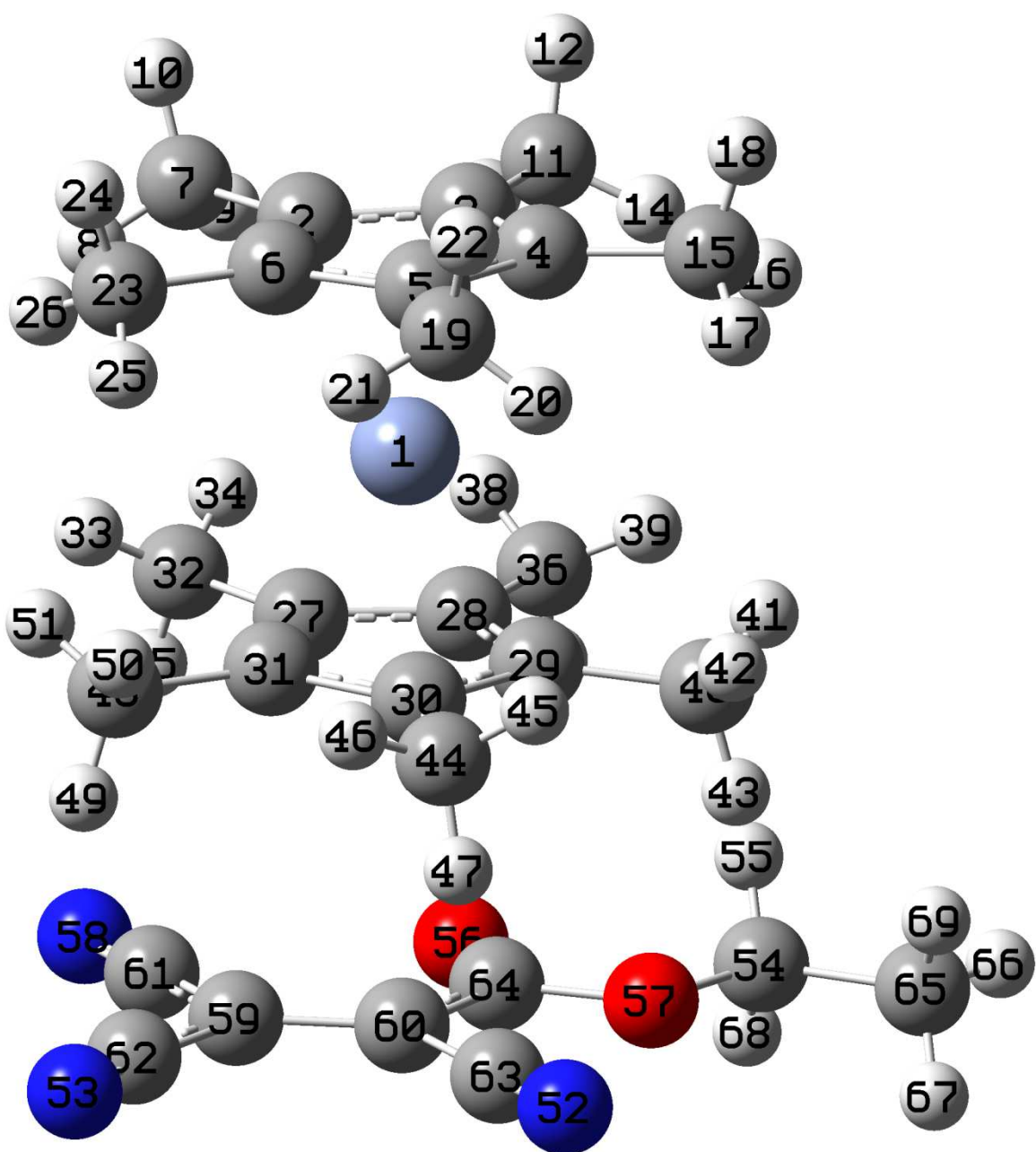
Spin state	Energy in a.u.	$\langle S^2 \rangle^*$	J in cm^{-1}
High spin (quintet)	-1486.6654340	6.100961	-107.24 cm^{-1}
Low spin (triplet)	-1486.6668841	3.133394	

* The $\langle S^2 \rangle$ values are obtained through unrestricted density functional approach. The unrestricted density functional calculation leads to the problem of spin contamination. Due to this spin contamination, the $\langle S^2 \rangle$ value is found to be deviated from the exact value of 6.000.^{B4, B5}

B4. (a) Bhattacharya, D.; Misra, A. *J. Phys. Chem. A*, **2009**, *113*, 5470; (b) Shil, S.; Misra, A. *J. Phys. Chem. A*, **2010**, *114*, 2022.

B5. Paul S.; Misra, A. *J. Chem. Theory and Comput.*, **2012**, *8*, 843.

Figure B.S2. Spin populations of the high-spin states at different functionals.



Spin populations at UBHandHLYP:

Mulliken atomic spin densities:

1	Cr	3.452088
2	C	-0.075705
3	C	-0.063121
4	C	-0.045285
5	C	-0.052738
6	C	-0.060055
7	C	0.015104
8	H	-0.000610
9	H	-0.000434
10	H	-0.000001
11	C	0.018556
12	H	0.000152
13	H	-0.000172
14	H	-0.001848
15	C	0.030128
16	H	-0.001165
17	H	-0.001640
18	H	0.000560
19	C	0.029040
20	H	-0.002802
21	H	-0.000792
22	H	0.000371
23	C	0.016175
24	H	0.000376
25	H	-0.001354
26	H	-0.000248
27	C	-0.108805
28	C	-0.062361
29	C	-0.021571
30	C	-0.120283
31	C	-0.119003
32	C	0.045692
33	H	0.000664
34	H	-0.002864
35	H	0.004106
36	C	0.082698
37	H	-0.006715
38	H	-0.000653
39	H	0.001546
40	C	-0.001421
41	H	-0.002097
42	H	-0.001464
43	H	-0.003589
44	C	0.031833
45	H	-0.000336
46	H	-0.000281
47	H	-0.001393
48	C	0.012664
49	H	0.006226
50	H	-0.002422
51	H	-0.001617

52	N	0.049340
53	N	0.167389
54	C	-0.004473
55	H	0.002348
56	O	0.099409
57	O	0.017629
58	N	0.223715
59	C	0.484294
60	C	0.408096
61	C	-0.231266
62	C	-0.136223
63	C	-0.085798
64	C	0.020922
65	C	-0.000062
66	H	-0.000062
67	H	-0.000007
68	H	0.001710
69	H	-0.000095

Sum of Mulliken spin densities= 4.00000

Spin populations at UB3LYP:

Mulliken atomic spin densities:

1	Cr	3.422894
2	C	-0.070972
3	C	-0.069556
4	C	-0.015448
5	C	-0.028181
6	C	-0.065246
7	C	-0.031425
8	H	0.000000
9	H	-0.000386
10	H	0.000826
11	C	0.002208
12	H	0.000927
13	H	0.001524
14	H	-0.001862
15	C	0.043588
16	H	0.000101
17	H	-0.001921
18	H	0.001478
19	C	0.046722
20	H	-0.003167
21	H	0.000387
22	H	0.001457
23	C	-0.001597
24	H	0.001098
25	H	-0.001779
26	H	0.001529
27	C	-0.109473
28	C	-0.067410
29	C	-0.018869
30	C	-0.078382
31	C	-0.099357

32	C	0.024940
33	H	0.000829
34	H	-0.001121
35	H	0.005098
36	C	0.063182
37	H	-0.002777
38	H	-0.000737
39	H	0.001107
40	C	0.002044
41	H	-0.001989
42	H	-0.002236
43	H	-0.002074
44	C	0.028099
45	H	-0.001191
46	H	-0.000268
47	H	0.000027
48	C	0.022861
49	H	0.008220
50	H	-0.002275
51	H	-0.001516
52	N	0.044192
53	N	0.138277
54	C	-0.003654
55	H	0.002692
56	O	0.087095
57	O	0.025861
58	N	0.177527
59	C	0.406035
60	C	0.383816
61	C	-0.148961
62	C	-0.083880
63	C	-0.064732
64	C	0.033645
65	C	0.000030
66	H	-0.000055
67	H	0.000007
68	H	0.002159
69	H	0.000015

Sum of Mulliken spin densities= 4.00000

Appendix C: Supplementary Information for Chapter 5

TDDFT results for *d-d* vertical excitation: The *d-d* excitations along with their oscillator strengths and orbital transition coefficients are listed in Tables C.S1, C.S2 and C.S3.

Table C.S1. Complex 1 TDDFT results.

Excitations	Oscillator Strengths (fosc)	Orbital transition coefficient
$d_{yz} \rightarrow d_{x^2-y^2}$ (HOMO \rightarrow LUMO)	0.003210117	0.713318
$d_{xz} \rightarrow d_{x^2-y^2}$	0.002323539	0.555789
$d_{yz} \rightarrow d_{z^2}$	0.000075149	0.280159

Table C.S2. Complex 2 TDDFT results.

Excitations	Oscillator Strengths (fosc)	Orbital transition coefficient
$d_{yz} \rightarrow d_{x^2-y^2}$ (HOMO \rightarrow LUMO)	0.007747317	0.838286
$d_{xz} \rightarrow d_{x^2-y^2}$	0.006952073	0.795980
$d_{yz} \rightarrow d_{z^2}$	0.006828186	0.426463

Table C.S3. Complex 3 TDDFT results.

Excitations	Oscillator Strengths (fosc)	Orbital transition coefficient
$d_{yz} \rightarrow d_{x^2-y^2}$ (HOMO \rightarrow LUMO)	0.004066582	0.953855
$d_{xz} \rightarrow d_{x^2-y^2}$	0.001813928	0.827064
$d_{yz} \rightarrow d_{z^2}$	0.001813928	0.101435

Appendix D: Supplementary Information for Chapter 6

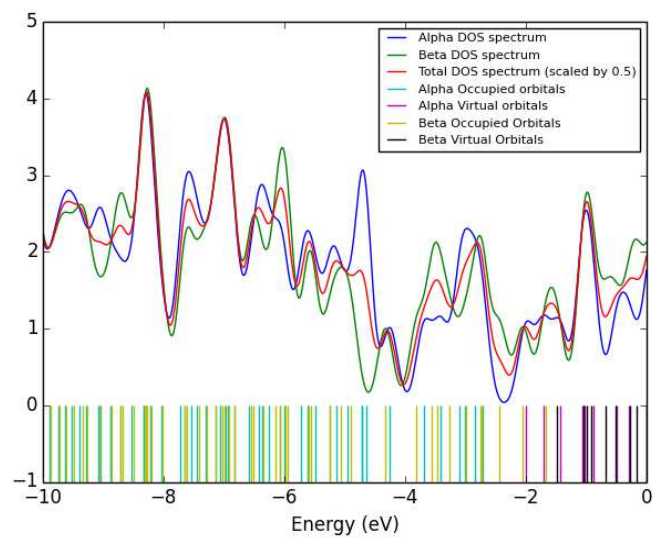
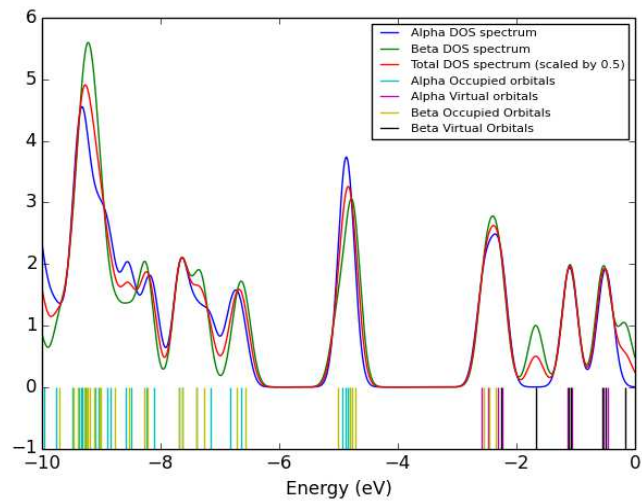
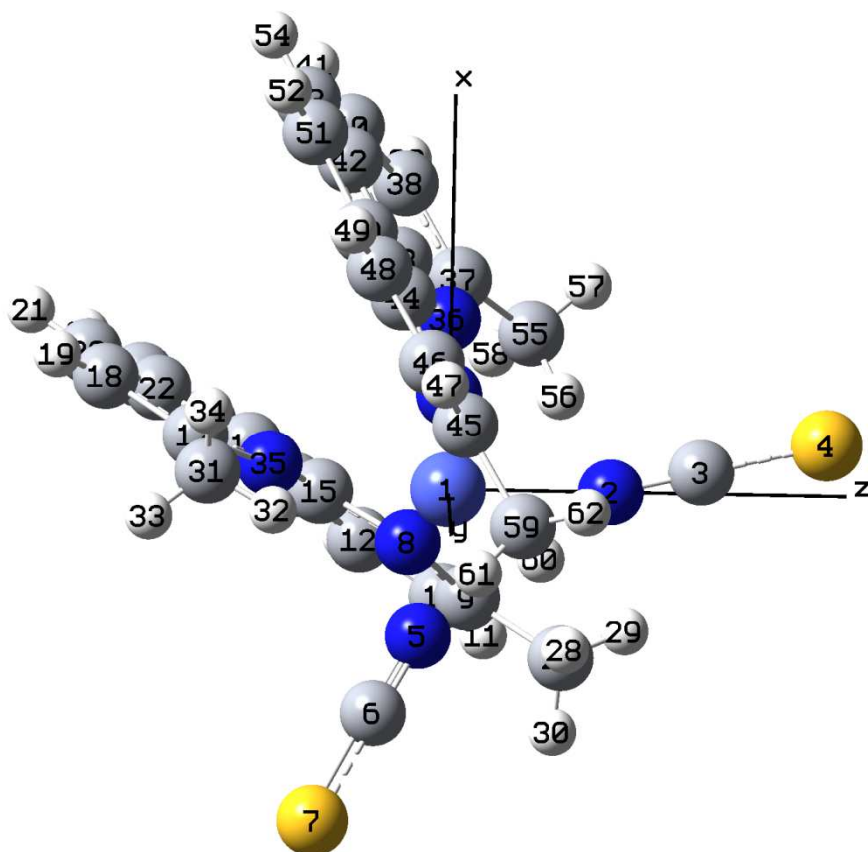


Figure D.S1. The Density of States (DOS) plots of the complex in (a) the unperturbed state and (b) under external electric field of magnitude 4.0×10^{-3} a.u.

Figure D.S2. Mulliken atomic spin densities at different applied electric fields.



Mulliken atomic spin densities at zero applied electric field:

Mulliken atomic spin densities:

1	Co	2.550419
2	N	0.087736
3	C	-0.014911
4	S	0.093805
5	N	0.086775
6	C	-0.012992
7	S	0.098080
8	N	0.046077
9	C	-0.013895
10	C	0.003092
11	H	0.000461
12	C	-0.011425
13	H	0.000928
14	C	0.002097
15	C	-0.007749
16	C	-0.002263
17	C	-0.007625
18	C	0.002948
19	H	0.000648
20	C	-0.007810
21	H	0.000629
22	C	0.002016
23	C	0.000185

24	H	0.000166
25	C	0.000688
26	H	0.000203
27	C	0.002883
28	H	-0.001242
29	H	-0.000366
30	H	-0.000355
31	C	0.002250
32	H	-0.000836
33	H	-0.000187
34	H	-0.000280
35	N	0.042802
36	N	0.042888
37	C	-0.007695
38	C	0.003491
39	H	0.000681
40	C	-0.008314
41	H	0.000664
42	C	0.002415
43	C	-0.002185
44	C	-0.008090
45	C	-0.012874
46	C	0.003260
47	H	0.000451
48	C	-0.012207
49	H	0.000967
50	C	0.002339
51	C	0.000745
52	H	0.000199
53	C	0.000244
54	H	0.000166
55	C	0.002395
56	H	-0.001026
57	H	-0.000174
58	H	-0.000265
59	C	0.002879
60	H	-0.001096
61	H	-0.000346
62	H	-0.000349
63	N	0.047884

Sum of Mulliken spin densities= 3.00000

Mulliken atomic spin densities at +0.004 a.u. applied electric field:

Mulliken atomic spin densities:

1	Co	2.353109
2	N	0.000980
3	C	-0.043498
4	S	0.009624
5	N	0.171036
6	C	-0.063613
7	S	0.338287
8	N	0.069482
9	C	-0.013454

10	C	0.006847
11	H	0.000433
12	C	-0.007254
13	H	0.000599
14	C	0.003165
15	C	-0.000119
16	C	0.000371
17	C	-0.010109
18	C	0.013356
19	H	-0.000223
20	C	0.002028
21	H	0.000079
22	C	0.001302
23	C	0.004147
24	H	0.000039
25	C	0.000981
26	H	0.000281
27	C	0.003795
28	H	-0.002503
29	H	-0.000363
30	H	-0.000388
31	C	0.003022
32	H	-0.000563
33	H	-0.000289
34	H	-0.000536
35	N	0.093918
36	N	0.038786
37	C	-0.005155
38	C	0.002692
39	H	0.000760
40	C	-0.004494
41	H	0.000300
42	C	0.000697
43	C	-0.000218
44	C	-0.005633
45	C	-0.011723
46	C	0.004682
47	H	0.000534
48	C	-0.010743
49	H	0.000779
50	C	0.002308
51	C	-0.000143
52	H	0.000252
53	C	0.000721
54	H	0.000152
55	C	0.002196
56	H	-0.000783
57	H	-0.000179
58	H	-0.000244
59	C	0.003581
60	H	-0.001746
61	H	-0.000328
62	H	-0.000321
63	N	0.049300

Sum of Mulliken atomic spin densities = 3.00000

Appendix E: List of Publications

List of published papers

1. Unique Bonding Pattern and Resulting Bond Stretch Isomerism in Be_3^{2-} (2015) **Goswami, T.**; Paul, S.; Mandal, S.; Misra, A.; Anoop, A. and Chattaraj, P. K. *Int. J. Quantum Chem.* 115, 426-433.
2. On the Control of Magnetic Anisotropy through External Electric Field (2014) **Goswami, T.** and Misra, A. *Chem. Eur. J.* 20, 13951-13956 (Selected as Back Cover & Very Important Paper).
3. On magnon mediated Cooper pair formation in ferromagnetic superconductors (2014) Kar, R.; **Goswami, T.**; Paul, B. C. and Misra, A. *AIP Adv.* 4, 087126.
4. A note on second-order nonlinear optical response of high-spin bis-TEMPO diradicals with possible application (2014) Bhattacharya, D.; Shil, S.; **Goswami, T.**; Misra, A. and Klein, D. *J. Comput. Theor. Chem.* 1039, 11-14.
5. Effect of Charge Transfer and Periodicity on the Magnetism of $[\text{Cr}(\text{Cp}^*)_2][\text{ETCE}]$ (2014) **Goswami, T.**; Paul, S. and Misra, A. *RSC Adv.* 4, 14847-14857.
6. The impact of surface structure and band gap on the optoelectronic properties of Cu_2O nanoclusters of varying size and symmetry (2014) Sinha, B.; **Goswami, T.**; Paul, S. and Misra, A. *RSC Adv.* 4, 5092–5104.
7. A Theoretical Study on Magnetic Properties of Bis-TEMPO Diradicals with Possible Application (2013) Bhattacharya, D.; Shil, S.; **Goswami, T.**; Misra, A.; Panda, A. and Klein, D. *J. Comput. Theor. Chem.* 1024, 15-23.
8. Intermolecular Interaction in 2-Aminopyridine: A Density Functional Study (2013) Majumder, M.; **Goswami, T.**; Misra, A.; Bardhan, S. and Saha, S. K. *Commun. Comput. Chem.* 1, 225-243.
9. Concurrent loss of aromaticity and onset of superexchange in Mg_3Na_2 with an increasing Na – Mg_3 distance (2013) Paul, S.; **Goswami, T.**; Misra, A. and Chattaraj, P. K. *Theor. Chem. Acc.* 132, 1391-10.
10. Ligand Effects toward the Modulation of Magnetic Anisotropy and Design of Magnetic Systems with Desired Anisotropy Characteristics (2012) **Goswami, T.** and Misra, A. *J. Phys. Chem. A.* 116, 5207-5215 (Highlighted in ACS Virtual Issue “Quantum Molecular Magnets”).
11. A Theoretical Study on Photomagnetic Fluorescent Protein Chromophore Coupled Diradicals and Their Possible Applications (2012) Bhattacharya, D.; Panda, A.; Shil, S.; **Goswami, T.** and Misra, A. *Phys. Chem. Chem. Phys.* 14, 6509-6913.

List of manuscripts under communication

12. Paul, S.; **Goswami, T.** and Misra, A., Noncomparative Scaling of Aromaticity through Electron Itinerancy (Manuscript under communication).
13. Sinha, B.; **Goswami, T.**; Paul, S. and Misra, A., Tailoring Retinal-Gold Nanoconjugate for Vision Enhancement (Manuscript under communication).
14. **Goswami, T.**; Homray, M.; Dasgupta, T.; Bhattacharya, D. and Misra, A., $C_2B_2F_4$: A new molecule deciphering unique aromaticity through electron donation (Manuscript under communication).

CHAPTER 1

Aromaticity and magnetism in metal based systems

Abstract

This chapter provides a brief account of the history and significant advances in the fields of aromaticity and magnetism. In this chapter a concise history of the origin and advancement of research in aromaticity is given which correlates the chronological development of the subjects with the evolution of new materials. The current status of the research in aromaticity, with special emphasis on the metal based aromatic molecules, is provided. Magnetism is also discussed according to the chronology of the advancement of the theory and explored materials. The effect of dimension in the magnetic properties is also discussed here. The emergence of new molecules for nanomagnets and the role of the theoretical advancement in designing such materials also discussed in this chapter.

1.1 Aromaticity

The concept of aromaticity is of central importance to the theory and practice of teaching and research in chemistry. The chemical term “aromatic” is first known to be used by August Wilhelm Hofmann in 1855.¹ Hofmann referred to a group of acids related to Benzoic acid as “aromatic acids” in his paper. In early 1860 “fatty” and “aromatic” compounds were differentiated by Kekulé.² The word aromatic was first chosen by Kekulé to refer benzene derivatives richer in carbon (kohlenstoffreichere). A precise definition of aromaticity was never given by Kekulé other than some partial definitions in the 1865/66 papers.³ In 1872, Kekulé described benzene as “a regular arrangement of the six carbon atoms”, thus implying a D_{6h} symmetric structure. However, initially benzene was drawn with alternating single and double bonds indicating a D_{3h} symmetric structure.⁴ The axiom, that “In allen sogenannten aromatischen Substanzen kann eine gemeinschaftliche Gruppe, ein Kern, angenommen werden, der aus 6 Kohlenstoffatomen besteht.” (In every so-called aromatic substance one common group, a kernel which consists of 6 carbon atoms, can be assumed) was contradicted by Erlenmeyer in the case of naphthalene,⁵ by Körner,⁶ and by Dewar for pyridine.⁷ In 1922 Crocker noticed that “aromatic structure is observed only in those combinations of elements which furnish *six* extra or aromatic electrons above those needed to complete a single-bonded ring”.⁸ He was thereby first to recognize the six aromatic electrons and in this way correctly described benzene, pyridine, thiophene, furan, and pyrrol. The circle, signifying the six aromatic electrons, was introduced by Armit and Robinson in 1925, but as they state that “the deletion of the central connecting bonds is more apparent than real”,⁹ it seems that they knew already from the beginning that their representation of polyaromatic hydrocarbons was flawed. In 1931, Hückel published the theory of cyclic $4n+2$ π -electron systems which forms the basis for Hückel’s rule for aromaticity.¹⁰ It was not until 1959 that Clar made the refinements to the resonance structures (Figure 1.1).¹¹

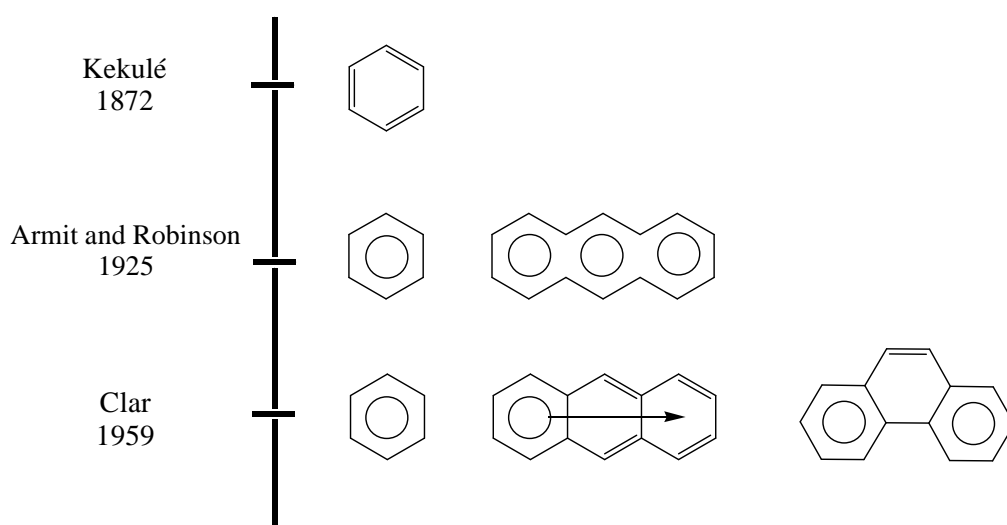


Figure 1.1. Evolution of resonance structures of benzene and polybenzenoid hydrocarbons from Kekulé to Clar.

The concept of aromaticity is to some extent intuitive. As a matter of fact the notion of “aromaticity” is controversial, difficult to understand or to explain in a few words. It implies that there is still a long way to go, and to dig, before we can conclude that this concept is of seminal value, useful in providing insight for the phenomenon. The core of aromatic nature is often defined by referring to a series of structural, energetic and spectroscopic characteristics, of which the following constitute the core: (i) a highly symmetric, delocalized structure involving six C–C bonds of equal length, each with partial double-bond character, (ii) enhanced thermodynamic stability, and (iii) reduced reactivity as compared to nonaromatic conjugated hydrocarbons.¹² Other properties that have been taken as symptoms of aromatic character are, for example, the down-field shift in proton NMR spectra, the exaltation of diamagnetic susceptibility, and a comparatively low reactivity.¹³ The counterpart of benzene is the antiaromatic 1,3-cyclobutadiene which, for example, shows localized double bonds instead of a regular delocalized structure with four C–C bonds of equal length.¹² There are many designations for aromaticity, but benzene is considered as the archetype of an aromatic molecule in all of the definitions. Soon after the designation of benzene as aromatic molecules, many characteristics of benzene were started to be used as benchmark to determine the aromaticity in other molecules. Often the degree of similarity of the characteristic between the molecule under study and benzene is then considered as a measure of Aromaticity. Aromaticity continues to be a topic in many studies associated not only with its relevance in chemistry, biology and technology, but also with the very concept itself. Indeed, despite many pioneering contributions on this issue, there is still a gap in our physical understanding of the nature of aromaticity.^{12,13,14} In the early twentieth century, Pauling and Hückel were the first to quantum chemically address the issue of benzene's structure and enhanced stability using valence bond (VB) and molecular orbital (MO) theory.¹⁵ In a VB-type approach, used by both Pauling and Hückel, the circular topology of benzene enables a resonance between the wave functions of two complementary sets of localized bonds, leading to an additional stabilization. In the MO approach applied by Hückel to the benzene problem, the enhanced stability of benzene compared, for example, to isolated or linearly conjugated double bonds, is attributed to an extra bonding contact (or resonance integral or interaction matrix element) in circularly conjugated hydrocarbons with $4n+2$ π -electrons^{15b,c} (a generalization to other than pericyclic topologies was later derived by Goldstein and Hoffmann).¹⁶

1.1.1. History and key advances

Since the isolation of benzene, the number of aromatic compounds has exponentially increased (See Table 1.1 for a summary of the main advances in the field of aromaticity). Before the end of the 19th century, the list was enlarged with benzene related monocyclic six membered rings. Then, the concept of aromaticity was extended to polycyclic rings such as naphthalene, anthracene, or phenanthrene and to rings with heteroatoms such as thiophene and pyrrole, and to annulenes and their ions e.g., tropylium cation. The work of Hückel helped to find a rule to discern between aromatic and non-aromatic compounds. With the concept of metalloaromaticity, aromaticity broke the confinements of organic chemistry. On the other hand, Heilbronner defined Möbius aromaticity, which follows exactly the opposite

behaviour of $4n+2$ rule. By means of theoretical calculations, Baird described a rule of triplet aromaticity which was experimentally validated by Wörner et al. in 2006.¹⁷ In 1978 Aihara introduced the three-dimensional aromaticity in boron clusters. Hirsch's rule allows one to predict the spherical aromaticity of recently discovered fullerenes and nanotubes.¹⁸ Finally, the most important recent breakthrough in the field of aromaticity took place in 2001, when Boldyrev, Wang et al., characterised the first all-metal aromatic cluster Al_4^{2-} . The properties of such molecules make them potentially useful for technical applications such as specific and very efficient catalysts, drugs, gas storage materials and other novel materials with as yet unimagined features. At variance with the classical aromatic organic molecules that possess only π -electron delocalization, these compounds present σ -, π -, and δ - (involving d -orbitals) or even ϕ - (involving f -orbitals) electron delocalization, exhibiting characteristics of what has been called multifold aromaticity. Figures 1.2 and 1.3 represent graphically the chronology of the advancement in aromaticity research.

Table 1.1. List of the key advances of the concept of aromaticity listed in chronological order.

Year	Main Contributors	Contributions
1825	Micheal Faraday ¹⁹	Isolation of benzene
1865	August Kekulé ²⁰	Cyclohexatriene benzene formula
1866	Ernlenmeyer ²¹	Reactivity basis for aromaticity
1922	Crocker ²²	Aromaticity sextet
1931	Hückel ²³	$(4n+2)\pi$ electron rule
1938	Evans, Warhurst ²⁴	Transition state stabilization by aromaticity
1945	Calvin, Wilson ²⁵	Metalloaromaticity
1959	Winstein ²⁶	Generalization of homoaromaticity
1964	Heilbronner ²⁷	Möbius aromaticity
1965	Breslow ²⁸	Recognition of aromaticity
1970	Osawa ²⁹	Superaromaticity
1972	Clar ³⁰	Clar aromatic sextet
1972	Baird ³¹	Triplet aromaticity
1978	Aihara ³²	Three-dimensional aromaticity
1979	Dewar ³³	σ -aromaticity
1979	Schleyer ³⁴	Double and in plane aromaticity
1985	Shaik and Hiberty ³⁵	π -electron distortivity
1985	Kroto ³⁶	Discovery of fullerenes
1991	Iijima ³⁷	Discovery of nanotubes
2001	Boldyrev and Wang ³⁸	All-metal aromaticity
2005	Schleyer ³⁹	d -orbital aromaticity
2007	Boldyrev and Wang ⁴⁰	δ -aromaticity
2008	Tsipis and Tsipis ⁴¹	ϕ -aromaticity

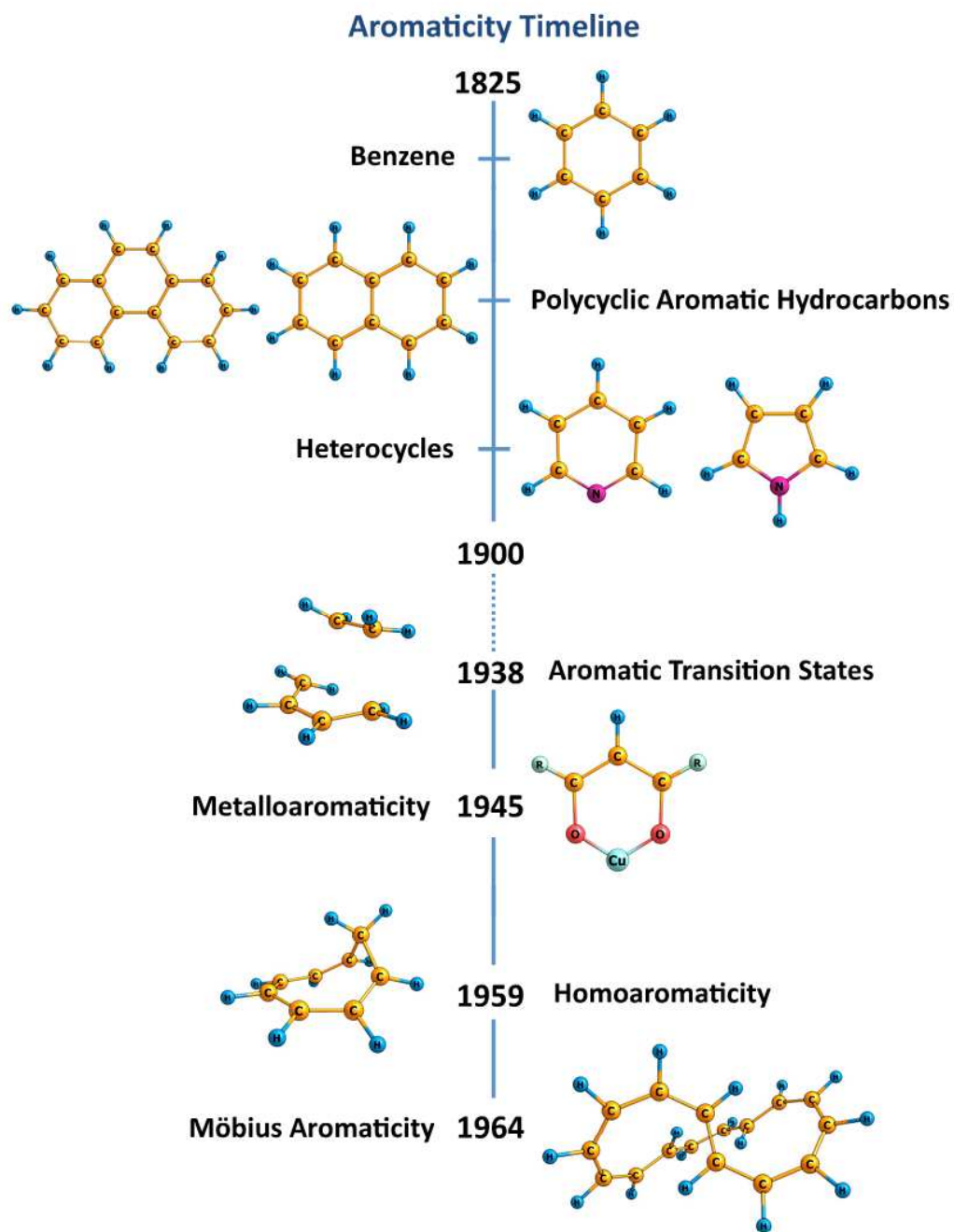


Figure 1.2. Most relevant advances of the concept of Aromaticity from 1825 to 1970.

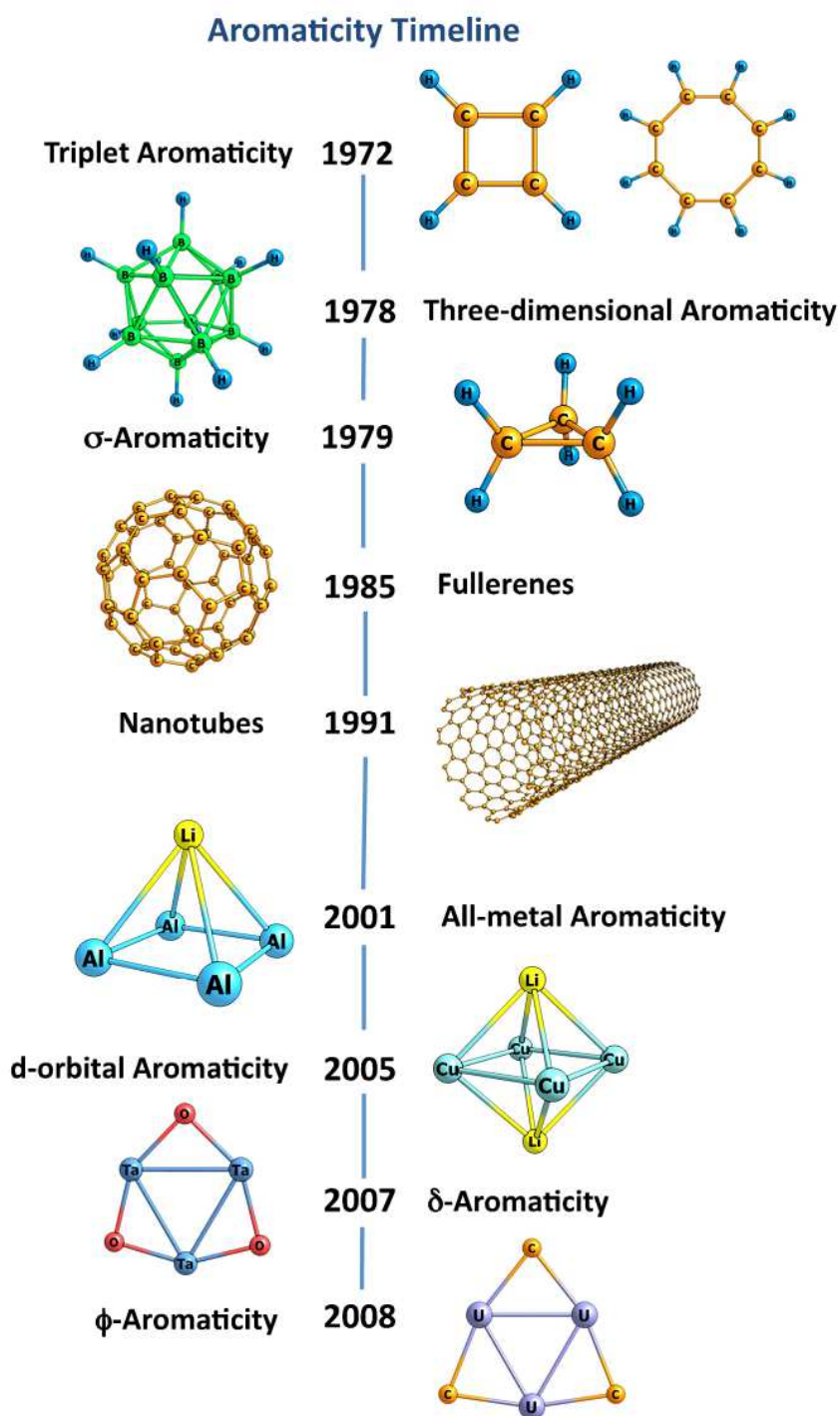


Figure 1.3. Most relevant advances of the concept of Aromaticity from 1970 to 2010.

1.1.2. Aromaticity in metal based systems

The concept of aromaticity is usually associated with organic compounds. The organometallic and inorganic aromatic species⁴² led the way to the discovery of σ -aromaticity⁴³ which was followed soon by the three dimensional aromaticity in certain spherical compounds.⁴⁴ The geometric, energetic and magnetic criteria are helpful to determine aromaticity in such species. However, the discovery of pure all-metal aromatic systems (AMAS) has made a prospect to the theoretical chemists due to the special nature of their chemical bonding leading to the existence of multi-fold aromaticity.⁴⁵ This discovery was followed by the searching of different novel all-transition metal aromatic as well as antiaromatic systems.⁴⁶ The presence of σ -, π -, and δ - or even ϕ -electron delocalization together, unlike classical π -electron delocalization in organic systems, enriches this special class of compounds. Besides, few of such systems drew attention to the scientific community due to the simultaneous presence of aromatic and antiaromatic ring current. The typical all-metal aromatic cluster Al_4^{2-} was reported to be a doubly aromatic system with the simultaneous existence of σ - radial- (σ_r -), σ -tangential- (σ_t -) and π -aromaticities. A number of metallo-aromatic compounds, e.g., Cu_3^+ ;⁴⁷ X_3^- (X=Sc, Y, La);⁴⁸ X_3^{2-} (X = Zn, Cd, Hg);⁴⁹ Hf_3 ;⁵⁰ Ta_3^- ;⁵¹ Au_5Zn^+ ;⁵² Cu_5Sc , Cu_6Sc^+ , Cu_7^{3-} and Cu_7Sc ;⁵³ M_4Li_2 (M = Cu, Ag, Au);⁵⁴ M_4L_2 and M_4L^- (M = Cu, Ag, Au; L = Li, Na)⁵⁵ etc. are also reported. This disparity of aromaticity in such metallo-aromatic systems, with their classical organic analogues, asked for a new definition which will resolve all the complexity and discrepancy to describe the phenomena of aromaticity.

1.2. Magnetism: History and Key Advancements

The first use of a loadstone compass can be found in China popular as *shao shih* or *tzhu shih*, which the Chinese meant loving stone more than four millennia ago. Then came the French word *l'aimant*, meaning attraction or friendship for magnet. The English word *magnet* came from the name of a region of the ancient Middle East, Magnesia, where magnetic ores were found. The amazing natural magic of magnets was known to the priests and people in Sumer, ancient Greece, China and pre-Colomban America. Zheng Gongliang in 1064, made a significant discovery that iron could acquire a resultant magnetization when quenched from red heat. Steel needles thus magnetized in the Earth's field were the first artificial permanent magnets. They aligned themselves with the field when floated or suitably suspended. A short step led to the invention of the navigational compass, which was described by Shen Kua around 1088. A lodestone sliced in the shape of a Chinese spoon was the lynchpin of an early magnetic device, the 'South pointer'. This 'South pointer' (Figure 1.4) were used for geomancy in China at the beginning of our era utilizing the property of the spoon turning on the base to align its handle with the Earth's magnetic field. Such permanent magnets are quite widespread in nature in the rocks rich in magnetite, the iron oxide Fe_3O_4 – which were magnetized by huge electric currents in lightning strikes.

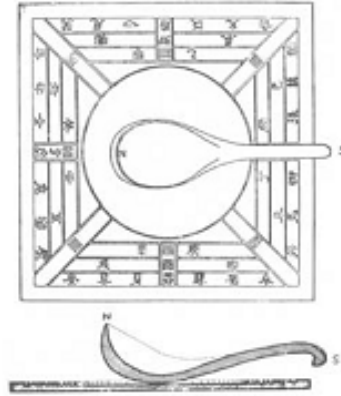


Figure 1.4. Some early magnetic devices: the ‘South pointer’ used for orientation in China around the beginning of the present era.

The Chinese are known to be the first to use abstract binary concepts such as yin/yang and male/ female, as well as understanding the concrete binary process of counting by the presence or absence of a bead in an abacus. But the development of a magnetic abacus, that is, a computer with binary magnetic information storage, took thousands more years to achieve. These magnetic memories were tiny toroids of ferrite that could be individually magnetized by simultaneous current pulses passing through two orthogonal wires. In this era of information technology the use of magnetic materials in tapes, floppy diskettes, and hard disks for the purpose of storing information are abundant in devices ranging from personal computers to supercomputers.

Magnetic materials are the backbone of progress of information technology in current days. Our seemingly insatiable appetite for more computer memory is satisfied by a variety of magnetic recording technologies based on nanocrystalline thin-film media and magneto-optic materials. Personal computers and many of our consumer and industrial electronics components are now powered largely by lightweight switch-mode power supplies using new magnetic materials technology that was unavailable 20 years ago. Magnetic materials touch many other aspects of our lives. Each automobile contains dozens of motors, actuators, sensors, inductors, and other electromagnetic and magneto-mechanical components using hard (permanent) as well as soft magnetic materials. Electric power generation, transformation, and distribution systems rely on hundreds of millions of transformers and generators that use various magnetic materials ranging from the standard 3% SiFe alloys to new amorphous magnetic alloys. Tiny strips or films of specially processed magnetic materials store one or more bits of information about an item or about the owner of an identification badge.

The magnetic properties of solids arise essentially from the magnetic moments of their atomic electrons. The quantum mechanics of electrons is described by Dirac equation which speaks that electrons have an additional degree of freedom, known as ‘spin’. The mathematical form of a “spin” is angular momentum and the genesis of magnetism is considered to be inherent within the interaction of such spins. The key advances in the field

of magnetism are given in Table 1.2. in chronological order. Magnetism can be divided into two groups. In one group, either there is no net spin moment or there is no interaction between the individual spin magnetic moments and each moment acts independently of the others. Congeners belonging to these groups are referred to as diamagnets and paramagnets respectively. In the other group, the individual moment couple to one another and form magnetically ordered materials. The coupling, which is quantum mechanical in nature, is known as the exchange interaction and is rooted in the overlap of electrons in conjunction with Pauli's exclusion principle. Most of the well known magnets are based on the compounds of iron, cobalt, nickel, gadolinium etc. which are ferromagnetic i.e. having unpaired spins in parallel orientation in their bulk state. The situation, where each spin is aligned antiparallel to its nearest neighbors, gives rise to antiferromagnetism. Metal compounds, MnO, MnF₂ or NiO are the archetypes of antiferromagnetic materials. In case, the numbers of antiparallel and parallel pair of spins are different or the antiparallely aligned spins are of unequal magnitude, a remnant magnetization develops in the material.

Table 1.2. List of the key advances in the field of magnetism in the chronological order.

Period	Dates	Icon	Materials
Ancient Period	-2000-1500	Compass	Iron, loadstone
Early modern age	1500-1820	Horseshoe magnet	Iron, loadstone
Electromagnetic age	1820-1900	Electromagnet	Electrical steel
Age of understanding	1900-1935	Pauli matrices	--
High-frequency age	1935-1960	Magnetic resonance	Ferrites
Age of Applications	1960-1995	Electric screw driver	Sm-Co, Nd-Fe-B
Age of spin electronics	1995-	Read head	Multilayers

1.2.1. Dimensionality and magnetic properties

An important branch of the molecular magnetism deals with molecular systems with bulk physical properties, such as long-range magnetic ordering. Molecular compounds with spontaneous magnetization below a critical temperature were reported during the eighties.⁵⁶ These pioneering reports encouraged many research groups in organic, inorganic, or organometallic chemistry to initiate activity on this subject, and many new molecule-based magnets have been designed and characterized. A tentative classification can arise from the chemical nature of the magnetic units involved in these materials— organic- or metal-based systems and mixed organic–inorganic compounds. The field of molecular magnetism is enriched with materials based on several families of magnetic metal complexes, such as the oxamato, oxamido, oxalato-bridged compounds and cyanide-bridged systems. The most extensively used spin carriers are 3*d* transition metal ions. The magnetic interactions between these ions are now well understood and enable the rational synthesis of materials. The heavier homologs from the second and third series have been envisaged only recently for the construction of hetero-bimetallic materials. In 1995 Olivier Kahn wrote a paper reviewing the magnetism of hetero-bimetallic compounds.⁵⁷ An important part of this review was devoted to finite polynuclear compounds, which can be considered as models for the study of exchange interactions. Magnetic ordering is a three dimensional property,

however, and the design of a molecule-based magnet requires control of the molecular architecture in the three directions of space.

1.2.2. Discrete molecules

One of the first high-spin molecules was prepared in 1988. It was a trinuclear linear CuMn₂ species synthesized by using [Cu(pba)]²⁻ as the core and [Mn(Me₆-[14]ane-N₄)]²⁺ as a peripheral complex.⁵⁸ However, no single crystal was obtained, and any structure in agreement with the magnetic properties was proposed for this species. The compound shows ferrimagnetic behavior with an irregular spin state structure resulting from the antiferromagnetic interaction between the peripheral Mn ions ($S_{\text{Mn}} = 5/2$) and the middle Cu ion ($S_{\text{Cu}} = 1/2$). The low-temperature magnetic behavior is the characteristic of a high-spin ground state equal to $S = 9/2$. Efforts were later made to obtain structural information for such species.⁵⁹ In this context it can be mentioned that Liao's group succeeded in isolating crystals of binuclear and trinuclear compounds with the Ni^{II} ion ($S_{\text{Ni}} = 1$).⁶⁰ These compounds were obtained by the reaction of CuL²⁻ (L = pba, pbaOH and opba) with NiL²⁺, L being tetraamine ligands, final compounds having formula (L Ni)CuL or (L Ni)₂CuL²⁺. These compounds have been magnetically characterized, and it is confirmed that they possess the expected ferrimagnetic behavior with an $S = 3/2$ ground state with a zero-field splitting. Another interesting example that can be cited here is by Ouahab and Kahn with the opbaCl₂ ligand and its Cu^{II} complex.⁶¹ The reaction of the Cu^{II} precursor with ethylenediamine, en, and Mn^{II} in the solvent DMSO led to an unprecedented trinuclear species Mn^{III}Cu^{II}Mn^{III}.

1.2.3. The importance of spin-nano magnets

The data storage industry is fast approaching the limit of the traditional bulk magnets used in computer hard drives. The ferromagnets that have been employed since IBM introduced the technology in 1953 are fundamentally limited, since the data becomes more volatile as the bit is made smaller. This has been termed the super-paramagnetic limit.⁶² Increasingly sophisticated methods are being used to dodge this limit, such as perpendicular storage⁶³ or using different substrates in disk construction. The issue is that as the domain of these bulk ferromagnets decreases, the potential for spontaneous demagnetisation (randomisation of spin orientation) becomes greater. Currently the bulk magnetic domain (which is made out of many small magnetic grains) is around the order of 100 nm.⁶⁴ Instead of continuing to evade this limit, it is possible to take a "bottom up" chemical approach for the construction of the magnetic bit. The ultimate goal of the nano-magnet is to create a molecule that is stable at room temperature, that retains its spin orientation for long periods and that can be easily read or manipulated. If this can be achieved then a new age of quantum storage is possible.

1.2.4. The single molecule magnet and the potential of quantum storage

The single molecule magnet (SMM) is one approach to create a molecular bit.⁶⁵ Each individual molecule is used to store data as the orientation of its electronic spin. The critical equation that governs the eligibility of an SMM takes the form

$$E = |D|S^2 \quad (1.1)$$

where E is the energy of the spin reversal barrier, S is the total spin of the system and D is the large component of the magnetic anisotropy. The energy barrier dictates the temperature up to which the spin retains its stability and thus controls the magnetic half-life of a nano-magnet. The issue of constructing large energy barriers is a chemical problem with two avenues to exploit; either the total spin of the system be large or the magnetic anisotropy could be increased. The current experimental trend is to construct ever larger clusters of inorganic molecules that contains multiple spin-unpaired electrons.⁶⁶ To create a molecule with a large paramagnetic ground state there are three main options, namely— (i) the use a hetero-metallic system where the metal spins are unbalanced, (ii) a homo-metallic system that contains an odd number of metal centres or (iii) a spin frustrated system. There is on-going research into the applicability of f -block elements⁶⁷ to attain ever higher ground state spins. A limitation of this approach is becoming apparent although the energy barrier scales as S^2 , the D tensor tends to scale as S^2 and thus renders the barrier increasing with spin of the order of S^0 .⁶⁸ A second factor in the construction of an SMM that must be considered is the magnetic anisotropy, D , which determines the spacing between the various spin states along the energy barrier.

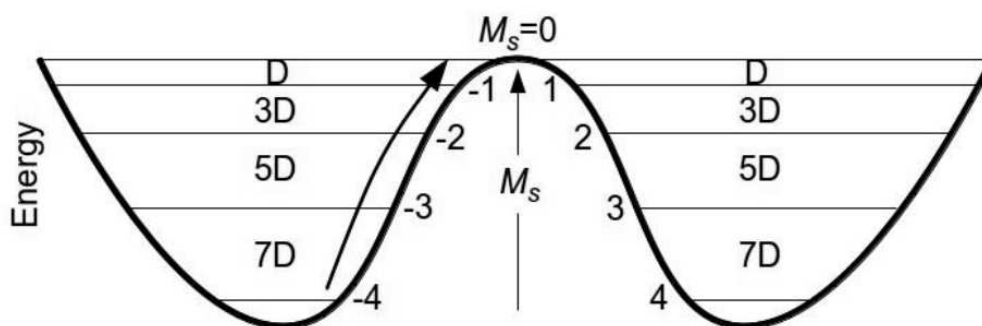


Figure 1.5. Diagram of the SMM energy barrier for an $S = 4$ system.

Here in Figure 1.5, M_s is the projection of spin in the S_z direction (the spin quantization axis). To create an SMM, D must be negative as this guarantees a ground state where the spin is all aligned along S_z and thus has a defined orientation for manipulation. As the molecule is excited and accesses higher lying M_s states, the spin is less orientated along S_z until it reaches the top of the energy barrier where $M_s = 0$ and is no longer orientated along that axis, at this point data would be lost. Nevertheless, a discussion of the quantum tunnelling mechanism is outside the work of this thesis. D is a difficult parameter to control

chemically as in inorganic systems it is dominated by spin-orbit coupling (SOC) and is extremely sensitive to ligand effects.

1.2.5. The role of theory in developing new magnetic molecules

Theoretical chemistry has some clear advantages in elucidating what is needed to create large D values. We are able to break D into its component factors of spin-spin interaction and spin-orbit coupling. Then, we are able to break down the spin-orbit coupling further and analyze the way its components influence its magnitude. Being able to calculate large SMMs is however out of the reach of pure wave-function methods due to their high computational cost; instead we must turn to density-functional theory (DFT), which has a much better scaling factor. Recently, Neese developed new methods of calculating the ZFS in a DFT framework; however it remains unclear if DFT in its current form is able to accurately model the coupling of the excited spin states needed to calculate D . Some analogy can be made to the electronic g-factor which is now readily studied in theory with a good degree of accuracy.⁶⁹ However, this is where the current limit of theoretical chemistry lies as the g-value only involves the coupling of electronic configurations of the same spin and the D value requires the coupling of excited states that can vary from the state of interest by $S \pm 1$. It is not clear that DFT is able to accurately model excited states of this nature as it is a theory of the ground state density. DFT studies so far show qualitative agreement with experiment.⁷⁰ The historic calculations of ZFS were done with ab initio methods.⁷¹

1.3. Objectives of the Thesis

The objective of the present thesis is to study the aromaticity of novel metal based system and the magnetic properties of metallo-organic complexes. The precise objectives of this thesis are defined in the following:

1. To study the aromaticity in metal based system and provide an insight about the onset of magnetism at the expense of aromaticity in such systems.
2. To study the effect of dimensionality on the magnetic exchange interaction of charge transfer transition metal complexes.
3. To study the effect of ligand-field on the magnetic anisotropy of the transition metal complexes.
4. To study the effect of external electric field in tuning the magnetic anisotropy of the metal base complexes.

Every chapter in this thesis is complete by itself; that is, it contains its own introduction, complete list of references, figures, tables, and interim conclusions etc.

1.4. References

1. Hofmann, A. *Proc. Roy. Soc. (London)* **1855**, 8, 1.
2. Kekulé, A. *Bull. Acad. R. Belg.* **1860**, 10, 347.
3. (a) Kekulé, A. *Bull. Soc. Chim. Soc. France*, **1865**, 3, 98; (b) Kekulé, A. *Bull. Acad. R. Belg.*, **1865**, 19, 501; (c) Kekulé, A. *Ann. Chem. Pharm.*, **1866**, 137, 129.
4. Kekulé, A. *Ann. Chem.* **1872**, 162, 77.
5. Erlenmeyer, E. *Ann. Chem. Pharm.* **1866**, 137, 327.
6. Körner, W. G. *Sci. Nat. Econ. Palermo*, **1869**, 5.
7. Dewar, J. *Trans. R. Soc. Edin.*, **1872**, 26, 195.
8. Crocker, E. C. *J. Am. Chem. Soc.* **1922**, 44, 1618.
9. Armit, J. W.; Robinson, R. *J. Chem. Soc.* **1925**, 127, 1604.
10. Hückel, E. *Z. Physik* **1931**, 70, 204.
11. (a) Clar, E. *Tetrahedron* **1959**, 6, 355; (b) Clar, E.; McCallum, A. *Tetrahedron* **1960**, 10, 171.
12. (a) Garratt, P. J. In *Aromaticity*, John Wiley & Sons, Inc, New York, 1986; (b) Minkin, V. I.; Glukhotsev, M. N.; Simkin, B. Y. In *Aromaticity and Antiaromaticity: Electronic and Structural Aspects*, John Wiley & Sons, Inc, New York, 1994; (c) Bickelhaupt, F.; de Wolf, W. H. *Recl. Trav. Chim. Pays-Bas* **1988**, 107, 459; (d) Kraakman, P. A.; Valk, J.-M.; Niederländer, H. A. G.; Brouwer, D. B. E.; Bickelhaupt, F. M.; de Wolf, W. H.; Bickelhaupt, F.; Stam, C. H. *J. Am. Chem. Soc.* **1990**, 112, 6638.
13. (a) Schleyer, P. v. R.; Jiao, H. J. *Pure Appl. Chem.* **1996**, 68, 209; (b) Carey, F. A.; Sundberg, R. J. In *Advanced Organic Chemistry: Structure And Mechanisms (Part A)*, Springer, New York, 2000; (c) Special issue on: Aromaticity, ed. Schleyer, P. v. R. *Chem. Rev.* **2001**, 101.
14. (a) Special issue on: Delocalization—pi and sigma, ed. Gladysz, J. A. *Chem. Rev.* **2005**, 105; (b) Breslow, R. *Acc. Chem. Res.* **1973**, 6, 393; (c) Krygowski, T. M.; Cyranski, M. K.; Czarnocki, Z.; Hafelinger, G.; Katritzky, A. R. *Tetrahedron* **2000**, 56, 1783; (d) Schleyer, P. v. R. *Chem. Rev.* **2001**, 101, 1115; (e) Cyranski, M. K.; Krygowski, T. M.; Katritzky, A. R.; Schleyer, P. v. R. *J. Org. Chem.* **2002**, 67, 1333.
15. (a) Pauling, L. *J. Am. Chem. Soc.* **1926**, 48, 1132; (b) Pauling, L. In *The Nature of the Chemical Bond*, 3rd ed., Cornell University Press: Ithaca, New York, 1960; (c) Hückel, E. *Z. Phys.* **1931**, 70, 204.
16. Goldstein, M. J.; Hoffmann, R. *J. Am. Chem. Soc.* **1971**, 93, 6193.

17. Wörner, H.; Merkt, F. *Angew Chem Int. Ed.* **2006**, *45*, 293.
18. Hirsch, A.; Chen, Z.; Jiao, H. *Angew. Chem. Int. Ed.* **2001**, *40*, 2834.
19. Faraday, M. *Phil trans. R. Soc. Lon.* **1825**, *115*, 440.
20. Kekulé, A. *Bulletin mensuel de la Société Chimique de Paris* **1865**, *3*, 98.
21. Erlenmeyer, E. *Ann.* **1866**, *137*, 327.
22. Crocker, E. *J. Am. Chem. Soc.* **1922**, *44*, 1618.
23. Hückel, E. *Z. Phys.* 1931, *70*, 207; Hückel, E. *Z. Phys.*, **1932**, *76*, 628.
24. Evans, M.; Warhurst, E. *Trans. Faraday Soc.* **1938**, *34*, 614.
25. Calvin, M.; Wilson, K. *J. Am. Chem. Soc.* **1945**, *67*, 2003.
26. Winstein, S.; Kosower, E. *J. Am. Chem. Soc.* **1959**, *81*, 4399.
27. Heilbronner, E. *Tetrahedron Lett.* **1964**, *5*, 1923.
28. Breslow, R. *Acc. Chem. Res.* **1973**, *6*, 393.
29. Osawa, E. *Kagaku (Kyoto)* **1970**, *25*, 854.
30. Clar, E. In *The aromatic sextet*; John Wiley & Sons, 1972.
31. Baird, N. *J. Am. Chem. Soc.* **1972**, *94*, 4941.
32. Aihara, J. *J. Am. Chem. Soc.* **1978**, *100*, 3339.
33. Dewar, M.; Mc.Kee, M. *Pure Appl. Chem.* **1980**, *6*, 1431.
34. Jemmis, E.; Schleyer, P. *J. Am. Chem. Soc.* **1982**, *104*, 4781.
35. Shaik, S.; Hiberty, P. *J. Am. Chem. Soc.* **1985**, *107*, 3089.
36. Kroto, H. *Nature*, **1985**, *318*, 162.
37. Iijima et al. *Nature*, **1991**, 354.
38. Li, X.; Kuznetsov, A. Zhang, H. Boldyrev, A. Wang, L. *Science*, **2001**, *291*, 859.
39. Wannare, C.; Corminboeuf, C.; Wang, Z.; Wodrich, M. King, R. Schleyer, P. *J. Am. Chem. Soc.* **2005**, *127*, 5701.
40. Zhai, H.; Averkeiv, B.; Zubarev, D.; Wang, L.; Boldyrev, A. *Angew. Chem. Int. Ed.* **2007**, *119*, 4355.
41. Tsipis, A.; Kefalidis, C.; Tsipis, C. *J. Am. Chem. Soc.*, **2008**, *130*, 9144.
42. Masui, H. *Coord. Chem. Rev.* **2001**, *219*, 957.

43. (a) Dewar, M. J. S.; McKee, M. L. *Pure Appl. Chem.* **1980**, *52*, 1431. (b) Dewar, M. J. S. *J. Am. Chem. Soc.* **1984**, *106*, 669. (c) Cremer, D.; Gauss, J. *J. Am. Chem. Soc.*, **1986**, *108*, 7467.
44. (a) Bühl, M.; Hirsch, A. *Chem. Rev.* **2001**, *101*, 1153. (b) Chen, Z.F.; King, R. *Chem. Rev.* **2005**, *105*, 3613.
45. Kuznetsov, A. E.; Boldyrev, A. I.; Li, X.; Wang, L. S. *J. Am. Chem. Soc.* **2001**, *123*, 8825.
46. Kuznetsov, A. E.; Birch, K. A.; Boldyrev, A. I.; Li, X.; Zhai, H. J.; Wang, L. S. *Science*, **2003**, *300*, 622.
47. Yong, L.; Wu, S. D.; Chi, X. X. *Int. J. Quant. Chem.*, **2007**, *107*, 722.
48. Chi, X. X. ; Liu, Y. *Int. J. Quant. Chem.*, **2007**, *107*, 1886.
49. Yong, L.; Chi, X. X. *J. Mol. Struct.*, **2007**, *818*, 93.
50. Averkiev, B. B.; Boldyrev, A. I. *J. Phys. Chem. A*, **2007**, *111*, 12864.
51. Wang, B.; Zhai, H. J.; Huang X.; Wang, L. S. *J. Phys. Chem. A*, **2008**, *112*, 10962.
52. Tanaka, H.; Neukemans, S.; Janssens, E.; Silverans, R. E.; Lievens, P. *J. Am. Chem. Soc.*, **2003**, *125*, 2862.
53. (a) Holtzl, T.; Janssens, E.; Veldeman, N.; Veszprem, T.; Lievens, P.; Nguyen, M. T. *Chem. Phys. Chem.*, **2008**, *9*, 833. (b) Holtzl, T.; Veldeman, N.; Veszpremi, T.; Lievens, P.; Nguyen, M. T. *Chem. Phys. Lett.*, **2009**, *469*, 304.
54. Wannere, C. S.; Corminboeuf, C.; Wang, Z. X.; Wodrich, M. D.; King, R. B.; Schleyer, P. v. R. *J. Am. Chem. Soc.*, **2005**, *127*, 5701.
55. Lin, Y. C.; Sundholm, D.; Juselius, J.; Cui, L. F.; Li, X.; Zhai, H. J.; Wang, L. S. *J. Phys. Chem. A*, **2006**, *110*, 4244.
56. (a) Miller, J. S.; Calabrese, J. C.; Rommelman, H.; Chittipedi, S. R.; Zang, J. H.; Reiff, W. M.; Epstein, A. J. *J. Am. Chem. Soc.* **1987**, *109*, 769; (b) Kahn, O.; Pei, Y.; Verdager, M.; Renard, J. P.; Sletten, J. *J. Am. Chem. Soc.* **1988**, *110*, 782.
57. Kahn, O. *Adv. Inorg. Chem.* **1995**, *43*, 179.
58. Pei, Y.; Journaux, Y.; Kahn, O. *Inorg. Chem.* **1988**, *27*, 399.
59. Mallah, T.; Marvilliers, A. In *Magnetism: From Molecules to Materials, Vol. 2*, Miller, J. S. Drillon M. (Eds.) Wiley-VCH, Weinheim 2001, p. 189.
60. Gao, E.-Q.; Tang, J.-K.; Liao, D.-Z.; Jiang, Z.-H.; Yan, S.-P.; Wang, G.-L. *Inorg. Chem.* **2001**, *40*, 3134.

- 61.** Fettouhi, M.;Ouahab, L.;Boukhari, A.;Cador, O.;Mathoniere, C.;Kahn, O. *Inorg. Chem.* **1996**, *35*, 4932.
- 62.** (a) Schiff,H.;Kirsensen, A. Handbook of Nanotechnology, B. Bhushan, Springer, 3rd ed. 2007, 264;(b) Richter, H. J. *J. Magn. Magn. Mater.***2009**, *321*, 467.
- 63.** Piramanayagam, S. N. *J. Appl. Phys.*, **2007**, *102*, 011301.
- 64.** (a) Wolf, E. L.; Medikonda, M. In *Understanding the Nanotechnology Revolution*, Wiley, New York, 2012, 181; (b) Wolf, E. L. In *Nanophysics and Nanotechnology*, Wiley, New York, 2nd ed, 2006, 11.
- 65.** (a) Friedman, J. R.;Sarachik, M. P. *Annu. Rev. Condens. Matter. Phys.*, **2010**, *1*, 109; (b) Christou, G.;Gatteschi, D.;Hendrickson, D. N.;Sessoli., R. *MRS Bulletin*, **2000**, *25*, 66.
- 66.** Soler, M.;Wernsdorfer, W.;Folting, K.;Pink, M.;Christou, G. *J. Am. Chem. Soc.*, **2004**, *126*, 2156.
- 67.** (a) Lin, P.; Burchell, T. J.; Ungur, L.; Chibotaru, L. F.; Wernsdorfer, W.; Murugesu, M. *Angew. Chem. Int. Ed.*, **2009**, *48*, 9489;(b) Woodruff, D. N.; Winpenny, R. E. P.; Layfield, R. A. *Chem. Rev.*, **2013**, 5110.
- 68.** (a) Waldmann, O. *Inorg. Chem.*, **2007**,*46*, 10035;(b) Neese, F.; Pantazis, D. A. *Faraday Discuss.* **2011**, *148*, 229.
- 69.** Neese, F. *J. Chem. Phys.***2001**, *115*, 11080.
- 70.** Cirera, J.; Ruiz, E.; Alvarez, S.; Neese, F.; Kortus, J. *Chem. Eur. J.*, **2009**, *15*, 4078.
- 71.** (a) Lounsbury, J. B. *J. Chem. Phys.*, **1965**, *42*, 1549; (b) Harrison, J. F. *J. Chem. Phys.*, **1971**, *54*, 5413.

CHAPTER 2

Theoretical methods to quantify aromaticity and magnetism

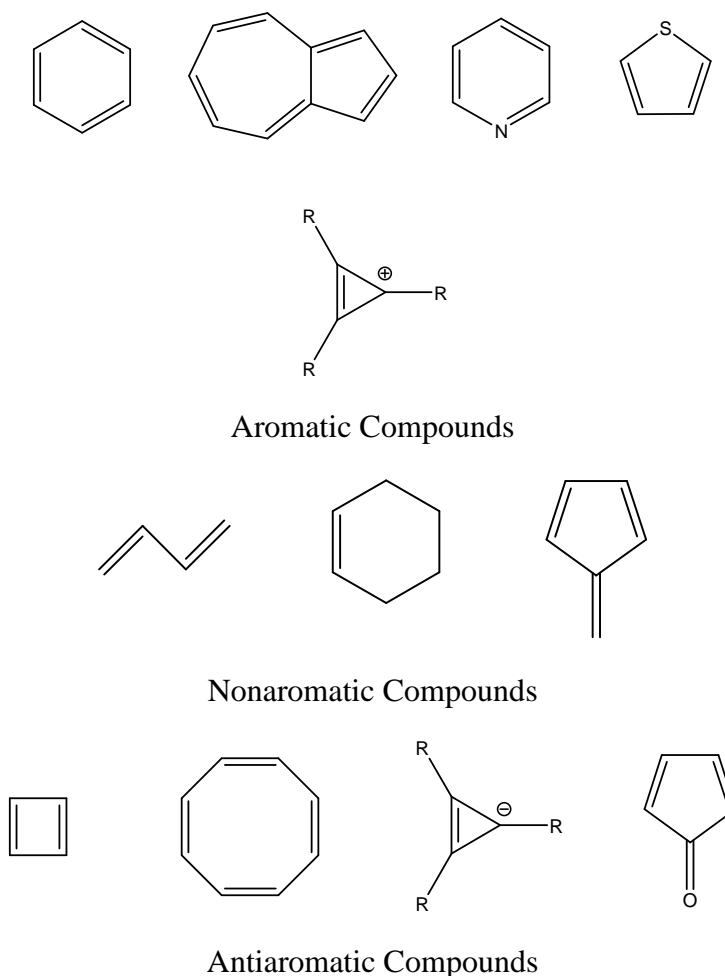
Abstract

The present chapter presents a brief account of the basic theoretical information related to aromaticity, magnetic exchange coupling constant and magnetic anisotropy. The significance of the quantification of aromaticity has been discussed with special emphasis on the fundamental categories based on which the assessment of aromaticity is performed. A short description of the available methods for quantification of aromaticity, which are of subsequent use in this work, is also presented. A brief background for the estimation of magnetic exchange coupling constant has been provided. Two different methods of determination of the magnetic exchange coupling constant (J) is given, namely, the broken symmetry approach and the spin-flip DFT approach. The theoretical approach behind these two methods are discussed elaborately. A short account of the basic theory behind the quantification of magnetic anisotropy is also provided here. There are two popular methods for the quantification of magnetic anisotropy. The Pederson-Khanna (PK) approach and the Neese method for quantification of zero-field splitting (ZFS) parameter D , in connection to the magnetic anisotropy are discussed with proper emphasis on the estimation of the spin-orbit coupling in spin-systems.

2.1 Quantification of Aromaticity

Aromaticity is one of the most pervasive concept in chemistry.¹ Although initially well defined in terms of cyclic electron delocalization in benzene and similar benzenoid rings,² the concept of aromaticity has been extended for many different classes of molecules, making it ambiguous over time. One can come to know about eight different classes of molecules that manifest aromatic property as defined by Minkin et al.,³ in their book “Aromaticity and Antiaromaticity, Electronic and Structural Aspects”, namely, (i) Aromaticity, (ii) Antiaromaticity, (iii) Heteroaromaticity, (iv) Homoaromaticity, (v) σ -aromaticity, (vi) In-plane aromaticity, (vii) Three-dimensional aromaticity and (viii) Spherical aromaticity. Although there are different classes of molecules that manifest aromaticity, there is no definite observable based on which one can classify a molecule as aromatic. The qualitative distinction of cyclic compounds into aromatic, nonaromatic, and antiaromatic (Scheme 2.1), is quite clear. However, it is also well documented that aromaticity is a qualitative as well as a quantitative concept.⁴

Scheme 2.1 Examples of Aromatic, Nonaromatic and Antiaromatic compounds



The features that distinguish an aromatic compound from a nonaromatic compound have been comprehended for a long time as —(1) cyclic compound with a large resonance energy (RE); (2) tendency to react by substitution rather than addition; (3) aromatic sextet and related Hückel rule of $(4n + 2)\pi$ electrons; (5) ability to sustain a diamagnetic ring current. Significant scrutiny of the concept of aromaticity prompts the scientific community for the proposition of some new indices to define aromaticity in a more precise and quantitative manner. Many different quantities have been derived to express the degree of aromaticity in various molecules. The existent aromaticity indices can be divided into a few fundamental categories, such as (i) energetic, (ii) structural, (iii) magnetic and (iv) electronic criteria. Also the techniques that are applied to obtain quantitative measures of aromaticity may be divided into four main groups:⁵ (1) measurements of the energy (heat of formation) of aromatic compounds and comparison of this with the estimated heat of formation of a hypothetical model analogue lacking cyclic conjugation; (2) measurement of the geometries of aromatic compounds and their comparison with geometries of nonaromatic analogues either measured or estimated; (3) measurement of magnetic properties of aromatic compounds and comparison with those expected for nonaromatic analogues; (4) quantum chemical calculations corresponding to all of these experimental approaches. It has now been convenient to choose physical methods over chemical techniques to provide a quantitative measure of aromaticity.

Depending on the nature of measured parameters and the physical state of the system when the measurement is being performed, the estimation of aromaticity encounters many inherent inconsistencies and discrepancies. Not only experimental techniques, theoretical approximations are also not free from inconsistencies and lead aromaticity as a contentious subject. These problems render the measurement, and indeed the definition of aromaticity to be multifaceted. Here we present an unbiased overview of some of the multifarious measures of aromaticity.⁴

2.1.1 Aromaticity indices

The multidimensional nature of aromaticity led scientists to quantify the effect that aromaticity exerts on different structural, magnetic, and electronic properties. There is a plethora of different aromaticity indices which measures the aromaticity of different class of aromatic compounds. The indices that have been used in this thesis are briefly discussed in the following subsections.

2.1.1.1. Nucleus Independent Chemical Shifts (NICS)

Nucleus independent chemical shifts (NICS) is a aromaticity index based on magnetic property manifested by an aromatic molecule.⁶ NICS index is calculated by taking the negative of the absolute magnetic shielding tensor of a dummy atom placed at the geometric center of an aromatic ring, the so-called NICS(0) index. Firstly, only this index was applied to estimate aromaticity in a molecule. The problem with this index was the large effect of the π -orbitals on the NICS(0) value. We are also concerned to estimate aromaticity that arises due to the participation of π -orbitals in the molecule. Hence, the dummy atom was later

moved to 1 Å above the molecular plane (NICS(1)), thus assessing the influence of the π -framework of the molecule (Figure 2.1).⁷ Negative NICS values indicate a diatropic ring current (aromaticity) while positive NICS values indicate a paratropic ring current (antiaromaticity). The isotropic chemical shift is represented as the average of the xx , yy , and zz tensor components. As the xy plane conventionally taken to be the molecular plane, and the magnetic field is applied along the z -direction, the zz tensor (out-of-plane) component reveals the most relevant information about aromaticity.⁸ The NICS index which only regards the zz component of the isotropic chemical shift tensor is designated as NICS(1)_{zz}, and is one of the most useful and reliable measures of aromaticity now a days.

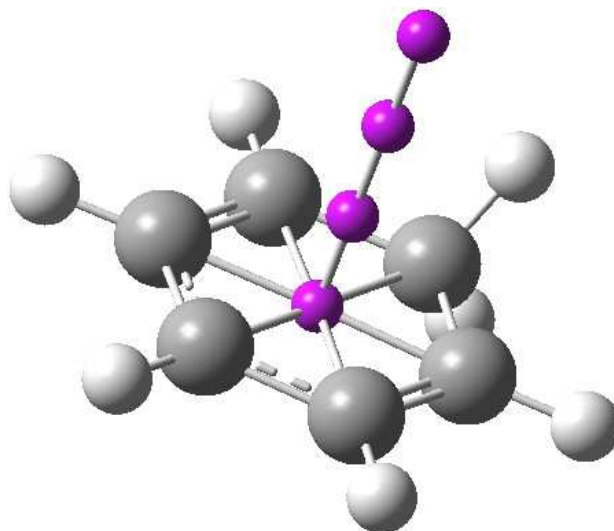


Figure 2.1. The scheme of calculation of NICS and NICS-scan by measuring the magnetic shielding at the ring centre and points above the ring plane.

2.1.1.2. NICS scan

Although NICS is widely accepted measure of aromaticity, one disadvantage of this index is a matter of concern, and that is only one point in space is regarded ofr the evaluation of NICS. Stanger introduced an alternative index based on the NICS index to alleviate the problems of using the NICS(0) and NICS(1) single point approaches.⁹ In this NICS-scan method the NICS values are calculated at each 0.1Å increment from the ring centre upto 5 Å above the ring (Figure 2.1). The plots of NICS-scan for aromatic compounds show deep minima for both the out-of-plane component and the overall isotropic chemical shift. On the other hand, antiaromatic compounds display a highly positive out-of-plane component close to the ring centre and then decrease to zero with increasing distance.

2.1.1.3. Electron Localization Function (ELF)

As electron delocalization is assessed as the main crux in the phenomenon of aromaticity, it is obvious that the aromaticity indices which reflect the electron delocalization are considered as the most appropriate measure.¹⁰ Hence another method to trace aromaticity is explored as the Electron Localization Function (ELF) based on the properties of the

electron localization function. The electron localization function is viewed as a mathematical description of the valence shell electron-pair repulsion (VSEPR) theory as presented in 1990 by Becke and Edgecombe.¹¹ The ELF and is defined as

$$ELF(r) = [1 + (\chi(r))^2]^{-1} = \left[1 + \left[\frac{T(r)}{T_h(r)} \right]^2 \right]^{-1} \quad (2.1)$$

where $\chi(r)$ is a dimensionless localization index referenced to the uniform electron gas. $T(r)$ is the local excess of kinetic energy due to the Pauli repulsion, and $T_h(r)$ is the Tomas-Fermi kinetic energy of the uniform electron gas.¹² The ELF can have values between 1 and 0. ELF attains values close to 1 where electrons are alone or paired with opposite spins, while in regions between the electron pairs ELF accomplish a smaller value due to Pauli repulsion.¹² The π -component of the electron localization function (ELF_π) is generally used as an indicator of aromaticity.

2.1.1.4. Multi-centre electron delocalization index

Electronic delocalization based descriptors of aromaticity are now-a-days being considered to play an important role in the characterization of aromaticity. Among these tools, the multicenter indices are the most versatile and are widely used to characterize different classes of aromaticity. The I_{ring} is the first among these descriptors, defined by Giambiagi et al.¹³ and is estimated as

$$I_{ring}(A) = \sum_{i_1, i_2, \dots, i_N} n_{i_1} \dots n_{i_N} S_{i_1 i_2}(A) S_{i_2 i_3}(A) \dots S_{i_N i_1}(A) \quad (2.2)$$

where n_i is the occupancy of i -th MO and $S_{ij}(A)$ is the overlap between MOs i and j within the molecular space assigned to atom A . The I_{ring} index measures the electron delocalization along the molecular ring.¹⁴ The multi-center index (MCI) is an improvement over I_{ring} that includes the delocalization across a ring.¹⁵ MCI is defined as the sum of all the I_{ring} values resulting from the permutations of indices A_1, A_2, \dots, A_N

$$MCI(A) = \frac{1}{2N} \sum_{P(A)} I_{ring}(A). \quad (2.3)$$

Here $P(A)$ is a permutation operator which interchanges the atomic labels A_1, A_2, \dots, A_N to generate up to the $N!$ permutations of the elements in the string A .¹⁶ A more positive MCI value indicates the ring to be more aromatic.

2.2. Estimation of Magnetic Exchange Coupling Constant (J)

Two electrons with parallel or antiparallel spins behave differently, even though the fundamental interaction is the same. If unpaired electrons are present on the metal centres of an oligonuclear transition metal complex, the spins of these electrons can couple either in parallel (ferromagnetic) or antiparallel fashion (antiferromagnetic) as is depicted in Figure 2.2. It is obvious that the atomic spin quantum numbers are no longer valid to describe the coupled spin system involving interaction between two spin-centres. A total spin quantum number S is now required. Hence, a proper description of the simplest system of one unpaired electron at each of the spin containing centres (e. g. Cu^{II}_2), would require S to be either 0 for the antiferromagnetically coupled state or 1 for the ferromagnetically coupled state.

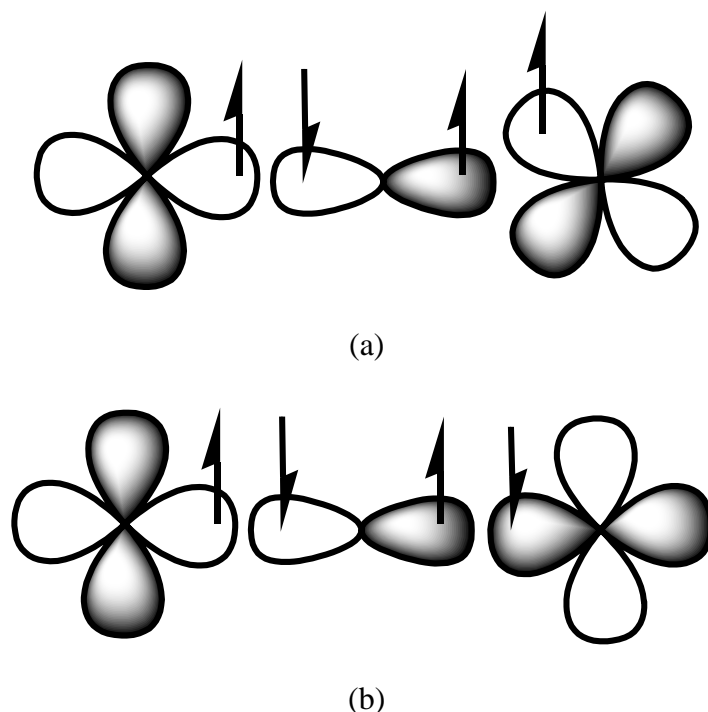


Figure 2.2. Ferromagnetic (a) and antiferromagnetic (b) coupling of two metal centers via σ -bonding.

The energy difference between these two states is described by the exchange coupling constant J . Negative value of J denotes an antiferromagnetic ground state while a positive value indicates a ferromagnetic ground state.¹⁷ The energy and the magnetic properties of such dinuclear systems can be described by the Heisenberg-Dirac-van Vleck (HDvV) Hamiltonian, popularly known as “Spin-Hamiltonian”

$$H = -2J_{ij}\hat{S}_i \cdot \hat{S}_j \quad (2.4)$$

where, \hat{S}_i and \hat{S}_j are the spin angular momentum operators on magnetic sites i and j and J_{ij} is the exchange coupling constant between them.¹⁸

2.2.1. Broken symmetry approach

Open-shell transition metal ions have several accessible electronic states which give rise to a number of different spin-states. Although the high spin state for a dinuclear system ($\uparrow\uparrow$) can easily be described in the density functional theory framework, the description of the low-spin state ($\uparrow\downarrow - \downarrow\uparrow$) requires multiple determinants and this is not possible in DFT.¹⁹ As a solution to this problem, one can guess the true low-spin state as a single determinant wave function ($\uparrow\downarrow$ or $\downarrow\uparrow$) and subsequently re-optimize the orbitals applying variational principle.²⁰ This method was first coined by Noodleman and is popularly known as the broken symmetry method.²¹ The optimized wave function is the broken symmetry solution to the problem. This method reproduces the correct charge density for the molecule, but as an artifact the spin density produced is incorrect. A broken symmetry solution for the simplest Cu^{II}_2 benchmark system should produce a single spin-up density at one Cu^{II} centre and single spin-down density at the other Cu^{II} atom. On the other hand, the true spin density of the low-spin state should be zero throughout the whole molecule. Hence, this is clearly not the case for the broken symmetry solution (Figure 2.3).

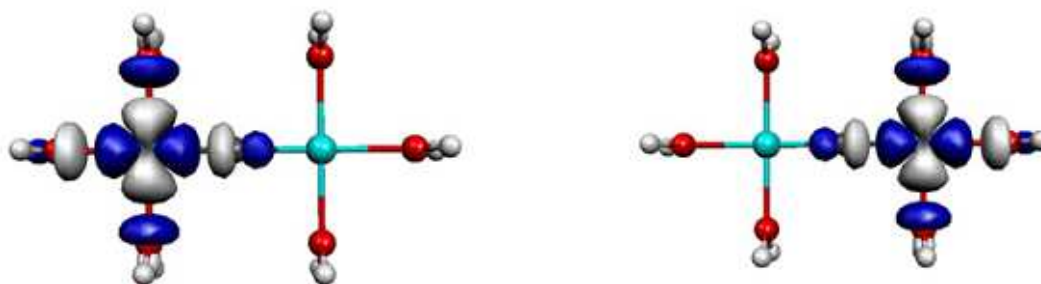


Figure 2.3. Spin densities of the broken symmetry solution for the Cu^{II}_2 benchmark system. The two uncoupled spins are in the $d_{x^2-y^2}$ orbitals of the two metal centers. Some spin density is also delocalized over the bridging atoms.

Once the correct charge density and thus the correct energy of the high- and low-spin states of the dinuclear complex are known, the exchange coupling constant between metal centres 1 and 2 can be computed with the help of the spin Hamiltonian (eqn. 2.4). Given the relation in eqn. 2.5 below, where \hat{S} is the total spin operator and \hat{S}_1, \hat{S}_2 are the spin operators for the individual magnetic centres

$$\hat{S}^2 = \hat{S}_1^2 + \hat{S}_2^2 + 2\hat{S}_1\hat{S}_2 \quad (2.5)$$

the HDvV Hamiltonian now becomes

$$\hat{H}_{HDvV} = -J(\hat{S}^2 - \hat{S}_1^2 - \hat{S}_2^2) \quad (2.6)$$

The energy expectation values of the high- and low-spin states can be calculated, assuming the wave functions are eigen functions of \hat{S}_1^2 and \hat{S}_2^2 , as

$$E_{HS} = -J[\langle \hat{S}^2 \rangle_{HS} - S_1(S_1 + 1) - S_2(S_2 + 1)] \quad (2.7)$$

$$E_{BS} = -J[\langle \hat{S}^2 \rangle_{BS} - S_1(S_1 + 1) - S_2(S_2 + 1)] \quad (2.8)$$

where $\langle \hat{S}^2 \rangle_{HS}$ and $\langle \hat{S}^2 \rangle_{BS}$ are the spin expectation values of the high- and low-spin states respectively. From eqns 2.7 and 2.8 the magnetic exchange coupling constant J comes out as

$$J = -\frac{E_{HS} - E_{BS}}{\langle \hat{S}^2 \rangle_{HS} - \langle \hat{S}^2 \rangle_{BS}} \quad (2.9)$$

Eqn. 2.9 represents the interpolative broken symmetry solution,²² as proposed by Yamaguchi et al.²³ In the extreme cases of an uncoupled system eqn 2.9 reduces to the so called spin-projected equation

$$J = -\frac{E_{HS} - E_{BS}}{S_{\max}^2}. \quad (2.10)$$

The spin-projected formalism has been directly implied by the treatment of Noodleman for the broken symmetry problem.²¹ On the other hand, for a fully coupled low-spin configuration, eqn. 2.9 reduces to the spin-unprojected equation

$$J = -\frac{E_{HS} - E_{BS}}{S_{\max}(S_{\max} + 1)}. \quad (2.11)$$

This approach was developed by Ruiz et al.²³ The general applicability of the expression of J given by Yamaguchi (eqn 2.9) can be understood through the following dependence of $\langle \hat{S}^2 \rangle$ of a Slater determinant on the overlap of magnetic orbitals.²⁴

$$\langle \hat{S}^2 \rangle = M_S(M_S + 1) + N_\beta - \sum_{i,j}^{N_\alpha, N_\beta} (O_{ij}^{\alpha\beta})^2 \quad (2.12)$$

where, $O_{ij}^{\alpha\beta}$ is the overlap between the spin orbitals referring to opposite spins. In case of the overlap among all pairs of α and β orbitals, the sum in eqn 2.12 is reduced to a summation over N^β with individual terms all equal to 1. Therefore, the sum equals N^β and the total spin expectation value indicates a pure spin state with $\langle S^2 \rangle_{BS} = 0$, and the denominator in eqn 2.9 transforms to $S_{\max}(S_{\max} + 1)$ which resembles eqn 2.11.

2.2.2. Spin-flip DFT approach

The exchange coupling constants J is related to the energy gap between the high- and low-spin states of a system (eqns 2.7 and 2.8). Hence, J can be calculated once the energies of two adjacent true spin states are known. Unfortunately, the true spin states are often multi-determinantal in nature and are not properly describable by single-determinantal ordinary KSDFT method as is discussed in the previous section. Thus a new methodology can be adopted based on the creation of single-determinantal micro-states by single electron spin-flip excitations from the high-spin reference state, which has a single-determinantal wave function. This methodology is known as spin-flip constricted variational DFT (SF-CV-DFT) formalism. The energy of the resulting single-determinantal micro-states are calculated relative to the high-spin reference as

$$A_{\bar{a}i, \bar{a}i} = \langle \psi_{i \rightarrow \bar{a}} | F^{KS} | \psi_{i \rightarrow \bar{a}} \rangle = \varepsilon_{\bar{a}} - \varepsilon_i + K_{\bar{a}i, \bar{a}i}^{KS} \quad (2.13)$$

where \bar{a} is a spin orbital of beta spin. The $K_{\bar{a}i, \bar{a}i}^{KS}$ terms for spin-flip excitations can be derived within the non-collinear DFT formalism.²⁵ The single-determinantal micro-states $\psi_{i \rightarrow \bar{a}}$ are eigenfunctions of the \hat{S}_z operator, but not of the \hat{S}^2 operator. However, the symmetrized linear combinations of the single-determinants $\psi_{i \rightarrow \bar{a}}$

$$\psi_\gamma = \sum_{\bar{a}i} C_{\bar{a}i, \gamma} \psi_{i \rightarrow \bar{a}} \quad (2.14)$$

are eigenfunctions of both \hat{S}_z and \hat{S}^2 , where the constants $C_{\bar{a}i, \gamma}$ are determined by symmetry only. The interaction matrix between the symmetrized spin micro-states ψ_γ can now be calculated as

$$A_{\gamma\tau} = \langle \psi_\gamma | F^{KS} | \psi_\tau \rangle \quad (2.15)$$

in terms of the corresponding matrix elements between single determinantal micro-states $\Psi_{i \rightarrow \bar{a}}$

$$A_{\bar{a}i, \bar{b}j} = \langle \Psi_{i \rightarrow \bar{a}} | F^{KS} | \Psi_{j \rightarrow \bar{b}} \rangle = K_{\bar{a}i, \bar{b}j}^{KS} + (\varepsilon_{\bar{a}} - \varepsilon_i) \delta_{ab} \delta_{ij}. \quad (2.16)$$

The state functions and energies can be calculated from orbitals optimized for the high-spin reference state. The energy difference ΔE is thus calculated on the basis of the so called unrestricted SF-CV-DFT scheme, which is directly related to the exchange coupling constant J .^{25a} However, this method suffers from some unavoidable spin contamination.

2.3. Quantification of Magnetic Anisotropy

The genesis of magnetic anisotropy in a molecule is the existence of two ground states of magnetization $+M_S$ and $-M_S$ separated by an energy barrier (U). Reorientation of spin in the magnetic molecules requires the energy U of amount $|D|S^2$ for molecules with integer spins and $|D|(S^2 - 1/4)$ for molecules with half integer spins, where D is the zero-field splitting (ZFS) parameter and S is the ground-state spin. ZFS is known to arise from the spin-orbit coupling (SOC) and the spin-spin coupling (SSC) predominantly.²⁶ The spin-orbit coupling interaction is generally described by the following Hamiltonian

$$\hat{H}_{SOC} = \lambda \hat{L} \cdot \hat{S} \quad (2.17)$$

where λ is the polyelectronic spin-orbit coupling constant and \hat{L} and \hat{S} refer to the orbital momentum and spin operators respectively. The basis for this Hamiltonian are $|L, M_L, S, M_{S_i}\rangle$ configurations belonging to the free-ion ground state.²⁷ In the regular DFT method, the SOC effects are included approximately by perturbation theory.

2.3.1. Pederson-Khanna (PK) method

The determination of the spin-orbit coupling with the help of eqn 2.17 requires that we take into account the electric field observed by the moving electrons. In the classical explanation, an electron moving with velocity v in an external electric field (E), experiences a magnetic field $v \times E/c$. A corresponding quantum-mechanical operator within a Hartree approximation would include $E = -\nabla\Phi(r)$, with Φ the Coulomb potential. Accordingly the velocity (v) is replaced by the momentum operator p and considering the spin of the electron, the interaction energy is given by

$$U = -\frac{1}{2c^2} L \cdot S \times \nabla \phi(r) \quad (2.18)$$

This is true only in the spherically symmetric potential. The interaction energy matrix elements is evaluated with single-electron wave functions, $\psi_{is} = \sum_{j\sigma} C_{j\sigma}^{is} \phi_j(r) \chi_\sigma$.²⁸ The interaction energy matrix thus takes the form

$$U_{j,\sigma,k,\sigma'} = \langle \phi_j \chi_\sigma | U | \phi_k \chi_{\sigma'} \rangle \quad (2.19)$$

The second-order correction to the total energy is then represented as

$$A_2 = \sum_{\sigma\sigma'} \sum_{ij} M_{ij}^{\sigma\sigma'} S_i^{\sigma\sigma'} S_j^{\sigma'\sigma} \quad (2.20)$$

where the matrix elements $M_{ij}^{\sigma\sigma'}$ are

$$M_{ij}^{\sigma\sigma'} = - \sum_{k,l} \frac{\langle \phi_{l\sigma} | U_i | \phi_{k\sigma'} \rangle \langle \phi_{k\sigma'} | U_j | \phi_{l\sigma} \rangle}{\epsilon_{l\sigma} - \epsilon_{k\sigma'}} \quad (2.21)$$

and

$$S_i^{\sigma\sigma'} = \langle \chi^\sigma | S_i | \chi^{\sigma'} \rangle \quad (2.22)$$

where χ^σ and $\chi^{\sigma'}$ are the spinors, $\phi_{l\sigma}$ and $\phi_{k\sigma'}$ are occupied and unoccupied orbitals with corresponding energies $\epsilon_{l\sigma}$ and $\epsilon_{k\sigma'}$, respectively. The second-order shift in energy can be represented in terms of anisotropy tensors as

$$\Delta_2 = \sum_{xy} \gamma_{xy} \langle S_x \rangle \langle S_y \rangle \quad (2.23)$$

After proper choice of co-ordinate system and diagonalizing the anisotropy tensor γ , eqn. 2.23 takes the form

$$\begin{aligned} \Delta_2 = & \frac{1}{3} (\gamma_{xx} + \gamma_{yy} + \gamma_{zz}) S(S+1) \\ & + \frac{1}{3} \left[\gamma_{zz} - \frac{1}{2} (\gamma_{xx} + \gamma_{yy}) \right] [3S_z^2 - S(S+1)] \\ & + \frac{1}{2} (\gamma_{xx} - \gamma_{yy}) (S_x^2 - S_y^2) \end{aligned} \quad (2.24)$$

Parameterization of the anisotropy tensor components (γ_{xx} , γ_{yy} , γ_{zz}) with D and E , which are the axial and the rhombic ZFS parameters, respectively, one can get the final simplified expression

$$H = DS_z^2 + E(S_x^2 - S_y^2) \quad (2.25)$$

In chapters 5 and 6 we have used this technique for ZFS computations.

2.3.2. The Neese technique

As is discussed in the previous sections, the SOC is described in the second-order in perturbation theory. The SOC operator can be approximated by an effective one electron operator $\hat{H}^{SOC} = \sum_i \hat{h}_i^{SOC} \hat{s}_i$. Here, \hat{h}_i^{SOC} can be represented as²⁹

$$h_i^{SOC}(\mu) = \sum_A \xi(r_{iA}) l_i^A(\mu) \quad (2.26)$$

where $l_i^A(\mu)$ is the μ th component of the orbital angular momentum operator relative to centre A and $\xi(r_{iA})$ is a suitable radial operator, i.e.

$$\xi(r_{iA}) = \frac{\alpha^2}{2} \frac{Z_A^{eff}}{|\vec{r}_i - \vec{R}_A|^3} \quad (2.27)$$

Here, Z_A^{eff} is an effective charge for center A situated at point \vec{R}_A and \vec{r}_i is the position operator of the i th electron. Neese et al. has prescribed sum-over state equations for components of the ZFS tensor in the second order contribution to SOC with given by³⁰

$$D_{KL}^{SOC-(0)} = -\frac{1}{S^2} \sum_{b(S_b=S)} \Delta_b^{-1} \langle 0^{SS} | \sum_i \hat{h}_i^{K;SOC} \hat{s}_{i,0} | b^{SS} \rangle \times \langle b^{SS} | \sum_i \hat{h}_i^{L;SOC} \hat{s}_{i,0} | 0^{SS} \rangle \quad (2.28)$$

$$D_{KL}^{SOC-(-1)} = -\frac{1}{S(2S-1)} \sum_{b(S_b=S-1)} \Delta_b^{-1} \langle 0^{SS} | \sum_i \hat{h}_i^{K;SOC} \hat{s}_{i,+1} | b^{S-1S-1} \rangle \times \langle b^{S-1S-1} | \sum_i \hat{h}_i^{L;SOC} \hat{s}_{i,-1} | 0^{SS} \rangle \quad (2.29)$$

$$D_{KL}^{SOC-(+1)} = -\frac{1}{(S+1)(2S+1)} \sum_{b(S_b=S+1)} \Delta_b^{-1} \langle 0^{SS} | \sum_i \hat{h}_i^{K;SOC} \hat{s}_{i,-1} | b^{S+1S+1} \rangle \times \langle b^{S+1S+1} | \sum_i \hat{h}_i^{L;SOC} \hat{s}_{i,+1} | 0^{SS} \rangle \quad (2.30)$$

Here the one-electron spin operator for electron i is written in terms of spherical vector operator components $\hat{s}_{i,m}$ with $m = 0, \pm 1$ and $\Delta_b = E_b - E_0$ is the excitation energy.³¹ After inclusion of proper prefactors for different spin excitations, the final form can be given as³²

$$D_{K,L}^0 = \frac{1}{4S^2} \sum_{\mu\nu} \langle \mu | h_{k,so} | \nu \rangle \left(\sum_{i_\alpha, a_\alpha} U_{a_\alpha i_\alpha}^{L;0} c_{\mu i}^\alpha c_{\mu a}^\alpha + \sum_{i_\alpha, a_\beta} U_{a_\beta i_\beta}^{L;0} c_{\mu i}^\beta c_{\mu a}^\beta \right) \quad (2.31)$$

$$D_{K,L}^{-1} = \frac{1}{2S(2S-1)} \sum_{\mu\nu} \langle \mu | h_{k,so} | \nu \rangle \left(\sum_{i_\alpha, a_\beta} U_{a_\alpha i_\alpha}^{L;-1} c_{\mu i}^\alpha c_{\mu a}^\beta + \sum_{i_\beta, a_\alpha} U_{a_\alpha i_\beta}^{L;-1} c_{\mu i}^\beta c_{\mu a}^\alpha \right) \quad (2.32)$$

$$D_{K,L}^{+1} = \frac{1}{2(S+1)(2S+1)} \sum_{\mu\nu} \langle \mu | h_{k,so} | \nu \rangle \left(\sum_{i_\alpha, a_\beta} U_{a_\beta i_\alpha}^{L;+1} c_{\mu i}^\alpha c_{\mu a}^\beta + \sum_{i_\beta, a_\alpha} U_{a_\alpha i_\beta}^{L;+1} c_{\mu i}^\beta c_{\mu a}^\alpha \right) \quad (2.33)$$

It is noteworthy that these coupled-perturbed CP equations are free from any contribution due to the Coulomb potential or any other local potential such as the exchange-correlation potential in DFT.

2.4. References

1. (a) Smith, M. B.; March, J. In *March's Advanced Organic Chemistry: Reactions, Mechanisms and Structure*, 5th ed.; John Wiley and Sons, New York, 2001; (b) Minkin, V.; Glukhovtsev, M.; Simkin, B. In *Aromaticity and Antiaromaticity*; Wiley Interscience, New York, 1994; (c) Schleyer, P. *Chem. Rev.* **2001**, *101*, 1115; (d) Schleyer, P. *Chem. Rev.* **2005**, *105*, 3433.
2. (a) Cremer, D. *Tetrahedron* **1988**, *44*, 7427; (b) Schleyer, P. v. R.; Jiao, H. *Pure Appl. Chem.* **1996**, *68*, 209; (c) Kekule, A. In *Lehrbuch der Organischen Chemie, Zweiter Band*; Ferdinand Enke Verlag, Erlangen, 1866.
3. Minkin, V.; Glukhovtsev, M.; Simkin, B. In *Aromaticity and Antiaromaticity*; Wiley Interscience, New York, 1994.
4. Katritzky, A. R.; Jug, K.; Oniciu, D. C. *Chem. Rev.* **2001**, *101*, 1421.
5. (a) Simkin, B. Y.; Minkin, V. I.; Glukhovtsev, M. N. *Adv. Heterocycl. Chem.* **1993**, *56*, 303; (b) Krygowski, T. M.; Cyranski, M. K.; Czarnocki, Z.; Hafelinger, G.; Katritzky, A. R. *Tetrahedron* **2000**, *56*, 1783.
6. Schleyer, P. v. R.; Maerker, C.; Dransfeld, A.; Jiao, H.; Hommes, N. J. R. v. E. *J. Am. Chem. Soc.* **1996**, *118*, 6317.

7. Schleyer, P. v. R.; Manoharan, M.; Wang, Z.-X.; Kiran, B.; Jiao, H.; Puchta, R.; Hommes, N. J. R. v. E. *Org. Lett.* **2001**, 3, 2465.
8. Fallah-Bagher-Shaidaei, H.; Wannere, C. S.; Corminboeuf, C.; Puchta, R.; Schleyer, P. v. R. *Org. Lett.* **2006**, 8, 863.
9. Stanger, A. *J. Org. Chem.* **2006**, 71, 883.
10. Feixas, F.; Matito, E.; Poater, J.; Solà, M. *J. Comput. Chem.* **2008**, 29, 1543.
11. (a) Becke, A. D.; Edgecombe, K. E. *J. Chem. Phys.* **1990**, 92, 5397; (b) Fourré, I.; Silvi, B.; Chaquin, P.; Sevin, A.; *J. Comput. Chem.* **1999**, 20, 897.
12. (a) Savin, A.; Nesper, R.; Wengert, S.; Fässler, T. F.; *Angew. Chem. Int. Ed. Engl.* **1997**, 36, 1808; (b) Chesnut, D. B.; Bartolotti, L. J.; *Chem. Phys.* **2000**, 253, 1.
13. Giambiagi, M.; Giambiagi, M. S. de; Santos, S.C. D. dos; Figueiredo, A. P. de *Phys. Chem. Chem. Phys.* **2000**, 2, 3381.
14. Jimenez-Halla, J. O. C.; Matito, E.; Solà, M.; Braunschweig, H.; Hörl, C.; Krummenacher, I.; Wahler, J. *Dalton Trans.* **2015**, 44, 6740.
15. Bultinck, P.; Ponec, R.; Damme, S. V. *J. Phys. Org. Chem.* **2005**, 18, 706.
16. Bultinck, P.; Rafat, M.; Ponec, R.; van Gheluwe, B.; Carbó-Dorca, R.; Popelier, P. J. *Phys. Chem. A* **2006**, 110, 7642.
17. Kahn, O. *Molecular Magnetism*; Wiley & Sons, Inc.: New York, 1993.
18. van Vleck, J. H. *The Theory of Electric and Magnetic Susceptibility*; Oxford University Press: Oxford, 1932.
19. Neese, F. *Coord. Chem. Rev.* **2009**, 253, 526.
20. Neese, F. *J. Phys. Chem. Solids* **2004**, 781.
21. Noodleman, L. *J. Chem. Phys.* **1981**, 74, 5737.
22. Rudra, I.; Wu, Q.; Voorhis, T. *J. Chem. Phys.* **2006**, 124, 024103.
23. Ruiz, E.; Alvarez, S.; Cano, J.; Polo, V. *J. Chem. Phys.* **2005**, 123, 164110.
24. (a) Szabo, A.; Ostlund, N. S. In *Modern Quantum Chemistry: Introduction to Advanced Electronic Structure Theory*; Dover Publications, New York, **1996**.; (b) Herrmann, C.; Yu, L.; Reiher, M. *J. Comput. Chem.* **2006**, 27, 1223.
25. (a) Zhekova, H.; Seth, M.; Ziegler, T. *J. Chem. Theory Comput.* **2011**, 7, 1858; (b) Wang, F.; Ziegler, T. *J. Chem. Phys.* **2004**, 121, 12191; (c) Wang, F.; Ziegler, T. *J. Chem. Phys.* **2005**, 122, 074109; (d) Wang, F.; Ziegler, T. *Int. J. Quant. Chem.* **2006**, 106, 2545.
26. McWeeny, R., *J. Chem. Phys.* **1965**, 42, 1717.

- 27.** Fedorov, D. G.; Koseki, S.; Schmidt, M. W.; Gordon, M. S. *Int. Rev. Phys. Chem.*, **2003**, 22, 551.
- 28.** Pederson M. R.; Khanna, S. N. *Phys. Rev. B*, **1999**, 60,13.
- 29.** (a) Koseki, S.; Schmidt, M. W.; Gordon, M. S. *J. Chem. Phys.* **1992**, 96, 10768. (b) Koseki, S.; Gordon, M. S.; Schmidt M. W., *J. Phys. Chem.* **1995**, 99, 12764; (c) Koseki, S.; Schmidt, M. W.; Gordon, M. S. *J. Phys. Chem. A*. **1998**, 102, 10430.
- 30.** Neese, F.; Solomon, E.I. *Inorg. Chem.*, **1998**, 37, 6568.
- 31.** Neese, F. *J. Chem. Phys.*, **2007**, 127, 164112.
- 32.** Zein S.; Neese, F. *J. Phys. Chem. A* **2008**, 112, 7976.

CHAPTER 3

Concurrent loss of aromaticity and onset of superexchange in Mg_3Na_2 with an increasing $Na-Mg_3$ distance

Abstract

Gradual migration of Na^+ from Mg_3^{2-} brings about fascinating change in aromatic and magnetic behavior of inorganic Mg_3Na_2 cluster, which is addressed at the B3LYP and QCISD levels. During this process, Na^+ takes away the electron density from Mg_3^{2-} causing a net decrease in aromaticity. A tug-of-war between the Pauli repulsion and the aromaticity is shown to be responsible for the observed stability and aromaticity trends in singlet and triplet states. Implications of a spin crossover vis-à-vis a possible superexchange are also explored.

3.1. Introduction

Triggered by the pioneering concept of ‘‘all metal aromaticity’’ by Boldyrev *et al.*,^{1,2} all-metal annular systems have received a keen attention in past decade. The exceptional nature of aromaticity in this class of molecules has led the researchers to go through several experimental and theoretical studies of such all-metal aromatic systems.³⁻³⁰ These systems include XAl_3^- ($X=Si, Ge, Sn, Pb$),^{3,4} M_4^{2-} ($M=Ga, In, Tl, Sb, Bi$),⁵⁻⁸ T_5^{6-} ($T=Ge, Sn, Pb$),^{9,10} M_4^{2+} ($M=Se, Te$),¹¹⁻¹⁵ M^{3-} ($M=Al, Ga$),¹⁶⁻¹⁹ Al_6^{2-} ,²⁰ Hg_4 ,^{5, 8} M_5^- ($M=Sb, Bi$),²⁴⁻²⁶ Au_5Zn^+ ,²⁷ Cu_3^{3+} ,²⁸ Cu_4^{2-} ,²⁹ $[Fe(X_5)]^+$ ($X=Sb, Bi$),³⁰ and so on. Ab initio and density functional theory (DFT)-based methods have been exercised to explain the stability and reactivity of a wide range of all-metal aromatic and antiaromatic systems.³¹ The dianionic annular systems containing main group metals have been perceived as stable building blocks for multi-decker sandwich complexes.³²⁻³⁶ The feasibility of using anionic annular systems to sandwich the cationic metal was first theoretically examined by Mercero and Ugalde, who found the proposed molecule $[Al_4TiAl_4]^{2-}$ to have large binding energy comparable to conventional metallocenes.³⁷ Apart from the metal, the annular system N_4^{2-} is found to fulfil all the aromaticity criteria³⁸ and is also able to form stable sandwich complexes with transition metals.³⁹ Among the anionic annular systems, Be_3^{2-} , Mg_3^{2-} , and Ca_3^{2-} have been paid a special attention for their interesting nature of stability, reactivity, and aromaticity.⁴⁰⁻⁴³ Such electron-surplus anions are unstable due to large inter-electronic repulsion⁴⁴⁻⁴⁶ and hence require suitable counterions to attain necessary stability.^{47, 48} In a recent work, Chakrabarty *et al.*⁴⁹ addressed the effect of Na^+ counterions on the bonding, stability, and aromaticity of Mg_3^{2-} in a neutral Mg_3Na_2 complex of D_{3h} symmetry, which can also be seen as an ‘‘inverted’’ sandwich compound with reference to the sandwich type clusters.^{37, 39} Chakrabarty *et al.*⁴⁹ have shown that with the increasing separation of Na^+ Ion from the Mg_3^{2-} triangular plane, the counterion is found to take away considerable amount of electron density from the planar dianion. Thus, the complex does not follow the common trend of ionic dissociation of inorganic salt and produces neutral Na and Mg_3 at large separation. Further, with an increase in separation of Na^+ from Mg_3^{2-} plane, the trigonal dianion cluster Mg_3^{2-} also experiences a gradual loss in its well-known π -aromaticity.^{40-43,47,48} All these interesting observations,⁴⁹ arising from gradual separation of Na from Mg_3 , prompted us to opt for the present theoretical investigation where the genesis of such observations in Mg_3Na_2 is thoroughly explored.

The molecule Mg_3Na_2 shows an interesting convergence in its singlet and triplet state at a 5 Å separation between the counterion Na^+ and triangular anion Mg_3^{2-} . This observation alludes toward the stabilization of the high spin state at some particular distance between the Mg_3 plane and Na. Moreover, during migration, Na^+ ion tends to pull away the loosely bound π -cloud of the trigonal Mg_3^{2-} ring,⁴⁹ and they accumulate unpaired spin in neutral Na atoms at fairly large distance. Hence, at this critical Na- Mg_3 distance, spins on two doublet sodium atoms can interact through planar Mg_3 ring and superexchange mechanism is switched on. Through the superexchange of spins on doublet sodium atoms, the molecule can turn magnetic and gain significant stability even with wide stretched axis joining Na and Mg_3 . This possibility of magnetic phase transition in Mg_3Na_2 is the crux of present investigation.

The extent of magnetic interaction is intimately related to the relative stability of the singlet and triplet states which may also vary with Mg₃–Na separation in the Mg₃Na₂ molecule. Thus, the change in the aromaticity may have some role in tuning the magnetic status of the molecule. In fact, an antagonistic relationship between aromaticity and magnetism has already been established in similar type of all-metal aromatic systems.⁵⁰ Hence, in the present work with continuous migration of Na⁺ ion from the Mg₃²⁻ plane, the possibility of appearance of magnetism due to onset of superexchange and its relation with the loss of aromaticity is put in focus. A part of the present results echoes and thus validates the fact in ref. 49, and another segment of this work describes the interplay between aromaticity and magnetism in Mg₃Na₂.

3.2. Theoretical background and computational details

The aromaticity of the present system is measured in terms of the magnetic criterion of aromaticity. The hypothesis that magnetic shielding tensor on a test dipole at the center of a ring can be used to quantify its magnetic property was first proposed by Elser and Haddon,⁵¹ which eventually became popular as nucleus-independent chemical shift (NICS). Negative (Positive) shielding tensor values are taken to indicate the presence of a diatropic (paratropic) ring current, and accordingly, the system is defined as aromatic (antiaromatic).⁵² However, the poor correlation between different measures has led the scientific community to debate about the proper characterization of aromaticity.^{53–57} At this circumstance, the use of more than one aromaticity indices to describe the aromaticity in molecules occurs to be a logical suggestion.⁶⁶ Although NICS is the most widely used descriptor of aromaticity in inorganic systems, nowadays delocalization-based indices are found to perform well in describing the aromaticity of materials.^{58–62} One of such indices is the delocalization index (DI), $\delta(A, B)$, based on quantum theory of atoms in molecules (QTAIM) methodology. This is estimated as the double integration of the exchange–correlation density over the atomic basins as defined by the QTAIM theory. This index gives a quantitative idea of the number of electrons delocalized between atoms A and B.⁶⁰ A larger DI value indicates more aromatic nature and corresponds to a more negative NICS. Being based directly on electron delocalization, which is the essence of aromaticity, NICS and the DI can be regarded as the absolute measure of aromaticity in the sense of not requiring reference standards for its quantification. Another such DI is the multicenter index (MCI) based on the extended delocalized bonding which is considered to be a typical characteristic of aromaticity.⁶³ Following the suggestions of Giambiagi *et al.*,⁶⁴ Bultinck *et al.*⁶³ formulated the MCI as

$$MCI_{ABC\dots K} = \eta \sum_{\mu \in A} \sum_{\nu \in B} \dots \sum_{\kappa \in K} \sum_i \Gamma_i [(PS)_{\mu\nu} (PS)_{\nu\rho} \dots (PS)_{\kappa\mu}] \quad (3.1)$$

where P and S represent charge density bond order and overlap matrices, respectively, and η is a normalization constant. Γ_i is the permutation operator which runs over the μ, ν, \dots, κ basis

to take into account all the terms of generalized population analysis. In the preceding section, a link between aromaticity and magnetism is outlined, at a fairly large separation between Na and Mg₃. According to ref. 40–43, the counterion Na⁺ moves away with the electron and eventually at a large distance becomes neutral. Na in the neutral state is expected to be in the doublet state which can undergo magnetic interaction with another doublet Na through diamagnetic Mg₃ ring. Hence, at some optimum distance, superexchange mechanism may be operative due to charge transfer from Mg₃ to Na. The second-order perturbation energy for such a charge transfer has been formulated by Anderson^{65–67} as follows,

$$\Delta E = \frac{t_{ij}^2}{U} \left(\frac{1}{2} + 2\hat{S}_i \hat{S}_j \right). \quad (3.2)$$

here, t_{ij} is the hopping integral which carries an electron from site i to site j , U is the single ion repulsion energy, and \hat{S}_i and \hat{S}_j are the spin angular momentum operators on magnetic sites i and j . However, this t^2/U term is well known in the Hubbard model and related to the coupling constant (J) of a spin exchange process.^{68,69} However, in a recent formalism, instead of direct estimation of this t^2/U term, the above expression is modified to estimate the coupling constant in terms of the second-order perturbation energy (ΔE) for charge transfer between sites and spin density on those centers (ρ_i and ρ_j).⁷⁰ This model suits in the present context, since here the magnetic interaction sets in due to charge migration from Mg₃ to Na,

$$J_{CT} = \frac{2\Delta E}{1 + \rho_i \cdot \rho_j}. \quad (3.3)$$

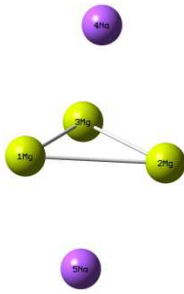
To study the system under investigation DFT as well as post Hartree–Fock level methods are used. In DFT, hybrid functional B3LYP, coupled with 6-311+g(d) basis set, is used in the unrestricted framework to optimize the structure. Besides, quadratic configuration interaction method QCISD is also employed with Dunning’s correlation consistent basis set aug-cc-pVDZ for geometry optimization. The shielding tensors on the dummy atoms are reported as the NICS value. While computing NICS, the sign convention coined by Schleyer *et al.*⁷¹ is followed. According to this convention, the signs of the computed values are reversed and negative (positive) sign is assigned for diamagnetic (paramagnetic) shielding. The choice of the gauge for the vector potential of the magnetic field is an important factor in the computation of shielding tensors. This well-known gauge problem had been resolved by adopting the gauge independent atomic orbitals (GIAO) method,^{72–75} and the same method is followed in the present work to compute the shielding tensors. To find out the contributions

of *r* and *p* electrons to aromaticity, NICS has been calculated both at the center of the ring [NICS(0)],⁷¹ and 1 Å above the plane [NICS(1)].^{76, 77} The second-order perturbation energies [ΔE in eqn (3.3)] due to the charge transfer from Mg_3^{2-} to Na^+ are obtained from the natural bond orbital (NBO) output, carried out in the Gaussian NBO version 3.1.^{78–81} Bond energy decomposition is performed using Amsterdam Density Functional (ADF) software.^{82–84} The DI, $\delta(A, B)$ terms are computed by the Proaim and Promega first-order algorithms as implemented in the AIMAll suite of programs.⁸⁵ To validate the DFT result, the NICS values of the singlet Mg_3Na_2 is also computed in CCSD method using DALTON.⁸⁶ The MCI index is calculated by ESI-3D suit of program,⁸⁷ which is popularly used for the calculation of electron sharing indices.^{88, 89} Other calculations are performed using Gaussian 09W suite of quantum chemical package.⁹⁰

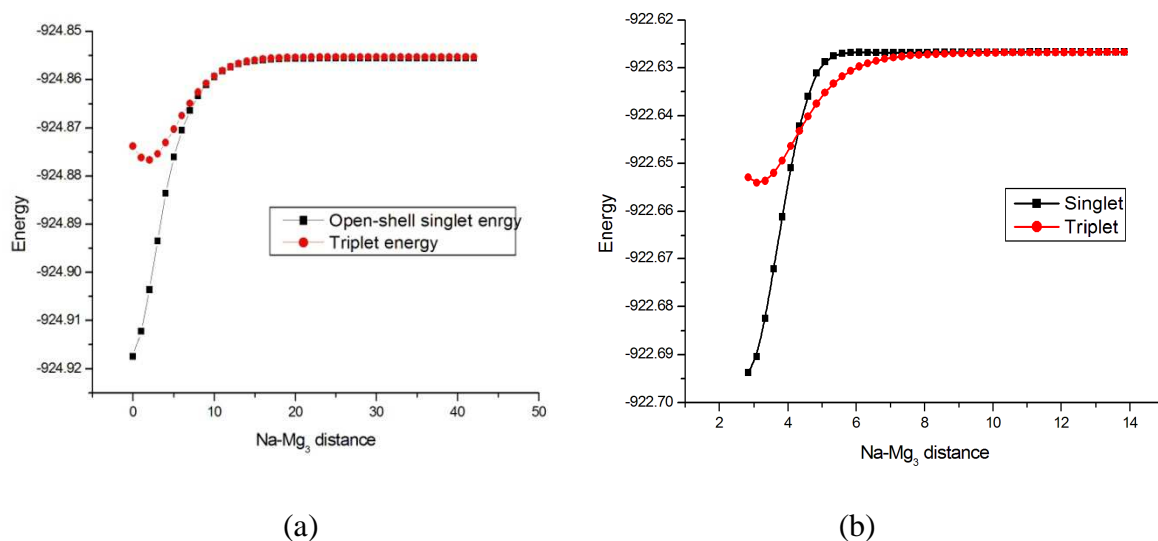
3.3. Results and discussion

The energy and geometry comparison of the system is reported in Table 3.1. It is interesting to observe that irrespective of the computational level, the system reserves its D_{3h} symmetry at its energy minima. It is also apparent from the Table 3.1 that the geometries in the singlet and triplet states only differ in the distance of Na^+ ion from the equatorial plane of Mg_3^{2-} , whereas the sides of Mg_3^{2-} triangle remains almost constant in both the spin states, irrespective of the methodology. Moreover, in both the methodologies, the triplet state of the molecule is found to have a longer separation between Na and Mg_3 compared to the singlet state. This dependence of spin state energies on the Na– Mg_3 separation is in agreement with the results in refs. 40–43. To further investigate the dependence of spin state energies on Na– Mg_3 separation, two Na^+ ions are allowed to move away by 0.25 Å from their ground state position along the axis lying perpendicular to the Mg_3^{2-} triangular plane till they reach a distance as large as ~14 Å (distance of Na is measured perpendicularly from the center of the Mg_3 ring).

Table 3.1. Energy and geometry comparison of the singlet and triplet states of Mg_3Na_2 , optimized at (a) UB3LYP/6-311+g(d) and (b) QCISD/aug-cc-pVDZ level of theories.

System	Singlet		Triplet	
	Bond Length (Å)	Energy (a.u)	Bond Length (Å)	Energy (a.u)
	(a)	(a)	(a)	(a)
	Mg – Mg = 3.13	– 924.918	Mg – Mg = 3.16	– 924. 877
	Mg ₃ – Na = 2.75		Mg ₃ – Na = 3.19	
	(b)	(b)	(b)	(b)
	Mg – Mg = 3.15	– 922.694	Mg – Mg = 3.17	– 922.654
	Mg ₃ – Na = 2.84		Mg ₃ – Na = 3.16	

It is interesting to note that in the DFT framework, the singlet state wave function with $\langle \hat{S} \rangle^2 = 0$ shows an internal instability at longer separation between Na and Mg₃. For this reason, the wave function corresponding to all the singlet states is optimized which results in the nonzero value of $\langle \hat{S} \rangle^2$ onward 3.7 Å distance between Na and Mg₃ (Table A.S1 and A.S2 in Appendix A). Moreover, the spin square value approaches toward unity with gradual stretching of Na–Mg₃ distance, indicating the attainment of open-shell singlet state (Table A.S1 and A.S2 in Appendix A). This observation is quite similar to that in the ref. 91, which says that for a two-electron two-radical system, if the bonding orbitals are beyond the range of any kind of interaction, the unrestricted solution is produced with an equal mixture of singlet state ($S=0$) and triplet state ($S=1$). Noodleman *et al.*^{92, 93} described such a spin state to be a broken symmetry (BS) state which is obtained by polarizing spins with antiparallel alignment at different magnetic sites within unrestricted formalism. The BS state, being a weighted average of high-spin and low-spin states,^{92, 93} is characterized by $\langle \hat{S} \rangle^2 = 1$. Hence, in the present case, the gradual separation of Na from Mg₃ plane causes the appearance of BS situation in Mg₃Na₂. Next, the potential energy scan is executed on the optimized geometry of singlet state (with optimized wave function) with spin multiplicities one and three, which provides the information of vertical excitation energy. In another scan, optimized geometries of both the spin states are used at their respective spin multiplicities, and thus, the adiabatic excitation energy can be figured out. Interestingly, all the plots delineate that the singlet state is gradually destabilized with the increase in Na–Mg₃ distance and ultimately overlaps with the triplet energy profile (Figure 3.1). However, the geometries and energies of the molecules in different spin states, the nature of the potential energy surface in Figure 3.1, obtained in the computational levels UB3LYP/6-311+g(d) and QCISD/aug-cc-pVDZ, are all found to be similar and concordant to each other. Hence, following computations on Mg₃Na₂ (with optimized wave function) are carried out only at UB3LYP/6-311+g(d) level with its geometry optimized at QCISD/aug-cc-pVDZ level (if not specified otherwise).



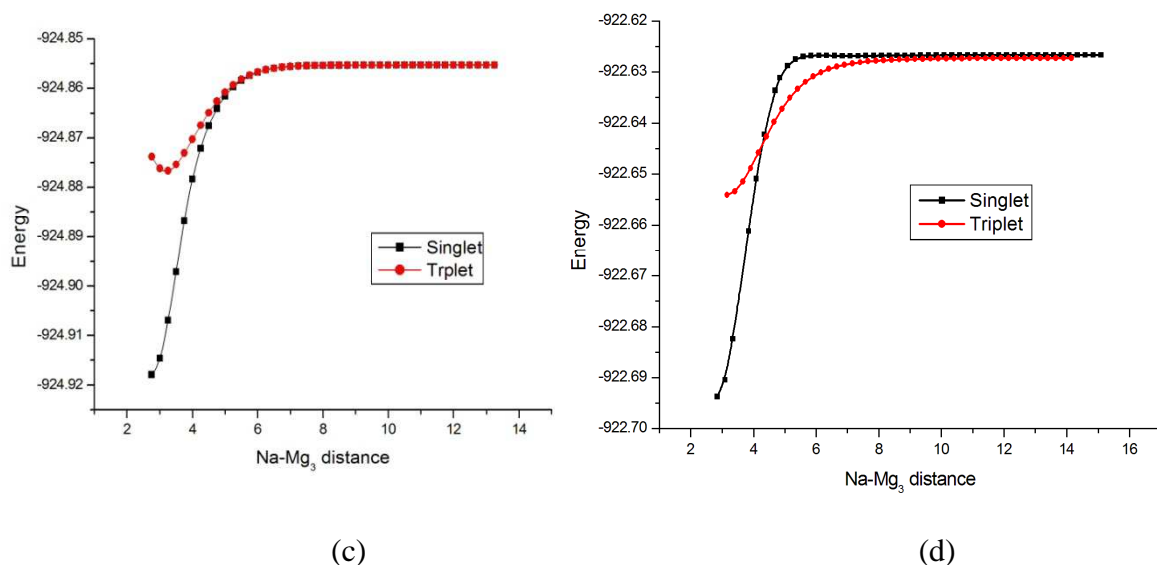


Figure 3.1. Energy (a.u.) profile of Mg_3Na_2 with increasing Na– Mg_3 distance (Å) on the (a) geometry of singlet state optimized at UB3LYP/6-311+g(d) level, (b) geometry of singlet state optimized at QCISD/aug-cc-pvdz level, (c) geometry of singlet and triplet states, both optimized at UB3LYP/6-311+g(d) level, and (d) geometry of singlet and triplet states, both optimized at QCISD/aug-cc-pvdz level of theory.

The explanation of the above schematics can be attributed to the gradual charge neutralization of Na^+ and Mg_3^{2-} with their increasing separation as evident from ref.49 as well as from the change in the pattern of highest occupied molecular orbital (HOMO) of singlet ground state (Figure 3.2). This is characterized by the delocalized electron density above and below the trigonal Mg_3 plane, which itself defines the nodal plane (Figure 3.2a). The electron density gradually migrates toward Na from Mg_3 and ultimately resorts solely on Na.

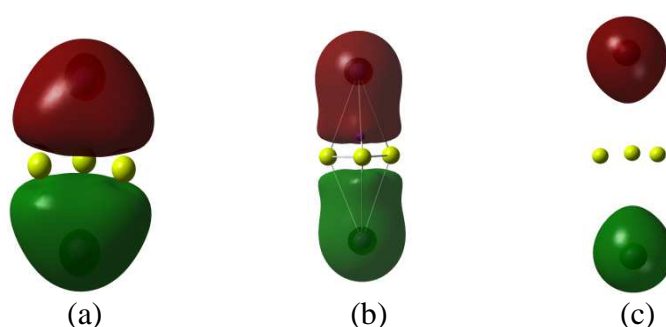


Figure 3.2. Schematics of the HOMO generated at (a) optimized geometry (b) Na– Mg_3 distance of 4.08 Å where the singlet energy approaches close to the triplet energy, and (c) Na – Mg_3 distance of 5.58 Å.

Since the HOMO of the singlet state retains two excess π -bonding electrons, they experience a repulsion which significantly reduces at large Na– Mg_3 distance owing to the charge accumulation on the Na atoms above and below the plane. The repulsion between the

bonding electrons is computed in terms of Pauli repulsion using ADF quantum chemical package.^{82–84} In ADF, the interaction energy between different fragments is split into

$$\Delta E_{bnd} = \Delta E_{Stat} + \Delta E_{Pauli} + \Delta E_{oi} \quad (3.4)$$

The first term usually corresponds to the attractive potential [94, 95], whereas ΔE_{Pauli} is usually repulsive in nature. In ADF, ΔE_{Pauli} is equated as the energy change associated with going from superposition of fragment densities ($\rho_A + \rho_B$) to the wave function $NA|\psi_A\psi_B|$ that properly obeys the Pauli principle through explicit antisymmetrization (A) and renormalization (N) of the product of fragment wave functions.⁸² ΔE_{oi} accounts for electron pair bonding, charge transfer, and polarization. However, due to charge migration, the Mg_3 plane becomes completely devoid of any electron, and the system loses the bonding energy. This fact is apparent from the following plot (Figure 3.3), where both the attractive potential and Pauli repulsion are found to decrease with an increase in the Na– Mg_3 distance. However, the stability gain by the system due to the decrease in Pauli repulsion energy cannot overcome the loss of attractive potential, resulting in a net decrease in binding energy.

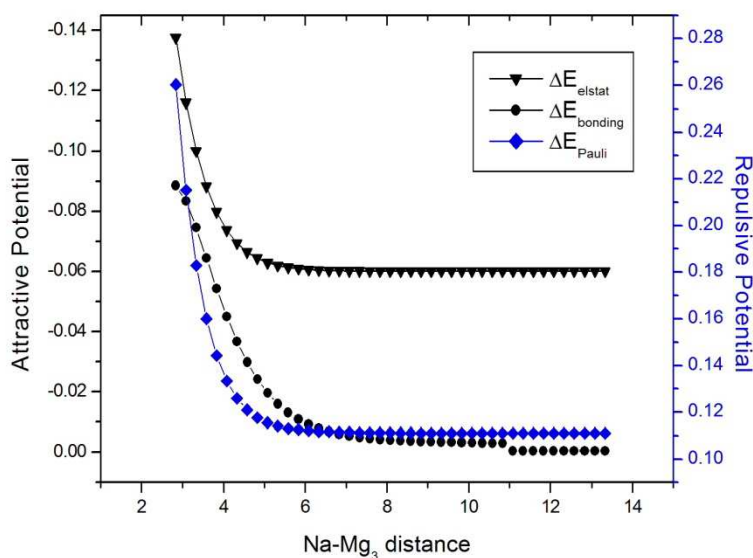
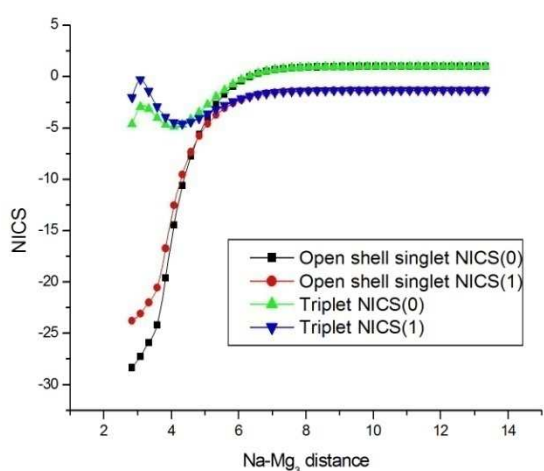


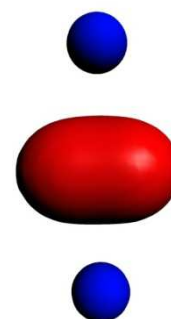
Figure 3.3. Bonding energy decomposition analysis in the singlet state of the molecule.

Next, to investigate the variation of aromaticity with increasing separation of Na from Mg_3 plane, NICS(0) and NICS(1) are scanned by varying the distance, at both the spin states of the system with its optimized geometry at the singlet state (Figure 3.4a). At the singlet ground state, large negative values of both NICS(0) and NICS(1) refer to the coexistence of σ - and π -aromaticity, rendering Mg_3Na_2 to be multiply aromatic. Existence of π -electron cloud above and below the Mg_3 plane in the HOMO can well explain π -aromaticity, whereas the maximum diamagnetic contribution toward the total NICS(0) value comes from the 26th MO (Figure 3.4b) of the system. As graphically represented in Figure 3.4b, this MO can evidently be narrated to be composed solely of Mg ‘s’ atomic orbitals. The contribution of

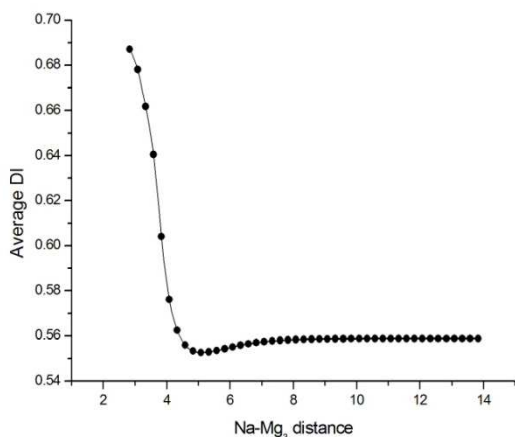
individual MOs toward the total NICS(0) value is computed in the ADF computational package. Contrary to the singlet state, low negative values of NICS(0) and NICS(1) are obtained near the ground state geometry of Mg_3Na_2 in its triplet state indicating lower degree of aromaticity than in the singlet state. This reduced aromaticity in the triplet state is due to the presence of unpaired spin in Na atoms which exalts the paratropic shielding tensor compared to its diatropic analog resulting in low aromaticity.⁵⁰ To further verify the variation of aromaticity, the average of DI among Mg atoms and the MCI values in the singlet state are also plotted against the increasing Na– Mg_3 separation (Figure 3.4c). A decaying nature of the average DI and MCI confirms the trend in the change of NICS. In addition to the DFT, ab initio method such as CCSD is also adopted to compute NICS. The plot shows the same trend of decreasing negativity of NICS particularly after spin density grows on Na atoms (Figure A.S1 in Appendix A) and hence once again solicits gradual loss of aromaticity with increasing Na– Mg_3 separation. However, with an increase in vertical distance of Na from the center of Mg_3 plane, the aromaticity in both the spin states decays almost to a null value, which is quite obvious, since Na atoms take away all the charge density which has been maintaining the ring current. Since two apical Na atoms are pulled apart which leave behind the Mg_3 moiety in the neutral state, the effect of dispersion can be argued to play a significant role in such scenario.⁹⁶ Hence, a verification of the effect of dispersion interaction in aromaticity of the singlet Mg_3Na_2 is performed at the DFT level with dispersion correction due to Grimme.^{97,98} From Figure A.S2 in Appendix A, it is apparent that the effect of dispersion on the NICS values is negligible which is also obvious from the literature.^{99–101} However, the dispersion may have effects on the energy of the molecule, and hence, the energy profiles of the system are compared with and without dispersion correction. The variation in energy with increase in Na– Mg_3 distance appears similar with and without the dispersion correction (Figure A.S3 in Appendix A).



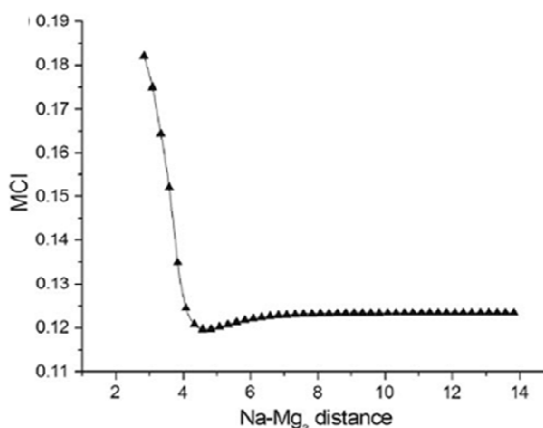
(a)



(b)



(c)



(d)

Figure 3.4. Plot of (a) NICS(0) and NICS(1) in the singlet and triplet state of Na_2Mg_3 at DFT level. (b) The 26th MO contributing maximum toward the diamagnetic NICS(0). (c) The average DI and (d) MCI index of aromaticity for the singlet state as a function of increasing Na–Mg₃ distance (Å).

Since, with an increase in Na–Mg₃ distance, Na move away with the pair of electrons responsible for maintaining the aromaticity, the system loses the aromatic stabilization energy though gains stability due to reduction in the Pauli repulsion, particularly in the singlet state. The loss of aromaticity with increasing Na–Mg₃ distance is formulated as

$$\delta_{NICS}(r) = NICS(r - \Delta r) - NICS(r) \quad (3.5)$$

where Δr is fixed at 0.25 Å in the present work. The plot of Pauli repulsion energy (ΔE_{Pauli}) and the loss of aromaticity with increasing separation between Na and Mg₃ are depicted in Figure 3.5, which clarifies that as in one hand, a minimization of Pauli repulsion energy tends to stabilize the system and on the other hand, loss of aromaticity acts as an instability factor. It is further interesting to note that the maximum loss of aromaticity occurs near to the critical value of Na–Mg₃ distance (4.33 Å) where the singlet and triplet state energies are converged (Figures 3.1b, d, 3.5). It is also noted here that the spin-crossover region corresponds to the zone of maximum change in the MCI and DI indices, which can be found from the derivative plots of the average DI and the MCI indices (Figure A.S4 of Appendix A). This observation advocates the fact that such spin-crossover occurs at the cost of the loss of delocalization which corroborates to aromaticity. This suggests that the appearance of BS state and consequent spin accumulation on the Na atoms at that point plays a definite role in reducing the aromaticity of the system. The localization of those two extra charges, which maintain the aromaticity, on the Na⁺ ions causes cessation in circulation of those electrons and explains the maximum loss of aromaticity as well the minimal ΔE_{Pauli} continuum after that point.

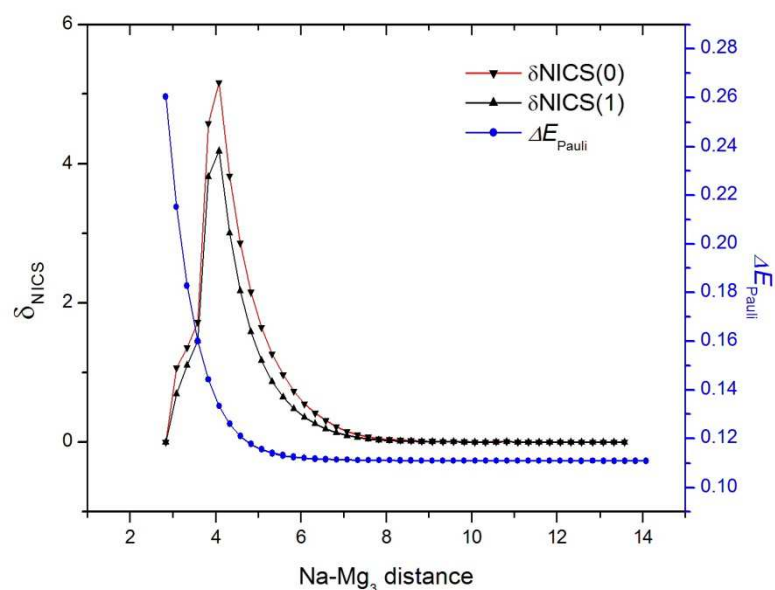


Figure 3.5. Plot of Pauli repulsion energy (ΔE_{Pauli}) and $\delta_{\text{NICS}}(0)$ and $\delta_{\text{NICS}}(1)$ with increasing Na–Mg₃ distance (Å) in the singlet state of Na₂Mg₃.

Since, with the gradual increase in the Na–Mg₃ separation, a charge transfer is occurred from Mg₃ to apical Na atoms, decrease in charge density in the Mg₃ plane causes weak bonding interaction (Figure 3.3). In this situation, the stability of the molecule can partly be compensated through the energy minimization due to charge migration from Mg₃ moiety to Na. The stability gained by such charge migration was given by Anderson in the framework of second-order perturbation theory and was equated with the energy of superexchange.^{65–67} In the present case also, the superexchange becomes possible between the spins accumulated on Na atoms as a consequence of charge transfer and gradual neutralization of Na⁺. The fact of gradual spin accumulation on Na with increase in Na–Mg₃ separation can be ascertained from the spin density plot in the Figure 3.6.

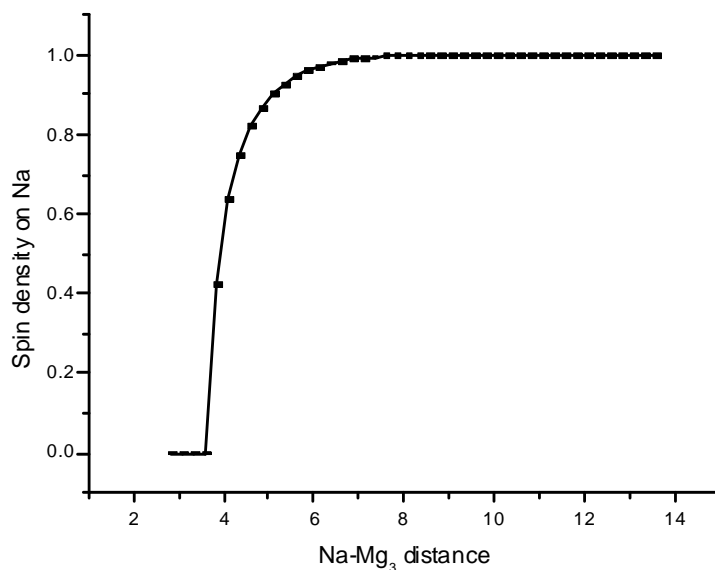


Figure 3.6. Plot of spin density on Na and Mg₃ in the ground state with increasing Na–Mg₃ distance (Å).

The value of coupling constant associated with the superexchange process can now be estimated through eqn (3.3). From the variation in MO with increase in Na–Mg₃ (Figure 3.2), it becomes evident that the charge migration involves the out-of-plane *p*-orbitals of all the three Mg atoms and *s* orbitals of the Na atoms particularly for low Na–Mg₃ distance. Thus, during NBO analysis, the out-of plane *p*-orbitals in Mg₃ plane and *s* orbitals in Na are only considered as the donor and acceptor orbitals for obtaining the appropriate value of second-order perturbation energy (ΔE) due to charge migration. To clarify this choice of relevant orbitals, a truncated part of the NBO output corresponding to the Na–Mg₃ distance of 5.08 Å, showing the donor and acceptor orbitals, and their composition are given in Table A.S3 in Appendix A as an example. From the plots in Figure 3.1 it appears that significant amount of spin density starts to grow on the Na atoms from the Na–Mg₃ distance of 4.08 Å. This open-shell singlet state is found to be more stable than the corresponding triplet state by a considerable amount up to ~6 Å distance between Na and Mg₃, beyond which the singlet–triplet energy gap almost vanishes. Thus, the superexchange energies (ΔE) are obtained from the NBO analysis of singlet state of Mg₃Na₂ with Na–Mg₃ separation in the range of 4.08–6.08 Å. While using this ΔE value in the estimation of coupling constant, the right-hand side of eqn (3.3) is multiplied by 2 since there are two such transitions from Mg₃ to first and second Na atoms. Moreover, these transitions leave almost zero spin density in Mg₃ plane, and thus, the denominator in the right-hand side of eqn (3.3) takes the value of one with which eqn (3.3) transforms into,

$$J = 4\Delta E \quad (3.6)$$

which is ultimately used in this work to estimate the exchange coupling constant associated with superexchange. Moreover, no contribution from the Na–Na direct exchange is taken into account due to their large separation. The interaction between two spins on Na atoms expectedly decreases with an increase in separation between Mg₃ and Na, and can be

understood from Table 3.2. The negative value of coupling constant indicates the antiferromagnetic interaction which is also attested by the spin density plot showing up-spin and down-spin on different Na atoms (Figure 3.7).

Table 3.2. ΔE and calculated J value on the basis of eqn (3.6).

Na – Mg ₃ distance (Å)	ΔE (kcal/mole)	J (cm ⁻¹)
4.33	0.37	– 518
4.58	0.295	– 413
4.83	0.225	– 315
5.08	0.17	– 238
5.33	0.115	– 161

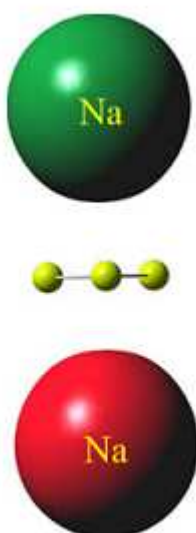


Figure 3.7. Spin density plot at a Na–Mg₃ separation onward 3.83 Å (green and red color denote up-spin and down-spin density).

3.4. Conclusion

Present study explains the change in the aromaticity and energy profile of the singlet state of Mg₃Na₂ molecule and gradual attainment of the BS state with an increase in Na–Mg₃ distance. Near the ground state, Mg atoms are held together by a pair of π -bonding electrons onto which Na⁺ ions are impregnated. The circulation of π -electron cloud above and below the Mg₃ plane also contributes to the σ - and π -aromaticity of the molecule. However, in this situation, the stability due to aromaticity has to compete with the Pauli repulsion. When the Na ions move away from Mg₃ plane with all the charge density, the aromaticity is also gradually lost, though the system gets stability due to decrease in Pauli repulsion. At a critical value (~4.33 Å) of Na–Mg₃ distance, the Pauli repulsion approaches a minimum due to localization of charge density on Na atoms above and below the plane. This charge accumulation on Na atoms makes these neutral doublet species with up-spin polarization at

one Na and down-spin at another. The spins on Na atoms undergo superexchange which is quantified through eqn (3.6). The stabilization due to superexchange and lowering of Pauli repulsion partly compensates the loss in bonding energy in the molecule for the charge migration to Na atoms. The Na spins are found to be engaged in antiferromagnetic interaction which gradually decreases with an increase in Na–Mg₃ separation.

3.5. References

1. Li, X.; Kuznetsov, A. E.; Zhang, H. F.; Boldyrev, A. I.; Wang, L. S. *Science* **2001**, *291*, 859.
2. Kuznetsov, A. E.; Birch, K. A.; Boldyrev, A. I.; Li, X.; Zhai, H. J.; Wang, L. S. *Science* **2003**, *300*, 622.
3. Li, X.; Zhang, H. F.; Wang, L. S.; Kuznetsov, A. E.; Cannon, N. A.; Boldyrev, A. I. *Angew Chem. Int. Ed.* **1867**, *40*, 1867.
4. Kuznetsov, A. E.; Boldyrev, A. I.; Li, X.; Wang, L. S. *J. Am. Chem. Soc.* **2001**, *123*, 8825.
5. Twamley, B.; Power, P. P. *Angew Chem. Int. Ed.* **2000**, *39*, 3500.
6. Cisar, A.; Corbett, J. D. *Inorg. Chem.* **1977**, *16*, 2482.
7. Critchlow, S. C.; Corbett, J. D. *Inorg. Chem.* **1984**, *23*, 770.
8. Tuononen, H. M.; Suontamo, R.; Valkonen, J.; Laitinen, R. S. *J. Phys. Chem. A* **2004**, *108*, 5670.
9. Todorov, I.; Sevov, S. C. *Inorg. Chem.* **2004**, *43*, 6490.
10. Todorov, I.; Sevov, S. C. *Inorg. Chem.* **2005**, *44*, 5361.
11. Gillespie, R. J.; Barr, J.; Kapoor, R.; Malhotra, K. C. *Can. J. Chem.* **1968**, *46*, 149.
12. Gillespie, R. J.; Barr, J.; Crump, D. B.; Kapoor, R.; Ummat, P. K. *Can. J. Chem.* **1968**, *46*, 3607.
13. Barr, J.; Gillespie, R. J.; Kapoor, R.; Pez, G. P. *J. Am. Chem. Soc.* **1968**, *90*, 6855.
14. Couch, T. W.; Lokken, D. A.; Corbett, J. D. *Inorg. Chem.* **1972**, *11*, 357.
15. Burford, N.; Passmore, J.; Sanders, J. C. P. In Liebman, J. F.; Greenburg, A. (Eds.) *From atoms to polymers. Isoelectronic analogies*. VCH, New York **1989**, p 53.
16. Li, X.; Wang, X. B.; Wang, L. S. *Phys. Rev. Lett.* **1998**, *81*, 1909.
17. Wu, H.; Li, X.; Wang, X. B.; Ding, C. F.; Wang, L. S. *J. Chem. Phys.* **1998**, *109*, 449.
18. Baek, K. K.; Bartlett, R. J. *J. Chem. Phys.* **1998**, *109*, 1334.

19. Kuznetsov, A. E.; Boldyrev, A. I. *Struct. Chem.* **2002**, 13, 141.
20. Kuznetsov, A. E.; Boldyrev, A. I.; Zhai, H. J.; Li, X.; Wang, L. S. *J. Am. Chem. Soc.* **2002**, 124, 11791.
21. Nielsen, J. W.; Baenziger, N. C. *Acta. Crystallogr.* **1954**, 7, 277.
22. Corbett, J. D. *Inorg. Nucl. Chem. Lett.* **1969**, 5, 81.
23. Kuznetsov, A. E.; Corbett, J. D.; Wang, L. S.; Boldyrev, A. I. *Angew Chem. Int. Ed.* **2001**, 40, 3369.
24. Gausa, M.; Kaschner, R.; Lutz, H.O.; Seifert, G.; Meiwes-Broer, K. H. *Chem. Phys. Lett.* **1994**, 230, 99.
25. Gausa, M.; Kaschner, R.; Seifert, G.; Faehrmann, J. H.; Lutz, H. O.; Meiwes, K. H. B. *J. Chem. Phys.* **1996**, 104, 9719.
26. Zhai, H. J.; Wang, L. S.; Kuznetsov, A. E.; Boldyrev, A. I. *J. Phys. Chem. A* **2002**, 106, 5600.
27. Tanaka, H.; Neukermans, S.; Janssens, E.; Silverans, R. E.; Lievens, P. *J. Am. Chem. Soc.* **2003**, 125, 2862.
28. Alexandrova, A. N.; Boldyrev, A. I.; Zhai, H. I.; Wang, L. S. *J. Phys. Chem. A* **2005**, 109, 562.
29. Wannere, C. S.; Corminboeuf, C.; Wang, Z. X.; Wodrich, M. D.; King, R. B.; Schleyer, P. V. R. *J. Am. Chem. Soc.* **2005**, 127, 5701.
30. Lein, M.; Frunzke, J.; Frenking, G. *Angew Chem. Int. Ed.* **2003**, 42, 1303.
31. Chattaraj, P. K.; Roy, D. R.; Elango, M.; Subramanian, V. *J. Phys. Chem. A* **2005**, 109, 9590.
32. Chattaraj, P. K.; Giri, S. *J. Mol. Struct. (Theochem)* **2008**, 865, 53.
33. Chattaraj, P. K.; Roy, D. R.; Duley, S. *Chem. Phys. Lett.* **2008**, 460, 382.
34. Roy, D. R.; Duley, S.; Chattaraj, P. K. *Proc. Indian Natl. Sci. Acad. Part-A* **2008**, 74, 11.
35. Chattaraj, P. K.; Giri, S. *Int. J. Quantum Chem.* **2009**, 109, 2373.
36. Chakrabarty, A.; Giri, S.; Chattaraj, P. K. *J. Mol. Struct. (Theochem)* **2009**, 913, 70.
37. Mercero, J. M.; Ugalde, J. M. *J. Am. Chem. Soc.* **2004**, 126, 3380.
38. Van Zandwijk, G.; Janssen, R. A. J.; Buck, H. M. *J. Am. Chem. Soc.* **1990**, 112, 4155.
39. Mercero, J. M.; Matxain, J. M.; Ugalde, J. M. *Angew Chem. Int. Ed.* **2004**, 43, 5485.

40. Giri, S.; Roy, D. R.; Duley, S.; Chakrabarty, A.; Parathasarathi, R.; Elango, M.; Vijayraj, R.; Subramaniam, V.; Islas, R.; Merino, G.; Chattaraj, P. K. *J. Comput. Chem.* **2010**, *31*, 1815.
41. Kuznetsov, A. E.; Boldyrev, A. I. *Chem. Phys. Lett.* **2004**, *388*, 452.
42. Roy, D. R.; Chattaraj, P. K. *J. Phys. Chem. A* **2008**, *112*, 1612.
43. Oscar, J.; Jimenez-Halla, C.; Matito, E.; Blancafort, L.; Robles, J.; Sola, M. *J. Comput. Chem.* **2009**, *30*, 2764.
44. Boldyrev, A. I.; Gutowski, M.; Simons, J. *Acc. Chem. Res.* **1996**, *29*, 497.
45. Boldyrev, A. I.; Simons, J. *J. Phys. Chem.* **1994**, *98*, 2298.
46. Janoschek, R. Z. *Z. Anorg. Allg. Chem.* **1992**, *616*, 101.
47. Wang, X. B.; Ding, C. F.; Nicholas, J. B.; Dixon, D. A.; Wang, L. S. *J. Phys. Chem. A* **1999**, *103*, 3423.
48. Wang, X. B.; Nicholas, J. B.; Wang, L. S. *J. Chem. Phys.* **2000**, *113*, 10837.
49. Chakrabarty, A.; Giri, S.; Duley, S.; Anoop, A.; Bultinck, P.; Chattaraj, P. K. *Phys. Chem. Chem. Phys.* **2011**, *13*, 14865.
50. Paul, S.; Misra, A. *Inorg. Chem.* **2011**, *50*, 3234.
51. Elser, V.; Haddon, R. C. *Nature (London)* **1987**, *325*, 792.
52. Lazzeretti, P. *Phys. Chem. Chem. Phys.* **2004**, *6*, 217.
53. Cyra, C.; Ski, M.; Krygowski, T. M.; Katritzky, A. R.; Schleyer, P. V. R. *J. Org. Chem.* **2002**, *67*, 1333.
54. Poater, J.; GarcFa-Cruz, I.; Illas, F.; Sol, V. M. *Phys. Chem. Chem. Phys.* **2004**, *6*, 314.
55. Katritzky, A. R.; Jug, K.; Oniciu, D. C. *Chem. Rev.* **2001**, *101*, 1421.
56. Krygowski, T. M.; Cyranfski, M. K. *Chem. Rev.* **2001**, *101*, 1385.
57. Katritzky, A. R.; Karelson, M.; Sild, S.; Krygowski, T. M.; Jug, K. *J. Org. Chem.* **1998**, *63*, 5228.
58. Fias, S.; Fowler, P. W.; Delgado, J. L.; Hahn, U.; Bultinck, P. *Chem. Eur. J.* **2008**, *14*, 3093.
59. Ghiasi, R.; Pasdar, H. *J. Mex. Chem. Soc.* **2012**, *56*, 426.
60. Poater, J.; Fradera, X.; Duran, M.; Sola, M. *Chem. Eur. J.* **2003**, *9*, 400.
61. Mandado, M.; Gonza ́lez-Moa, M. J.; Mosquera, R. A. *J. Comput. Chem.* **2007**, *28*, 127.

62. Foroutan-Nejad, C. *Phys. Chem. Chem. Phys.* **2012**, *14*, 9738.
63. Bultinck, P.; Rafat, M.; Ponec, R.; Gheluwe, B. V.; Carbo-Dorca, R.; Popelier, P. *J. Phys. Chem. A* **2006**, *110*, 7642.
64. Giambiagi, M.; de Giambiagi, M. S.; dos Santos Silva, C. D.; PaivadeFigueiredo, A. *Phys. Chem. Chem. Phys.* **2000**, *2*, 3381.
65. Anderson, P. W. *Phys. Rev.* **1950**, *79*, 350.
66. Anderson, P. W. *Phys. Rev.* **1959**, *115*, 2.
67. Anderson, P. W. In *Solid state physics*, vol 14 Seitz F, Turnbull D (Eds.) Academic Press Inc., New York **1963**, p 99.
68. Munoz, D.; Illas, F.; de Moreira, I. P. R. *Phys. Rev. Lett.* **2000**, *84*, 1579.
69. Caballol, R.; Castell, O.; Illas, F.; de Moreira, I. P. R.; Malrieu, J. P. *J. Phys. Chem. A* **1997**, *101*, 7860.
70. Paul, S.; Misra, A. *J. Chem. Theory Comput.* **2012**, *8*, 843.
71. Schleyer, P. V. R.; Maerker, C.; Dransfeld, A.; Jiao, H.; Hommes, N. J. R. V. E. *J. Am. Chem. Soc.* **1996**, *118*, 6317.
72. Ditchfield, R. *Mol. Phys.* **1974**, *27*, 789.
73. Fukui, H. *Magn. Res. Rev.* **1987**, *11*, 205.
74. Freidrich, K.; Seifert, G.; Grossmann, G. *Z. Phys. D.* **1990**, *17*, 45.
75. Malkin, V. G.; Malkina, O. L.; Erikson, L. A.; Salahub, D. R. In: *Politzer, P.; Seminario, J. M. (eds) Modern density functional theory: a tool for chemistry, vol 2. Elsevier, Amsterdam 1995.*
76. Schleyer, P. V. R.; Jiao, H.; Hommes, N. J. R. V. E.; Malkin, V. G.; Malkina, O. *J. Am. Chem. Soc.* **1997**, *119*, 12669.
77. Schleyer, P. V. R.; Manoharan, M.; Wang, Z. X.; Kiran, B.; Jiao, H.; Pachta, R.; Hommes, N. J. R. V. E. *Org. Lett.* **2001**, *3*, 2465.
78. Foster, J. P.; Weinhold, F. *J. Am. Chem. Soc.* **1980**, *102*, 7211.
79. Carpenter, J. E. *Extension of Lewis structure concepts to open shell and excited state molecular species. Ph. D. Thesis, University of Wisconsin, Madison, 1987.*
80. Reed, A. E.; Curtiss, L. A.; Weinhold, F. *Chem. Rev.* **1988**, *88*, 899.
81. Weinhold, F.; Carpenter, J. E. In *The structure of small molecules and ions*. Naaman, R.; Vager, Z. (Eds.) Plenum, New York, **1988**, p 227.

- 82.** teVelde, G.; Bickelhaupt, F. M.; van Gisbergen, S. J. A.; Guerra, C. F.; Baerends, E. J.; Snijders, J. G.; Ziegler, T. *J. Comput. Chem.* **2001**, *22*, 931.
- 83.** Guerra, C. F.; Snijders, J. G.; teVelde, G.; Baerends, E. J. *Theor. Chem. Acc.* **1998**, *99*, 391.
- 84.** ADF (2012) SCM, theoretical chemistry. Vrije Universiteit, Amsterdam, The Netherlands, <http://www.scm.com>
- 85.** AIMAll (version 13.05.06), Keith, T. A. **2011**, <http://aim.tkgristmill.com>
- 86.** Angeli, C.; Bak, K. L.; Bakken, V.; Christiansen, O.; Cimiraglia, R.; Coriani, S.; Dahle, P.; Dalskov, E. K.; Enevoldsen, T.; Fernandez, B.; Ferrighi, L.; Frediani, L.; Hattig, C.; Hald, K.; Halkier, A.; Heiberg, H.; Helgaker, T.; Hetttema, H.; Jansik, B.; Jensen, H. J. A.; Jonsson, D.; Jørgensen, P.; Kirpekar, S.; Klopper, W.; Knecht, S.; Kobayashi, R.; Kongsted, J.; Koch, H.; Ligabue, A.; Lutnæs, O. B.; Mikkelsen, K. V.; Nielsen, C. B.; Norman, P.; Olsen, J.; Osted, A.; Packer, M. J.; Pedersen, T. B.; Rinkevicius, Z.; Rudberg, E.; Ruden, T. A.; Ruud, K.; Salek, P.; Samson, C. C. M.; Sanchez de Meras, A.; Saue, T.; Sauer, S. P. A.; Schimmelpfennig, B.; Steindal, A. H.; Sylvester-Hvid, K. O.; Taylor, P. R.; Vahtras, O.; Wilson, D. J.; Ågren, H.; Dalton et al. **2011**, amolecular electronic structure program, Release Dalton 2011 see <http://daltonprogram.org>
- 87.** Matito, E. **2006**, ESI-3D: electron sharing indices program for 3D molecular space partitioning. Institute of Computational chemistry and Catalysis (IQCC), University of Girona, Catalonia, Spain, http://iqc.udg.es/*eduard/ESI.
- 88.** Matito, E.; Duran, M.; Solà, M. *J. Chem. Phys.* **2005**, *122*, 014109.
- 89.** Matito, E.; Solà, M.; Salvador, P.; Duran, M. *Faraday Discuss* **2007**, *135*, 325.
- 90.** Frisch, M. J.; Trucks, G. W.; Schlegel, H. B.; Scuseria, G. E.; Robb, M. A.; Cheesman, J. R.; Zakrzewski, V. G.; Montgomery, J. A.; Strtmann, R. E.; Burant, J. C.; Dapprich, S.; Milliam, J. M.; Daniels, A. D.; Kudin, K. N.; Strain, M. C.; Farkas, O.; Tomasi, J.; Barone, V.; Cossi, M.; Camme, R.; Mennucci, B.; Pomelli, C.; Adamo, C.; Clifford, S.; Ochterski, J.; Petersson, G. A.; Ayala, P. Y.; Cui, Q.; Morokuma, K.; Rega, N.; Salvador, P.; Dannenberg, J. J.; Malich, D. K.; Rabuck, A. D.; Raghavachari, K.; Foresman, J. B.; Cioslowski, J.; Ortiz, J. V.; Baboul, A. G.; Stetanov, B. B.; Liu, G.; Liashenko, A.; Piskorz, P.; Komaromi, I.; Gomperts, R.; Martin, R. L.; Fox, D. J.; Keith, T.; Al-Laham, M. A.; Peng, C. Y.; Nnsyskkara, A.; Challacombe, M.; Gill, P. M. W.; Johnson, B.; Chen, W.; Wong, M. W.; Andres, J. L.; Gonzalez, C.; Head-Gordon, M.; Replogle, E. S.; Pople, J. A. GAUSSIAN09, Revision A.02, Gaussian Inc., Pittsburgh (2009).
- 91.** Chen, W.; Schelgel, H. B. *J. Chem. Phys.* **1994**, *101*, 5957.
- 92.** Noodleman, L. *J. Chem. Phys.* **1981**, *74*, 5737.
- 93.** Noodleman, L.; Case, D. A. *Adv. Inorg. Chem.* **1992**, *38*, 423.

- 94.** Bickelhaupt, F. M.; Baerends, E. J. In *Reviews of computational chemistry*, vol 15. Lipkowitz, K. B.; Boyd, D. B. (Eds.) Wiley VCH, New York, **2000**, p 1.
- 95.** Baerends, E. J. In *Cluster models for surface and bulk phenomena*, Nato ASI series B, vol 283 Pacchioni, G.; Bagus, P. S. (Eds.) Plenum Press, New York, **1992**, p 189
- 96.** Chattaraj, P. K. (ed) *In: Aromaticity and metal clusters*. CRC, New York, **2011**.
- 97.** Grimme, S. J. *Comput. Chem.* **2004**, 25, 1463.
- 98.** Grimme, S. J. *Comput. Chem.* **2006**, 27, 1787.
- 99.** Ochsenfeld, C.; Koziol, F.; Brown, S. P.; Schaller, T.; Seelbach, U. P.; Klärner, F. G. *Solid State Nucl. Magn. Reson.* **2002**, 22, 128.
- 100.** Ochsenfeld, C. *Phys. Chem. Chem. Phys.* **2000**, 2, 2153.
- 101.** Ochsenfeld, C.; Brown, S. P.; Schnell, I.; Gauss, J.; Spiess, H. W. *J. Am. Chem. Soc.* **2001**, 123, 2597.

CHAPTER 4

Effect of charge transfer and periodicity on the magnetism of [Cr(Cp)₂][ETCE]*

Abstract

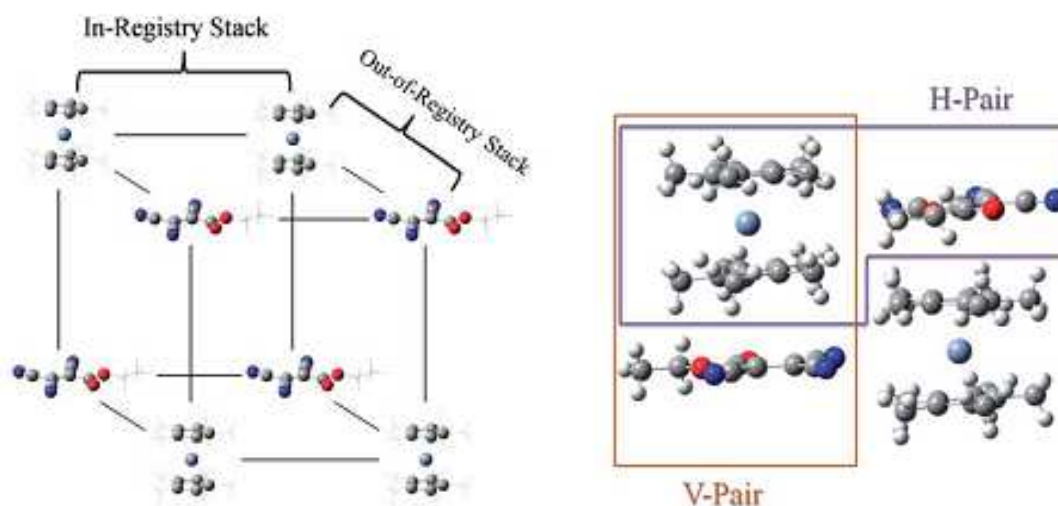
Magnetism in metallocene based donor–acceptor complexes stems from the donor to acceptor charge transfer. Thus, to correlate the exchange coupling constant J and the charge transfer integral, a formalism is developed which enables one to obtain the coupling constant from the value of the charge transfer integral and the spin topology of the system. The variance in the magnetic interaction between donor and acceptor is also investigated along two perpendicular directions in the three dimensional crystal structure of the reference system, decamethylchromocenium ethyl tricyanoethylenecarboxylate [Cr(Cp*)₂][ETCE]. These donor–acceptor pairs (V-pair and H-pair), oriented along vertical and horizontal directions respectively, are found to have different extents of J , which is attributed to the difference in exchange coupling mechanisms, viz., direct exchange and superexchange. Next, V-pair and H-pair are taken together to treat both the intrachain and interchain magnetic interactions, since this competition is necessary to decipher the overall magnetic ordering in the bulk phase. In fact, this truncated model produces a small positive value of J supporting the weak ferromagnetic nature of the complex. Lastly, a periodic condition is imposed on the system to comprehend the nature of magnetism in the extended system. Interestingly, the ferromagnetism, prevailing in the aperiodic system, turns into weak antiferromagnetism in the periodic environment. This is explained through the comparison of density of states (DOS) plots in aperiodic and periodic systems. This DOS analysis reveals proximity of the donor and acceptor orbitals, facilitating their mixing in periodic conditions. This mixing causes the antiferromagnetic interaction to prevail over the ferromagnetic one, and imparts an overall antiferromagnetic nature in periodic conditions. This change over in magnetic nature with the imposition of periodicity may be useful to understand the dependence of magnetic behavior with dimensionality in extended systems.

4.1. Introduction

The synthesis and characterization of charge transfer (CT) ferromagnetic compound $[\text{Fe}(\text{Cp}^*)_2][\text{TCNE}]$ ($\text{Cp}^* = \eta^5\text{-C}_5\text{Me}_5$ and $\text{TCNE} = \text{tetracyanoethylene}$) by Miller *et al.* in 1985 was a breakthrough in the field of metallocene-based magnets.¹ This was the first reported complex where the unpaired electron of a p -orbital also participates in the exchange interaction along with metal d -electrons. Nanoscale charge transfer is also known to have widespread application in sensors, photonics, electrocatalysis, solar photoconversion, molecular electronics and soon.² The occurrence of charge transfer in organoligand–metal fragments is found to induce a high dielectric polarization and concomitant intense nonlinear optical (NLO) response.³ Long spin coherence time in such materials renders them as potential candidates for high-density information storage and also for quantum computing.⁴ Their applicability can further be proliferated by simply tuning their magnetic interaction through simple adjustment of organic fragments therein. All these facts tantalize the scientific community to explore a plethora of such metallocene based charge transfer complexes (MBCTCs).^{5–7} In these compounds such as $[\text{M}(\text{Cp}^*)_2][\text{TCNE}]$ ($\text{M} = \text{Cr}, \text{Mn}$ or Fe); $[\text{M}(\text{Cp}^*)_2]$ fragment donates one electron from the magnetic orbital of the metal to the initially diamagnetic $[\text{TCNE}]$ part. This leads to ferromagnetic interaction among the localized spins on the donor part (D^+) and the acceptor part (A^-).⁷ Divergent mechanisms have been proposed for the spin exchange in these CT salts. One such proposition is the McConnell-II mechanism where the stability of a particular spin state is attributed to the interaction of ground spin state and lowest excited state of same spin multiplicity.⁸ Miller *et al.* supported this mechanism assuming a forward charge transfer from the donor to the acceptor leading to the triplet excited state.^{7b} In $[\text{Fe}(\text{Cp}^*)_2]^+[\text{TCNE}]^-$, the triplet ground state becomes stabilized through its interaction with the lowest lying triplet excited state.^{8c} However, in case of $[\text{Mn}(\text{Cp}^*)_2]^+[\text{TCNE}]^-$ and $[\text{Cr}(\text{Cp}^*)_2]^+[\text{TCNE}]^-$, the interaction between the ground and excited states leads to the stabilization of the antiferromagnetic situation which is in opposition to the experimentally reported high spin state of the molecules. Hence, the McConnell-II mechanism based explanation appears insufficient to justify this observation.^{7b,c,9} To explain this anomaly, Kollmar and Kahn coined a new mechanism of back charge transfer from A^- to D^+ , which is justified by the presence of positive spin density on Cp^* ring.^{9b} Another proposition is McConnell-I mechanism,¹⁰ where a large positive spin density on the transition metal induces a negative spin density on Cp^* ring, which again induces a positive spin density on the acceptor. These conflicting mechanisms about the origin of magnetic nature in MBCTCs urge for the development of a complete theoretical model.^{7b}

To investigate the charge transfer induced magnetic interaction in the MBCTCs, the compound *decamethylchromocenium ethyl tricyanoethylenecarboxylate* $[\text{Cr}(\text{Cp}^*)_2][\text{ETCE}]$ is taken as the representative system in the present work. This complex is recently synthesized by Wang *et al.* and found to have a ferrimagnetic ordering.¹¹ This ferrimagnetism may arise from the competition of ferro- and antiferro-magnetic interactions in three different lattice dimensions as interestingly probed by Datta and Misra.¹² The $[\text{Cr}(\text{Cp}^*)_2][\text{ETCE}]$ is known to crystallize in orthorhombic geometry with parallel arrangement of vertical one dimensional

D^+A^- chains. These one dimensional chains in a crystal can have two possible parallel orientations. In one type, the D^+ segments are oriented side by side and termed as in registry chains (Figure 4.1a). On the other hand, in the out of registry chains, D^+ finds A^- in the neighboring chain in its nearest position (Figure 4.1).^{11,13} The D^+A^- pair of a vertical chain is defined as the V-pair in this work (Figure 4.1b). As the nearest neighbor spin interaction is known to govern the magnetic nature of any system,¹³ a nearest D^+A^- pair from the horizontally stacked out of registry chains is selected for this investigation. This D^+A^- pair, where the D^+ and A^- belong to two different vertical columns arranged in an out of registry manner which is termed as H-pair in this work (Figure 4.1b). Although, the origin of ferromagnetism in the V-pair has been well explained by McConnell-I mechanism,¹⁰ the weak ferromagnetic ordering of H-pair is not yet addressed properly.¹¹



(a) Three dimensional motif of $[Cr(Cp^*)_2][ETCE]$ (b) Out of registry D^+A^- pairs

Figure 4.1. (a) Representation of the in registry and out of registry chains (b) blue and brown rectangles in the out of registry chains designate the H-pair and V-pair respectively.

This study makes an attempt to address the charge transfer induced magnetism in a particular MBCTC, $[Cr(Cp^*)_2][ETCE]$, keeping three different goals in its focus. Primarily, the charge transfer in between donor and acceptor is explored and the donor–acceptor magnetic coupling is quantified in terms of this charge transfer energy. Secondly, the architecture of this complex hints towards a different degree of magnetic interaction between the donor and the acceptor in V-pair and H-pair. In the V-pair, the d -electrons on Cr can be transferred to the acceptor via Cp^* bridge;¹⁴ whereas, absence of any such mediator in case of H-pair obstacles the CT process. The difference in horizontal and vertical direction definitely has an important role in governing the overall magnetic nature of this crystal. This stimulates us to investigate the nature of magnetic interaction in the V-pair and H-pair individually and

in presence of each other. Lastly, we cultivate the role of periodicity in governing charge transfer and concomitant magnetic interaction. Dealing with such extended system also enables one to explore the effect of dimension on magnetic characteristics. The systems in reduced dimension are found to depart from their usual bulk behavior which inspires the study of electronic properties in nano scale.¹⁵ Intensified magnetism in the reduced dimension has recently been the subject of several theoretical and experimental investigations.¹⁶ This fact has already been realized in cases of Au-nanoparticle, alkali metal clusters, Mn nanosheet and many other systems.^{16e,h,17} All these facts spur the study of the effect of periodicity on the magnetic behavior of $[\text{Cr}(\text{Cp}^*)_2][\text{ETCE}]$.

4.2. Theoretical Framework

The magnetic sites in a system are characterized by a non-vanishing spin angular momentum quantum number, S_i . Interaction among these localized spin moments govern the overall magnetic nature of the system. The magnetic interaction, often termed as exchange coupling is described by the well-known phenomenological Heisenberg–Dirac–van Vleck (HDvV) Hamiltonian, which describes the isotropic interaction between localized magnetic moments S_i and S_j as

$$\hat{H} = -\sum_{i<j} J_{ij} S_i S_j \quad (4.1)$$

where, J_{ij} is the exchange coupling constant between the localized spin moments, and the i, j symbols indicate that the sum extends to the nearest neighbor interactions only. According to the spin Hamiltonian in eqn (4.1), a positive (negative) value of J_{ij} corresponds to a ferromagnetic (antiferromagnetic) interaction, thus favoring a situation with parallel (antiparallel) spins. Symmetrically equivalent magnetic sites must necessarily have equal amplitude of spin density which imposes a delocalized solution for the system. Thus, such “full-symmetry” calculations are unable to consider the weakly coupled limit, where the electrons are fully localized.¹⁸ Therefore, the removal of all symmetry elements connecting the magnetic centers is necessary to account for weak coupling limit. Noodleman and co-workers worked out a “broken-symmetry” (BS) approach, where the space and spin symmetry can be removed by polarizing the up-spin and down-spin onto different magnetic centers.¹⁹ Later on, Bencini and Ruiz modified this expression for the limit of strongly interacting magnetic sites.²⁰ On the other hand, Yamaguchi's expression encompasses the appropriate limit, depending on the interaction strength and thus fulfils the criterion of general applicability,²¹

$$J_{ij} = \frac{E^{HS} - E^{BS}}{\langle \hat{S}^2 \rangle^{BS} - \langle \hat{S}^2 \rangle^{HS}}. \quad (4.2)$$

The general applicability of the eqn (4.2) can be understood through the following dependence of $\langle \hat{S}^2 \rangle$ on the overlap of magnetic orbitals²²

$$\langle \hat{S}^2 \rangle = M_S(M_S + 1) + N_\beta - \sum_{i,j}^{N_\alpha, N_\beta} (O_{ij}^{\alpha\beta})^2. \quad (4.3)$$

Here, $O_{ij}^{\alpha\beta}$ is an integral describing the overlap between the spatial parts of α and β spin orbitals.^{22,23} In the strong coupling limit, all pairs of α and β orbitals overlap and the double sum in eqn (4.3) is reduced to N_β . Therefore, the total spin expectation value indicates a pure spin state with $\langle \hat{S}^2 \rangle_{BS} = 0$ for a diradical with equal number of α and β electrons. Hence, the denominator in eqn (4.2) transforms to $S_{HS}(S_{HS} + 1)$ which resembles the Noodleman–Bencini–Ruiz formula.²⁰ On the other hand, if magnetic orbitals do not overlap (BS determinant), the sum in eqn (4.3) becomes $N_\beta - 2S_A$, where S_A is the sum of α and β magnetic orbitals. In this weakly coupled limit, $\langle \hat{S}^2 \rangle_{BS} = 2S_A = S_{HS}$ and resembles Noodleman's original expression.²³ The BS state is usually constructed by mixing two magnetic orbitals which usually belongs to different irreducible representations.^{19,20b} So, the magnetic orbitals should be close enough in order to interact with each other. Hence, for the remote magnetic sites, the construction of BS state becomes difficult. However, the BS state is usually achieved by performing HF or DFT in spin-unrestricted formalism where up-spin and down-spin densities are allowed to localize on different centers.^{20b} Though an open shell singlet state can best be represented through multi-configuration techniques;²⁴ DFT uses a single Slater determinant to describe the BS state and thus becomes more advantageous than post-HF methods in handling larger systems.^{20b}

As discussed in the introduction, the donor–acceptor magnetic coupling is induced by electron transfer from donor to acceptor. Among the various models of charge transfer in electronic systems, a perturbative treatment has widely been adopted to account for the electron tunnelling process.²⁵ Anderson in his pioneering work, derived the second order perturbation energy (DE) for such an intersite charge transfer and correlated this energy with magnetic interaction as,²⁶

$$\Delta E = \frac{t_{ij}^2}{U} \left(\frac{1}{2} + 2\hat{S}_i \hat{S}_j \right). \quad (4.4)$$

Here, t_{ij} is the hopping integral which carries an electron from site i to site j and U is the single ion repulsion energy. However, this t^2/U term is well-known in the Hubbard model and related to the exchange coupling constant (J).²⁷ In their seminal works Calzado et al. Applied ab initio CI techniques to compute these individual contributions to the magnetic coupling constant using effective Hamiltonian theory.²⁸ However, in a recent formalism, instead of direct estimation of this t^2/U term; the above expression is modified to estimate the coupling constant (J_{SX}) in a superexchange process in terms of the second order perturbation energy (ΔE) for charge transfer between sites and spin population on those centers (ρ_i and ρ_j),²⁹

$$J_{SX} = \frac{2\Delta E}{1 + \rho_i \rho_j}. \quad (4.5)$$

The charge transfer matrix element between the donor and acceptor can be expressed as^{30–33}

$$H_{DA} = \frac{E_D - E_A}{2}. \quad (4.6)$$

where, H_{DA} is a pure one electron matrix element, coupling the effective donor and acceptor orbitals as

$$H_{DA} = \langle \phi_D | \hat{H} | \phi_A \rangle. \quad (4.7)$$

and, E_D and E_A are the energies of the LUMO in cationic donor and neutral acceptor. Again, the second order perturbation energy (ΔE) for the charge transfer process is related to the transfer matrix element H_{DA} for the donor–acceptor pair in the following manner,³⁴

$$\Delta E = \frac{|H_{DA}|^2}{E_D - E_A}. \quad (4.8)$$

Now, substituting $2\Delta E$ term in eqn (4.5), using eqn (4.8) and (4.6), the following modified form is obtained,

$$J_T = \frac{H_{DA}}{1 + \rho_D \rho_A}. \quad (4.9)$$

This can be conveniently used to calculate the exchange coupling constant value (J_T) in electron transfer systems.

4.3. Computational Details

In the present work, the effective exchange integral J is estimated in two approaches, one of which is the state-of-the-art spin projection technique of Yamaguchi (eqn (4.2)). In the second approach, the electron transfer matrix element for charge transfer from donor to acceptor and the spin populations on the donor and acceptor sites are used to estimate J through presently derived eqn (4.9). The eqn (4.2) is generally implemented through an unrestricted or spin polarized formalism, where the up-spin and down-spin densities are allowed to localize on magnetic sites.^{21,22} Thus, in the present work unrestricted DFT (U-DFT) is applied to compute the coupling constant. The same U-DFT method is adopted to derive the parameters in eqn (4.9). The U-DFT method is reported to produce a reliable estimate of such transfer integrals, at least in cases of metal-based systems.³⁵ To evaluate J through eqn (4.9), standard DFT calculation on the isolated donor and acceptor molecules is first carried out to extract the energies of the LUMO of the cationic fragment $[\text{Cr}(\text{Cp}^*)_2]^+$ and that of the neutral acceptor [ETCE]. These energy values along with the spin populations on the donor and acceptor in the ground state of dimer $[\text{Cr}(\text{Cp}^*)_2]^+[\text{ETCE}]^-$ are utilized to compute the J_T in eqn (4.9).

To understand the magnetic effect of V-pair on H-pair and vice versa in the crystal motif of $[\text{Cr}(\text{Cp}^*)_2][\text{ETCE}]$, it becomes necessary to estimate the exchange-coupling constant between every D^+A^- pair in vertical and horizontal directions in presence of each other. A recently adopted technique to determine J in a system with multiple magnetic sites becomes useful in this regard.³¹ In this particular strategy, which is mentioned as the “dummy approach” in the present work; first the effect of all the magnetic sites on each other is realized in the form of ground state spin population. Then the exchange coupling constant between any two magnetic sites is calculated on the basis of their ground state spin population while regarding other magnetic sites inert. However, in the present context the computational scheme of ref. 31 is applied on a 2D crystal motif displayed in Figure 4.1b so as to consider both the direct exchange and superexchange in the H-pair and V-pair respectively. The spin density distribution of this system is first obtained. Next, the exchange coupling for one V-pair is computed while its neighboring V-pair is made dummy. Although, other than a specific magnetic pair all other magnetic sites are made dummy, their effect is imposed on the specific pair in terms of pre-calculated spin population which can be understood from the spin density parameterization of the Heisenberg Hamiltonian.³¹

In order to investigate the effect of periodicity on the magnetic interaction, the periodic boundary condition is imposed on the system. To deal with the extended solid, different level of theoretical platforms are used which ranges from the simple tight-binding model to the ab initio periodic Hartree–Fock and modern DFT based methods.³³ The eigenstates of such periodic system can be labelled by the reciprocal lattice vectors, \mathbf{k} , in the first Brillouin zone (BZ).³³ Since the system is infinite, the quantum numbers \mathbf{k} are continuous. Calculation of the total energy requires a self-consistent calculation of the eigenvalues, which are performed at a finite number of points in the Brillouin zone.³⁴ A recent work expresses the charge transfer integral as the function of \mathbf{k} point³⁶ and thus

stimulates us to investigate the influence of increasing k point (within the first BZ) on the charge transfer induced magnetism.

The structure of the complex is available in crystallographic file format,¹¹ this geometry of the complex is taken as its ground state structure. While doing the periodic boundary calculation with different k points, the Perdew–Burke–Ernzerhof exchange and correlation functional (PBE) is employed.³⁷ This exchange correlation functional is found to produce superior accuracy for a broad variety of systems under periodic boundary conditions.³⁸ This advanced GGA functional includes some electron correlation effects at larger distances. The LANL2DZ basis set is chosen selectively for Cr atoms and 6-311++g(d,p) for all other atoms and this has been maintained throughout for DFT calculations. The success of exchange correlation functionals in accurate estimation of J is believed to be intrinsically linked to the introduction of an amount of Hartree–Fock (HF) exchange.³⁹ In this regard, the B(X)LYP functional is prescribed as the optimum performer, where X is related to the percentage of Fock exchange.⁴⁰ However, Martin and Illas have shown that the coupling constant vary with X and the result becomes satisfactory with X=50.⁴¹ Hence, in this work we use BHandHLYP functional with X=50, which has already been found efficient to reproduce the experimental value of coupling constant.⁴² This particular functional is characterized to be a 1 : 1 mixture of DFT and exact exchange energies which can be represented as $E_{XC}=0.5E_{HF}^X + 0.5E_{LSDA}^X + 0.5\Delta E_{Becke88}^X + E_{LYP}^C$.⁴³ This is also supported by Caballolet *al.*⁴⁴ who have concluded that functionals assuming fully delocalized open shell magnetic orbitals, such as B3LYP, produce a poor description of local moments.⁴¹ Particularly, the B3LYP functional is reported to produce inaccurate structural and thermochemical parameters in the extended systems due to its failure to attain homogeneous electron gas limit.⁴⁵ On the contrary, another school of thought advocate the use of B3LYP with less amount of HF exchange to get a reliable estimate of J .⁴⁶ Nevertheless, the hybrid functionals are questioned for their tendency to overstabilize the higher spin multiplet, whereas the GGA functionals overestimate the stability of the ground state.⁴⁷ On the other hand, the hybrid meta GGA functional TPSSh with 10% HF exchange shows a minimum deviation (10–15%) in the J value compared to experiment.⁴⁸ Thus, among several other functionals, the TPSSh functional is chosen by several groups for evaluating the exchange coupling constant.⁴⁹ In order to get a self-consistent result, here also a set of exchange correlational functionals is applied to compute the exchange coupling constant. The results obtained with DFT are also validated with the multireference Complete Active Space Self-Consistent Field (CASSCF) technique, based on the active electron approximation. This technique incorporates several important physical effects in both direct exchange and superexchange cases for the calculation of magnetic interaction.⁵⁰ However, the CAS method disregards important physical mechanisms like ligand-spin polarization, dynamic spin polarization, double spin polarization etc. and underestimates the coupling constant in effect.⁵¹ These effects can be included through the second order perturbation theory based upon the UHF wave function. The complete active space second-order perturbation theory (CASPT2) is a method which imposes second order correction to the CAS wave functions, and found useful in producing J close to experimental values.⁵² This method can further be refined by considering “external correlation” through multireference configuration interaction

(MRCI) tools,⁵³ among which the difference dedicated CI(DDCI) approach by Miralles et al. has been particularly successful to produce the desired degree of accuracy.⁵⁴ However, to avoid computational rigor associated with such sophisticated methods, in the present work the CASSCF is used with a large active space which includes different configurations connected to charge transfer excitation,⁵⁵ and thus partially overrule the limitations of CASSCF. An active space often electrons in nine orbitals [CASSCF (10, 9)] is used to calculate the exchange coupling constant of the V-pair in this work. All calculations are performed using Gaussian 09W suite of quantum chemical package.⁵⁶ The density of states (DOS) plots are generated with GaussSum 2.2.⁵⁷

4.4. Results and Discussion

Before dealing with the present dimeric system $[\text{Cr}(\text{Cp}^*)_2][\text{ETCE}]$, first the ground states of monomers (D and A) are taken for pursuit. Since, there exists a probability for the neutral $[\text{Cr}^{\text{II}}(\text{Cp}^*)_2]$ to remain in the low-spin triplet or high-spin quintet state, it requires a theoretical confirmation. The ground state of the monomers is thus checked with different DFT functional. These results are also compared with multireference CASSCF to verify the reliability of DFT methods in properly describing the ground state of the monomers. Everywhere, the ground state is recognized as the low-spin triplet (Table B.S1 in Appendix B), which is also reported experimentally.⁴² Concerning to an orbitally degenerate ground state of $[\text{Cr}^{\text{II}}(\text{Cp}^*)_2]$, Cr^{2+} ion is supposed to experience a quenching of the orbital angular momentum due to static Jahn–Teller (JT) effect.⁵⁸ Moreover, the Cr ion in the D^+A^- species is also reported to be reluctant to magnetic hysteresis and exhibit no magnetic anisotropy.¹¹ The neutral acceptor unit, which initially exists in singlet ground state, turns into an anionic doublet after accepting an electron from neutral donor, leaving the donor in cationic quartet state. The overall quintet spin state in $[\text{Cr}(\text{Cp}^*)_2][\text{ETCE}]$ dimer, with three *d*-electrons on the Cr atom and one in the acceptor unit finds validation in its spin density plot and references of similar systems.^{11,9b} From the molecular orbital (MO) analysis of V-pair and H-pair, 131 to 134 MOs appear as singly occupied molecular orbitals (SOMO), of which 133 α MO is found to be composed of the acceptor orbitals solely in both the pairs (Figure 4.2). Since, the computations are performed at U-DFT level, all the occupied orbitals are in fact possessed by single electrons. Thus, here the SOMOs are referred to as the α -occupied MOs which do not have any β -counterpart of comparable energy.

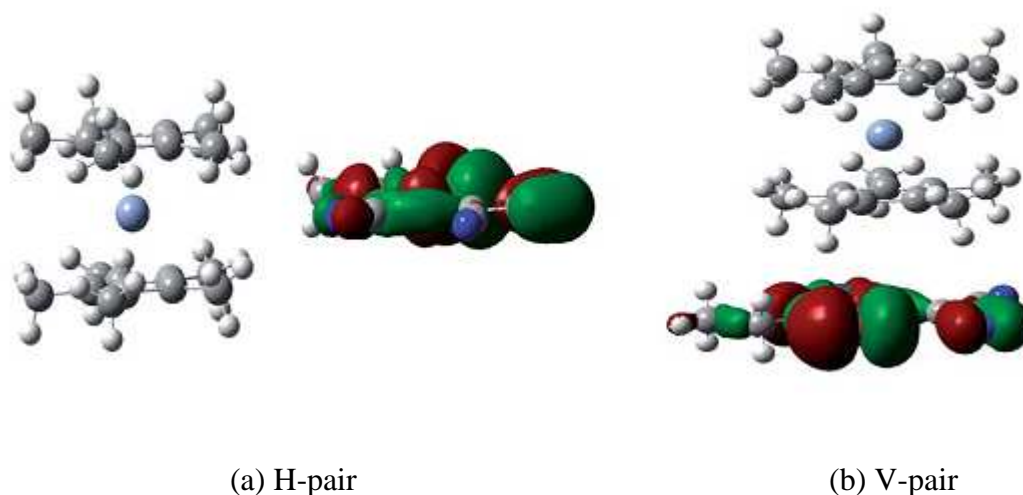


Figure 4.2. The 133rd α -SOMO in (a) H-pair, and (b) V-pair, solely centered on the acceptor.

Existence of this MO advocates for the single electron transfer to the acceptor moiety. Rest of the SOMOs shows an equitable contribution of Cp* and ETCE orbitals. Although in such complexes metal d -orbitals are reported as magnetic orbitals,¹³ in the present case any contribution from Cr d -orbitals is found surprisingly missing in the construction of the highest occupied α -MOs. This contradiction probably stems from the non-Aufbau kind of behavior, where the singly occupied metal orbitals are buried below doubly occupied orbitals.⁴⁴ The density of states (DOS) plot which shows the highest occupied β -spin orbitals at higher energy levels than the highest occupied α -MOs (Figure 4.3) also supports this observation. This problem is often encountered in systems having bonds with prevalently ionic character. Due to this rearrangement of the electrons in shuffled MOs, the contribution of d -orbitals is found in 126, 127 and 128 α -MOs which are below the so called SOMOs. However, applying spin projection technique (eqn (4.2)), the coupling is found to be very weak ($J = 0.004 \text{ cm}^{-1}$) in the H-pair, compared to V-pair ($J = 511 \text{ cm}^{-1}$). Though weakly coupled, the H-pair takes a decisive role in setting up the gross magnetic behavior in such crystals.^{6b}

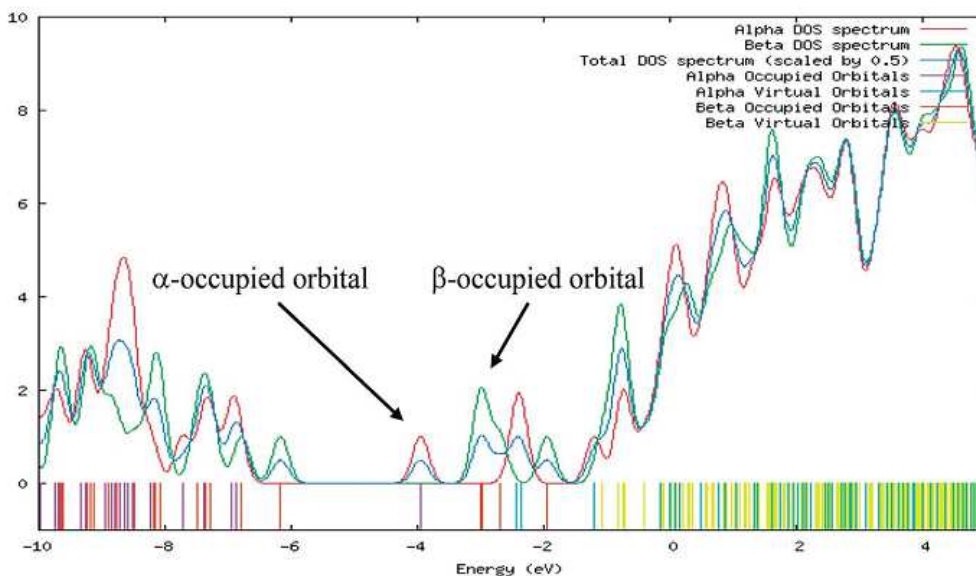


Figure 4.3. The DOS plot of the V-pair.

Now, to understand the charge transfer phenomenon, the electronic configuration of D^+ and A^- in the V-pair is compared with its neutral analogues (D^0 and A^0). From the comparison of the molecular orbitals of the individual D^0 and A^0 units, it appears that the electron transits from the 86th β -orbital of D^0 to the 46th α -MO of A^0 . In the receptor part, the antibonding nature of the olefinic C–C orbitals further clarifies that this is the π^* MO (Figure 4.4). This analysis, performed in the background of monomer approach, also provides necessary information for the appropriate selection of donor and acceptor orbitals, participating in the charge transfer process. To trace the charge transfer process, the system is analyzed at the transition state, when one electron is being transferred from the donor β -orbital to the π^* MO of the acceptor. It has been shown previously that the superexchange electronic charge resonance energy, which we have denoted here as $2\Delta E$ in eqn (4.5), can be substituted by the charge transfer integral (H_{DA}) or the direct vacuum electronic coupling term.⁵⁹ The initial and final states of electron transfer has been crucial in the determination of the two-state approximation. In determining the initial and final states of the electron transfer, the β -LUMO of the isolated donor D^+ is taken as the donor orbital since the electron was initially localized on that particular orbital. Whereas, in the acceptor part A, the α -LUMO is taken as the recipient orbital since the hopping electron is going to be localized on that orbital.⁴⁶ Using the energies of the concerned orbitals, the magnetic exchange coupling constant is estimated as 514 cm^{-1} through eqn (4.9) (at UBH and HLYP/6-311++g(d,p) with LANL2DZ extrabasis on Cr) which is in reasonable agreement with the J , estimated at same level of theory through the famous spin projection technique (eqn (4.2)) of Yamaguchi (Table 4.1). To compare these values obtained through DFT, a more accurate CASSCF technique is adopted as well, which is capable to describe the multireference character of involved radicals. The CASSCF wave function is constructed allowing all possible combination of ten electrons in nine orbitals resulting in a CASSCF (10,9) active space. The active space includes SOMOs, i.e., Cr d_z^2 , $d_{x^2-y^2}$ and d_{xy} -orbitals on the donor fragment and also the singly occupied π^* -orbital on the acceptor fragment. The orbitals, which on a test calculation using a

larger active space (namely a 14 electrons and 11 orbitals space), shows an occupancy of 1.99 electrons, are moved to core orbitals. The chosen active orbitals are shown in Figure 4.5. From Table 1, the chosen functional BHandHLYP and CASSCF are found to produce similar value of exchange coupling constant. Moreover, in all the methodologies, same kind of spin density alternation (up–down–up) in Cr–Cp*–ETCE is observed, which is indicative of the superexchange mechanism (see Table B.S2 in Appendix B).

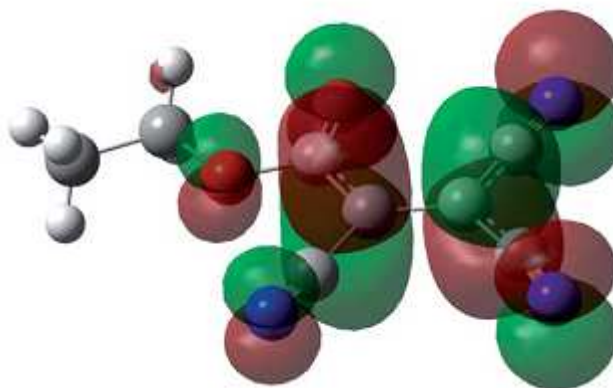


Figure 4.4. The 46th α -MO of acceptor unit in both of the V-pair and H-pair.

Table 4.1. Comparison of coupling constant values (J) for the V-pair, obtained through different methodology.

Level of theory	J in cm^{-1}
BHandHLYP/6-311++g(d,p) with LANL2DZ extrabasis on Cr	511
CASSCF(10,9)/LANL2DZ	439

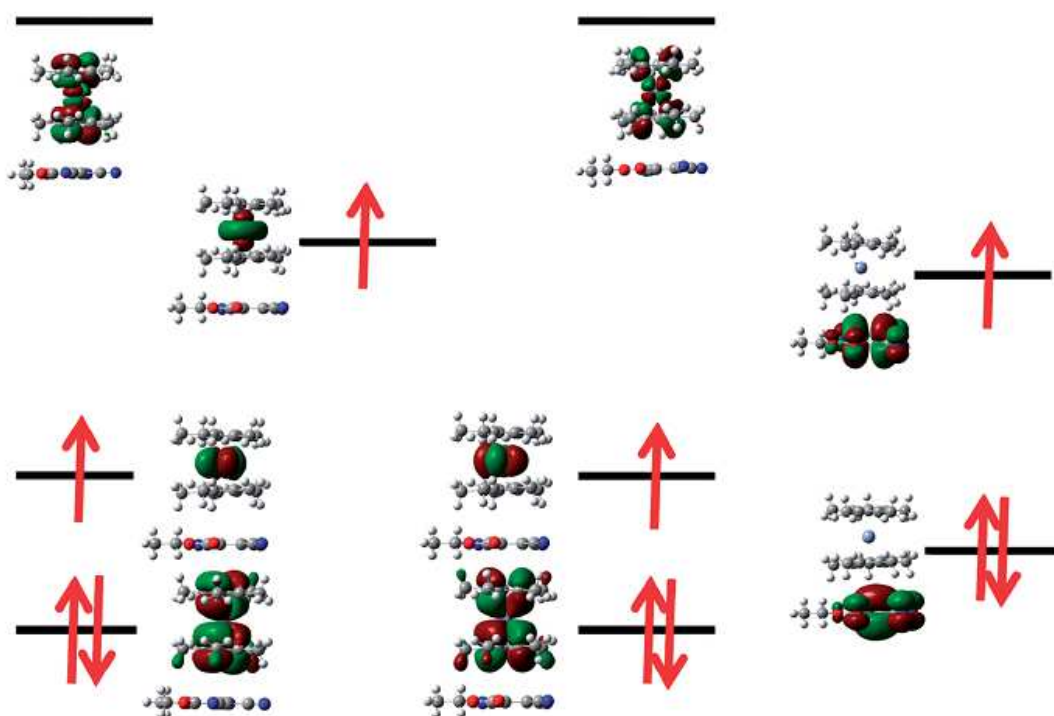


Figure 4.5. A qualitative MO diagram of the chosen active space for the CASSCF calculation, containing 10 electrons in 9 orbitals.

4.4.1. Competition between exchange mechanisms

So far the spin topology of the V-pair is concerned, it is interesting to note significant spin density on Cp* moiety which intervenes the magnetic sites Cr and the acceptor ETCE. This observation suggests that bridging Cp* ligand is playing a role to couple the spins on Cr and ETCE through superexchange process. The spin density alternation further affirms the possibility of superexchange.⁴⁷ The spin density alternation in the V-pair also justifies the McConnell-I mechanism, according to which, the majority spin on the metal atom induces a negative spin density on the Cp* motif, which in its turn spawns positive spin density on the acceptor part. On the other hand, absence of any such bridging ligand in between the magnetic sites of H-pair makes direct exchange the only mechanism for the interaction of spins. Earlier studies pointed out two such contributions to the magnetic coupling;

$$\begin{aligned}
 J &\equiv J_F \left(\text{for FM interaction} \right) + J_{AF} \left(\text{for AFM interaction} \right) \\
 &= 2K_{ij} - 4 \frac{t_{ij}^2}{U}
 \end{aligned}
 \tag{4.10}$$

where K_{ij} describes direct exchange between magnetic orbitals and generally considered as ferromagnetic contribution.⁴⁸ The second part, including the hopping integral t_{ij}^2 and the on-

site Coulomb repulsion U , is usually termed as kinetic exchange in Anderson's interpretation and antiferromagnetically contributes to the total coupling constant.⁴⁹ In a model proposed by Heitler and London, J is similarly split into ferro- and antiferro-magnetic parts

$$J = K + 2\beta S . \quad (4.11)$$

The first part, being the two-electron exchange integral is necessarily positive; whereas the second part contains resonance integral (β) and an overlap integral (S), which are of opposite sign and thus their product becomes negative. Hence, the value of overlap integral plays a crucial role in controlling the overall nature of magnetic interaction.^{9b} However, the value of direct exchange coupling constant, estimated through spin projection technique, in case of H-pair is found to be very weak (0.004 cm^{-1}) compared to that (511 cm^{-1}) in case of V-pair, where the superexchange is operative. This observation is in agreement with Anderson's explanation where the superexchange is argued to be more intense than direct exchange on the basis of metal–ligand overlap.^{48b} The direct exchange interaction is considered to be comparatively weaker because it operates between spatially orthogonal wave functions.⁵⁰ Further, the degree of exchange is found to be largely affected from the distance between the magnetic sites.⁵¹ Hence, the large distance of 7.248\AA between the donor and acceptor in H-pair is another reason for the weaker direct exchange compared to superexchange. This observation is in agreement with the result of theoretical and experimental works, executed on similar systems,⁵⁷ where the intrachain (V-pair) magnetic interaction is found to be much stronger than interchain (H-pair) interaction.

Though weak, the interchain coupling takes a significant role in deciding the overall magnetic ordering of the system.^{6b,11,57} Hence, both of these V-pair superexchange and H-pair direct exchange are to be simultaneously taken into account to explain the bulk magnetic behavior. As a replica of the bulk system, a two-dimensional (2D) motif of the crystal (Figure 4.1b) is scooped out where both H-pair and V-pair are present. Next, following the computational strategy stated in ref. 31, the second vertical column is made dummy in order to compute the coupling constant in the 1st V-pair. The exchange interaction between the donor–acceptor pair in horizontal direction is quantified through similar approach. A comparable approach requires embedding the central unit in a field of point charges.⁶⁰ Inclusion of neighboring units is found to be a good approximation to the bulk property.⁶¹ The value of coupling constant (J_D), obtained in this way for the V-pair considerably decreased to 13 cm^{-1} compared to the earlier computed J value of 511 cm^{-1} (Table 4.1). On the other hand, in the H-pair there is a slight increase (0.007 cm^{-1}). This indicates some kind of antagonism between direct exchange and superexchange. Since this truncated model reproduces the bulk-behavior, the coupling constant of this system is ideal to compare with that obtained from experimental data.

The value of J drastically decreases in a two-dimensional system, compared to that in the single V-pair. A close comparison of the parameters, required to get coupling constant from eqn (4.2), reveals that except the energy of BS state all other factors are nearly same in single pair and 2D model. This clearly indicates that in the 2D model the BS state gets more stability compared to single D^+A^- pair, which can be attributed to the interchain interaction.

In the extended model, one single D^+A^- pair finds another such A^-D^+ pair in its neighbor, which causes a distortion in its equilibrium configuration.⁵⁷ Following the second order perturbation it can be shown that there is an orbital interaction between neighboring chains, which eventually stabilizes the broken-symmetry state.⁶² Moreover, the difference of spin density in these two situations, also contributes to such steep change in the value of coupling constant (see Figure B.S1 in Appendix B). A decrease of spin density is noticed in the two dimensional array due to dispersion of spin densities from magnetic sites, which affect the coupling constants. This fact finds its support from the recent works which advocate for an intimate relationship between the spin population and coupling constant.^{29,31}

4.4.2. Effect of periodicity

For a proper understanding of the magnetic interaction in the extended system, one must concentrate on studying the magnetic interaction as a periodic function. To gain an insight to the magnetic property in the periodic lattice system, periodic boundary condition is imposed on the system with the translational vectors 10.796 Å in the vertical direction and 16.161 Å in the horizontal direction. An attempt to compute the J value in the periodic boundary is failed in case of the horizontal pair because of the non-convergence of BS solution. This can be attributed to the large distance between donor and acceptor which does not allow mixing of the orbitals on magnetic centers and the BS state cannot be constructed in consequence. This fact is also ensured from a very weak value of coupling constant for H-pair. The electron tunnelling rate is also found to decay exponentially with distance.^{59,63} For this, the vertical pair is only chosen to investigate the effect of periodicity on its magnetism.

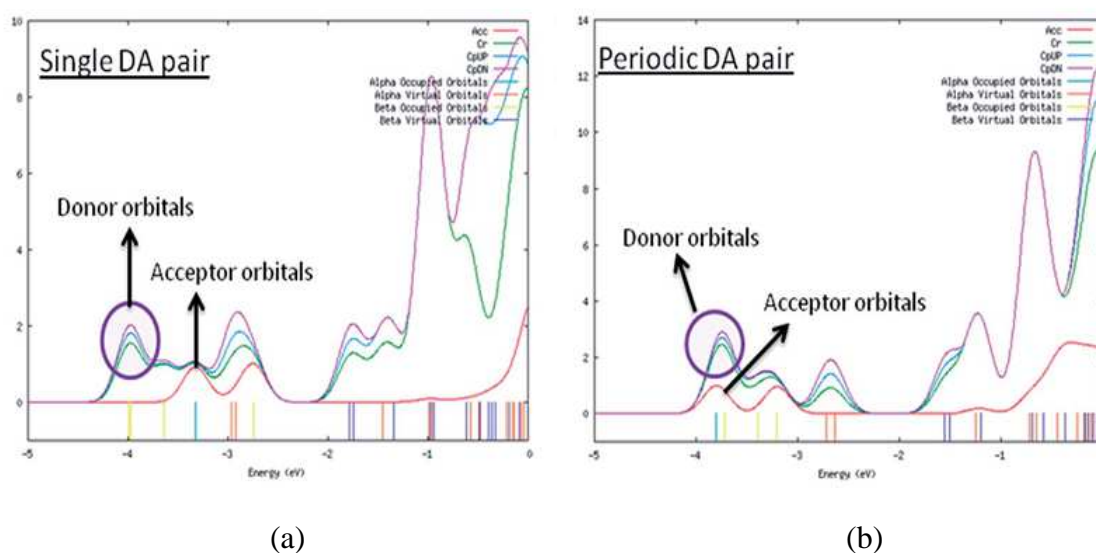


Figure 4.6. The density of states plots of the V-pair in (a) gas phase and (b) under periodic boundary condition.

It has been previously anticipated that the prediction of a local property, e.g., spin density for a system in cluster or in PBC are similar for a particular functional.⁶⁴ The comparison of spin density in PBE functional can be found in Tables B.S2 and B.S3 of Appendix B. A close inspection of Tables B.S2 and B.S3 reveals a change in the spin density

under PBC (see Table B.S3 in Appendix B). This is expected to bring about the variation in magnetic interaction. However, a variation in the choice of the k -point grid shows that after the 3rd k -point, the change in spin density becomes insignificant which implies the attainment of the bulk limit. Computation of magnetic exchange coupling constant with the constraint of periodic boundary reveals an antiferromagnetic (AFM) interaction in vertical direction. The AFM interaction in the V-pair under periodic boundary condition (PBC) is in the stark contrast to the positive value of coupling constant in absence of PBC. The change over from FM to AFM exchange within the periodic boundary condition may be argued to be arising out of this difference in functionals. To verify this, in absence of PBC the exchange coupling constant for the V-pair is also estimated using PBE functional in unrestricted framework which results in the J value of 133 cm^{-1} . This result shows that from the methodological point of concern, though the functional may alter the extent of coupling,⁶⁵ it cannot overturn the magnetic nature at least in the present case. Thus imposition of periodicity only can be attributed to such change in the magnetic behavior. This spin crossover can be understood in terms of charge transfer integral t_{ij} in eqn (4.4).⁶⁶ In this extended model, a particular donor (D^+) finds two acceptor units (A^-) below and above it unlike in the single V-pair. This increases the possibility of charge transfer, leading to the stabilization of AFM state. The exchange coupling constant under PBC is also calculated in the hybrid PBE0 functional for convenience,⁶⁷ which also predicts antiferromagnetic exchange in the periodic lattice. The results are given in Table B.S4 of Appendix B. The larger estimate of J produced by the hybrid PBE0 functional, in comparison to the pure PBE functional, can be explained due to the presence of a fraction of exact exchange which has a much larger extent than the DFT exchange considered in the pure functional. The AFM exchange coupling within the periodic boundary approach can further be envisaged as the effect induced by increasing the degrees of freedom of an electron. Thus the system gains stabilization in presence of PBC which can be confirmed from the energy comparison of V-pair, computed at same theoretical level [UPBEPBE/6-311++g(d,p) level with LANL2DZ as extrabasis on Cr atom]. The energy of the system without periodic boundary is -2445.135 a.u. and with the periodic boundary the energy is -2445.142 a.u. The periodic electron density can thus be assumed to be more delocalized which in turn induces a decreasing shift in Hubbard U parameter.⁶⁸ Now, there is a report of the lowering of energy of the d -states with increase in U parameter.⁶⁹ So, a decreasing shift in U should uplift the energy levels of d -states, which is apparent from the DOS plots in aperiodic and periodic conditions (Figure 4.6). Hence, a small value of U is expected in a periodic boundary formulation.⁶⁸ From the comparison of DOS plots in aperiodic and periodic systems, not only the upliftment of Cr d -states, but also the destabilization of Cp* ligands can be noticed. In addition, the up-spin orbital of acceptor lowers down in energy in the periodic condition. This situation brings the down-spin orbital of lower Cp* ring and the up-spin orbital of acceptor unit within the same energy range and thus facilitate their overlap in the periodic condition of the system. Hence, a small value of U together with non-zero value of S result in a stronger AFM interaction, which eventually supersedes the FM interaction and turns the system into a weak antiferromagnet in the periodic condition. However, the overall ferromagnetism in the bulk is manifested through an ensemble of different mechanisms.^{6b,66,70,71}

4.5. Conclusion

The phenomenon of charge transfer (CT) is of paramount impact in guiding the courses of several biological and chemical processes. In the present study, the charge transfer process is also found effective in governing the magnetic behavior of metallocene based charge transfer complexes. A recently synthesized system, $[\text{Cr}(\text{Cp}^*)_2][\text{ETCE}]$ is taken as the representative MBCTC to explore the influence of charge transfer on the magnetic behavior of such donor–acceptor complexes. Anderson in his pioneering work ascribed charge transfer as the origin of kinetic exchange and correlated this exchange with the second order perturbation energy for such charge transfer. In a recent work, using this approach of Anderson, the coupling constant is parameterized with spin population (eqn (4.5)). However, eqn (4.5) is employed to account for through bond charge transfer in a superexchange process. On the contrary, NBO analysis for the present system clarifies a zero overlap status in between the donor and acceptor, which necessitates the tunnelling of electron in its journey from the donor to the acceptor. Hence, in the present work, eqn (4.5) is modified to take the electron tunnelling matrix element (H_{DA}) into account to determine the coupling constant. This integral, is evaluated from the zeroth order eigenvalues of pure donor and acceptor at the transition state of the electron transfer process. The exchange coupling constant (J_{T}), obtained in this way (eqn (4.9)) is well in agreement with J , the coupling constant derived through well-known spin projection technique of Yamaguchi (eqn (4.2)). The charge transfer interaction happens to be the central in such type of complexes where the magnetic interaction begins after the charge dislocates from the donor to the acceptor creating one magnetic site at the acceptor.

The topological difference of V-pair and H-pair leads to the possibility of concurrent and competitive exchange interactions at different directions. In V-pair, the intervening Cp^* ring assists the transfer of electron from metal to acceptor unit and hence there operates the superexchange process in this direction. In the other direction, the donor and acceptor are far separated and there is no such aid for the spins to be transferred from the donor to the acceptor. Hence the direct exchange process becomes only viable in H-pair. From the comparison of the coupling constant values, the superexchange interaction is found dominant in between two exchange processes in $[\text{Cr}(\text{Cp}^*)_2][\text{ETCE}]$. Since, the weak interaction in the horizontal direction takes a decisive role to render overall magnetic ordering; the V- and H-pairs are simultaneously taken into account. This situation opens up the possibility of several exchange interactions among multiple magnetic sites, which is estimated through one of our earlier developed computational scheme, referred to as dummy approach within the text. The coupling constant value for the V-pair, obtained through this approach is found to be very low compared to the previous value, where only the V-pair is considered. The drastic decrease in the J value through dummy approach is attributed to the interchain interaction. The coexistence of competitive superexchange and direct exchange in this truncated model replicates the bulk behavior. The small positive value of J supports the weak ferromagnetic nature of this MBCTC by Wang *et al.*¹¹

It has been of optimal challenge to investigate the nature of magnetism in a crystal system. The best way to mimic the real network of spins of a cluster demands the application

of periodic boundary condition. The PBC can treat systems in bulk condition with much less computational effort without taking the finite size-effect and border-effect. Our calculation clearly shows that the magnetic interaction in one dimensional periodic lattice of such kind of system in the vertical direction is antiferromagnetic and the extent of magnetism is too low. Moreover, it is interesting to note that the FM system turns into an AFM one with imposition of periodic boundary condition. This change over in the magnetic status of the system is explained with the rearrangement of the density of states in $[\text{Cr}(\text{Cp}^*)_2][\text{ETCE}]$. In this condition, there occurs a simultaneous higher and lower energy shifts in the donor and acceptor orbitals respectively and the donor–acceptor overlap integral gains a non-zero value, which is otherwise zero in the system. This lift in energy of the d -states is also supported from the easy dispersion of alpha spin to the Cp^* ligand orbital. Hence, this situation facilitates electron delocalization and results a lower Hubbard U value. As a consequence of all these facts the $[\text{Cr}(\text{Cp}^*)_2][\text{ETCE}]$ which exhibits ferromagnetic coupling in the single D^+A^- pair, turns into a antiferromagnetic system in the periodic condition along vertical direction. However, the convolution of different exchanges pervading the crystal makes it a weak ferromagnet. An extended review on MBCTC divulges that there is a delicate balance in the sign of coupling constant in horizontal direction.⁶⁵ This weak, still competing magnetic interaction is regarded as the principle criterion for metamagnetism.⁷² However, this work suggests a delicate poise of magnetic interaction in the vertical direction as well.

4.6. References

1. (a) Miller, J. S.; Epstein, A. J.; Reiff, W. M. *Mol. Cryst. Liq. Cryst.*, **1985**, *120*, 27; (b) Miller, J. S.; Calabrese, J. C.; Rommelmann, H.; Chittipeddi, S. R.; Zang, J. H.; Reiff W. M.; Epstein, A. J. *J. Am. Chem. Soc.* **1987**, *109*, 769.
2. (a) Jortner J. and Ratner, M.; *Molecular Electronics, Blackwell Science, Cambridge, MA, 1997*; (b) Aviram A. and Ratner, M. *Molecular Electronics: Science and Technology (Annals of the New York Academy of Sciences), The New York Academy of Sciences, New York, NY. 1998*, vol. 852.
3. (a) Goovaerts, E.; Wenseleers, W. E.; Garcia M. H.; and Cross, G. H. *Nonlinear Optical Materials, in Handbook of Advanced Electronic and Photonic Materials and Devices, Academic Press, New York. 2001*; (b) Morall, J. P.; Dalton, G. T.; Humphrey M. G. Samoc, M. *Adv. Organomet. Chem.* **2008**, *55*, 61; (c) Powell C. E.; Humphrey, M. G. *Coord. Chem. Rev.* **2004**, *248*, 725; (d) Long, N. J. *Angew. Chem. Int. Ed. Engl.* **1995**, *34*, 21; (e) Di Bella, S.; Dragonetti, C.; Pizzotti, M.; Roberto, D.; Tessore F. Ugo, R. *Top. Organomet. Chem.* **2010**, *28*, 1; (f) Astruc, D. *Organometallic Chemistry and Catalysis, Springer, Heidelberg. 2007*; (g) Fuentealba, M.; Toupet, L.; Manzur, C.; Carrillo, D.; Ledoux-Rak, I. Hamon, J.R. *J. Organomet. Chem.* **2007**, *692*, 1099; (h) Lambert, C.; Gaschler, W.; Zabel, M.; Matschiner R. Wortmann, R.; *J. Organomet. Chem.* **1999**, *592*, 109.
4. (a) Carretta, S.; Santini, P.; Amoretti, G.; Guidi, T.; Copley, J. R. D.; Qiu, Y.; Caciuffo, R.; Timco G. Winpenny, R. E. P. *Phys. Rev. Lett.* **2007**, *98*, 167401; (b) Ardavan, A.; Rival, O.; Morton, J. J. L.; Blundell, S. J.; Tyryshkin, A. M.; Timco G. Winpenny, R. E. P. *Phys. Rev.*

- Lett.* **2007**, 98, 057201; (c) Leuenberger M. N. Loss, D. *Nature* **2001**, 410, 789; (d) Troiani, F.; Ghirri, A.; Affronte, M.; Carretta, S.; Santini, P.; Amoretti, G.; Piligkos, S.; Timco G. Winpenny, R. E. P. *Phys. Rev. Lett.* **2005**, 94, 207208; (e) Lehmann, J.; Gaita-Arino, A.; Coronado E. Loss, D. *Nat. Nanotechnol.* **2007**, 2, 312.
5. Yee, G. T.; Whitton, M. J.; Sommet, R. D.; Frommen C. M.; Reiff, W. M. *Inorg. Chem.* **2000**, 39, 1874.
6. (a) Kaul, B. B.; Durfee W. S. Yee, G. T. *J. Am. Chem. Soc.* **1999**, 121, 6862; (b) Kaul, B. B.; Sommer, R. D.; Noll B. C. Yee, G. T. *Inorg. Chem.* **2000**, 39, 865.
7. (a) Boderick, W. E.; Liu X. Hoffman, B. M. *J. Am. Chem. Soc.* **1991**, 113, 6334; (b) Miller, J. S.; McLean, R. S.; Vazquez, C.; Calabrese, J. C.; Zuo F. Epstein, A. J.; *J. Mater. Chem.* **1993**, 3, 215; (c) Yee, G. T.; Manriquez, J. M.; Dixon, D. A.; McLean, R. S.; Groski, D. M.; Flippen, R. B.; Narayan, K. S.; Epstein A. J. Miller, J. S. *Adv. Mater.* **1991**, 3, 309.
8. (a) McConnell, H. M.; *Proc. Robert A. Welch Found. Conf. Chem. Res.* **1967**, 11, 144; (b) Breslow, R. *Pure Appl. Chem.* **1982**, 54, 927; (c) Kahn, O. *Molecular Magnetism*, VCH, New York, **1993**.
9. (a) Schweizer, J.; Golhen, S.; Lelièvre-Berna, E.; Ouahab, L.; Pontillon Y. Ressouche, E. *Phys. B* **2001**, 297, 213; (b) Kollmar C. Kahn, O. *Acc. Chem. Res.* **1993**, 26, 259.
10. McConnell, H. D. *J. Chem. Phys.* **1963**, 39, 1910.
11. Wang, G.; Sledobnick, C.; Butcher R. J. Yee, G. T. *Inorg. Chim. Acta* **2009**, 362, 2423.
12. Datta S. N. Misra, A. *J. Chem. Phys.* **1999**, 111, 9009.
13. Tyree, W. S. *Thesis submitted to the faculty of the Virginia Polytechnic Institute and State University for the degree of Master of Science in Chemistry.* **2005**.
14. Okamura, T.; Takano, Y.; Yoshioka, Y.; Ueyama, N.; Nakamura A. Yamaguchi, K. *J. Organomet. Chem.* **1998**, 569, 177.
15. Brune, H.; Röder, H.; Boragno H. Kern, K. *Phys. Rev. Lett.* **1994**, 73, 1955.
16. (a) Pederson, M. R.; Reuse F. Khanna, S. N. *Phys. Rev. B: Condens. Matter Mater. Phys.* **1998**, 58, 5632; (b) Nayak, S. K.; Rao B. K. Jena, P. *J. Phys.: Condens. Matter* **1998**, 10, 10863; (c) Nayak S. K. Jena, P. *Chem. Phys. Lett.* **1998**, 289, 473; (d) Nickelbein, M. B. *Phys. Rev. Lett.* **2001**, 86, 5255; (e) Michael, F.; Gonzalez, C.; Mujica, V.; Marquez M. Ratner, M. A. *Phys. Rev. B: Condens. Matter Mater. Phys.* **2007**, 76, 224409; (f) Sosa-Hernandez, E. M.; Alvarado-Leyva, P. G.; Montezano-Carrizales J. M. Aguilera-Granja, F. *Rev. Mex. Fis.* **2004**, 50, 30; (g) Liu, F.; Khanna S. N. Jena, P. *Phys. Rev. B: Condens. Matter Mater. Phys.* **1991**, 43, 8179; (h) Mitra, S.; Mandal, A.; Datta, A.; Banerjee, S.; Chakravorty, J. D. *Phys. Chem. C* **2011**, 115, 14673.

17. (a) Reddy, B. V.; Khanna S. N.; Dunlap, B. I. *Phys. Rev. Lett.* **1993**, *70*, 3323; (b) Nozue, Y.; Kodaira T.; Goto, T. *Phys. Rev. Lett.* **1992**, *68*, 3789; (c) Cox, A. J.; Loudereback J. G.; Bloomfield, L. A. *Phys. Rev. Lett.* **1993**, *71*, 923; (d) Villaseñor-González, P.; DorantesDávila, J.; Dreyysé H.; Pastor, G. M.; *Phys. Rev. B: Condens. Matter Mater. Phys.* **1997**, *55*, 15084; (e) Guirado-López, R.; Spanjaard D.; Desjonqueres, M. C. *Phys. Rev. B: Condens. Matter Mater. Phys.* **1998**, *57*, 6305.
18. McGrady, J. E.; Stranger R.; Lovell, T. *J. Phys. Chem. A* **1997**, *101*, 6265.
19. Noodleman, L. *J. Chem. Phys.* **1981**, *74*, 5737.
20. (a) Bencini, A.; Totti, F.; Daul, C. A.; Doclo, K.; Fantucci P.; Barone, V. *Inorg. Chem.* **1997**, *36*, 5022; (b) Ruiz, E.; Cano, J.; Alvarez S.; Alemany, P. *J. Comput. Chem.* **1999**, *20*, 1391.
21. Soda, T.; Kitagawa, Y.; Onishi, T.; Takano, Y.; Shigeta, Y.; Nagao, H.; Yoshioka Y.; Yamaguchi, K. *Chem. Phys. Lett.* **2000**, *319*, 223.
22. Szabo A.; Ostlund, N. S. *Modern Quantum Chemistry: Introduction to Advanced Electronic Structure Theory*, Dover Publications, New York. **1996**.
23. Herrmann, C.; Yu L.; Reiher, M. *J. Comput. Chem.* **2006**, *27*, 1223.
24. Binning Jr, R. C.; Babelo, D. E. *J. Comput. Chem.* **2008**, *29*, 716.
25. Galperin, M.; Segal D.; Nitzam, A. *J. Chem. Phys.* **1999**, *111*, 1569.
26. (a) Anderson, P. W. *Phys. Rev.* **1950**, *79*, 350; (b) Anderson, P. W. *Phys. Rev.* **1959**, *115*, 2; (c) Anderson, P. W. In *Theory of the Magnetic Interaction: Exchange in Insulators and Superconductors*, *Solid State Physics*, vol. 14, Academic, New York, **1963**, p. 99.
27. Munoz, D.; Illas F.; de Moreira, I. P. R. *Phys. Rev. Lett.* **2000**, *84*, 1579.
28. (a) Calzado, C. J.; Cabrero, J.; Malrieu J. P.; Caballol, R.; *J. Chem. Phys.* **2002**, *116*, 2728; (b) Calzado, C. J.; Cabrero, J.; Malrieu J. P. and Caballol, R. *J. Chem. Phys.* **2002**, *116*, 3985; (c) Calzado, C. J.; Angeli, C.; Taratiel, D.; Caballol R.; Malrieu, J. P. *J. Chem. Phys.* **2009**, *131*, 044327.
29. (a) Paul S.; Misra, A. *J. Chem. Theory Comput.* **2012**, *8*, 843; (b) Shil, S.; Paul S.; Misra, A. *J. Phys. Chem. C* **2013**, *117*, 2016.
30. Petrov, E. G.; Shevchenko, Y. V.; Teslenko V. I.; May, V. *J. Chem. Phys.* **2001**, *115*, 7107.
31. Paul S.; Misra, A. *J. Phys. Chem. A* **2010**, *114*, 6641.
32. (a) Daizadeh, I.; Medvedev D. M.; Stuchebrukhov, A. A. *Mol. Biol. Evol.* **2002**, *19*, 406; (b) Mikolajczyk, M. M.; Zale'sny, R.; Czy'znikowska, Z.; Toman, P.; Leszczynski J.; Bartkowiak, W.; *J. Mol. Model.* **2011**, *17*, 2143.

33. Makov, G.; Shah R.; Payne, M. C. *Phys. Rev. B: Condens.Matter Mater. Phys.* **1996**, *53*, 15513.
34. (a) Foster J. P.; Weinhold, F. *J. Am. Chem. Soc.* **1980**, *102*, 7211; (b) Reed, A. E.; Curtiss L. A.; Weinhold, F. *Chem. Rev.* **1988**, *88*, 899.
35. Baumeier, B.; Kirkpatrick J.; Andrienko, D. *Phys. Chem. Chem. Phys.* **2010**, *12*, 11103.
36. Huang J.; Kertesz, M. *J. Chem. Phys.* **2005**, *122*, 234707.
37. Perdew, J. P.; Burke K.; Ernzerhof, M. *Phys. Rev. Lett.* **1996**, *77*, 3865.
38. (a) Improta, R.; Barone, V.; Kudin K. N.; Scuseria, G. E. *J. Chem. Phys.* **2001**, *114*, 254; (b) Zhao, G.; Jiang, L.; He, Y.; Li, J.; Dong, H.; Wang X.; Hu, W. *Adv. Mater.* **2011**, *23*, 3959; (c) Improta, R.; Barone, V.; Kudin K. N.; Scuseria, G. E. *J. Am. Chem. Soc.* **2001**, *123*, 3311.
39. (a) Becke, A. D. *J. Chem. Phys.* **1993**, *98*, 5648; (b) Stephens, J.; Devlin, F. J.; Chabalowski C. F.; Frisch, M. J. *J. Phys.Chem.* **1994**, *98*, 11623; (c) Adamo C.; Barone, V. *J. Chem. Phys.* **1999**, *110*, 6158; (d) Ernzerhof M.; Scuseria, G. E. *J. Chem. Phys.* **1999**, *110*, 5029; (e) Jacquemin, D.; Perpète, E. A.; Ciofini I.; Adamo, C. *Chem. Phys. Lett.* **2005**, *405*, 376.
40. (a) Chevrau, H.; de Moreira, I. P. R.; Silvi B.; Illas, F. *J. Phys.Chem. A* **2001**, *105*, 3570; (b) Ruiz, E.; Alemany, P.; Alvarez S.; Cano, S.; *J. Am. Chem. Soc.* **1997**, *119*, 1297.
41. (a) Martin R. L.; Illas, F. *Phys. Rev. Lett.* **1997**, *79*, 1539;(b) Illas F.; Martin, R. L. *J. Chem. Phys.* **1998**, *108*, 2519.
42. Onishi, T.; Takano, Y.; Kitagawa, Y.; Kawakami, T.; Yoshioka Y.; Yamaguchi, K. *Polyhedron* **2001**, *20*, 1177.
43. Becke, A. D. *J. Chem. Phys.* **1993**, *98*, 1372.
44. Caballol, R.; Castell, O.; Illas, F.; Malrieu J. P.; Moreira, I. deP. R. *J. Phys. Chem. A* **1997**, *101*, 7860.
45. Paier, J.; Marsman M.; Kreese, G. *J. Chem. Phys.* **2007**, *127*, 024103.
46. Atanasov, M.; Delley, B.; Neese, F.; Tregenna-Piggott P. L.; Sigrist, M. *Inorg. Chem.* **2011**, *50*, 2112.
47. Pantazis, D. A.; Orio, M.; Petrenko, T.; Zein, S.; Bill, E.; Lubitz, W.; Messinger J. Neese, F. *Chem. Eur. J.* **2009**, *15*, 5108.
48. (a) Orio, M.; Pantazis, D. A.; Petrenko T.; Neese, F. *Inorg.Chem.* **2009**, *48*, 7251; (b) Pantazis, D. A.; Krewald, V.; Orio M.; Neese, F. *Dalton Trans.* **2010**, *39*, 4959.
49. (a) Pantazis, D. A.; Orio, M.; Petrenko, T.; Zein, S.; Lubitz, W.; Messinger J.; Neese, F. *Phys. Chem. Chem. Phys.* **2009**, *11*, 6788; (b) Tao, J.; Perdew, J. P.; Staroverov V. N.;

Scuseria, G. E. *Phys. Rev. Lett.* **2003**, *91*, 146401; (c) Staroverov, V. N.; Scuseria, G. E.; Tao J.; Perdew, J. P. *J. Chem. Phys.* **2003**, *119*, 12129.

50. Mödl, M.; Dolg, M.; Fulde P.; Stoll, H. *J. Chem. Phys.* **1997**, *106*, 1836.

51. (a) Mouesca, J. M.; Noodleman L.; Case, D. A. *Int.J. Quantum Chem., Quantum Biol. Symp.* **1995**, *22*, 95; (b) Daudey, J. P.; de Loth P.; Malrieu, J. P. In *Magnetic Structural Correlation in Exchange Coupled Systems*, NATO Symposium, D. Gatteschi, O. Kahn and R. D. Willett (Eds.), Reidel, Dordrecht, **1984**.

52. (a) Andersson, K.; Malmqvist, P. A.; Roos, B. O.; Sadlej A. J.; Wolinski, K. *J. Phys. Chem.* **1990**, *94*, 5483; (b) Andersson, K.; Malmqvist P. A.; Roos, B. O. *J. Chem. Phys.* **1992**, *96*, 1218; (c) de Graaf, C.; Sousa, C.; de Moreira I. P. R.; Illas, F. *J. Phys. Chem. A* **2001**, *105*, 11371.

53. Calzado, C. J.; Celestino, A.; Caballol R.; Malrieu, J. P. *Theor. Chem. Acc.* **2010**, *126*, 185.

54. (a) Miralles, J.; Daudey J. P.; Caballol, R. *Chem. Phys. Lett.* **1992**, *198*, 555; (b) Miralles, J.; Castell, O.; Caballol R.; Malrieu, J. P. *Chem. Phys.* **1993**, *172*, 33.

55. de Graaf, C.; Broe R.; Nieuwpoort, W. C. *Chem. Phys. Lett.* **1997**, *271*, 372.

56. Frisch, M. J.; Trucks, G. W.; Schlegel, H. B.; Scuseria, G. E.; Robb, M. A.; Cheesman, J. R.; Zakrzewski, V. G.; Montgomery, J. A.; Strtmann, R. E.; Burant, J. C.; Dapprich, S.; Milliam, J. M.; Daniels, A. D.; Kudin, K. N.; Strain, M. C.; Farkas, O.; Tomasi, J.; Barone, V.; Cossi, M.; Camme, R.; Mennucci, B.; Pomelli, C.; Adamo, C.; Clifford, S.; Ochterski, J.; Petersson, G. A.; Ayala, P. Y.; Cui, Q.; Morokuma, K.; Rega, N.; Salvador, P.; Dannenberg, J. J.; Malich, D. K.; Rabuck, A. D.; Raghavachari, K.; Foresman, J. B.; Cioslowski, J.; Ortiz, J. V.; Baboul, A. G.; Stetanov, B. B.; Liu, G.; Liashenko, A.; Piskorz, P.; Komaromi, I.; Gomperts, R.; Martin, R. L.; Fox, D. J.; Keith, T.; Al-Laham, M. A.; Peng, C. Y.; Nnsyskkara, A.; Challacombe, M.; Gill, P. M. W.; Johnson, B.; Chen, W.; Wong, M. W.; Andres, J. L.; Gonzalez, C.; Head-Gordon, M.; Replogle E. S.; Pople, J. A. GAUSSIAN09, Revision A.02, Gaussian Inc., Pittsburgh (2009).

57. O'Boyle, N. M.; Tenderholt A. L.; Langner, K. M. *J. Comput. Chem.* **2008**, *29*, 839.

58. (a) Castellani, M. P.; Geib, S. J.; Rheingold A. L.; Trogler, W. C. *Organometallics* **1987**, *6*, 1703; (b) Stroppa, A.; Barone, P.; Jain, P.; Perez-Mato J. M.; Picozzi, S. *Adv. Mater.* **2013**, *25*, 2284.

59. Gruschus J. M.; Kuki, A. *J. Phys. Chem.* **1993**, *97*, 5581.

60. (a) Staemmler V.; Fink, K. *Chem. Phys.* **2002**, *278*, 79; (b) Stoll H.; Doll, K. *J. Chem. Phys.* **2012**, *136*, 074106.

61. Noga, J.; Baňacký, P.; Biskupič, S.; Boča, R.; Pelikán, P.; Svrček M.; Zajac, A. *J. Comput. Chem.* **1999**, *20*, 253.

62. (a) Yoshizawa K.; Hoffmann, R. *J. Chem. Phys.* **1995**, *103*, 2126; (b) Wang, W. J.; Yao K. L.; Lin, H. Q.; *J. Chem. Phys.* **1998**, *108*, 2867.
63. Bicout D. J.; Kats, E. *Phys. Lett. A* **2002**, *300*, 479.
64. de Moreira, I. P. R.; Illas F.; Martin, R. L. *Phys. Rev. B: Condens. Matter Mater. Phys.* **2002**, *65*, 155102.
65. Imbrota, R.; Kudin, K. N.; Scuseria G. E.; Barone, V. *J. Am. Chem. Soc.* **2002**, *124*, 113.
66. Miller, J. S.; Epstein A. J.; Reiff, W. M. *Chem. Rev.* **1988**, *201*.
67. (a) Cramer C. J.; Truhlar, D. G. *Phys. Chem. Chem. Phys.* **2009**, *11*, 10757; (b) Marsman, M.; Paier, J.; Stroppa A.; Kresse, G.; *J. Phys.: Condens. Matter* **2008**, *20*, 064201; (c) Stroppa A.; Picozzi, S. *Phys. Chem. Chem. Phys.* **2010**, *12*, 5405.
68. Gangopadhyay, S.; Masunov, A. E.; Poalelungi E.; Leuenberger, M. N. *J. Chem. Phys.* **2010**, *132*, 244104.
69. Ederer C.; Komelj, M. *Phys. Rev. B: Condens. Matter Mater. Phys.* **2007**, *76*, 064409.
70. Wynn, C. M.; Girtu, M. A.; Brinckerhoff, W. B.; Suguira, K. I.; Miller J. S.; Epstein A. J. *Chem. Mater.* **1997**, *9*, 2156.
71. Miller, J. S. *J. Mater. Chem.* **2010**, *20*, 1846.
72. Stryjewski E.; Giordano, N. *Adv. Phys.* **1977**, *26*, 487.

CHAPTER 5

Ligand Effects toward the Modulation of Magnetic Anisotropy and Design of Magnetic Systems with Desired Anisotropy Characteristics

Abstract

Magnetic anisotropy of a set of octahedral Cr(III) complexes is studied theoretically. The magnetic anisotropy is quantified in terms of zero-field splitting (ZFS) parameter D , which appeared sensitive toward ligand substitution. The increased π -donation capacity of the ligand enhances the magnetic anisotropy of the complexes. The axial π -donor ligand of a complex is found to produce an easy-plane type ($D > 0$) magnetic anisotropy, while the placement of the axial ligands with π -acceptors entails the inversion of magnetic anisotropy into the easy-axis type ($D < 0$). This observation enables one to fabricate a single molecule magnet for which easy-axis type magnetic anisotropy is an indispensable criterion. The equatorial ligands are also found to play a role in tuning the magnetic anisotropy. The magnetic anisotropy property is also correlated with the nonlinear optical (NLO) response. The value of the first hyperpolarizability varies proportionately with the magnitude of the ZFS parameter. Finally, it has also been shown that a rational design of simple octahedral complexes with desired anisotropy characteristics is possible through the proper ligand selection.

5.1. Introduction

Magnetically interacting open-shell transition metal ion clusters have been a topic of thorough investigation in the past few decades, which has caused the divergent areas of chemistry and physics to meet.¹ Interesting catalytic, biochemical, and physical properties of paramagnetic metal complexes have drawn the attention of many researchers and material scientists.² Magnetic materials based on molecular lattices, rather than continuous lattices of classical magnets, have been designed and synthesized.³ Recently, polynuclear clusters assembled from mononuclear coordination complexes have become a subject of increased interest since it is relevant for the study of “single molecule magnets” (SMMs).⁴ A phenomenon hindering spin inversion causes certain molecules to exhibit slow relaxation of the magnetization after removal of an applied magnetic field, thus showing SMM behavior.^{5,6} The discovery that some metal coordination clusters may behave as SMMs^{5,7,8} has provoked plentiful research in the direction of their potential applications in high-density information storage and quantum computing.^{9–11}

The genesis of SMM behavior is a large easy-axis magnetic anisotropy and concomitant high energy barrier that needs to be overcome for the reversal of the magnetic moment. The barrier to reorient spin in magnetic molecules can be given by $|D|S^2$ for molecules with integer spins and $|D|(S^2-1/4)$ for molecules with half integer spins, where D is the zero-field splitting (ZFS) parameter and S is the ground state spin.¹² Molecular systems containing a large number of paramagnetic centers with significant negative D are the most suitable candidates to be used as SMMs.⁵ However, most of these species show either low negative or positive D value in spite of having high ground state spin. Recently, a few lanthanide complexes have been reported to show slow magnetic relaxation behavior. For example, phthalocyanine double-decker complexes with Tb(IV) and Er(III) encapsulated in a polyoxometalate framework exhibit an extremely high negative anisotropy barrier.^{13,14} Several complexes of Fe(II), U(III) and Dy(III) also show similar characteristics.^{15–17} Another novel class of nanomagnets called the single-chain magnets (SCMs), can be formed by combination of the SMMs.^{18–23} A series of one-dimensional cyano-bridged coordination solids $(\text{DMF})_4\text{MReCl}_4(\text{CN})_2$, with $\text{M} = \text{Mn}, \text{Fe}, \text{Co}, \text{Ni}$, have been reported to show a slow relaxation of magnetization.²⁴ Moreover, in the combination of SMMs in which the easy axes of anisotropies are linked in a parallel manner, can lead to a large easy-axis type ($D < 0$) anisotropy in the long-chain range, and manifestation of a slow relaxation of magnetization can occur.²⁵

The dependence of the ZFS parameter (D) on the nature of ligands has long been a subject of enormous interest.²⁶ For example, the synthesis and characterization of a series of high spin hexa-coordinated dihalide Mn(II) complexes $[\text{Mn}(\text{tpa})\text{X}_2]$ (tpa = tris-2-picolyamine; $\text{X} = \text{I}, \text{Br}, \text{and Cl}$) advocate for the presence of such ligand effects showing an increase in the D value with I relative to that with Br and Cl ($D_{\text{I}} > D_{\text{Br}} > D_{\text{Cl}}$).^{26b} Recently

Karunadasa et al. have shown the variation in magnetic anisotropy in a few pseudo-octahedral first-row transition metal complexes by varying ligands.²⁷ A series of octahedral complexes $[\text{Cr}(\text{dmpe})_2(\text{CN})\text{X}]^+$ (dmpe = 1,2-bis-(dimethylphosphino)ethane, X = Cl, Br, I) and $\text{Cr}(\text{dmpe})_2(\text{CN})\text{X}$ (X = Cl, I) has been studied, and a similar trend as that discussed above has been observed. Logically, the observed trends can be attributed to factors such as changes in *d*-orbital splitting with the nature of the halide, the influence of ligand spin-orbit coupling, and so on. A simple computational model may be useful for a clear analysis of the observed changes in *D* as a function of the nature of the ligands. One of the interesting properties that such types of organometallic complexes manifest is the nonlinear optical (NLO) property.²⁸ Molecular NLO materials are of considerable scientific interest due to their potential application in the field of optoelectronics and all-optical data processing technologies.^{29,30} In a number of works, the magnetic property of materials has been related to the NLO response.^{31,32} Therefore, it can be intuited that there exists a correlation between NLO response and ZFS parameter.

In order to understand the effect of the ligands to tune the magnetic anisotropy in transition metal complexes, a systematic DFT study was carried out on a few chosen systems (Figure 5.1). The observed trends in the *D* values of the octahedral complexes $[\text{Cr}(\text{dmpe})_2(\text{CN})\text{X}]^+$ (dmpe=1,2-bis-(dimethylphosphino)ethane, X = Cl, Br, I) enable one to estimate the contribution of the halides toward the ZFS of the whole molecule. Such contributions of the ligands are correlated with the energy difference between the highest occupied molecular orbital (HOMO) and lowest unoccupied molecular orbital (LUMO), and second-order NLO response. A positive value of *D* would correspond to an easy-plane type (i.e., $D > 0$) magnetic anisotropy. On the other hand, a negative value relating to the easy-axis type (i.e., $D < 0$) magnetic anisotropy would make the systems more interesting for various applications. As a logical consequence, the second part of our work involves the study of the magnetic nature of the complexes in which both the axial positions of the complex are replaced either by π -donor or π -acceptor ligands to inspect the magnetic nature of the complexes as a function of ligand substitution.

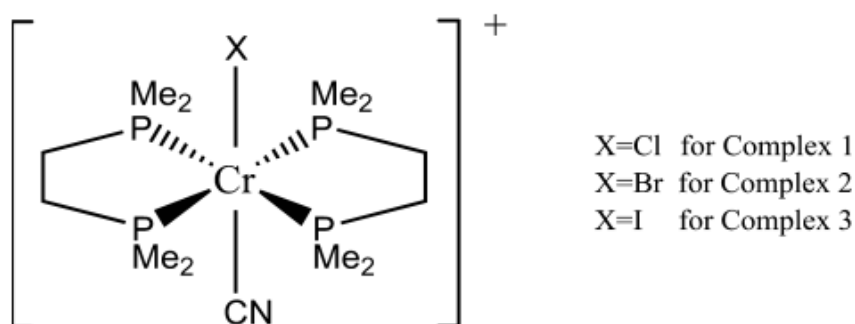


Figure 5.1. Structures of the octahedral complexes $[\text{Cr}(\text{dmpe})_2(\text{CN})\text{X}]^+$, (X = Cl, Br, I for complexes 1, 2, and 3, respectively).

5.2. Theoretical Background

Magnetic anisotropy leads to the splitting of $2S+1$ magnetic sublevels even in the absence of an external magnetic field, and this phenomenon is called ZFS. The degeneracy of the M_s states is lifted due to ZFS in molecules having $S > 1/2$. Prediction of the ZFS in transition-metal complexes using density functional theory (DFT)-based methods has been a subject of scientific interest.^{26b} The uncoupled perturbation theoretical approach in the framework of unrestricted Kohn-Sham formalism is adopted to determine the spin-orbit coupling contribution to ZFS.³³ The second-order correction to the total energy of a system due to spin-orbit coupling can be expressed as³⁴

$$\Delta_2 = \sum_{\sigma\sigma'} \sum_{ij} M_{ij}^{\sigma\sigma'} S_i^{\sigma\sigma'} S_j^{\sigma'\sigma}, \quad (5.1)$$

Where σ is used to denote different spin degrees of freedom and i and j denote coordinate labels, x , y , and z . Here $S_i^{\sigma\sigma'}$ is defined as

$$S_i^{\sigma\sigma'} = \left\langle \chi^\sigma \mid S_i \mid \chi^{\sigma'} \right\rangle \quad (5.2)$$

χ^σ and $\chi^{\sigma'}$ are a set of spinors that are constructed from a unitary transformation on the S_z eigenstates. The matrix elements $M_{ij}^{\sigma\sigma'}$ are described as

$$M_{ij}^{\sigma\sigma'} = - \sum_{kl} \frac{\langle \varphi_{l\sigma} \mid V_i \mid \varphi_{k\sigma'} \rangle \langle \varphi_{k\sigma'} \mid V_j \mid \varphi_{l\sigma} \rangle}{\varepsilon_{l\sigma} - \varepsilon_{k\sigma'}}. \quad (5.3)$$

In this equation, $\varphi_{l\sigma}$ and $\varphi_{k\sigma'}$ are occupied and unoccupied states with energies $\varepsilon_{l\sigma}$ and $\varepsilon_{k\sigma'}$, respectively. The operator V_x is related to the derivative of coulomb potential. In the absence of magnetic field, the change in energy of the system in the second-order can be written as

$$\Delta_2 = \sum_{ij} \gamma_{ij} \langle S_i \rangle \langle S_j \rangle. \quad (5.4)$$

Diagonalizing the anisotropy tensor γ , one can obtain the eigenvalues γ_{xx} , γ_{yy} , and γ_{zz} , and, consequently, the second-order perturbation energy can be written as

$$\begin{aligned}
\Delta_2 = & \frac{1}{3}(\gamma_{xx} + \gamma_{yy} + \gamma_{zz})S(S + 1) \\
& + \frac{1}{3}\left[\gamma_{zz} - \frac{1}{2}(\gamma_{xx} + \gamma_{yy})\right]\left[3S_z^2 - S(S + 1)\right] \\
& + \frac{1}{2}(\gamma_{xx} - \gamma_{yy})(S_x^2 - S_y^2)
\end{aligned} \tag{5.5}$$

Parameterization of the anisotropy tensor components (γ_{xx} , γ_{yy} , γ_{zz}) with D and E , which are the axial and the rhombic ZFS parameters, respectively, gives rise to the following simplified expression

$$H_{ZFS} = D\left[S_z^2 - \frac{1}{3}S(S + 1)\right] + E[S_x^2 - S_y^2]. \tag{5.6}$$

The sign of the axial ZFS parameter D is important in determining the nature of the magnetic property associated with the system. For a positive value of D , the system cannot show magnetic phenomena, and the magnetic anisotropy is termed easy-plane anisotropy. On the other hand, the negative value of D is the basic requirement for a material to become SMM.³⁵

5.3. Computational Details

Single-point calculations on the chosen octahedral Cr(III) complexes (Figure 5.1) are carried out on the crystallographic geometries obtained from ref 27. Following the methodology proposed by Pederson and Khanna,³⁴ the ORCA³⁶ code is used to calculate the ZFS tensor in DFT formalism. We have calculated the ZFS parameters using the BPW91 functional,³⁷ and TZV basis set,³⁸ and taking advantage of the resolution of the identity (RI) approximation with the auxiliary TZV/J Coulomb fitting basis set,³⁹ under unrestricted Kohn–Sham formalism. This methodology, as adopted in this work, is being widely used to compute the ZFS parameter.^{37b,c,40} Although there are several methods available for the computation of the ZFS parameter, the Pederson and Khanna (PK) method is known to produce the correct sign of the ZFS parameter.^{37b,c} Moreover, it has also been observed that the ZFS contributions predicted by this method show fair agreement with accurate ab initio and experimental results. With regard to the computation of the ZFS parameter, other DFT methods that are being used are Neese’s quasi-restricted (QR) approach,⁴¹ and the coupled perturbed spin orbit coupling (CP-SOC) method.⁴² Recently, some more sophisticated ab initio techniques have proven to produce excellent results.⁴³ Nevertheless, the justification of using the PK method in the case of Mn(II) systems by Neese and co-workers solicits for the

selection of this method in the present work.³³ Earlier studies have concluded that magnetic anisotropy values have strong dependence on the functionals; however, the same is less dependent on basis sets.^{37a,44} It has also been previously explained that the performance of the nonhybrid functionals toward the prediction of the D parameter is excellent.⁴⁵ Thus it can be expected that the BPW91 functional will be a good choice for the calculation of the ZFS parameter, which has also been shown by Rodriguez et al.^{37b,c} The second-order NLO response β has been calculated using the Gaussian 09W⁴⁶ suite of software, using the same methodology as the ZFS parameter. As the Gaussian suit of software does not allow the use of TZV basis set for the element iodine, we supply the midi-x basis set as an extrabasis for the element iodine. The midi-x basis set is a heteroatom-polarized valence-double- ζ basis set that is known to be good at predicting partial atomic charges accurately.⁴⁷

5.4. Results and Discussions

5.4.1. Role of π -donation from ligand

The ZFS parameters are computed for complexes 1, 2, and 3 (Figure 5.1). The agreement between the calculated and the experimental values can be followed from Table 5.1. The ZFS is known to arise from small differences of various contributions; thus, a better agreement with the experimental results can rarely be expected.⁴⁸ However, the order of magnitude of the ZFS parameters are in parity with experimental observations. Moreover, similar to the experimental trend, the magnitude of D increases gradually from complex 1 to 3 in the present study.

Table 5.1. Experimental (D_{exp}) and calculated (D_{calc}) ZFS parameters for the complexes 1, 2, and 3.

complex	formula	$ D_{exp} $ (cm^{-1})	D_{calc} (cm^{-1})
1	$[\text{Cr}(\text{dmpe})_2(\text{CN})\text{Cl}]^+$	0.11	0.27
2	$[\text{Cr}(\text{dmpe})_2(\text{CN})\text{Br}]^+$	1.28	1.45
3	$[\text{Cr}(\text{dmpe})_2(\text{CN})\text{I}]^+$	2.30	5.66

Although it is difficult to relate the electron pulling capacity of a ligand with the help of electronegativity of the ligand in the complex, the effect of covalency cannot be ignored. A covalent interaction of the central metal with the ligand aids in the delocalization of unpaired spins away from the metal.⁴⁹ This phenomenon is often explained through the orbital reduction factor k , which is defined by Stevens as the decrease in the orbital angular

momentum of an unpaired electron in the d -orbital.⁵⁰ Previously, it has been shown that the orbital reduction factor is associated with the time spent by the unpaired electron in the adjacent ligands.⁵¹ The orbital reduction factor is expressed as follows:

$$k = \frac{\langle \Psi_i | l | \Psi_i \rangle}{\langle d_i | l | d_i \rangle} \quad (5.7)$$

where l is the orbital angular momentum operator, and $|d\rangle$ and $|\Psi\rangle$ are free ion d -orbitals and molecular orbitals, respectively.⁵² However, k can be reduced to the following working equation for computational realization:

$$k = \frac{\sum_{i=1}^{2l+1} \sum_{\mu=1}^{2l+1} c(i, \mu)^2}{2l + 1} \quad (5.8)$$

for $l=2$, i runs over d atomic orbitals (AOs) and μ runs over molecular orbitals (MOs) with dominant d -contributions, with $c(i, \mu)$ being the contribution of i th AO to the μ th MO.⁵³ The orbital reduction factor value obtained for complexes 1, 2, and 3 are 1.16, 0.95, and 0.85, respectively. A reduction in the orbital angular momentum from the free ion value can be taken as evidence of covalency between the central ion and the ligand.⁵⁴ Following Pellow and Vala,⁵⁵ it clearly appears that the value of orbital reduction factor is dependent on the ratio of the metal and the ligand spin-orbit coupling. Hence, a smaller value of the orbital reduction factor depicts a larger spin-orbit coupling contribution from the ligand to the overall magnetic anisotropy characteristics of the complex. Although the conventional orbital reduction factor has values within 0 and 1, a k value larger than 1 can arise due to the admixture of states with different multiplicity.⁵⁶ A value of k greater than 1 signifies that the spin-orbit coupling of the complex is greater than the free ion value.⁵⁵ This point has been explained thoroughly by Griffith on the basis of the delocalization of the d -orbitals.^{56b} The halogen ligands are also known for their π -donation ability, which increases down the halogen group. Hence gradual increase in the magnitude of D parameter can primarily be attributed to the π -donation strength or the basicity of the halide ligands. The ZFS parameters are usually understood in the framework of ligand-field (LF) theory as many other properties of transition metal complexes.³³ In an octahedral field, the degenerate d -orbitals of the metal ion is split into two levels, namely, t_{2g} and e_g . The ground state of Cr(III) in an octahedral environment has the electronic configuration t_{2g}^3 which gives rise to the $^4A_{2g}$ state. The three unpaired electrons in this d^3 system remain in the nonbonding d_{xy} , d_{yz} , and d_{zx} orbitals of the t_{2g} group. There are six one-electron promotions that give rise to $^4T_{1g}$ and $^4T_{2g}$ excited states. These two states are different in energy, but only the $^4T_{2g}$ state can couple to the ground state.⁵⁷ However $t_{2g}^2 e_g^1$ configuration corresponds to a 4T state, and, particularly, these excitations within the metal d -shell make the most important contributions to the ZFS.⁵⁸ Four

types of excitations that are found to contribute to the D tensor are SOMO–VMO ($\alpha \rightarrow \alpha$), SOMO–SOMO ($\alpha \rightarrow \beta$), DOMO–VMO ($\beta \rightarrow \alpha$), and DOMO–SOMO ($\beta \rightarrow \beta$), where SOMO, VMO, and DOMO refer to singly occupied, virtual, and doubly occupied MOs, respectively. In the unrestricted formalism, all the orbitals are singly occupied by up-spin or down-spin. Thus, the SOMOs are referred to as those occupied up-spin MOs that do not have any population in their down-spin counter parts. Similarly, those orbitals having population in both the up and their corresponding down spin MOs are considered here as DOMOs. In Table 5.2, these individual excitation contributions to the D are listed. It can be seen from Table 5.2 that all the individual contributions are more or less in accordance with the experimentally observed trend in the values of ZFS parameters, i.e., these contributions also increase from Cl to I in almost all cases. The crucial dependence of the ZFS parameter on various important $d \rightarrow d$ excited states, involving spin-allowed and forbidden intra-SOMO spin flip excitations can be observed from Table 5.2.⁵⁹ Among the four excitations, two important contributions stem from $\alpha \rightarrow \alpha$ and $\beta \rightarrow \alpha$ excitations, which correspond to the SOMO \rightarrow VMO and DOMO \rightarrow VMO transitions, respectively. The first one has maximum positive contribution toward the overall D of the molecule, while the DOMO \rightarrow VMO has the highest negative contribution for the same. The magnetic response of the electronic ground state is largely determined by the $d-d$ excited states of the same multiplicity as that of the ground state.⁵⁸ The HOMO \rightarrow LUMO transition is so spin conserving that the $d-d$ transition can exclusively be made responsible for the ZFS.⁴¹ This observation draws our attention to the HOMO–LUMO gap of the molecules, where HOMO is the highest energy SOMO. TDDFT calculations for the study of the $d-d$ vertical excitations are carried out with the same basis set and functional to see which of these excitations are most important for the ZFS. The TDDFT results (see Appendix C) for all three complexes reveal that, among the $d-d$ transitions, those transitions that correspond to the highest oscillator strength are HOMO–LUMO transitions.

Table 5.2. Individual excitation contribution to the total ZFS parameter D .

complexes	SOMO–SOMO ($\alpha \rightarrow \beta$)	DOMO–VMO ($\beta \rightarrow \alpha$)	SOMO–VMO ($\alpha \rightarrow \alpha$)	DOMO–SOMO ($\beta \rightarrow \beta$)
complex 1	0.02	−0.35	0.29	0.31
complex 2	1.53	−4.78	3.64	1.06
complex 3	11.87	−25.22	17.99	1.02

The HOMOs in all three cases are $p\pi-d\pi$ antibonding orbitals (Figure 5.2), while the LUMOs are mainly concentrated on the metal d -orbitals with no contribution from the ligands. Since the LUMOs, mainly composed of metal $d_{x^2-y^2}$ orbitals, are not in a desired

orientation to interact with halides, they are found to be almost constant in energy with the variation in halides (Figure 5.3). Interaction of halide p -orbitals with the metal d -orbitals leads to destabilization of those orbitals by mixing with them in an antibonding fashion. The extent of destabilization increases with the donation property of the halide π -donor. Hence, the HOMO–LUMO gap eventually reduces from the chloride complex to the iodide complex (Figure 5.3). Thus, it is expected that in case of the chloride complex, the D value will be lowest in magnitude as the denominator in eqn 5.3 is largest. Hence the increase in the D value from complex 1 to 3 is justifiable from the standpoint of the reducing HOMO–LUMO gap.



Figure 5.2. The HOMOs and the LUMOs of the octahedral Cr(III) complexes. The equatorial ligands are in tube form for clarity.

Moreover, a reduction in the HOMO–LUMO gap has its manifestation in the NLO properties of materials.³¹ This single parameter, the HOMO–LUMO gap, is established as a key factor to tune both the magnetic behavior and the NLO response simultaneously.³¹ Electronic charge-transfer transition is responsible for NLO response in materials. Analysis of the results obtained from the calculation of the second-order NLO response reveals that there is a unidirectional charge-transfer transition, as one particular tensorial component of β , namely β_{zzz} , is the dominating term, with z -axis being parallel to the metal halogen bond.⁶⁰ A good π -donation from the ligand increases the diffusibility of the electronic cloud in between the metal and the ligand, which in turn is responsible for the hyperpolarizability of the molecule. Hence, the physical origin of the high β_{zzz} for complex 3 can be correlated with the strong π -donation ability of iodine. On the other hand, it is clear from eqn 5.3 that the denominator of the tensorial component of magnetic anisotropy corresponds to the energy difference between the occupied and unoccupied energy levels. In that case, an increase in first hyperpolarizability value can be envisaged as a tool toward the prediction of increasing magnetic anisotropy. Keeping this view in mind, we have also computed the first hyperpolarizability that is the second-order NLO response of the complexes. The first hyperpolarizability values are given in Table 5.3 along with the HOMO–LUMO energy gap.

Scrutiny of Table 5.3 shows that as we go from complex 1 to complex 3 with increased π -donation of one axial ligand, the value of β_{zzz} is increased, showing the validity of the idea of getting a prediction over the magnitude of ZFS from the NLO response.

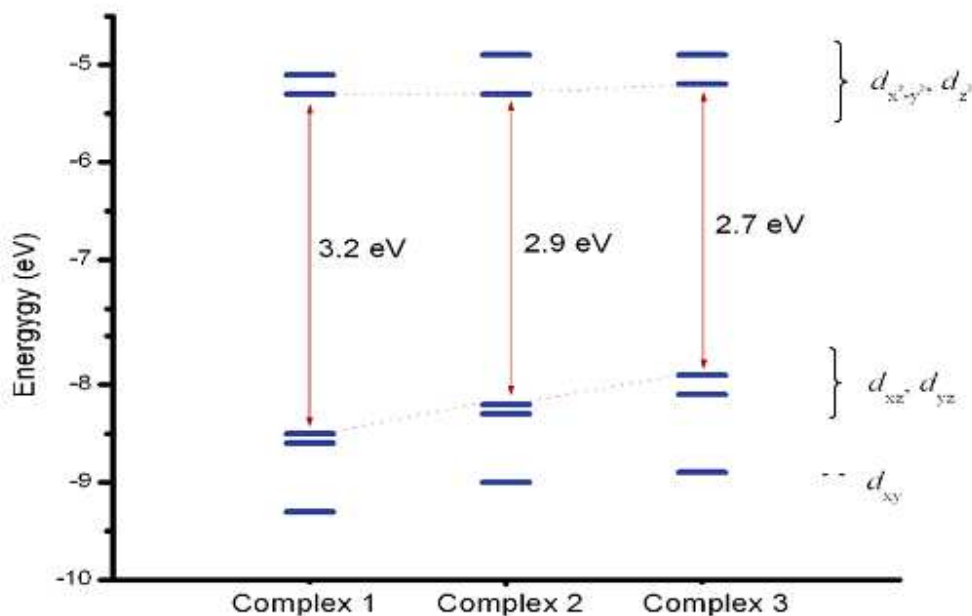


Figure 5.3. Decrease in the HOMO–LUMO gap on going from complex 1 to complex 3, with the increase in π -donation strength from Cl to I.

Table 5.3. The first hyperpolarizability values of complexes 1, 2, and 3 and corresponding HOMO–LUMO gaps (ΔE_{HL}).

complexes	HOMO–LUMO energy gap (ΔE_{HL}) (in eV)	hyperpolarizability (β_{zzz}) (in a.u.)
1	3.2	–146.61
2	2.9	–393.90
3	2.7	–546.01

5.4.2. Effect of individual ligands toward the ZFS of a molecule

The interaction of the π -donor ligand with the d orbitals in the t_{2g} group is shown in Figure 5.4. The π -interaction lifts the SOMOs containing d_{xz} and d_{yz} orbitals upward by forming $p\pi-d\pi$ antibonding orbitals. In order to study the effect imparted by the ligands, a

DFT calculation is performed by replacing the ligands of focus by point charges of same magnitude as that on the ligand. The purpose of this model is to nullify the π -interaction between the ligand orbitals and the metal d -orbitals. The charge in place of the ligand is retained to model the same crystal field environment as in the original complex and enforces a similar occupation of the orbitals.⁶¹ When the ligand is replaced by a point charge, the D value, which is denoted here as D_X , corresponds to the ZFS of the complex, excluding that specific ligand. The idea as coined by Neese and Solomon⁴⁷ is that the ligand contribution to the total D can be estimated from the difference of the D_X from the molecular D values. The use of point charges in the calculation of the electronic spectra of complexes is known as the “Sparkle” model.⁶² Hence, the method employing the point charge, described above, can be used as a scheme for getting a fingerprint of the ligand contribution toward the total SOC of the complex in the DFT framework. The results given in Table 5.4 depict that there is a considerable contribution from the halide ligands to the magnetic anisotropy of the complexes, i.e., the participation of the halide ligands in the spin–orbit coupling is very pronounced. The contribution from ligand is also increased from chloride to iodide. This result is quite consistent with the fact that, as iodine has a very heavy nucleus, the spin–orbit coupling imparted by this ligand will be higher than bromide, which will in turn be greater than chloride. The comparison of the D values with and without π -donor explores that, in the cases of complexes 2 and 3, the halide ligands play a significant role to make the value of D positive and there placement of ligand with point charge brings forth a negative D_X value. The π -acceptor ligand on the other side, which has been kept intact, may be responsible for the switch in the D value. However, for complex 1, the D_X value is not altered much and is of positive sign. This apparent anomaly in D_X values can be attributed to the altering electron availability at the Cr(III) atom, which in its turn increases the π -acceptor capacity of the CN^- ligand.⁶³ In the presence of a weak donor Cl^- ligand in complex 1, the π -accepting tendency of the CN^- is less efficient. Hence, in the case of complex 1, the cyanide ligand cannot act as an effective π -acceptor, and, consequently, the effect is less prominent. As bromide or iodide effectively donates electrons to the metal ion, the electron density on the metal in complex 2 and 3 is much higher than that in complex 1. The availability of electrons in the metal ion in bromide and iodide complexes is much higher, and the π -accepting tendencies of the CN^- ligands are very similar. So, the replacement of these groups with point charge produces D values that differ so little that rounding off leads to the same value of D_X , and both are of negative sign. This reversal in D in the case of complexes 2 and 3 is explained below from the arrangement of the MOs and d -orbital splitting of the Cr(III) ion in the octahedral ligand field. At zero applied magnetic field, the ligand field Hamiltonian is written as

$$\hat{H}_{LF} = \Delta_{ax} \left[\hat{L}_z^2 - \frac{1}{3} L(L+1) \right] + \Delta_{rh} \left[\hat{L}_x^2 - \hat{L}_y^2 \right] - A\lambda L \cdot S \quad (5.9)$$

where Δ_{ax} and Δ_{rh} are the axial and rhombic splitting parameters, respectively, λ is the spin–orbit coupling constant, and A is a constant having a value between 1.0 (strong ligand

field) and 1.5 (weak ligand field).⁶⁴ The Δ_{ax} is the splitting of the d_{xy} -orbital relative to the d_{xz} and d_{yz} -orbitals ($\Delta_{ax} = E_{xz,yz} - E_{xy}$).⁶⁵ The sign of Δ_{ax} determines the sign of the D parameter. The positive sign of D requires Δ_{ax} to be positive, which indicates that the d_{xz} and d_{yz} -orbitals are at higher energy than the d_{xy} -orbital. A negative Δ_{ax} would certainly give rise to a state where the d_{xy} -orbital lies higher in the energy level diagram than the d_{xz} and d_{yz} -orbitals.⁶⁶ Figure 5.4 clearly explains the positive sign of the ZFS parameter in the cases of complexes 1, 2, and 3. Thus, the MO analysis of the complexes with different ligands can serve as a good indicator to forecast the sign of the ZFS parameter.

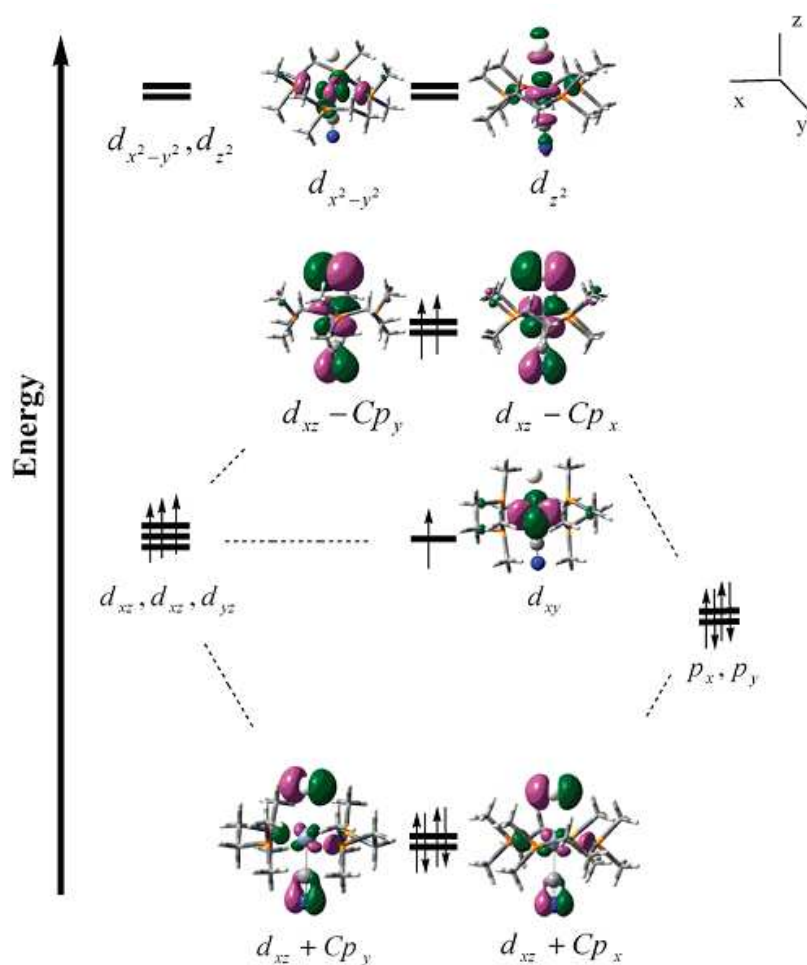


Figure 5.4. A qualitative MO diagram of $[\text{Cr}(\text{dmpe})_2(\text{CN})\text{X}]^+$ showing interaction of the metal d -orbitals with π -donor ligands.

Table 5.4. The values of the total ZFS parameter (D) and after replacement of the halide ligands with point charges of the same magnitude (D_X with $X = \text{Cl}, \text{Br}, \text{and I}$).

complex	D (cm^{-1})	D_X (cm^{-1})
1	0.27	0.23
2	1.45	-0.14
3	5.66	-0.14

5.4.3. Effect of axial ligand substitution

To examine the effect of π -donation and π -acceptance from the axial positions on the magnetic anisotropy of a complex, two sets of test calculations were performed. The first set of calculations was carried out with complexes where both the axial positions occupied by π -donor ligands and the other set of calculations are performed with the complexes containing π -acceptor ligands in axial positions.

SET-I. Set-I includes complexes of formula $[\text{Cr}(\text{dmpe})_2\text{L}_2]^+$, with $\text{L} = \text{Cl}, \text{Br}, \text{and I}$ (Figure 5.5). These structures are also available in crystallographic information file format in ref 27. The intention to carry out the first set of calculations arose from the observation of Table 5.4, as there we can see that the presence of a π -donor is found to increase the value of D . Hence further replacement of the other axial ligand with the same π -donor is made, and the results are tabulated in Table 5.5.

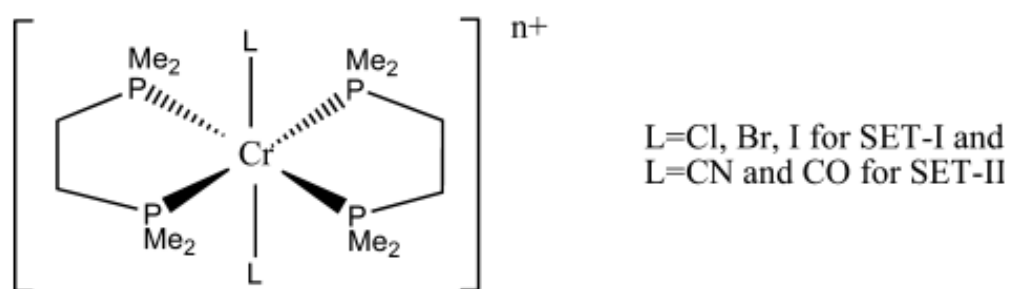


Figure 5.5. Schematic representation of the complexes used in SET-I and SET-II.

Table 5.5. Calculated ZFS parameters for complex series $[\text{Cr}(\text{dmpe})_2\text{X}_2]^+$, with X = Cl, Br, and I.

$[\text{Cr}(\text{dmpe})_2\text{X}_2]^+$	Calculated ZFS Parameter D in cm^{-1}
L=Cl	0.38
L=Br	3.80
L=I	16.98

From the results it is clear that when both the axial ligands are halides, the magnitude of D is much higher than those complexes with only one halide ligand in an axial position. The d -orbital splitting in such complexes are such that the d_{xy} -orbital lies at a lower energy than the d_{xz} or d_{yz} -orbital, i.e., in these cases, Δ_{ax} is positive. The positive sign of the axial splitting parameter Δ_{ax} explains the positive ZFS value. It is also obvious from Tables 1 and 5 that this ligand effect is additive in nature.

SET-II. While the effect of the π -donor ligands can be understood as a controlling factor of the sign and magnitude of D , it is obvious that with a π -acceptor ligand, the sign of D would be negative. A negative D value is desired for making SMMs. So, this set of numerical experiment is carried out with the π -acceptor ligands in the axial positions, and ZFS parameters are calculated. The calculated values of D are kept in Table 5.6. A qualitative MO diagram for such set of complexes is given in Figure 5.6. An alteration in the position of the singly occupied d_{xy} orbital in the energy spectrum of these complexes compared to that in Set-I complexes is observed. Hence, from the discussions given in the previous section, the change in the sign of the D values for this set of complexes can be explained. Moreover, a higher negative D is obtained with a stronger π -accepting carbonyl (CO) ligand. It has been reported previously that if easy-axis anisotropies are linked in tandem, they can lead to a large easy-axis type anisotropy in the long chain range, and exhibition of a slow relaxation of magnetization can be realized.²⁵ Hence it seems to be quite a general effect that, while a π -donor ligand causes an easy-plane anisotropy, a π -acid ligand on the other hand makes the nature of the anisotropy of the complexes to be of easy-axis type.

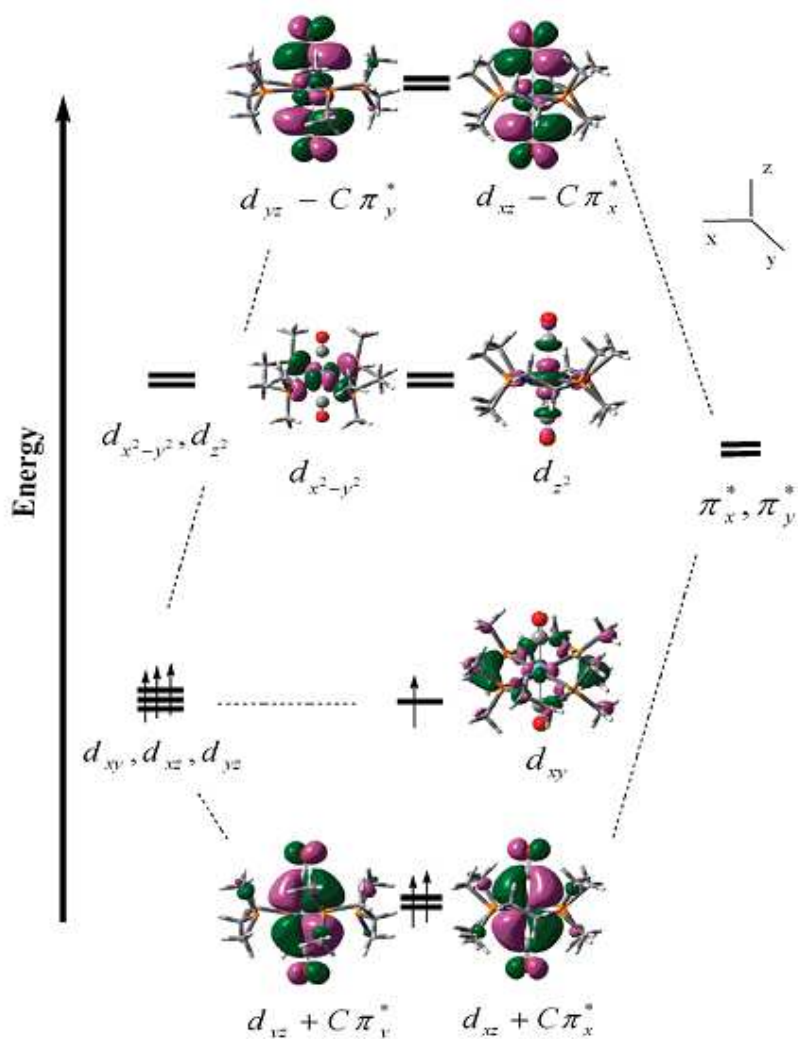


Figure 5.6. A qualitative MO diagram of $[\text{Cr}(\text{dmpe})_2(\text{CN})\text{X}/\text{CN}]^+$ showing interaction of the metal d -orbitals with π -acceptor ligands.

Table 5.6. Calculated ZFS parameters for complex series $[\text{Cr}(\text{dmpe})_2\text{L}_2]^{n+}$, with L = CN and CO.

$[\text{Cr}(\text{dmpe})_2\text{L}_2]^{n+}$	Calculated ZFS Parameter D in cm^{-1}
$[\text{Cr}(\text{dmpe})_2(\text{CN})_2]^+$	-0.09
$[\text{Cr}(\text{dmpe})_2(\text{CO})_2]^{3+}$	-0.14

5.4.4. Effect of equatorial ligand substitution

On the basis of the results of the numerical experiment employing point charge given in Table 5.4, the effect of the axial ligand substitution is carried out as described in the above sections. It seems from the discussion in Table 5.4 that the electron density on the metal ion is vital when π -acceptor ligands are employed from both axial positions. The greater the electron density on the metal, the more effective the π -acceptor ligands will be. The equatorial ligands here can aid in the increment of electron density on the central metal, which in turn can lead to greater π -acceptance of the axial ligands. Hence, for the verification of the above speculation, a few complexes are designed with two π -acceptor ligands in the axial positions, and the equatorial ligands are changed through the halides (Figure 5.7). The designed octahedral complexes contain chloride, bromide, and iodide ligands, respectively, in their equatorial positions. First we have tried out three octahedral Cr(III) complexes with CN^- as two axial ligands. Here we see that, as the donation from the equatorial ligands increase, the magnitude of the negative D is increased (Table 5.7). Thus following the interplay between the nature of the ligand and the axial crystal field splitting (Δ_{ax}), one can systematically change the magnetic anisotropy of a complex. To sum up, we can say that a negative D value can be achieved if there is sufficient donation of electrons from the equatorial ligands to the metal, so that a larger availability of electrons on the metal occurs and the designing of single molecule magnets with a high degree of magnetic anisotropy is possible by suitable placement of the π -acid ligands in the axial positions of octahedral metal complexes.

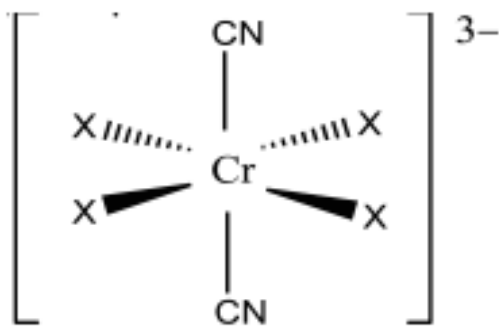


Figure 5.7. Schematic representation of the designed complexes where equatorial positions are replaced with halides ($X = \text{Cl}, \text{Br}, \text{and I}$).

Table 5.7. Calculated ZFS parameters for complex Series $[\text{CrX}_4(\text{CN})_2]^{3-}$, with X= Cl, Br, and I.

X=	Calculated ZFS Parameter D in cm^{-1} for Complex $[\text{CrX}_4(\text{CN})_2]^{3-}$
Cl	-0.13
Br	-0.69
I	-5.18

5.5. Conclusion

In the present work, the magnetic anisotropy property of a series of octahedral Cr(III) complexes is studied. It has been shown that π -donor and π -acceptor ligands, in the axial position of the octahedral complexes, have different effects on the magnetic anisotropy of the complexes. The interaction of the ligands with the metal d -orbitals gives rise to two different situations responsible for this kind of switch in the ZFS parameter. The π -donor ligands play a role in making the magnitude of ZFS larger with an increased π -donation from the halide ligands, while a π -acceptor ligand causes the anisotropy property to be of easy-axis type ($D < 0$). Moreover, a π -acceptor ligand in both the axial positions imparts single molecular magnetic nature to the system having an easy-axis of the magnetic anisotropy. An increased donation from the equatorial positions is seen to enhance the magnitude of easy axis type magnetic anisotropy. This can be attributed to the increased π -accepting efficiency of the axial ligands due to an enhanced metallic electron density, pushed by the equatorial ligands. On the basis of the above observations regarding the ligand replacement, octahedral Cr(III) complexes can be designed in such a way that it can meet our desired anisotropy characteristics. The NLO response is found to vary with π -donation similarly as the magnetic anisotropy. The second order NLO response, β , has been related to the magnetic anisotropy in the case of the non-centrosymmetric octahedral complexes, where we can see that the NLO response can lead us to good anticipation of magnetic anisotropy.

From the systematic DFT study with these octahedral complexes, a clear understanding about the influence of the ligands on modulating the magnetic anisotropy of the Cr(III) complexes is possible. For convenience, we perform a few numerical experimentations. The D value for $[\text{CrBr}_4(\text{CN})_2]^{3-}$, as we recollect from Table 7, is -0.69 cm^{-1} . We calculate the ZFS parameter for $[\text{CrBr}_4(\text{CO})_2]^-$, which comes out to be -2.51 cm^{-1} . Now relying on the above method of prediction, we design a complex of formula $[\text{CrBr}_4(\text{CN})(\text{CO})]^{2-}$ and expect

the D value to be in between -0.69 cm^{-1} and -2.51 cm^{-1} and get a value of -0.94 cm^{-1} . Thus, from this observation, a general conclusion can be drawn that the anisotropy of such metal complexes is greatly controlled by the ligands. To summarize, this work explicates a simple application of DFT to calculate anisotropy parameters in metal complexes to devise a rule of thumb for the occurrence of SMM behavior in such complexes.

5.6. References

1. Kahn, O. *Molecular Magnetism*; VCH: New York, 1993.
2. Oshio, H.; Nakano, M. *Chem. -Eur. J.* **2005**, *11*, 5178.
3. Gatteschi, D.; Sessoli, R. *J. Magn. Magn. Mater.* **2004**, *272*, 1030.
4. Krzystek, J.; Ozarowski, A.; Telser, J. *Coord. Chem. Rev.* **2006**, *250*, 2308.
5. (a) Sessoli, R.; Tsai, H. L.; Schake, A. R.; Wang, S.; Vincent, J. B.; Folting, K.; Gatteschi, D.; Christou, G.; Hendricson, D. N. *J. Am. Chem. Soc.* **1993**, *115*, 1804; (b) Sessoli, R.; Gatteschi, D.; Caneschi, A.; Novak, M. A. *Nature* **1993**, *365*, 141.
6. (a) Gatteschi, D.; Sessoli, R.; Villain, J. *Molecular Nanomagnets*; Oxford University Press: New York, 2006; (b) Milios, C. J.; Vinslava, A.; Wernsdorfer, W.; Moggach, S.; Parsons, S.; Perlepes, S. P.; Christou, G.; Brechin, E. K. *J. Am. Chem. Soc.* **2007**, *129*, 2754; (c) Freedman, D. E.; Jenkins, D. M.; Ivarone, A. T.; Long, J. R. *J. Am. Chem. Soc.* **2008**, *130*, 2884; (d) Yoshihara, D.; Karasawa, S.; Koga, N. *J. Am. Chem. Soc.* **2008**, *130*, 10460.
7. Gatteschi, D.; Caneschi, A.; Pardi, L.; Sessoli, R. *Science* **1994**, *265*, 1054.
8. Aubin, S. M. J.; Wemple, M. W.; Adams, D. M.; Tsai, H. L.; Christou, G.; Hendricson, D. N. *J. Am. Chem. Soc.* **1996**, *118*, 7746.
9. Ritter, S. K. *Chem. Eng. News* **2004**, *82*, 29.
10. (a) Garanin, D. A.; Chudnovsky, E. M. *Phys. Rev. B* **1997**, *56*, 11102; (b) Leuenberger, M. N.; Loss, D. *Nature* **2001**, *410*, 789; (c) Jo, M. H.; Grose, J. E.; Baheti, K.; Deshmukh, M. M.; Sokol, J. J.; Rumberger, E. M.; Hendrickson, D. N.; Long, J. R.; Park, H.; Ralph, D. C. *Nano Lett.* **2006**, *6*, 2014; (d) Ardavan, A.; Rival, O.; Morton, J. J. L.; Blundell, S. J.; Tyryshkin, A. M.; Timco, G. A.; Winpenny, R. E. P. *Phys. Rev. Lett.* **2007**, *98*, 572011; (e) Bogani, L.; Wernsdorfer, W. *Nat. Mater.* **2008**, *7*, 179; (f) Stamp, P. C. E.; Gaita-Arino, A. *J. Mater. Chem.* **2009**, *19*, 1718.
11. (a) Affronte, M.; Troiani, F.; Ghirri, A.; Candini, A.; Evangelisti, M.; Corradini, V.; Carretta, S.; Santini, P.; Amoretti, G.; Tuna, F.; Timco, G.; Winpenny, R. E. P. *J. Phys. D*

Appl. Phys. **2007**, *40*, 2999; (b) Manoli, M.; Johnstone, R. D. L.; Parsons, S.; Murrie, M.; Affronte, M.; Evangelisti, M.; Brechin, E. K. *Angew. Chem., Int. Ed.* **2007**, *46*, 4456; (c) Mannini, M.; Pineider, F.; Sainctavit, P.; Danieli, C.; Otero, E.; Sciancalepore, C.; Talarico, A. M.; Arrio, M. A.; Cornia, A.; Gatteschi, D.; Sessoli, R. *Nat. Mater.* **2009**, *8*, 194; (d) Loth, S.; von Bergmann, K.; Ternes, M.; Otte, A. F.; Lutz, C. P.; Heinrich, A. J. *Nat. Phys.* **2010**, *6*, 340.

12. (a) Collison, D.; Murrie, M.; Oganessian, V. S.; Piligkos, S.; Poolton, N. R. J.; Rajaraman, G.; Smith, G. M.; Thomson, A. J.; Timko, G. A.; Wernsdorfer, W.; Winpenny, R. E. P.; McInnes, E. J. L. *Inorg. Chem.*, **2003**, *42*, 5293; (b) Vallejo, J.; Castro, I.; Cañadillas-Delgado, L.; Ruiz-Pérez, C.; Ferrando-Soria, J.; Ruiz-García, R.; Cano, J.; Lloret, F.; Julve, M. *Dalton Trans.* **2010**, *39*, 2350.

13. (a) AlDamen, M. A.; Clemente-Juan, J. M.; Coronado, E.; Marti-Gastaldo, C.; Gaita-Arino, A. *J. Am. Chem. Soc.* **2008**, *130*, 8874; (b) AlDamen, M. A.; Cardona-Serra, S.; Clemente-Juan, J. M.; Coronado, E.; Gaita-Arino, A.; Marti-Gastaldo, C.; Luis, F.; Montero, O. *Inorg. Chem.* **2009**, *48*, 3467–3479.

14. (a) Branzoli, F.; Carretta, P.; Filibian, M.; Zoppellaro, G.; Graf, M. J.; Galan-Mascaros, J. R.; Fuhr, O.; Brink, S.; Ruben, M. *J. Am. Chem. Soc.* **2009**, *131*, 4387; (b) Kyatskaya, S.; Galan-Mascaros, J. R.; Bogani, L.; Hennrich, F.; Kappes, M.; Wernsdorfer, W.; Ruben, M. *J. Am. Chem. Soc.* **2009**, *131*, 15143.

15. Jiang, S. D.; Wang, B. W.; Su, G.; Wang, Z. M.; Gao, S. *Angew. Chem., Int. Ed.* **2010**, *49*, 7448.

16. (a) Rinehart, J. D.; Long, J. R. *J. Am. Chem. Soc.* **2009**, *131*, 12558; (b) Rinehart, J. D.; Meihaus, K. R.; Long, J. R. *J. Am. Chem. Soc.* **2010**, *132*, 7572.

17. Freedman, D. E.; Harman, W. H.; Harris, T. D.; Long, G. J.; Chang, C. J.; Long, J. R. *J. Am. Chem. Soc.* **2010**, *132*, 1224.

18. Clerac, R.; Miyasaka, H.; Yamashita, M.; Coulon, C. *J. Am. Chem. Soc.* **2002**, *124*, 12837.

19. Ferbinteanu, M.; Miyasaka, H.; Wernsdorfer, W.; Nakata, K.; Sugiura, K.; Yamashita, M.; Coulon, C.; Clerac, R. *J. Am. Chem. Soc.* **2005**, *127*, 3090.

20. Miyasaka, H.; Nezu, T.; Sugimoto, K.; Sugiura, K.; Yamashita, M.; Clerac, R. *Chem.–Eur. J.* **2005**, *11*, 1592.

21. Kajiwara, T.; Nakano, M.; Kaneko, Y.; Takaishi, S.; Ito, T.; Yamashita, M.; Kamiyama, A. I.; Nojiri, H.; Ono, Y.; Kojima, N. *J. Am. Chem. Soc.* **2005**, *127*, 10150.

22. Miyasaka, H.; Madanbashi, T.; Sugimoto, K.; Nakazawa, Y.; Wernsdorfer, W.; Sugiura, K.; Yamashita, M.; Coulon, C.; Clerac, R. *Chem.–Eur. J.* **2006**, *12*, 7028.
23. Caneschi, A.; Gatteschi, D.; Lalioti, N.; Sangregorio, C.; Sessoli, R.; Venturi, G.; Vindigni, A.; Rettori, A.; Pini, M. G.; Novak, M. A. *Angew. Chem., Int. Ed.* **2001**, *40*, 1760.
24. Harris, T. D.; Bennett, M. V.; Clerac, R.; Long, J. R. *J. Am. Chem. Soc.* **2010**, *132*, 3980.
25. Nakano, M.; Oshio, H. *Chem. Soc. Rev.* **2011**, *40*, 3239.
26. (a) Busey, R. H.; Sonder, E. *J. Chem. Phys.* **1962**, *36*, 93; (b) Desrochers, P. J.; Telser, J.; Zvyagin, S. A.; Ozarowski, A.; Krzystek, J.; Vicic, D. A. *Inorg. Chem.* **2006**, *45*, 8930; (c) Duboc, C.; Phoeung, T.; Zein, S.; Pecaut, J.; Collomb, M.-N.; Neese, F. *Inorg. Chem.* **2007**, *46*, 4905.
27. Karunadasa, H. I.; Arquero, K. D.; Berben, L. A.; Long, J. R. *Inorg. Chem.* **2010**, *49*, 4738.
28. Kanis, D. R.; Lacroix, P. G.; Ratner, M. A.; Marks, T. J. *J. Am. Chem. Soc.* **1994**, *116*, 10089.
29. Zyss, J. *Molecular Nonlinear Optics: Materials, Physics and Devices*; Academic: Boston, MA, 1994; *Nonlinear Optical Properties of Matter: From Molecules to Condensed Phases*; Papadopoulos, M. G., Leszczynski, J., Sadlej, A. J., Eds.; Kluwer: Dordrecht, The Netherlands, 2005.
30. (a) Marder, S. R.; Gorman, C. B.; Meyers, F.; Perry, J. W.; Bourhill, G.; Bré das, J. L.; Pierce, B. M. *Science* **1994**, *265*, 632; (b) Marder, S. R. *Chem. Commun.* **2006**, 131; (c) Kang, H.; Evmenenko, G.; Dutta, P.; Clays, K.; Song, K.; Marks, T. J. *J. Am. Chem. Soc.* **2006**, *128*, 6194; (d) Yang, M.; Champagne, B. *J. Phys. Chem. A* **2003**, *107*, 3942; (e) Liao, Y.; Bhattacharjee, S.; Firestone, K. A.; Eichinger, B. E.; Paranj, R.; Anderson, C. A.; Robinson, B. H.; Reid, P. J.; Dalton, L. R. *J. Am. Chem. Soc.* **2006**, *128*, 6847; (f) Kang, H.; Facchetti, A.; Jiang, H.; Cariati, E.; Righetto, S.; Ugo, R.; Zuccaccia, C.; Macchioni, A.; Stern, C. L.; Liu, Z.; Ho, S.-T.; Brown, E. C.; Ratner, M. A.; Marks, T. J. *J. Am. Chem. Soc.* **2007**, *129*, 3267.
31. Paul, S.; Misra, A. *Inorg. Chem.* **2011**, *50*, 3234.
32. (a) Cariati, E.; Ugo, R.; Santoro, G.; Tordin, E.; Sorace, L.; Caneschi, A.; Sironi, A.; Macchi, P.; Casati, N. *Inorg. Chem.* **2010**, *49*, 10894; (b) Lacroix, P. G.; Malfant, I.; Bé nard, S.; Yu, P.; Riviè re, E.; Nakatani, K. *Chem. Mater.* **2001**, *13*, 441; (c) Dragonetti, C.; Righetto, S.; Roberto, D.; Ugo, R.; Valore, A.; Fantacci, S.; Sgamellotti, A.; Angelis, F. D. *Chem. Commun.* **2007**, 4116; (d) Janjua, M. R. S. A.; Guan, W.; Yan, L.; Su, Z. -M.; Ali, M.; Bukhari, I. H. *J. Mol. Graph. Model.* **2010**, *28*, 735.

33. Zein, S.; Duboc, C.; Lubitz, W.; Neese, F. *Inorg. Chem.* **2008**, *47*, 134.
34. Pederson, M. R.; Khanna, S. N. *Phys. Rev. B* **1999**, *60*, 9566.
35. Neese, F.; Pantazis, D. A. *Faraday Discuss.* **2011**, *148*, 229.
36. Neese, F.; Neese, F. ORCA 2.8.0; University of Bonn: Bonn, Germany, 2010.
37. (a) van Wüllen, C. *J. Chem. Phys.* **2009**, *130*, 194109;(b) Aquino, F.; Rodriguez, J. H. *J. Phys. Chem. A* **2009**, *113*, 9150; (c) Aquino, F.; Rodriguez, J. H. *J. Chem. Phys.* **2005**, *123*, 204902.
38. (a) Schäfer, A.; Horn, H.; Ahlrichs, R. *J. Chem. Phys.* **1992**, *97*,2571; (b) Schäfer, A.; Huber, C.; Ahlrichs, R. *J. Chem. Phys.* **1994**, *100*, 5829.
39. Weigend, F. *Phys. Chem. Chem. Phys.* **2006**, *8*, 1057.
40. (a) Takeda, R.; Mitsuo, S.; Yamanaka, S.; Yamaguchi, K. *Polyhedron* **2005**, *24*, 2238; (b) Kortus, J.; Pederson, M. R.; Baruah, T.; Bernstein, N.; Hellberg, C. S. *Polyhedron* **2003**, *22*, 1871; (c) Park, K.; Pederson, M. R.; Richardson, S. L.; Aliaga-Alcalde, N.; Christou, G. *Phys. Rev. B* **2003**, *68*, 020405;(d) Baruah, T.; Pederson, M. R. *Int. J. Quantum Chem.* **2003**, *93*,324; (e) Ribas-Ariño, J.; Baruah, T.; Pederson, M. R. *J. Am. Chem. Soc.* **2006**, *128*, 9497.
41. Neese, F. *J. Am. Chem. Soc.* **2006**, *128*, 10213.
42. Neese, F. *J. Chem. Phys.* **2007**, *127*, 164112.
43. Maurice, R.; Sivalingam, K.; Ganyushin, D.; Guihéry, N.; de Graaf, C.; Neese, F. *Inorg. Chem.* **2011**, *50*, 6229.
44. Reviakine, R.; Arbuznikov, A. V.; Tremblay, J. C.; Remenyi, C.; Malkina, O. L.; Malkin, V. G.; Kaupp, M. *J. Chem. Phys.* **2006**, *125*, 054110.
45. Misochko, E. Y.; Korchagin, D. V.; Bozhenko, K. V.; Chapyshev, S. V.; Aldoshin, S. M. *J. Chem. Phys.* **2010**, *133*, 064101.
46. Frisch, M. J.; Trucks, G. W.; Schlegel, H. B.; Scuseria, G. E.; Robb, M. A.; Cheesman, J. R.; Zakrzewski, V. G.; Montgomery, J. A.; Strtmann, R. E.; Burant, J. C.; Dapprich, S.; Milliam, J. M.; Daniels, A. D.; Kudin, K. N.; Strain, M. C.; Farkas, O.; Tomasi, J.; Barone, V.; Cossi, M.; Camme, R.; Mennucci, B.; Pomelli, C.; Adamo, C.; Clifford, S.; Ochterski, J.; Petersson, G. A.; Ayala, P. Y.; Cui, Q.; Morokuma, K.; Rega, N.; Salvador, P.; Dannenberg, J. J.; Malich, D. K.; Rabuck, A. D.; Raghavachari, K.; Foresman, J. B.; Cioslowski, J.; Ortiz, J. V.; Baboul, A. G.; Stetanov, B. B.; Liu, G.; Liashenko, A.; Piskorz, P.; Komaromi, I.; Gomperts, R.; Martin, R. L.; Fox, D. J.; Keith, T.; Al-Laham, M. A.; Peng, C. Y.; Nnsyskkara, A.; Challacombe, M.; Gill, P. M. W.; Johnson, B.; Chen, W.; Wong, M. W.;

Andres, J. L.; Gonzalez, C.; Head-Gordon, M.; Replogle E. S.; Pople, J. A. GAUSSIAN09, Revision A.02, Gaussian Inc., Pittsburgh (2009).

47. (a) Easton, R. E.; Giesen, D. J.; Welch, A.; Cramer, C. J.; Truhlar, D. G. *Theor. Chim. Acta* **1996**, *93*, 281; (b) Li, J.; Cramer, C. J.; Truhlar, D. G. *Theor. Chem. Acc.* **1998**, *99*, 192.

48. Neese, F.; Solomon, E. I. *Inorg. Chem.* **1998**, *37*, 6568.

49. Solomon, E. I. *Inorg. Chem.* **2006**, *45*, 8012.

50. Stevens, K. W. H. *Proc. R. Soc. A (London)* **1953**, *219*, 542.

51. Nyholm, R. S. *Pure Appl. Chem.* **1968**, *17*, 1.

52. Tofield, B. C. *J. Phys. Colloq.* **1976**, *37*, C6–539.

53. Atanasov, M.; Baerends, E. J.; Baettig, P.; Bruyndonckx, R.; Daul, C.; Rauzy, C.; Zbiri, M. *Chem. Phys. Lett.* **2004**, *399*, 433.

54. O'Reilly, T. J.; Offenbacher, E. L. *J. Chem. Phys.* **1971**, *54*, 3065.

55. Pellow, R.; Vala, M. *J. Chem. Phys.* **1989**, *90*, 5612.

56. (a) Debrunner, P. G.; Dexter, A. F.; Schulz, C. E.; Xia, Y.-M.; Hager, L. P. *Proc. Natl. Acad. Sci. U.S.A.* **1996**, *93*, 12791; (b) Griffith, J. S. *Mol. Phys.* **1971**, *21*, 135.

57. Neese, F.; Solomon, E. I., Magnetism: Molecules to Materials IV; Miller, J. S., Drillon, M., Eds; Wiley-VCH: Weinheim, 2002; Chapter 9, p 406.

58. Schöneboom, J. C.; Neese, F.; Thiel, W. *J. Am. Chem. Soc.* **2005**, *127*, 5840.

59. Maganas, D.; Sottini, S; Kyritsis, P.; Groenen, E. J. J.; Neese, F. *Inorg. Chem.* **2011**, *50*, 8741.

60. Kanis, D. R.; Ratner, M. A.; Marks, T. J. *Chem. Rev.* **1994**, *94*, 195.

61. Boguslawski, K.; Jacob, C. R.; Reiher, M. *J. Chem. Theory. Comput.* **2011**, *7*, 2740.

62. de Andrade, A. V. M; da Costa, N. B., Jr.; Longo, R. L.; Malta, O. L.; Simas, A. M.; de Sá, G.F. *Mol. Eng.* **1997**, *7*, 293.

63. (a) Meissler, G. L.; Tarr, D. A. *Inorganic Chemistry*; Pearson Education and Pearson Prentice Hall: Upper Saddle River, NJ, 2004. (b) Caughey, W. S.; Eberspaecher, H.; Fuchsman, W. H.; McCoy, S.; Alben, J. O. *Ann. N.Y. Acad. Sci.* **1969**, *153*, 722.

64. Kittilstved, K. R.; Sorgho, L. A.; Amstutz, N.; Tregenna-Piggott, P. L. W.; Hauser, A. *Inorg. Chem.* **2009**, *48*, 7750.

65. Solomon, E. I.; Brunold, T. C.; Davis, M. I.; Kemsley, J. N.; Lee, S.-K.; Lehnert, N.; Neese, F.; Skulan, A. J.; Yang, Y.-S.; Zhou, J. *Chem. Rev.* **2000**, *100*, 235.

66. Solomon, E. I.; Pavel, E. G.; Loeb, K. E.; Campochiaro, C. *Coord. Chem. Rev.* **1995**, *144*, 369.

CHAPTER 6

On the control of magnetic anisotropy through an external electric field

Abstract

The effect of an external electric field on the magnetic anisotropy of a single-molecule magnet has been investigated, with the help of DFT. The magnetic anisotropy of a pseudo-octahedral Co(II) complex namely, [Co^{II}(dmphen)₂(NCS)₂], has been investigated in the present chapter in connection to the tunability of the magnetic anisotropy through external electric field. The application of an electric field can alter the magnetic anisotropy from “easy-plane” ($D > 0$) to “easy-axis” ($D < 0$) type. The alteration in the magnetic anisotropy is found due to the change in the Rashba spin-orbit coupling by the external electric field. This variation in the Rashba spin-orbit coupling is further confirmed by the generation of the spin dependent force in the molecule which is later found to manifest separation of α - and β - spins in opposite ends of the molecule. The excitation analysis performed through time-dependent DFT also predicts that the external electric field facilitates metal to π -acceptor ligand charge transfer, leading to uniaxial magnetic anisotropy and concomitant spin Hall effect in a single molecule.

6.1. Introduction

Magnetic anisotropy is of central importance in the understanding of single-molecule magnets (SMM).¹ Molecules that exhibit slow relaxation of their magnetization, leading to a magnetic hysteresis at low temperatures, are termed as SMMs.² The genesis of this interesting magnetic property in a molecule is the existence of two ground states of magnetization $+M_S$ and $-M_S$ separated by an energy barrier. This bistability of the SMMs makes them indispensable in the domain of data storage³ and quantum computing.⁴ SMMs are often characterized by a large easy-axis-type magnetic anisotropy and concomitant high energy barrier (U), which restricts the reversal of the magnetization from $+M_S$ to $-M_S$. To reorient spin in the magnetic molecules, the barrier U can be given by $|D|S^2$ for molecules with integer spins and $|D|(S^2 - 1/4)$ for molecules with half integer spins. D is the zero-field splitting (ZFS) parameter and S is the ground-state spin. The large negative ZFS parameter (D) causes the spin (S) of the molecule to point along a preferred easy-axis and makes it a nanomagnet. The requirement of proper SMMs for apposite needs prompted researchers to study the tuning of magnetic anisotropy.

The most investigated molecule of this type is $[\text{Mn}_{12}\text{O}_{12}(\text{CH}_3\text{COO})_{16}(\text{H}_2\text{O})_4]$, which is popularly known as $\text{Mn}_{12}\text{-ac}$.⁵ A central tetrahedron of four Mn^{4+} ions ($S=3/2$) and eight surrounding Mn^{3+} ($S=2$) ions construct the magnetic core of $\text{Mn}_{12}\text{-ac}$. This compound, which was first synthesized by Lis,⁶ has drawn the attention of the scientific community because it has a strikingly large molecular magnetic moment,⁷ and magnetic bistability with a high magnetization reversal barrier.⁸ It is evident from the above discussion that the spin-reversal barrier is dependent on the total spin, S , and the ZFS parameter, D . The most convenient way to increase the energy barrier within a SMM is through the ground-state spin S . However, increasing S leads to an effective reduction in the ZFS parameter, D ,⁹ which results in a net decrease in the spin-reorientation barrier, U . Thus, the only way to control U is through modulation of the ZFS parameter, D . Although a plethora of compounds with properties that resemble those of $\text{Mn}_{12}\text{-ac}$ have been synthesized to date,¹⁰ the rational design of SMMs with tunable S and D is far from being achieved. Thus, modulation of the ZFS parameter is now a promising field of research for its wide-ranging applications in high-density information storage, quantum computing, and spintronic devices.¹¹

Cobalt(II) complexes are known to exhibit strong spin-orbit coupling in comparison to manganese(II-IV), iron(III), or nickel(-II), to which the distinguished members of the SMM family belong.¹² This is because such octahedral or pseudo-octahedral cobalt(II) ions are known to exert strong first-order orbital magnetism. The ground-state spin configuration for Co(II) in an octahedral coordination environment is $t_{2g}^5 e_g^2$, which designates a 4F ground state.¹³ The 4F ground state is split into two triplet states ($^4T_{1g}, ^4T_{2g}$) and one singlet state ($^4A_{2g}$). The triplet nature of the $^4T_{1g}$ ground state is responsible for first-order orbital momentum.¹³ The large unquenched orbital angular momentum in Co^{II} makes it an important candidate for the study of magnetic anisotropy. Current literature in the domain of SMM research suggests a drift towards the tuning of the magnetic anisotropy through various means.

The modulation of the ZFS parameter by ligand substitution has recently been studied in the framework of DFT.¹⁴ Structural modification in an octahedral Cr^{III} system can switch the magnetization behavior of a molecule from easy-plane to easy-axis type. Herein, we investigate the effect of an external electric field on the ZFS parameter of a pseudo-octahedral [Co^{II}-(dmphen)₂(NCS)₂] complex (dmphen=2,9-dimethyl-1,10-phenanthroline; Figure 6.1) to control magnetization through external stimuli. The use of an electric field in tuning magnetic and transport properties has also been demonstrated recently.¹⁵ To control magnetization, the use of an electric field is highly advantageous.¹⁶ Although the bulk properties of SMMs are well documented in their unperturbed state,¹⁷ the study of the effect of an external electric field on the magnetization of SMMs is relatively recent.¹⁸

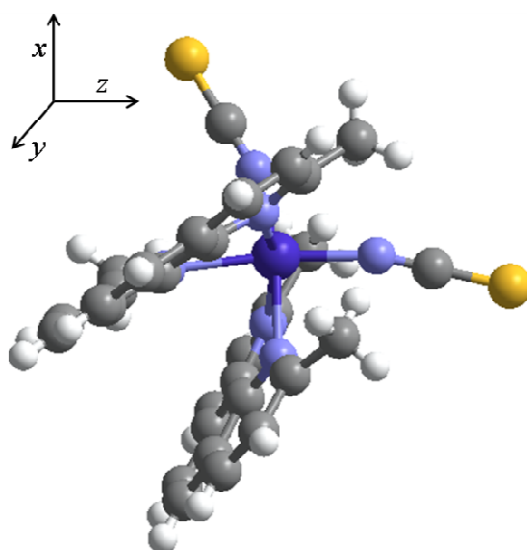


Figure 6.1. Structure of the pseudo-octahedral Co^{II}-complex, [Co^{II}(dmphen)₂(NCS)₂].

6.2. Theoretical Background and Method

The formation of a static electric field between two oppositely charged parallel plates is well known from the laws of classical electrophysics. It is also common practice to create a uniform static field between the central area of large parallel plates because in that area the electric lines of force become parallel. This simple concept from elementary physics encouraged us to construct a device to calculate ZFS under the influence of an external electric field. Thus, to realize the magnetization behavior of the molecule under an electric pulse, we placed the molecule between two oppositely charged parallel plates with an area of about 600 Å². We chose the atomic arrangements of the Pt (111) surface, and subsequently, replaced the atoms with point charges uniformly to create the charged plates. The plates were 40 Å apart, which maintained a distance of at least 18 Å from the molecule and would avoid any structural deformation due to point charges. The whole arrangement is pictorially represented in Figure 6.2. This is typically the same arrangement as a parallel-plate capacitor.

The left plate is charged as positive, while the right plate contains negative point charges of the same magnitude in the platinum atomic positions. In this way, we create an electric field along the positive z -axis. Calculations of the ZFS parameters were performed by following the methodology discussed in the following paragraphs.

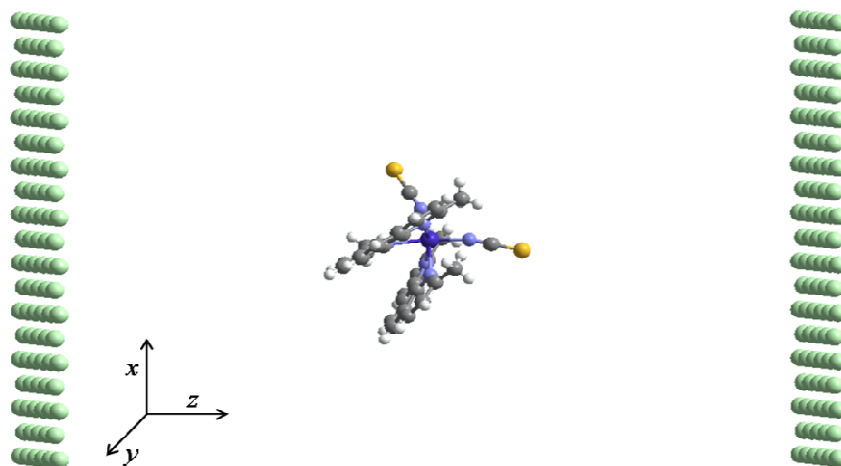


Figure 6.2. The arrangement of $[\text{Co}^{\text{II}}(\text{dmphen})_2(\text{NCS})_2]$ complex between two oppositely charged parallel plates.

ZFS lifts the degeneracy of the M_S states in a molecule with $S > 1/2$, in the absence of an external magnetic field. It is customary to treat the spin-orbit coupling contribution to ZFS through an uncoupled perturbation theoretical approach in unrestricted Kohn-Sham formalism.¹⁹ The corresponding correction to the total energy can be expressed as eqn (6.1):²⁰

$$\Delta_2 = \sum_{\sigma\sigma'} \sum_{ij} M_{ij}^{\sigma\sigma'} S_i^{\sigma\sigma'} S_j^{\sigma'\sigma}, \quad (6.1)$$

in which $S_i^{\sigma\sigma'} = \langle \chi^\sigma | S_i | \chi^{\sigma'} \rangle$; χ^σ and $\chi^{\sigma'}$ are different spinors; σ denotes different spin degrees of freedom and the coordinate labels, x , y , and z are represented by i , j , and so forth. The matrix elements $M_{ij}^{\sigma\sigma'}$ in eqn (6.1) are described by eqn (6.2)

$$M_{ij}^{\sigma\sigma'} = - \sum_{kl} \frac{\langle \varphi_{l\sigma} | V_i | \varphi_{k\sigma'} \rangle \langle \varphi_{k\sigma'} | V_j | \varphi_{l\sigma} \rangle}{\varepsilon_{l\sigma} - \varepsilon_{k\sigma'}}. \quad (6.2)$$

In this equation $\varepsilon_{l\sigma}$ and $\varepsilon_{k\sigma'}$ are energies of the occupied, $\varphi_{l\sigma}$, and unoccupied, $\varphi_{k\sigma'}$, states, respectively. In the absence of a magnetic field, the change in energy of the system in the second-order is written as eqn (6.3):

$$\Delta_2 = \sum_{ij} \gamma_{ij} \langle S_i | \langle S_j \rangle. \quad (6.3)$$

Upon diagonalization of the anisotropy tensor, γ , the eigenvalues γ_{xx} , γ_{yy} , and γ_{zz} are obtained and the second-order perturbation energy can now be written as eqn (6.4)

$$\begin{aligned} \Delta_2 = & \frac{1}{3}(\gamma_{xx} + \gamma_{yy} + \gamma_{zz})S(S+1) \\ & + \frac{1}{3}\left[\gamma_{zz} - \frac{1}{2}(\gamma_{xx} + \gamma_{yy})\right][3S_z^2 - S(S+1)] \\ & + \frac{1}{2}(\gamma_{xx} - \gamma_{yy})(S_x^2 - S_y^2) \end{aligned} \quad (6.4)$$

These anisotropy tensor components (γ_{xx} , γ_{yy} , γ_{zz}) are parameterized to obtain eqn (6.5) as a simplified expression:

$$H_{ZFS} = D[S_z^2 - \frac{1}{3}S(S+1)] + E[S_x^2 - S_y^2] \quad (6.5)$$

in which D and E are axial and rhombic ZFS parameters, respectively. Calculation of parameters D and E was performed in the ORCA suit of a density functional package.²¹ The methodology adopted herein was the BPW91 functional,²² TZV basis set,²³ with the auxiliary TZV/J Coulomb-fitting basis set.²⁴ This methodology, under unrestricted Kohn--Sham formalism, as adopted herein, is being widely used to compute ZFS parameters.^{22a,25} Although there are several methods available for the computation of the ZFS parameter, the Pederson and Khanna (PK) method is known to produce the correct sign of the ZFS parameter;^{22a,26} therefore, we use this methodology²⁰ to calculate the ZFS parameters. The ZFS contributions predicted by this method show fair agreement with accurate ab initio and experimental results.

6.3. Results and Discussions

Single-point calculations on the crystallographic structure, which are available in ref.28, were performed and used for further calculations. It is known from the EPR spectra of complex $[\text{Co}^{\text{II}}(\text{dmphen})_2(\text{NCS})_2]$ that it has ground-state spin $S=3/2$. The value of D is calculated for the complex in its unperturbed ground state and also under the application of bias voltage in the range of -4×10^{-3} to 4×10^{-3} a.u. Herein, the positive and negative values of the external electric field are designated with the application of the field along the positive direction of the z axis, that is, along one axial direction of the Co-NCS bond. The complex is put under a static electric field of different strengths, according to the arrangement discussed in the previous section. It was shown previously that typically a critical electric field in the order of 0.01a.u. was required to bring about ionization in a molecule.²⁷ Hence, application of an electric field in the order of 0.004a.u., as in the present case, is not expected to bring about any undesired polarization or ionization of the molecule.

In the ground state, the ZFS parameter of the complex is positive, which signifies easy-plane type magnetic anisotropy. The computed value of D is given in Table 6.1, along with individual excitation contributions. The MAE barrier, U , was also computed and compared with experimental values.²⁸ We found reasonable agreement of the calculated value of U with the experimentally obtained MAE barrier. However, from experimental results reported previously,²⁸ we also find an ab initio CASSCF result of $D = +196 \text{ cm}^{-1}$ with a clear dictation of the disagreement between the calculated and experimental values of U . There has been a debate about whether DFT is better than ab initio methods in the logical prediction of ZFS parameters. Nevertheless, in a recent study, it was categorically shown that DFT provided efficient estimates of the ZFS parameters compared with popular ab initio methods.²⁹

Table 6.1. A comparison of the experimental magnetic anisotropy energy (MAE) barrier with that computed at the BPW91/TZV level and the individual excitation contributions towards the ZFS parameter in the ground state.

Computed ZFS parameter D and U at BPW91/TZV level			Experimental ²⁸ MAE barrier in cm^{-1}
Individual excitation contributions to ZFS	Calculated ZFS Parameter D in cm^{-1}	Calculated MAE barrier in cm^{-1}	
$\alpha \rightarrow \alpha$	0.178	6.561	~17
$\alpha \rightarrow \beta$	1.385		
$\beta \rightarrow \alpha$	-0.266		
$\beta \rightarrow \beta$	5.265		

Computation of the ZFS parameters is also executed under different external electric fields. The values of D , along with the individual excitation contributions towards ZFS, are given in Table 6.2. A plot of the variation in D with applied electric field in Figure 6.3 suggests that after certain critical field strength the easy-plane magnetization of the Co^{II} complex changes to easy-axis type. Thus, it can be interpreted that, after a threshold field, the molecule starts to behave as an SMM. Moreover, the switch in the D value in both field directions is also clear from Figure 6.3. This flip in D is in the range of 1.6×10^{-3} and 1.7×10^{-3} a.u of electric field strength when the field is applied along the positive z axis.

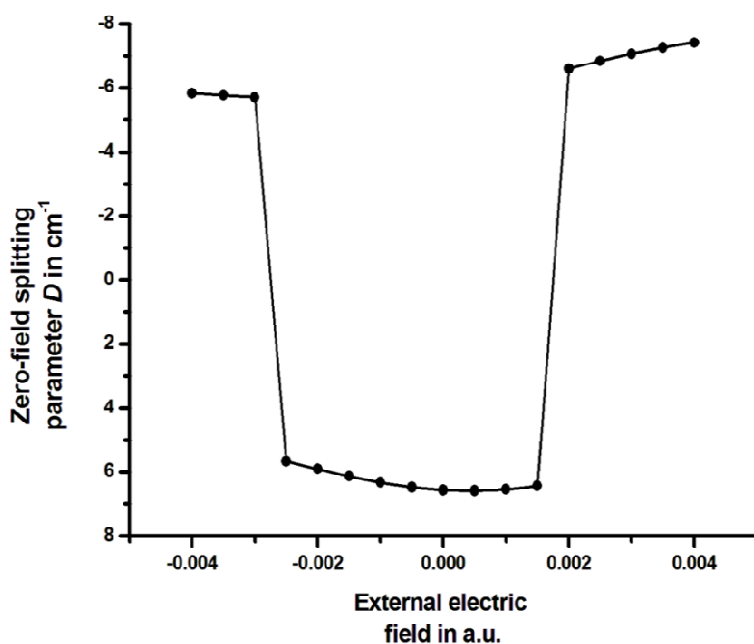


Figure 6.3. A plot of the variation in D with external electric field.

Table 6.2. The ZFS parameters computed at the BPW91/TZV level and the individual excitation contributions towards ZFS under the influence of a finite electric field.

External Electric Field (in a.u.)	ZFS parameter D (in cm^{-1})	Different Excitation Contributions to D			
		$\alpha \rightarrow \alpha$	$\alpha \rightarrow \beta$	$\beta \rightarrow \alpha$	$\beta \rightarrow \beta$
Under negative applied field					
-0.0040	-5.828	-0.132	-1.288	0.211	-4.619
-0.0035	-5.762	-0.131	-1.267	0.216	-4.580
-0.0030	-5.700	-0.130	-1.236	0.222	-4.557
-0.0025	5.668	0.168	1.429	-0.230	4.301
-0.0020	5.909	0.172	1.451	-0.238	4.524
-0.0015	6.133	0.175	1.463	-0.247	4.742
-0.0010	6.325	0.177	1.460	-0.255	4.943
-0.0005	6.470	0.178	1.436	-0.261	5.117
Under positive applied field					
0.0005	6.578	0.177	1.323	-0.268	5.347
0.0010	6.537	0.177	1.231	-0.270	5.399
0.0015	6.428	0.179	1.105	-0.273	5.418
0.0020	-6.593	-0.107	-0.646	0.258	-6.096
0.0025	-6.835	-0.107	-0.602	0.255	-6.380
0.0030	-7.059	-0.104	-0.560	0.249	-6.644
0.0035	-7.254	-0.107	-0.516	0.248	-6.879
0.0040	-7.406	-0.110	-0.477	0.246	-7.066

It can be seen from Tables 6.1 and 6.2 that the major excitation contribution towards D comes from the $\beta \rightarrow \beta$ excitation. To further investigate the effect of electric field on the excitation pattern of the molecule, we performed time-dependent (TD) DFT calculations at the same computational level by using the Gaussian09W³⁰ suite of programs. Excitations with maximum oscillator strengths are characterized to involve β electrons only. The molecular orbitals (MOs) from and to which excitation occurs are summarized in Table 6.3. In the ground state, the source MO involves the metal d orbitals and the thiocyanate ligands. The destination MOs in the unperturbed state corroborate the interaction of the dmphen ligand with the central metal ion. No significant change in the picture is observed for a field strength lower than that of the critical value at which D is still positive. On the other hand, above the critical field strength, the excitation spectrum reverses. At a field strength of 0.004 a.u., the source MO is essentially centered on the dmphen ligand, whereas the destination is the MO based on the NCS ligands. Hence, from the above discussion, it is evident that the natural tendency of the electrons to flow towards the π -acceptor NCS ligands is developed at a field strength higher than that of the critical field. It follows from our previous work that the π -accepting tendency of the ligands exerts easy-axis-type magnetic anisotropy ($D < 0$) in a molecule.¹⁴ Thus, it can be concluded that the switch in the D value arises from metal-to-ligand back charge transfer in the molecule facilitated by exposure to the external electric field.

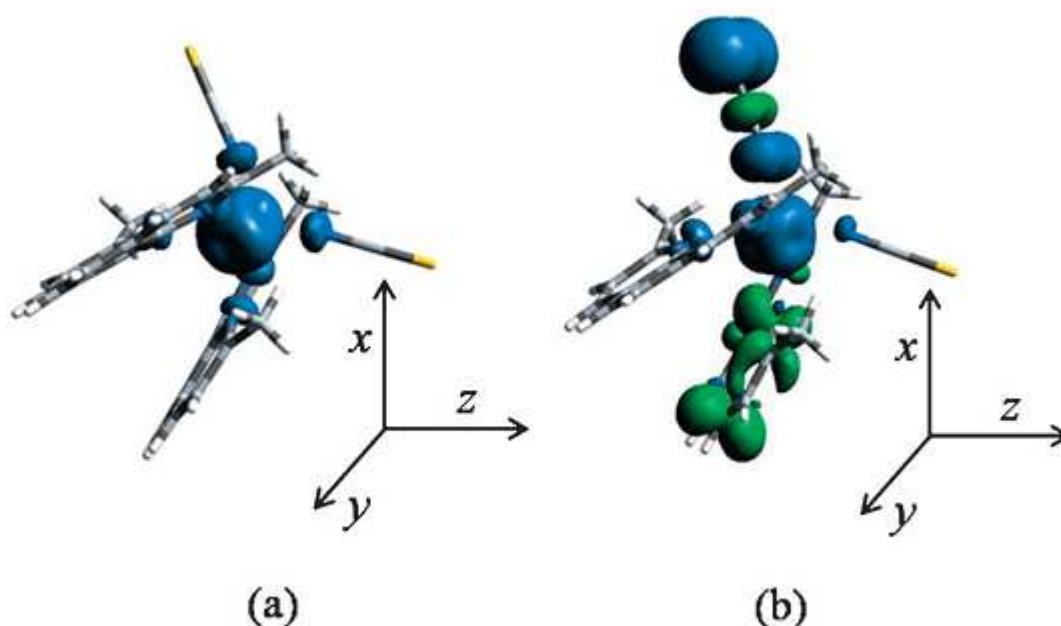
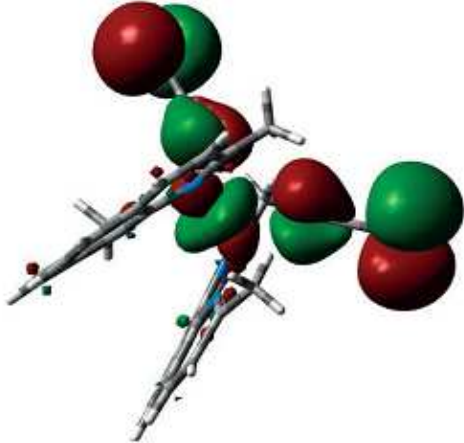
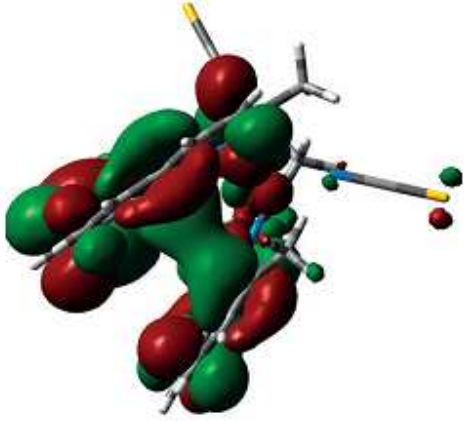
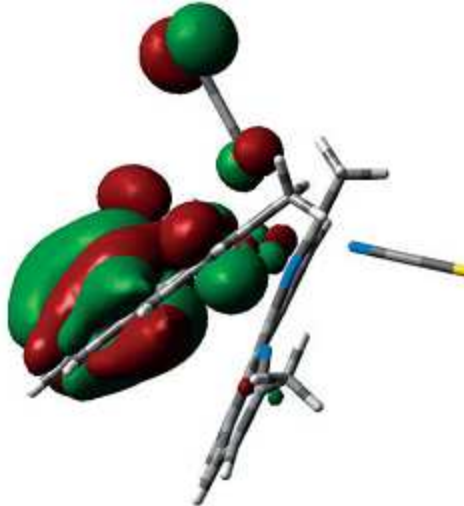
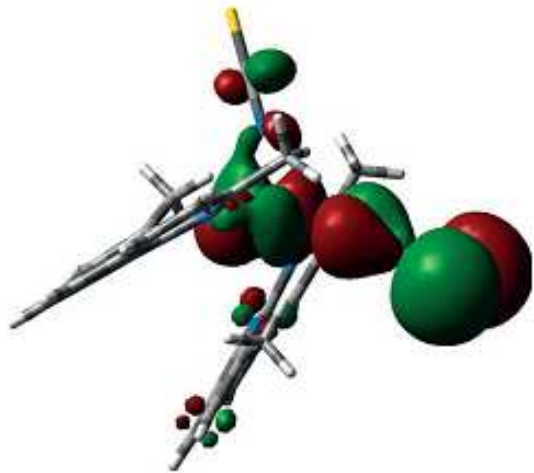


Figure 6.4. The spin-density plots (at an isosurface value of 0.004) of the Co(II) complex in a) the ground state and b) under the applied electric field with a magnitude of 4.0×10^3 a.u. The blue color specifies α -spin density and the green color indicates β -spin density.

Table 6.3. The excitation behavior of [CoII(dmphen)2(NCS)2] in the ground state and under application of a finite electric field computed at the BPW91/TZV level.

Applied electric field strength h [a.u.]	Source MO	Destination MO
0.000		
	136 β	138 β
0.004		
	134 β	137 β

A similar and more interesting portrayal of the phenomenon is found in the spin density plots depicted in Figure 6.4. We compared the spin densities of the complex at zero-external field and finite external electric fields above the critical field. Separation of the α and β spins is observed at a higher electric field strength than that of the unperturbed state. This dispersion of the β spin is further confirmed from a comparison of the density of states (DOS)

plots at different electric fields given in Figure D.S1 in the Supporting Information. Close inspection of the DOS plots reveals the shift in the energies of the α and β electrons. Although electrons of both spins show a shift in the energy level, an alteration in the energy of the β spin is specifically observed. This interesting feature of a shift in the energy levels of different spins due to opposite spin accumulation on two different sides of a molecule is termed as the spin Hall effect.³¹

The molecular origin of this correlation of the electron spin and applied electric field is steered by spin-orbit coupling. In this context, the Rashba-type spin-orbit interaction draws the attention of the scientific community due to its tunable nature under an applied electric field.³² The spin-orbit coupling Hamiltonian in eqn (6.6) describes the coupling of electron spin σ and momentum p under an external electric field E :

$$\hat{H}_{\text{SO}} = -\mu_{\text{B}}\sigma\left(p\frac{E}{2mc^2}\right) \quad (6.6)$$

in which σ , μ_{B} , and c are Pauli spin matrices, the Bohr magneton, and the velocity of light, respectively. It is evident from eqn (6.6) that a momentum-dependent internal magnetic field is generated, as shown in eqn (6.7):

$$B_{\text{int}} = p\frac{E}{2mc^2} \quad (6.7)$$

and the resulting spin polarization is crucially dependent on both p and E and their relative directions.³³ It can be argued that there is a generalized tendency of the electrons to move towards the π -accepting NCS ligands, and hence, the direction of the resultant momentum of the electrons can be along the $+x$ axis (see Appendix D). The interaction of the electron momentum with the external electric field generates an internal magnetic field. A magnetic field thus generated, in turn, accelerates the α and β electrons in opposite directions through a spin-dependent force, represented by eqn(6.8)

$$F_{\uparrow\downarrow} = \pm g\mu_{\text{B}}\frac{dB_{\text{int}}}{dq} \quad (6.8)$$

in which g is the electronic g factor and μ_{B} is the Bohr magneton. The clear bifurcation of the α and β spin densities in opposite directions in the present complex indicates a modification in the spin-orbit interaction. It is also commonly understood that the ZFS in metal systems originates from spin-orbit coupling. Thus, modification in the spin-orbit coupling is further established through alteration to the ZFS parameter under an external electric field.

6.4. Conclusion

Emerging interest in mononuclear complexes, in comparison to polynuclear ones, has meant that the field of quantum magnets has turned to tuning of the ZFS parameter D through structural modification or external aids. This study contemplated the magnetic anisotropy of

an octahedral Co^{II} complex, namely, $[\text{Co}^{\text{II}}(\text{dmphen})_2(\text{NCS})_2]$, in connection with the tunability of ZFS parameter D by exploiting an electric field as an external stimuli. Previously, it was shown that the presence of a π -accepting ligand in the axial position of an octahedral complex could result in magnetization of the molecular magnetic dipole along a specific direction. The external electric field in the present situation assisted such metal-to-ligand charge transfer and led to a switchover in the anisotropic characteristics. A spin-Hall spatial spin separation was also observed due to modulation in the Rashba spin-orbit coupling in a single molecule, for the first time, rather than in mesoscopic systems.

6.5. References

1. (a) Boussac, A.; Girerd, J. J.; Rutherford, A. W. *Biochemistry* **1996**, *35*, 6984; (b) Horner, O.; Rivire, E.; Blondin, G.; Un, S.; Rutherford, A. W.; Girerd, J. J.; Boussac, A. *J. Am. Chem. Soc.* **1998**, *120*, 7924 – 7928; (c) Dub, C. E.; Sessoli, R.; Hendrich, M. P.; Gatteschi, D.; Armstrong, W. H. *J. Am. Chem. Soc.* **1999**, *121*, 3537 – 3538; (d) Wernsdorfer, W.; Sessoli, R. *Science* **1999**, *284*, 133.
2. (a) Sessoli, R.; Tsai, H. L.; Schake, A. R.; Wang, S. Y.; Vincent, J. B.; Folting, K.; Gatteschi, D.; Christou, G.; Hendrickson, D. N. *J. Am. Chem. Soc.* **1993**, *115*, 1804 – 1816; (b) Gatteschi, D.; Sessoli, R.; Villain, J. In *Molecular Nanomagnets*, Oxford University Press, New York, **2006**; (c) Milios, C. J.; Vinslava, A.; Wernsdorfer, W.; Moggach, S.; Parsons, S.; Perlepes, S. P.; Christou, G.; Brechin, E. K. *J. Am. Chem. Soc.* **2007**, *129*, 2754 – 2755; (d) Yoshihara, D.; Karasawa, S.; Koga, N. *J. Am. Chem. Soc.* **2008**, *130*, 10460 – 10461.
3. Mannini, M.; Pineider, F.; Sainctavit, P.; Danieli, C.; Otero, E.; Sciancalepore, C.; Talarico, M.; Arrio, M. A.; Cornia, A.; Gatteschi, D.; Sessoli, R. *Nat. Mater.* **2009**, *8*, 194 – 197.
4. (a) Leuenberger, M. N.; Loss, D.; *Nature* **2001**, *410*, 789 – 793; (b) Ardavan, A.; Rival, O.; Morton, J. J. L.; Blundell, S. J.; Tyryshkin, A. M.; Timco, G. A.; Winpenny, R. E. P.; *Phys. Rev. Lett.* **2007**, *98*, 057201; (c) Stamp, P. C. E.; Gaita-Arino, A. *J. Mater. Chem.* **2009**, *19*, 1718 – 1730.
5. Sessoli, R., Gatteschi, D.; Caneschi, A.; Novak, M. A. *Nature* **1993**, *365*, 141 – 143.
6. Lis, T. *Acta Cryst. B* **1980**, *36*, 2042 – 2046.
7. Caneschi, A.; Gatteschi, D.; Sessoli, R.; Barra, A. L.; Brunel, L. C.; Guillot, M. *J. Am. Chem. Soc.* **1991**, *113*, 5873 – 5874.
8. Lawrence, J.; Lee, S. C.; Kim, S.; Anderson, N.; Hill, S.; Murugesu, M.; Christou, G. *AIP Conf. Proc.* **2006**, *850*, 1133 – 1134.
9. (a) Waldmann, O. *Inorg. Chem.* **2007**, *46*, 10035 – 10037; (b) Kirchner, N.; van Slageren, J.; Dressel, M. *Inorg. Chim. Acta.* **2007**, *360*, 3813 – 3819.

10. Arom, G.; Brechin, E. K. *Struct. Bonding (Berlin)* **2006**, *122*, 1 – 67.
11. (a) Bogani, L.; Wernsdorfer, W. *Nat. Mater.* **2008**, *7*, 179 – 186; (b) Urdampilleta, M.; Klyatskaya, S.; Cleuziou, J.P.; Ruben, M.; Wernsdorfer, W.; *Nat. Mater.* **2011**, *10*, 502 – 506; (c) Ritter, S. K. *Chem. Eng. News* **2004**, *82*, 29–32.
12. Liu, J.; Datta, S.; Bolin, E.; Lawrence, J.; Beedle, C. C.; Yang, E. C.; Goy, P.; Hendrickson, D. N.; Hill, S.; *Polyhedron* **2009**, *28*, 1922 – 1926.
13. (a) Lloret, F.; Julve, M.; Cano, J.; Ruiz-Garca, R.; Pardo, E. *Inorg. Chim. Acta* **2008**, *361*, 3432 – 3445; (b) Palii, A.; Tsukerblat, B.; Clemente-Juan, J. M.; Coronado, E.; *Int. Rev. Phys. Chem.* **2010**, *29*, 135 – 230.
14. Goswami, T.; Misra, A. *J. Phys. Chem. A* **2012**, *116*, 5207 – 5215.
15. Shil, S.; Misra, A.; *RSC Adv.* **2013**, *3*, 14352 – 14362.
16. (a) Chiba, D.; Sawicki, M.; Nishitani, Y.; Nakatani, Y.; Matsukura, F.; Ohno, H. *Nature* **2008**, *455*, 515 – 518; (b) Lebeugle, D.; Mougín, A.; Viret, M.; Colson, D.; Ranno, L. *Phys. Rev. Lett.* **2009**, *103*, 257601.
17. (a) Accorsi, S.; Barra, A. L.; Caneschi, A.; Chastanet, G.; Cornia, A.; Fabretti, A. C.; Gatteschi, D.; Mortalo, C.; Olivieri, E.; Parenti, F.; Rosa, P.; Sessoli, R.; Sorace, L.; Wernsdorfer, W.; Zoppi, L. *J. Am. Chem. Soc.* **2006**, *128*, 4742 – 4755; (b) Gregoli, L.; Danieli, C.; Barra, A. L.; Neugebauer, P.; Pellegrino, G.; Poneti, G.; Sessoli, R.; Cornia, A.; *Chem. Eur. J.* **2009**, *15*, 6456 – 6467.
18. Zyazin, A. S.; van den Berg, J. W. G.; Osorio, E. A.; van der Zant, H. S. J.; Konstantinidis, N. P.; Leijnse, M.; Wegewijs, M. R.; May, F.; Hofstetter, W.; Danieli, C.; Cornia, A. *Nano Lett.* **2010**, *10*, 3307 – 3311.
19. Zein, S.; Duboc, C.; Lubitz, W.; Neese, F. *Inorg. Chem.* **2008**, *47*, 134.
20. Pederson, M. R.; Khanna, S. N. *Phys. Rev. B* **1999**, *60*, 9566 – 9572.
21. Neese, F. *ORCA 2.8.0; University of Bonn, Bonn, Germany*, **2010**.
22. (a) van Wllen, C. *J. Chem. Phys.* **2009**, *130*, 194109; (b) Aquino, F.; Rodriguez, J. H. *J. Phys. Chem. A* **2009**, *113*, 9150 – 9156.
23. (a) Schfer, A.; Horn, H.; Ahlrichs, R. *J. Chem. Phys.* **1992**, *97*, 2571 – 2577; (b) Schfer, A.; Huber, C.; Ahlrichs, R. *J. Chem. Phys.* **1994**, *100*, 5829 – 5835.
24. Weigend, F. *Phys. Chem. Chem. Phys.* **2006**, *8*, 1057 – 1065.
25. (a) Park, K.; Pederson, M. R.; Richardson, S. L.; Aliaga-Alcalde, N.; Christou, G. *Phys. Rev. B* **2003**, *68*, 020405; (b) Ribas-Ariço, J.; Baruah, T.; Pederson, M. R. *J. Am. Chem. Soc.* **2006**, *128*, 9497 – 9505.
26. Aquino, F.; Rodriguez, J. H. *J. Chem. Phys.* **2005**, *123*, 204902.

27. (a) Davari, N.; P.-O. strand, Ingebrigtsen, S.; Unge, M. *J. Appl. Phys.* **2013**, *113*, 143707; (b) Davari, N.; P.-O. strand, Van Voorhis, T.; *Mol. Phys.* **2013**, *111*, 1456 – 1461; (c) Smirnov, M. B.; Krainov, V. P. *J. Exp. Theor. Phys.* **1997**, *85*, 447 – 450.
28. Vallejo, J.; Castro, I.; Ruiz-Garca, R.; Cano, J.; Julve, M.; Lloret, F.; Munno, G. D.; Wernsdorfer, W.; Pardo, E. *J. Am. Chem. Soc.* **2012**, *134*, 15704 –15707.
29. Singh, S. K.; Rajaraman, G. *Chem. Eur. J.* **2013**, *19*, 1 – 12.
30. Frisch, M. J.; Trucks, G. W.; Schlegel, H. B.; Scuseria, G. E.; Robb, M. A.; Cheesman, J. R.; Zakrzewski, V. G.; Montgomery, J. A.; Strtmann, R. E.; Burant, J. C.; Dapprich, S.; Milliam, J. M.; Daniels, A. D.; Kudin, K. N.; Strain, M. C.; Farkas, O.; Tomasi, J.; Barone, V.; Cossi, M.; Camme, R.; Mennucci, B.; Pomelli, C.; Adamo, C.; Clifford, S.; Ochterski, J.; Petersson, G. A.; Ayala, P. Y.; Cui, Q.; Morokuma, K.; Rega, N.; Salvador, P.; Dannenberg, J. J.; Malich, D. K.; Rabuck, A. D.; Raghavachari, K.; Foresman, J. B.; Cioslowski, J.; Ortiz, J. V.; Baboul, A. G.; Stetanov, B. B.; Liu, G.; Liashenko, A.; Piskorz, P.; Komaromi, I.; Gomperts, R.; Martin, R. L.; Fox, D. J.; Keith, T.; Al-Laham, M. A.; Peng, C. Y.; Nnsyskkara, A.; Challacombe, M.; Gill, P. M. W.; Johnson, B.; Chen, W.; Wong, M. W.; Andres, J. L.; Gonzalez, C.; Head-Gordon, M.; Replogle E. S.; Pople, J. A. GAUSSIAN09, Revision A.02, Gaussian Inc., Pittsburgh (2009).
31. Beeler, M. C.; Williams, R. A.; Jimenez-Garcia, K.; LeBlanc, L. J.; Perry, A. R.; Spielman, I. B. *Nature* **2013**, *498*, 201 – 204.
32. Nitta, J.; Akazaki, T.; Takayanagi, H.; Enoki, T.; *Phys. Rev. Lett.* **1997**, *78*, 1335.
33. Dresselhaus, G. *Phys. Rev.* **1955**, *100*, 580 – 586.

CHAPTER 7

Conclusion

Abstract

This chapter presents a general and comprehensive conclusion of all the chapters.

This chapter deals with the general conclusive remarks drawn from the previous chapters. The first chapter provides a brief introduction to the origin and advancement of research in aromaticity, magnetic exchange coupling and magnetic anisotropy of the metal based systems. The development of the theory of aromaticity with the advent of the synthesis of new materials based on transition metals, heavy metals or alkaline earth metals have been discussed. The origin and the chronological advancement of the theory and synthetic research of metal complexes have been elaborated with special emphasis on the application of the magnetic materials as data storage devices and nanomagnets. Finally, the role of theoretical research in the progression of the field of magnetism is explained.

The second chapter presents a brief theoretical framework of the measurements of aromaticity based on energetic, magnetic and structural criteria are discussed. Some of the methods that are utilised in this thesis to quantify aromaticity are explained in detail. The estimation of magnetic exchange coupling constant based on density functional theory based methodology is explicated elaborately. The most popular broken symmetry approach and spin flip approach are elucidated thoroughly. Finally, the estimation of magnetic anisotropy through density functional methods is enlightened. The Pederson-Khanna (PK) method and the Neese methods of quantification of axial and rhombic ZFS parameter D are also explained.

Chapter three explains the change in the aromaticity and energy profile of the singlet state of Mg_3Na_2 molecule and gradual attainment of the BS state with an increase in Na– Mg_3 distance. Near the ground state, Mg atoms are held together by a pair of π -bonding electrons onto which Na^+ ions are impregnated. The circulation of π -electron cloud above and below the Mg_3 plane also contributes to the σ - and π -aromaticity of the molecule. However, in this situation, the stability due to aromaticity has to compete with the Pauli repulsion. When the Na ions move away from Mg_3 plane with all the charge density, the aromaticity is also gradually lost, though the system gets stability due to decrease in Pauli repulsion. At a critical value (~ 4.33 Å) of Na– Mg_3 distance, the Pauli repulsion approaches a minimum due to localization of charge density on Na atoms above and below the plane. This charge accumulation on Na atoms makes these neutral doublet species with up-spin polarization at one Na and down-spin at another. The spins on Na atoms undergo superexchange. The stabilization due to superexchange and lowering of Pauli repulsion partly compensates the loss in bonding energy in the molecule for the charge migration to Na atoms. The Na spins are found to be engaged in antiferromagnetic interaction which gradually decreases with an increase in Na– Mg_3 separation.

Chapter four explains that the phenomenon of charge transfer (CT) is of paramount impact in guiding the courses of several magnetic processes. In the present study, the charge transfer process is also found effective in governing the magnetic behavior of metallocene based charge transfer complexes. A recently synthesized system, $[\text{Cr}(\text{Cp}^*)_2][\text{ETCE}]$ is taken as the representative MBCTC to explore the influence of charge transfer on the magnetic behavior of such donor–acceptor complexes. Anderson in his pioneering work ascribed charge transfer as the origin of kinetic exchange and correlated this exchange with the second order perturbation energy for such charge transfer. In a recent work, using this approach of

Anderson, the coupling constant is parameterized with spin population. However, through bond charge transfer in a superexchange process is accounted for with the help of a newly developed equation in this chapter. On the contrary, NBO analysis for the present system clarifies a zero overlap status in between the donor and acceptor, which necessitates the tunnelling of electron in its journey from the donor to the acceptor. The electron tunnelling matrix element (H_{DA}) integral, is evaluated from the zeroth order eigenvalues of pure donor and acceptor at the transition state of the electron transfer process. The exchange coupling constant (J_T), obtained in this way is well in agreement with J , the coupling constant derived through well-known spin projection technique of Yamaguchi. The charge transfer interaction happens to be the central in such type of complexes where the magnetic interaction begins after the charge dislocates from the donor to the acceptor creating one magnetic site at the acceptor. The topological difference of V-pair and H-pair leads to the possibility of concurrent and competitive exchange interactions at different directions. In V-pair, the intervening Cp* ring assists the transfer of electron from metal to acceptor unit and hence there operates the superexchange process in this direction. In the other direction, the donor and acceptor are far separated and there is no such aid for the spins to be transferred from the donor to the acceptor. Hence the direct exchange process becomes only viable in H-pair. From the comparison of the coupling constant values, the superexchange interaction is found dominant in between two exchange processes in $[\text{Cr}(\text{Cp}^*)_2][\text{ETCE}]$. Since, the weak interaction in the horizontal direction takes a decisive role to render overall magnetic ordering; the V- and H-pairs are simultaneously taken into account. This situation opens up the possibility of several exchange interactions among multiple magnetic sites, which is estimated through a newly developed computational scheme, referred to as dummy approach within the text. The coupling constant value for the V-pair, obtained through this approach is found to be very low compared to the previous value, where only the V-pair is considered. The drastic decrease in the J value through dummy approach is attributed to the interchain interaction. The coexistence of competitive superexchange and direct exchange in this truncated model replicates the bulk behavior. It has been of optimal challenge to investigate the nature of magnetism in a crystal system. The best way to mimic the real network of spins of a cluster demands the application of periodic boundary condition. The PBC can treat systems in bulk condition with much less computational effort without taking the finite size-effect and border-effect. Our calculation clearly shows that the magnetic interaction in one dimensional periodic lattice of such kind of system in the vertical direction is antiferromagnetic and the extent of magnetism is too low. Moreover, it is interesting to note that the FM system turns into an AFM one with imposition of periodic boundary condition. This change over in the magnetic status of the system is explained with the rearrangement of the density of states in $[\text{Cr}(\text{Cp}^*)_2][\text{ETCE}]$. In this condition, there occurs a simultaneous higher and lower energy shifts in the donor and acceptor orbitals respectively and the donor–acceptor overlap integral gains a non-zero value, which is otherwise zero in the system. This lift in energy of the d -states is also supported from the easy dispersion of alpha spin to the Cp* ligand orbital. Hence, this situation facilitates electron delocalization and results a lower Hubbard U value. As a consequence of all these facts the $[\text{Cr}(\text{Cp}^*)_2][\text{ETCE}]$ which exhibits ferromagnetic coupling in the single D^+A^- pair, turns into an antiferromagnetic system in the periodic condition along vertical direction. However, the convolution of different exchanges

pervading the crystal makes it a weak ferromagnet. An extended review on MBCTC divulges that there is a delicate balance in the sign of coupling constant in horizontal direction. This weak, still competing magnetic interaction is regarded as the principle criterion for metamagnetism. However, this work suggests a delicate poise of magnetic interaction in the vertical direction as well.

In chapter five, the magnetic anisotropy property of a series of octahedral Cr(III) complexes is studied. It has been shown that π -donor and π -acceptor ligands, in the axial position of the octahedral complexes, have different effects on the magnetic anisotropy of the complexes. The interaction of the ligands with the metal d -orbitals gives rise to two different situations responsible for this kind of switch in the ZFS parameter. The π -donor ligands play a role in making the magnitude of ZFS larger with an increased π -donation from the halide ligands, while a π -acceptor ligand causes the anisotropy property to be of easy-axis type ($D < 0$). Moreover, a π -acceptor ligand in both the axial positions imparts single molecular magnetic nature to the system having an easy-axis of the magnetic anisotropy. An increased donation from the equatorial positions is seen to enhance the magnitude of easy axis type magnetic anisotropy. This can be attributed to the increased π -accepting efficiency of the axial ligands due to an enhanced metallic electron density, pushed by the equatorial ligands. On the basis of the above observations regarding the ligand replacement, octahedral Cr(III) complexes can be designed in such a way that it can meet our desired anisotropy characteristics. The NLO response is found to vary with π -donation similarly as the magnetic anisotropy. The second-order NLO response, β , has been related to the magnetic anisotropy in the case of the non-centrosymmetric octahedral complexes, where we can see that the NLO response can lead us to good anticipation of magnetic anisotropy. From the systematic DFT study with these octahedral complexes, a clear understanding about the influence of the ligands on modulating the magnetic anisotropy of the Cr(III) complexes is possible. For convenience, we perform a few numerical experimentations. The D value for $[\text{CrBr}_4(\text{CN})_2]^{3-}$, is -0.69 cm^{-1} . We calculate the ZFS parameter for $[\text{CrBr}_4(\text{CO})_2]^-$, which comes out to be -2.51 cm^{-1} . Now relying on the above method of prediction, we design a complex of formula $[\text{CrBr}_4(\text{CN})(\text{CO})]^{2-}$ and expect the D value to be in between -0.69 cm^{-1} and -2.51 cm^{-1} and get a value of -0.94 cm^{-1} . Thus, from this observation, a general conclusion can be drawn that the anisotropy of such metal complexes is greatly controlled by the ligands. To summarize, this work explicates a simple application of DFT to calculate anisotropy parameters in metal complexes to devise a rule of thumb for the occurrence of SMM behaviour in such complexes.

Emerging interest in mononuclear complexes, in comparison to polynuclear ones, has meant that the field of quantum magnets has turned to tuning of the ZFS parameter D through structural modification or external aids. Chapter six contemplated the magnetic anisotropy of an octahedral Co^{II} complex, namely, $[\text{Co}^{\text{II}}(\text{dmphen})_2(\text{NCS})_2]$, in connection with the tunability of ZFS parameter D by exploiting an electric field as an external stimuli. Previously, it was shown that the presence of a π -accepting ligand in the axial position of an octahedral complex could result in magnetization of the molecular magnetic dipole along a specific direction. The external electric field in the present situation assisted such metal-to-

ligand charge transfer and led to a switch over in the anisotropic characteristics. A spin-Hall spatial spin separation was also observed due to modulation in the Rashba spin-orbit coupling in a single molecule, for the first time, rather than in mesoscopic systems.

BIBLIOGRAPHY

Chapter 1.

1. Hofmann, A. *Proc. Roy. Soc. (London)* **1855**, 8, 1.
2. Kekulé, A. *Bull. Acad. R. Belg.* **1860**, 10, 347.
3. (a) Kekulé, A. *Bull. Soc. Chim. Soc. France*, **1865**, 3, 98; (b) Kekulé, A. *Bull. Acad. R. Belg.*, **1865**, 19, 501; (c) Kekulé, A. *Ann. Chem. Pharm.*, **1866**, 137, 129.
4. Kekulé, A. *Ann. Chem.* **1872**, 162, 77.
5. Erlenmeyer, E. *Ann. Chem. Pharm.* **1866**, 137, 327.
6. Körner, W. *G. Sci. Nat. Econ. Palermo*, **1869**, 5.
7. Dewar, J. *Trans. R. Soc. Edin.*, **1872**, 26, 195.
8. Crocker, E. C. *J. Am. Chem. Soc.* **1922**, 44, 1618.
9. Armit, J. W.; Robinson, R. *J. Chem. Soc.* **1925**, 127, 1604.
10. Hückel, E. *Z. Physik* **1931**, 70, 204.
11. (a) Clar, E. *Tetrahedron* **1959**, 6, 355; (b) Clar, E.; McCallum, A. *Tetrahedron* **1960**, 10, 171.
12. (a) Garratt, P. J. In *Aromaticity*, John Wiley & Sons, Inc, New York, 1986; (b) Minkin, V. I.; Glukhotsev, M. N.; Simkin, B. Y. In *Aromaticity and Antiaromaticity: Electronic and Structural Aspects*, John Wiley & Sons, Inc, New York, 1994; (c) Bickelhaupt, F.; de Wolf, W. H. *Recl. Trav. Chim. Pays-Bas* **1988**, 107, 459; (d) Kraakman, P. A.; Valk, J.-M.; Niederländer, H. A. G.; Brouwer, D. B. E.; Bickelhaupt, F. M.; de Wolf, W. H.; Bickelhaupt, F.; Stam, C. H. *J. Am. Chem. Soc.* **1990**, 112, 6638.
13. (a) Schleyer, P. v. R.; Jiao, H. *J. Pure Appl. Chem.* **1996**, 68, 209; (b) Carey, F. A.; Sundberg, R. J. In *Advanced Organic Chemistry: Structure And Mechanisms (Part A)*, Springer, New York, 2000; (c) Special issue on: Aromaticity, ed. Schleyer, P. v. R. *Chem. Rev.* **2001**, 101.
14. (a) Special issue on: Delocalization—pi and sigma, ed. Gladysz, J. A. *Chem. Rev.* **2005**, 105; (b) Breslow, R. *Acc. Chem. Res.* **1973**, 6, 393; (c) Krygowski, T. M.; Cyranski, M. K.; Czarnocki, Z.; Hafelinger, G.; Katritzky, A. R. *Tetrahedron* **2000**, 56, 1783; (d) Schleyer, P. v. R. *Chem. Rev.* **2001**, 101, 1115; (e) Cyranski, M. K.; Krygowski, T. M.; Katritzky, A. R.; Schleyer, P. v. R. *J. Org. Chem.* **2002**, 67, 1333.
15. (a) Pauling, L. *J. Am. Chem. Soc.* **1926**, 48, 1132; (b) Pauling, L. In *The Nature of the Chemical Bond*, 3rd ed., Cornell University Press: Ithaca, New York, 1960; (c) Hückel, E. *Z. Phys.* **1931**, 70, 204.
16. Goldstein, M. J.; Hoffmann, R. *J. Am. Chem. Soc.* **1971**, 93, 6193.
17. Wörner, H.; Merkt, F. *Angew Chem Int. Ed.* **2006**, 45, 293.
18. Hirsch, A.; Chen, Z.; Jiao, H. *Angew. Chem. Int. Ed.* **2001**, 40, 2834.

19. Faraday, M. *Phil trans. R. Soc. Lon.* **1825**, 115, 440.
20. Kekulé, A. *Bulletin mensuel de la Société Chimique de Paris* **1865**, 3, 98.
21. Erlenmeyer, E. *Ann.* **1866**, 137, 327.
22. Crocker, E. *J. Am. Chem. Soc.* **1922**, 44, 1618.
23. Hückel, E. *Z. Phys.* 1931, 70, 207; Hückel, E. *Z. Phys.*, **1932**, 76, 628.
24. Evans, M.; Warhurst, E. *Trans. Faraday Soc.* **1938**, 34, 614.
25. Calvin, M.; Wilson, K. *J. Am. Chem. Soc.* **1945**, 67, 2003.
26. Winstein, S.; Kosower, E. *J. Am. Chem. Soc.* **1959**, 81, 4399.
27. Heilbronner, E. *Tetrahedron Lett.* **1964**, 5, 1923.
28. Breslow, R. *Acc. Chem. Res.* **1973**, 6, 393.
29. Osawa, E. *Kagaku (Kyoto)* **1970**, 25, 854.
30. Clar, E. In *The aromatic sextet*; John Wiley & Sons, 1972.
31. Baird, N. *J. Am. Chem. Soc.* **1972**, 94, 4941.
32. Aihara, J. *J. Am. Chem. Soc.* **1978**, 100, 3339.
33. Dewar, M.; Mc.Kee, M. *Pure Appl. Chem.* **1980**, 6, 1431.
34. Jemmis, E.; Schleyer, P. *J. Am. Chem. Soc.* **1982**, 104, 4781.
35. Shaik, S.; Hiberty, P. *J. Am. Chem. Soc.* **1985**, 107, 3089.
36. Kroto, H. *Nature*, **1985**, 318, 162.
37. Iijima et al. *Nature*, **1991**, 354.
38. Li, X.; Kuznetsov, A. Zhang, H. Boldyrev, A. Wang, L. *Science*, **2001**, 291, 859.
39. Wannare, C.; Corminboeuf, C.; Wang, Z.; Wodrich, M. King, R. Schleyer, P. *J. Am. Chem. Soc.* **2005**, 127, 5701.
40. Zhai, H.; Averkeiv, B.; Zubarev, D.; Wang, L.; Boldyrev, A. *Angew. Chem. Int. Ed.* **2007**, 119, 4355.
41. Tsipis, A.; Kefalidis, C.; Tsipis, C. *J. Am. Chem. Soc.*, **2008**, 130, 9144.
42. Masui, H. *Coord. Chem. Rev.* **2001**, 219, 957.
43. (a) Dewar, M. J. S.; McKee, M. L. *Pure Appl. Chem.* **1980**, 52, 1431. (b) Dewar, M. J. S. *J. Am. Chem. Soc.* **1984**, 106, 669. (c) Cremer, D.; Gauss, J. *J. Am. Chem. Soc.*, **1986**, 108, 7467.
44. (a) Bühl, M.; Hirsch, A. *Chem. Rev.* **2001**, 101, 1153. (b) Chen, Z.F.; King, R. *Chem. Rev.* **2005**, 105, 3613.

45. Kuznetsov, A. E.; Boldyrev, A. I.; Li, X.; Wang, L. S. *J. Am. Chem. Soc.* **2001**, *123*, 8825.
46. Kuznetsov, A. E.; Birch, K. A.; Boldyrev, A. I.; Li, X.; Zhai, H. J.; Wang, L. S. *Science*, **2003**, *300*, 622.
47. Yong, L.; Wu, S. D.; Chi, X. X. *Int. J. Quant. Chem.*, **2007**, *107*, 722.
48. Chi, X. X. ; Liu, Y. *Int. J. Quant. Chem.*, **2007**, *107*, 1886.
49. Yong, L.; Chi, X. X. *J. Mol. Struct.*, **2007**, *818*, 93.
50. Averkiev, B. B.; Boldyrev, A. I. *J. Phys. Chem. A*, **2007**, *111*, 12864.
51. Wang, B.; Zhai, H. J.; Huang X.; Wang, L. S. *J. Phys. Chem. A*, **2008**, *112*, 10962.
52. Tanaka, H.; Neukemans, S.; Janssens, E.; Silverans, R. E.; Lievens, P. *J. Am. Chem. Soc.*, **2003**, *125*, 2862.
53. (a) Holtzl, T.; Janssens, E.; Veldeman, N.; Veszprem, T.; Lievens, P.; Nguyen, M. T. *Chem. Phys. Chem.*, **2008**, *9*, 833. (b) Holtzl, T.; Veldeman, N.; Veszpremi, T.; Lievens, P.; Nguyen, M. T. *Chem. Phys. Lett.*, **2009**, *469*, 304.
54. Wannere, C. S.; Corminboeuf, C.; Wang, Z. X.; Wodrich, M. D.; King, R. B.; Schleyer, P. v. R. *J. Am. Chem. Soc.*, **2005**, *127*, 5701.
55. Lin, Y. C.; Sundholm, D.; Juselius, J.; Cui, L. F.; Li, X.; Zhai, H. J.; Wang, L. S. *J. Phys. Chem. A*, **2006**, *110*, 4244.
56. (a) Miller, J. S.; Calabrese, J. C.; Rommelman, H.; Chittipedi, S. R.; Zang, J. H.; Reiff, W. M.; Epstein, A. J. *J. Am. Chem. Soc.* **1987**, *109*, 769; (b) Kahn, O.; Pei, Y.; Verdaguer, M.; Renard, J. P.; Sletten, J. *J. Am. Chem. Soc.* **1988**, *110*, 782.
57. Kahn, O. *Adv. Inorg. Chem.* **1995**, *43*, 179.
58. Pei, Y.; Journaux, Y.; Kahn, O. *Inorg. Chem.* **1988**, *27*, 399.
59. Mallah, T.; Marvilliers, A. In *Magnetism: From Molecules to Materials, Vol. 2*, Miller, J. S. Drillon M. (Eds.) Wiley-VCH, Weinheim 2001, p. 189.
60. Gao, E.-Q.; Tang, J.-K.; Liao, D.-Z.; Jiang, Z.-H.; Yan, S.-P.; Wang, G.-L. *Inorg. Chem.* **2001**, *40*, 3134.
61. Fettouhi, M.; Ouahab, L.; Boukhari, A.; Cador, O.; Mathoniere, C.; Kahn, O. *Inorg. Chem.* **1996**, *35*, 4932.
62. (a) Schiff, H.; Kirsensen, A. *Handbook of Nanotechnology*, B. Bhushan, Springer, 3rd ed. 2007, 264; (b) Richter, H. J. *J. Magn. Magn. Mater.* **2009**, *321*, 467.
63. Piramanayagam, S. N. *J. Appl. Phys.*, **2007**, *102*, 011301.
64. (a) Wolf, E. L.; Medikonda, M. In *Understanding the Nanotechnology Revolution*, Wiley, New York, 2012, 181; (b) Wolf, E. L. In *Nanophysics and Nanotechnology*, Wiley, New York, 2nd ed, 2006, 11.

65. (a) Friedman, J. R.; Sarachik, M. P. *Annu. Rev. Condens. Matter. Phys.*, **2010**, *1*, 109; (b) Christou, G.; Gatteschi, D.; Hendrickson, D. N.; Sessoli, R. *MRS Bulletin*, **2000**, *25*, 66.
66. Soler, M.; Wernsdorfer, W.; Folting, K.; Pink, M.; Christou, G. *J. Am. Chem. Soc.*, **2004**, *126*, 2156.
67. (a) Lin, P.; Burchell, T. J.; Ungur, L.; Chibotaru, L. F.; Wernsdorfer, W.; Murugesu, M. *Angew. Chem. Int. Ed.*, **2009**, *48*, 9489; (b) Woodruff, D. N.; Winpenny, R. E. P.; Layfield, R. A. *Chem. Rev.*, **2013**, 5110.
68. (a) Waldmann, O. *Inorg. Chem.*, **2007**, *46*, 10035; (b) Neese, F.; Pantazis, D. A. *Faraday Discuss.* **2011**, *148*, 229.
69. Neese, F. *J. Chem. Phys.* **2001**, *115*, 11080.
70. Cirera, J.; Ruiz, E.; Alvarez, S.; Neese, F.; Kortus, J. *Chem. Eur. J.*, **2009**, *15*, 4078.
71. (a) Lounsbury, J. B. *J. Chem. Phys.*, **1965**, *42*, 1549; (b) Harrison, J. F. *J. Chem. Phys.*, **1971**, *54*, 5413.

Chapter 2.

1. (a) Smith, M. B.; March, J. In *March's Advanced Organic Chemistry: Reactions, Mechanisms and Structure*, 5th ed.; John Wiley and Sons, New York, 2001; (b) Minkin, V.; Glukhovtsev, M.; Simkin, B. In *Aromaticity and Antiaromaticity*; Wiley Interscience, New York, 1994; (c) Schleyer, P. *Chem. Rev.* **2001**, *101*, 1115; (d) Schleyer, P. *Chem. Rev.* **2005**, *105*, 3433.
2. (a) Cremer, D. *Tetrahedron* **1988**, *44*, 7427; (b) Schleyer, P. v. R.; Jiao, H. *Pure Appl. Chem.* **1996**, *68*, 209; (c) Kekule, A. In *Lehrbuch der Organischen Chemie, Zweiter Band*; Ferdinand Enke Verlag, Erlangen, 1866.
3. Minkin, V.; Glukhovtsev, M.; Simkin, B. In *Aromaticity and Antiaromaticity*; Wiley Interscience, New York, 1994.
4. Katritzky, A. R.; Jug, K.; Oniciu, D. C. *Chem. Rev.* **2001**, *101*, 1421.
5. (a) Simkin, B. Y.; Minkin, V. I.; Glukhovtsev, M. N. *Adv. Heterocycl. Chem.* **1993**, *56*, 303; (b) Krygowski, T. M.; Cyranski, M. K.; Czarnocki, Z.; Hafelinger, G.; Katritzky, A. R. *Tetrahedron* **2000**, *56*, 1783.
6. Schleyer, P. v. R.; Maerker, C.; Dransfeld, A.; Jiao, H.; Hommes, N. J. R. v. E. *J. Am. Chem. Soc.* **1996**, *118*, 6317.
7. Schleyer, P. v. R.; Manoharan, M.; Wang, Z.-X.; Kiran, B.; Jiao, H.; Puchta, R.; Hommes, N. J. R. v. E. *Org. Lett.* **2001**, *3*, 2465.
8. Fallah-Bagher-Shaidaei, H.; Wannere, C. S.; Corminboeuf, C.; Puchta, R.; Schleyer, P. v. R. *Org. Lett.* **2006**, *8*, 863.

9. Stanger, A. *J. Org. Chem.* **2006**, *71*, 883.
10. Feixas, F.; Matito, E.; Poater, J.; Solà, M. *J. Comput. Chem.* **2008**, *29*, 1543.
11. (a) Becke, A. D.; Edgecombe, K. E. *J. Chem. Phys.* **1990**, *92*, 5397; (b) Fourré, I.; Silvi, B.; Chaquin, P.; Sevin, A.; *J. Comput. Chem.* **1999**, *20*, 897.
12. (a) Savin, A.; Nesper, R.; Wengert, S.; Fässler, T. F.; *Angew. Chem. Int. Ed. Engl.* **1997**, *36*, 1808; (b) Chesnut, D. B.; Bartolotti, L. J.; *Chem. Phys.* **2000**, *253*, 1.
13. Giambiagi, M.; Giambiagi, M. S. de; Santos, S. C. D. dos; Figueiredo, A. P. de *Phys. Chem. Chem. Phys.* **2000**, *2*, 3381.
14. Jimenez-Halla, J. O. C.; Matito, E.; Solà, M.; Braunschweig, H.; Hörl, C.; Krummenacher, I.; Wahler, J. *Dalton Trans.* **2015**, *44*, 6740.
15. Bultinck, P.; Ponec, R.; Damme, S. V. *J. Phys. Org. Chem.* **2005**, *18*, 706.
16. Bultinck, P.; Rafat, M.; Ponec, R.; van Gheluwe, B.; Carbó-Dorca, R.; Popelier, P. J. *Phys. Chem. A* **2006**, *110*, 7642.
17. Kahn, O. *Molecular Magnetism*; Wiley & Sons, Inc.: New York, 1993.
18. van Vleck, J. H. *The Theory of Electric and Magnetic Susceptibility*; Oxford University Press: Oxford, 1932.
19. Neese, F. *Coord. Chem. Rev.* **2009**, *253*, 526.
20. Neese, F. *J. Phys. Chem. Solids* **2004**, *781*.
21. Noodleman, L. *J. Chem. Phys.* **1981**, *74*, 5737.
22. Rudra, I.; Wu, Q.; Voorhis, T. *J. Chem. Phys.* **2006**, *124*, 024103.
23. Ruiz, E.; Alvarez, S.; Cano, J.; Polo, V. *J. Chem. Phys.* **2005**, *123*, 164110.
24. (a) Szabo, A.; Ostlund, N. S. In *Modern Quantum Chemistry: Introduction to Advanced Electronic Structure Theory*; Dover Publications, New York, **1996**.; (b) Herrmann, C.; Yu, L.; Reiher, M. *J. Comput. Chem.* **2006**, *27*, 1223.
25. (a) Zhekova, H.; Seth, M.; Ziegler, T. *J. Chem. Theory Comput.* **2011**, *7*, 1858; (b) Wang, F.; Ziegler, T. *J. Chem. Phys.* **2004**, *121*, 12191; (c) Wang, F.; Ziegler, T. *J. Chem. Phys.* **2005**, *122*, 074109; (d) Wang, F.; Ziegler, T. *Int. J. Quant. Chem.* **2006**, *106*, 2545.
26. McWeeny, R., *J. Chem. Phys.* **1965**, *42*, 1717.
27. Fedorov, D. G.; Koseki, S.; Schmidt, M. W.; Gordon, M. S. *Int. Rev. Phys. Chem.*, **2003**, *22*, 551.
28. Pederson M. R.; Khanna, S. N. *Phys. Rev. B*, **1999**, *60*, 13.

29. (a) Koseki, S.; Schmidt, M. W.; Gordon, M. S. *J. Chem. Phys.* **1992**, *96*, 10768. (b) Koseki, S.; Gordon, M. S.; Schmidt M. W., *J. Phys. Chem.* **1995**, *99*, 12764; (c) Koseki, S.; Schmidt, M. W.; Gordon, M. S. *J. Phys. Chem. A* **1998**, *102*, 10430.
30. Neese, F.; Solomon, E.I. *Inorg. Chem.*, **1998**, *37*, 6568.
31. Neese, F. *J. Chem. Phys.*, **2007**, *127*, 164112.
32. Zein S.; Neese, F. *J. Phys. Chem. A* **2008**, *112*, 7976.

Chapter 3.

1. Li, X.; Kuznetsov, A. E.; Zhang, H. F.; Boldyrev, A. I.; Wang, L. S. *Science* **2001**, *291*, 859.
2. Kuznetsov, A. E.; Birch, K. A.; Boldyrev, A. I.; Li, X.; Zhai, H. J.; Wang, L. S. *Science* **2003**, *300*, 622.
3. Li, X.; Zhang, H. F.; Wang, L. S.; Kuznetsov, A. E.; Cannon, N. A.; Boldyrev, A. I. *Angew Chem. Int. Ed.* **1867**, *40*, 1867.
4. Kuznetsov, A. E.; Boldyrev, A. I.; Li, X.; Wang, L. S. *J. Am. Chem. Soc.* **2001**, *123*, 8825.
5. Twamley, B.; Power, P. P. *Angew Chem. Int. Ed.* **2000**, *39*, 3500.
6. Cisar, A.; Corbett, J. D. *Inorg. Chem.* **1977**, *16*, 2482.
7. Critchlow, S. C.; Corbett, J. D. *Inorg. Chem.* **1984**, *23*, 770.
8. Tuononen, H. M.; Suontamo, R.; Valkonen, J.; Laitinen, R. S. *J. Phys. Chem. A* **2004**, *108*, 5670.
9. Todorov, I.; Sevov, S. C. *Inorg. Chem.* **2004**, *43*, 6490.
10. Todorov, I.; Sevov, S. C. *Inorg. Chem.* **2005**, *44*, 5361.
11. Gillespie, R. J.; Barr, J.; Kapoor, R.; Malhotra, K. C. *Can. J. Chem.* **1968**, *46*, 149.
12. Gillespie, R.J.; Barr, J.; Crump, D. B.; Kapoor, R.; Ummat, P. K. *Can. J. Chem.* **1968**, *46*, 3607.
13. Barr, J.; Gillespie, R. J.; Kapoor, R.; Pez, G. P. *J. Am. Chem. Soc.* **6855**, *90*, 6855.
14. Couch, T. W.; Lokken, D. A.; Corbett, J. D. *Inorg. Chem.* **1972**, *11*, 357.
15. Burford, N.; Passmore, J.; Sanders, J. C. P. In Liebman, J. F.; Greenburg, A. (Eds.) *From atoms to polymers. Isoelectronic analogies*. VCH, New York **1989**, p 53.
16. Li, X.; Wang, X. B.; Wang, L. S. *Phys. Rev. Lett.* **1998**, *81*, 1909.
17. Wu, H.; Li, X.; Wang, X. B.; Ding, C. F.; Wang, L. S. *J. Chem. Phys.* **1998**, *109*, 449.
18. Baeck, K. K.; Bartlett, R. J. *J. Chem. Phys.* **1998**, *109*, 1334.
19. Kuznetsov, A. E.; Boldyrev, A. I. *Struct. Chem.* **2002**, *13*, 141.

20. Kuznetsov, A. E.; Boldyrev, A. I.; Zhai, H. J.; Li, X.; Wang, L. S. *J. Am. Chem. Soc.* **2002**, *124*, 11791.
21. Nielsen, J. W.; Baenziger, N. C. *Acta. Crystallogr.* **1954**, *7*, 277.
22. Corbett, J. D. *Inorg. Nucl. Chem. Lett.* **1969**, *5*, 81.
23. Kuznetsov, A. E.; Corbett, J. D.; Wang, L. S.; Boldyrev, A. I. *Angew Chem. Int. Ed.* **2001**, *40*, 3369.
24. Gausa, M.; Kaschner, R.; Lutz, H.O.; Seifert, G.; Meiwes-Broer, K. H. *Chem. Phys. Lett.* **1994**, *230*, 99.
25. Gausa, M.; Kaschner, R.; Seifert, G.; Faehrmann, J. H.; Lutz, H. O.; Meiwes, K. H. B. *J. Chem. Phys.* **1996**, *104*, 9719.
26. Zhai, H. J.; Wang, L. S.; Kuznetsov, A. E.; Boldyrev, A. I. *J. Phys. Chem. A* **2002**, *106*, 5600.
27. Tanaka, H.; Neukermans, S.; Janssens, E.; Silverans, R. E.; Lievens, P. *J. Am. Chem. Soc.* **2003**, *125*, 2862.
28. Alexandrova, A. N.; Boldyrev, A. I.; Zhai, H. I.; Wang, L. S. *J. Phys. Chem. A* **2005**, *109*, 562.
29. Wannere, C. S.; Corminboeuf, C.; Wang, Z. X.; Wodrich, M. D.; King, R. B.; Schleyer, P. V. R. *J. Am. Chem. Soc.* **2005**, *127*, 5701.
30. Lein, M.; Frunzke, J.; Frenking, G. *Angew Chem. Int. Ed.* **2003**, *42*, 1303.
31. Chattaraj, P. K.; Roy, D. R.; Elango, M.; Subramanian, V. *J. Phys. Chem. A* **2005**, *109*, 9590.
32. Chattaraj, P. K.; Giri, S. *J. Mol. Struct. (Theochem)* **2008**, *865*, 53.
33. Chattaraj, P. K.; Roy, D. R.; Duley, S. *Chem. Phys. Lett.* **2008**, *460*, 382.
34. Roy, D. R.; Duley, S.; Chattaraj, P. K. *Proc. Indian Natl. Sci. Acad. Part-A* **2008**, *74*, 11.
35. Chattaraj, P. K.; Giri, S. *Int. J. Quantum Chem.* **2009**, *109*, 2373.
36. Chakrabarty, A.; Giri, S.; Chattaraj, P. K. *J. Mol. Struct. (Theochem)* **2009**, *913*, 70.
37. Mercero, J. M.; Ugalde, J. M. *J. Am. Chem. Soc.* **2004**, *126*, 3380.
38. Van Zandwijk, G.; Janssen, R. A. J.; Buck, H. M. *J. Am. Chem. Soc.* **1990**, *112*, 4155.
39. Mercero, J. M.; Matxain, J. M.; Ugalde, J. M. *Angew Chem. Int. Ed.* **2004**, *43*, 5485.
40. Giri, S.; Roy, D. R.; Duley, S.; Chakrabarty, A.; Parathasarathi, R.; Elango, M.; Vijayraj, R.; Subramanian, V.; Islas, R.; Merino, G.; Chattaraj, P. K. *J. Comput. Chem.* **2010**, *31*, 1815.
41. Kuznetsov, A. E.; Boldyrev, A. I. *Chem. Phys. Lett.* **2004**, *388*, 452.
42. Roy, D. R.; Chattaraj, P. K. *J. Phys. Chem. A* **2008**, *112*, 1612.

43. Oscar, J.; Jimenez-Halla, C.; Matito, E.; Blancafort, L.; Robles, J.; Sola, M. *J. Comput. Chem.* **2009**, *30*, 2764.
44. Boldyrev, A. I.; Gutowski, M.; Simons, J. *Acc. Chem. Res.* **1996**, *29*, 497.
45. Boldyrev, A. I.; Simons, J. *J. Phys. Chem.* **1994**, *98*, 2298.
46. Janoschek, R. Z. *Z. Anorg. Allg. Chem.* **1992**, *616*, 101.
47. Wang, X. B.; Ding, C. F.; Nicholas, J. B.; Dixon, D. A.; Wang, L. S. *J. Phys. Chem. A* **1999**, *103*, 3423.
48. Wang, X. B.; Nicholas, J. B.; Wang, L. S. *J. Chem. Phys.* **2000**, *113*, 10837.
49. Chakrabarty, A.; Giri, S.; Duley, S.; Anoop, A.; Bultinck, P.; Chattaraj, P. K. *Phys. Chem. Chem. Phys.* **2011**, *13*, 14865.
50. Paul, S.; Misra, A. *Inorg. Chem.* **2011**, *50*, 3234.
51. Elser, V.; Haddon, R. C. *Nature (London)* **1987**, *325*, 792.
52. Lazzeretti, P. *Phys. Chem. Chem. Phys.* **2004**, *6*, 217.
53. Cyra, C.; Ski, M.; Krygowski, T. M.; Katritzky, A. R.; Schleyer, P. V. R. *J. Org. Chem.* **2002**, *67*, 1333.
54. Poater, J.; GarcFa-Cruz, I.; Illas, F.; Sol, V. M. *Phys. Chem. Chem. Phys.* **2004**, *6*, 314.
55. Katritzky, A. R.; Jug, K.; Oniciu, D. C. *Chem. Rev.* **2001**, *101*, 1421.
56. Krygowski, T. M.; Cyranski, M. K. *Chem. Rev.* **2001**, *101*, 1385.
57. Katritzky, A. R.; Karelson, M.; Sild, S.; Krygowski, T. M.; Jug, K. *J. Org. Chem.* **1998**, *63*, 5228.
58. Fias, S.; Fowler, P. W.; Delgado, J. L.; Hahn, U.; Bultinck, P. *Chem. Eur. J.* **2008**, *14*, 3093.
59. Ghiasi, R.; Pasdar, H. *J. Mex. Chem. Soc.* **2012**, *56*, 426.
60. Poater, J.; Fradera, X.; Duran, M.; Sola, M. *Chem. Eur. J.* **2003**, *9*, 400.
61. Mandado, M.; González-Moa, M. J.; Mosquera, R. A. *J. Comput. Chem.* **2007**, *28*, 127.
62. Foroutan-Nejad, C. *Phys. Chem. Chem. Phys.* **2012**, *14*, 9738.
63. Bultinck, P.; Rafat, M.; Ponec, R.; Gheluwe, B. V.; Carbo-Dorca, R.; Popelier, P. *J. Phys. Chem. A* **2006**, *110*, 7642.
64. Giambiagi, M.; de Giambiagi, M. S.; dos Santos Silva, C. D.; PaivadeFigueiredo, A. *Phys. Chem. Chem. Phys.* **2000**, *2*, 3381.
65. Anderson, P. W. *Phys. Rev.* **1950**, *79*, 350.
66. Anderson, P. W. *Phys. Rev.* **1959**, *115*, 2.
67. Anderson, P. W. In *Solid state physics*, vol 14 Seitz F, Turnbull D (Eds.) Academic Press Inc., New York **1963**, p 99.

68. Munoz, D.; Illas, F.; de Moreira, I. P. R. *Phys. Rev. Lett.* **2000**, *84*, 1579.
69. Caballol, R.; Castell, O.; Illas, F.; de Moreira, I. P. R.; Malrieu, J. P. *J. Phys. Chem. A* **1997**, *101*, 7860.
70. Paul, S.; Misra, A. *J. Chem. Theory Comput.* **2012**, *8*, 843.
71. Schleyer, P. V. R.; Maerker, C.; Dransfeld, A.; Jiao, H.; Hommes, N. J. R. V. E. *J. Am. Chem. Soc.* **1996**, *118*, 6317.
72. Ditchfield, R. *Mol. Phys.* **1974**, *27*, 789.
73. Fukui, H. *Magn. Res. Rev.* **1987**, *11*, 205.
74. Freidrich, K.; Seifert, G.; Grossmann, G. Z. *Phys. D.* **1990**, *17*, 45.
75. Malkin, V. G.; Malkina, O. L.; Erikson, L. A.; Salahub, D. R. In: *Politzer, P.; Seminario, J. M. (eds) Modern density functional theory: a tool for chemistry, vol 2. Elsevier, Amsterdam 1995.*
76. Schleyer, P. V. R.; Jiao, H.; Hommes, N. J. R. V. E.; Malkin, V. G.; Malkina, O. *J. Am. Chem. Soc.* **1997**, *119*, 12669.
77. Schleyer, P. V. R.; Manoharan, M.; Wang, Z. X.; Kiran, B.; Jiao, H.; Pachta, R.; Hommes, N. J. R. V. E. *Org. Lett.* **2001**, *3*, 2465.
78. Foster, J. P.; Weinhold, F. *J. Am. Chem. Soc.* **1980**, *102*, 7211.
79. Carpenter, J. E. *Extension of Lewis structure concepts to open shell and excited state molecular species. Ph. D. Thesis, University of Wisconsin, Madison, 1987.*
80. Reed, A. E.; Curtiss, L. A.; Weinhold, F. *Chem. Rev.* **1988**, *88*, 899.
81. Weinhold, F.; Carpenter, J. E. In *The structure of small molecules and ions*. Naaman, R.; Vager, Z. (Eds.) Plenum, New York, **1988**, p 227.
82. teVelde, G.; Bickelhaupt, F. M.; van Gisbergen, S. J. A.; Guerra, C. F.; Baerends, E. J.; Snijders, J. G.; Ziegler, T. *J. Comput. Chem.* **2001**, *22*, 931.
83. Guerra, C. F.; Snijders, J. G.; teVelde, G.; Baerends, E. J. *Theor. Chem. Acc.* **1998**, *99*, 391.
84. ADF (2012) SCM, theoretical chemistry. VrijeUniversiteit, Amsterdam, TheNetherlands, <http://www.scm.com>
85. AIMAll (version 13.05.06), Keith, T. A. **2011**, <http://aim.tkgristmill.com>
86. Angeli, C.; Bak, K. L.; Bakken, V.; Christiansen, O.; Cimiraglia, R.; Coriani, S.; Dahle, P.; Dalskov, E. K.; Enevoldsen, T.; Fernandez, B.; Ferrighi, L.; Frediani, L.; Hattig, C.; Hald, K.; Halkier, A.; Heiberg, H.; Helgaker, T.; Hettema, H.; Jansik, B.; Jensen, H. J. A.; Jonsson, D.; Jørgensen, P.; Kirpekar, S.; Klopper, W.; Knecht, S.; Kobayashi, R.; Kongsted, J.; Koch, H.; Ligabue, A.; Lutnæs, O. B.; Mikkelsen, K. V.; Nielsen, C. B.; Norman, P.; Olsen, J.; Osted, A.; Packer, M. J.; Pedersen, T. B.; Rinkevicius, Z.; Rudberg, E.; Ruden, T. A.; Ruud, K.; Salek, P.; Samson, C. C. M.; Sanchez de Meras, A.; Saue, T.; Sauer, S. P. A.; Schimmelpfennig, B.; Steindal, A. H.; Sylvester-Hvid, K. O.; Taylor, P. R.; Vahtras, O.;

Wilson, D. J.; Ågren, H.; Dalton et al. **2011**, amolecular electronic structure program, Release Dalton 2011 see <http://daltonprogram.org>

87. Matito, E. **2006**, ESI-3D: electron sharing indices program for 3D molecular space partitioning. Institute of Computational chemistry and Catalysis (IQCC), University of Girona, Catalonia, Spain, <http://iqc.udg.es/~eduard/ESI>.

88. Matito, E.; Duran, M.; Solà, M. *J. Chem. Phys.* **2005**, *122*, 014109.

89. Matito, E.; Solà, M.; Salvador, P.; Duran, M. *Faraday Discuss* **2007**, *135*, 325.

90. Frisch, M. J.; Trucks, G. W.; Schlegel, H. B.; Scuseria, G. E.; Robb, M. A.; Cheesman, J. R.; Zakrzewski, V. G.; Montgomery, J. A.; Strtmann, R. E.; Burant, J. C.; Dapprich, S.; Milliam, J. M.; Daniels, A. D.; Kudin, K. N.; Strain, M. C.; Farkas, O.; Tomasi, J.; Barone, V.; Cossi, M.; Camme, R.; Mennucci, B.; Pomelli, C.; Adamo, C.; Clifford, S.; Ochterski, J.; Petersson, G. A.; Ayala, P. Y.; Cui, Q.; Morokuma, K.; Rega, N.; Salvador, P.; Dannenberg, J. J.; Malich, D. K.; Rabuck, A. D.; Raghavachari, K.; Foresman, J. B.; Cioslowski, J.; Ortiz, J. V.; Baboul, A. G.; Stetanov, B. B.; Liu, G.; Liashenko, A.; Piskorz, P.; Komaromi, I.; Gomperts, R.; Martin, R. L.; Fox, D. J.; Keith, T.; Al-Laham, M. A.; Peng, C. Y.; Nnsyskkara, A.; Challacombe, M.; Gill, P. M. W.; Johnson, B.; Chen, W.; Wong, M. W.; Andres, J. L.; Gonzalez, C.; Head-Gordon, M.; Replogle, E. S.; Pople, J. A. GAUSSIAN09, Revision A.02, Gaussian Inc., Pittsburgh (2009).

91. Chen, W.; Schlegel, H. B. *J. Chem. Phys.* **1994**, *101*, 5957.

92. Noodleman, L. *J. Chem. Phys.* **1981**, *74*, 5737.

93. Noodleman, L.; Case, D. A. *Adv. Inorg. Chem.* **1992**, *38*, 423.

94. Bickelhaupt, F. M.; Baerends, E. J. In *Reviews of computational chemistry*, vol 15. Lipkowitz, K. B.; Boyd, D. B. (Eds.) Wiley VCH, New York, **2000**, p 1.

95. Baerends, E. J. In *Cluster models for surface and bulk phenomena*, Nato ASI series B, vol 283 Pacchioni, G.; Bagus, P. S. (Eds.) Plenum Press, New York, **1992**, p 189

96. Chattaraj, P. K. (ed) *In: Aromaticity and metal clusters*. CRC, New York, **2011**.

97. Grimme, S. *J. Comput. Chem.* **2004**, *25*, 1463.

98. Grimme, S. *J. Comput. Chem.* **2006**, *27*, 1787.

99. Ochsenfeld, C.; Koziol, F.; Brown, S. P.; Schaller, T.; Seelbach, U. P.; Klärner, F. G. *Solid State Nucl. Magn. Reson.* **2002**, *22*, 128.

100. Ochsenfeld, C. *Phys. Chem. Chem. Phys.* **2000**, *2*, 2153.

101. Ochsenfeld, C.; Brown, S. P.; Schnell, I.; Gauss, J.; Spiess, H. W. *J. Am. Chem. Soc.* **2001**, *123*, 2597.

Chapter 4.

1. (a) Miller, J. S.; Epstein, A. J.; Reiff, W. M. *Mol. Cryst. Liq. Cryst.*, **1985**, *120*, 27; (b) Miller, J. S.; Calabrese, J. C.; Rommelmann, H.; Chittipeddi, S. R.; Zang, J. H.; Reiff W. M.; Epstein, A. J. *J. Am. Chem. Soc.* **1987**, *109*, 769.
2. (a) Jortner J. and Ratner, M.; *Molecular Electronics, Blackwell Science, Cambridge, MA, 1997*; (b) Aviram A. and Ratner, M. *Molecular Electronics: Science and Technology (Annals of the New York Academy of Sciences)*, *The New York Academy of Sciences, New York, NY. 1998*, vol. 852.
3. (a) Goovaerts, E.; Wenseleers, W. E.; Garcia M. H.; and Cross, G. H. *Nonlinear Optical Materials, in Handbook of Advanced Electronic and Photonic Materials and Devices, Academic Press, New York. 2001*; (b) Morall, J. P.; Dalton, G. T.; Humphrey M. G. Samoc, M. *Adv. Organomet. Chem.* **2008**, *55*, 61; (c) Powell C. E.; Humphrey, M. G. *Coord. Chem. Rev.* **2004**, *248*, 725; (d) Long, N. J. *Angew. Chem. Int. Ed. Engl.* **1995**, *34*, 21; (e) Di Bella, S.; Dragonetti, C.; Pizzotti, M.; Roberto, D.; Tessore F. Ugo, R. *Top. Organomet. Chem.* **2010**, *28*, 1; (f) Astruc, D. *Organometallic Chemistry and Catalysis, Springer, Heidelberg. 2007*; (g) Fuentealba, M.; Toupet, L.; Manzur, C.; Carrillo, D.; Ledoux-Rak, I. Hamon, J.R. *J. Organomet. Chem.* **2007**, *692*, 1099; (h) Lambert, C.; Gaschler, W.; Zabel, M.; Matschiner R. Wortmann, R.; *J. Organomet. Chem.* **1999**, *592*, 109.
4. (a) Carretta, S.; Santini, P.; Amoretti, G.; Guidi, T.; Copley, J. R. D.; Qiu, Y.; Caciuffo, R.; Timco G. Winpenny, R. E. P. *Phys. Rev. Lett.* **2007**, *98*, 167401; (b) Ardavan, A.; Rival, O.; Morton, J. J. L.; Blundell, S. J.; Tyryshkin, A. M.; Timco G. Winpenny, R. E. P. *Phys. Rev. Lett.* **2007**, *98*, 057201; (c) Leuenberger M. N. Loss, D. *Nature* **2001**, *410*, 789; (d) Troiani, F.; Ghirri, A.; Affronte, M.; Carretta, S.; Santini, P.; Amoretti, G.; Piligkos, S.; Timco G. Winpenny, R. E. P. *Phys. Rev. Lett.* **2005**, *94*, 207208; (e) Lehmann, J.; Gaita-Arino, A.; Coronado E. Loss, D. *Nat. Nanotechnol.* **2007**, *2*, 312.
5. Yee, G. T.; Whitton, M. J.; Sommet, R. D.; Frommen C. M.; Reiff, W. M. *Inorg. Chem.* **2000**, *39*, 1874.
6. (a) Kaul, B. B.; Durfee W. S. Yee, G. T. *J. Am. Chem. Soc.* **1999**, *121*, 6862; (b) Kaul, B. B.; Sommer, R. D.; Noll B. C. Yee, G. T. *Inorg. Chem.* **2000**, *39*, 865.
7. (a) Boderick, W. E.; Liu X. Hoffman, B. M. *J. Am. Chem. Soc.* **1991**, *113*, 6334; (b) Miller, J. S.; McLean, R. S.; Vazquez, C.; Calabrese, J. C.; Zuo F. Epstein, A. J.; *J. Mater. Chem.* **1993**, *3*, 215; (c) Yee, G. T.; Manriquez, J. M.; Dixon, D. A.; McLean, R. S.; Groski, D. M.; Flippen, R. B.; Narayan, K. S.; Epstein A. J. Miller, J. S. *Adv. Mater.* **1991**, *3*, 309.
8. (a) McConnell, H. M.; *Proc. Robert A. Welch Found. Conf. Chem. Res.* **1967**, *11*, 144; (b) Breslow, R. *Pure Appl. Chem.* **1982**, *54*, 927; (c) Kahn, O. *Molecular Magnetism, VCH, New York, 1993*.
9. (a) Schweizer, J.; Golhen, S.; Lelièvre-Berna, E.; Ouahab, L.; Pontillon Y. Ressouche, E. *Phys. B* **2001**, *297*, 213; (b) Kollmar C. Kahn, O. *Acc. Chem. Res.* **1993**, *26*, 259.
10. McConnell, H. D. *J. Chem. Phys.* **1963**, *39*, 1910.
11. Wang, G.; Slebodnick, C.; Butcher R. J. Yee, G. T. *Inorg. Chim. Acta* **2009**, *362*, 2423.

12. Datta S. N. Misra, A. *J. Chem. Phys.* **1999**, *111*, 9009.
13. Tyree, W. S. *Thesis submitted to the faculty of the Virginia Polytechnic Institute and State University for the degree of Master of Science in Chemistry.* **2005**.
14. Okamura, T.; Takano, Y.; Yoshioka, Y.; Ueyama, N.; Nakamura A. Yamaguchi, K. *J. Organomet. Chem.* **1998**, *569*, 177.
15. Brune, H.; Röder, H.; Boragno H. Kern, K. *Phys. Rev. Lett.* **1994**, *73*, 1955.
16. (a) Pederson, M. R.; Reuse F. Khanna, S. N. *Phys. Rev. B: Condens. Matter Mater. Phys.* **1998**, *58*, 5632; (b) Nayak, S. K.; Rao B. K. Jena, P. *J. Phys.: Condens. Matter* **1998**, *10*, 10863; (c) Nayak S. K. Jena, P. *Chem. Phys. Lett.* **1998**, *289*, 473; (d) Nickelbein, M. B. *Phys. Rev. Lett.* **2001**, *86*, 5255; (e) Michael, F.; Gonzalez, C.; Mujica, V.; Marquez M. Ratner, M. A. *Phys. Rev. B: Condens. Matter Mater. Phys.* **2007**, *76*, 224409; (f) Sosa-Hernandez, E. M.; Alvarado-Leyva, P. G.; Montezano-Carrizales J. M. Aguilera-Granja, F. *Rev. Mex. Fis.* **2004**, *50*, 30; (g) Liu, F.; Khanna S. N. Jena, P. *Phys. Rev. B: Condens. Matter Mater. Phys.* **1991**, *43*, 8179; (h) Mitra, S.; Mandal, A.; Datta, A.; Banerjee, S.; Chakravorty, J. D. *Phys. Chem. C* **2011**, *115*, 14673.
17. (a) Reddy, B. V.; Khanna S. N.; Dunlap, B. I. *Phys. Rev. Lett.* **1993**, *70*, 3323; (b) Nozue, Y.; Kodaira T.; Goto, T. *Phys. Rev. Lett.* **1992**, *68*, 3789; (c) Cox, A. J.; Louderback J. G.; Bloomfield, L. A. *Phys. Rev. Lett.* **1993**, *71*, 923; (d) Villaseñor-González, P.; DorantesDávila, J.; Dreyysé H.; Pastor, G. M.; *Phys. Rev. B: Condens. Matter Mater. Phys.* **1997**, *55*, 15084; (e) Guirado-López, R.; Spanjaard D.; Desjonqueres, M. C. *Phys. Rev. B: Condens. Matter Mater. Phys.* **1998**, *57*, 6305.
18. McGrady, J. E.; Stranger R.; Lovell, T. *J. Phys. Chem. A* **1997**, *101*, 6265.
19. Noodleman, L. *J. Chem. Phys.* **1981**, *74*, 5737.
20. (a) Bencini, A.; Totti, F.; Daul, C. A.; Doclo, K.; Fantucci P.; Barone, V. *Inorg. Chem.* **1997**, *36*, 5022; (b) Ruiz, E.; Cano, J.; Alvarez S.; Alemany, P. *J. Comput. Chem.* **1999**, *20*, 1391.
21. Soda, T.; Kitagawa, Y.; Onishi, T.; Takano, Y.; Shigeta, Y.; Nagao, H.; Yoshioka Y.; Yamaguchi, K. *Chem. Phys. Lett.* **2000**, *319*, 223.
22. Szabo A.; Ostlund, N. S. *Modern Quantum Chemistry: Introduction to Advanced Electronic Structure Theory*, Dover Publications, New York. **1996**.
23. Herrmann, C.; Yu L.; Reiher, M. *J. Comput. Chem.* **2006**, *27*, 1223.
24. Binning Jr, R. C.; Babelo, D. E. *J. Comput. Chem.* **2008**, *29*, 716.
25. Galperin, M.; Segal D.; Nitzam, A. *J. Chem. Phys.* **1999**, *111*, 1569.
26. (a) Anderson, P. W. *Phys. Rev.* **1950**, *79*, 350; (b) Anderson, P. W. *Phys. Rev.* **1959**, *115*, 2; (c) Anderson, P. W. In *Theory of the Magnetic Interaction: Exchange in Insulators and Superconductors*, *Solid State Physics*, vol. 14, Academic, New York, **1963**, p. 99.
27. Munoz, D.; Illas F.; de Moreira, I. P. R. *Phys. Rev. Lett.* **2000**, *84*, 1579.

28. (a) Calzado, C. J.; Cabrero, J.; Malrieu J. P.; Caballol, R.; *J. Chem. Phys.* **2002**, *116*, 2728; (b) Calzado, C. J.; Cabrero, J.; Malrieu J. P. and Caballol, R. *J. Chem. Phys.* **2002**, *116*, 3985; (c) Calzado, C. J.; Angeli, C.; Taratiel, D.; Caballol R.; Malrieu, J. P. *J. Chem. Phys.* **2009**, *131*, 044327.
29. (a) Paul S.; Misra, A. *J. Chem. Theory Comput.* **2012**, *8*, 843; (b) Shil, S.; Paul S.; Misra, A. *J. Phys. Chem. C* **2013**, *117*, 2016.
30. Petrov, E. G.; Shevchenko, Y. V.; Teslenko V. I.; May, V. *J. Chem. Phys.* **2001**, *115*, 7107.
31. Paul S.; Misra, A. *J. Phys. Chem. A* **2010**, *114*, 6641.
32. (a) Daizadeh, I.; Medvedev D. M.; Stuchebrukhov, A. A. *Mol. Biol. Evol.* **2002**, *19*, 406; (b) Mikolajczyk, M. M.; Zaleśny, R.; Czyżnikowska, Z.; Toman, P.; Leszczynski J.; Bartkowiak, W.; *J. Mol. Model.* **2011**, *17*, 2143.
33. Makov, G.; Shah R.; Payne, M. C. *Phys. Rev. B: Condens.Matter Mater. Phys.* **1996**, *53*, 15513.
34. (a) Foster J. P.; Weinhold, F. *J. Am. Chem. Soc.* **1980**, *102*, 7211; (b) Reed, A. E.; Curtiss L. A.; Weinhold, F. *Chem. Rev.* **1988**, *88*, 899.
35. Baumeier, B.; Kirkpatrick J.; Andrienko, D. *Phys. Chem. Chem. Phys.* **2010**, *12*, 11103.
36. Huang J.; Kertesz, M. *J. Chem. Phys.* **2005**, *122*, 234707.
37. Perdew, J. P.; Burke K.; Ernzerhof, M. *Phys. Rev. Lett.* **1996**, *77*, 3865.
38. (a) Improta, R.; Barone, V.; Kudin K. N.; Scuseria, G. E. *J. Chem. Phys.* **2001**, *114*, 254; (b) Zhao, G.; Jiang, L.; He, Y.; Li, J.; Dong, H.; Wang X.; Hu, W. *Adv. Mater.* **2011**, *23*, 3959; (c) Improta, R.; Barone, V.; Kudin K. N.; Scuseria, G. E. *J. Am. Chem. Soc.* **2001**, *123*, 3311.
39. (a) Becke, A. D. *J. Chem. Phys.* **1993**, *98*, 5648; (b) Stephens, J.; Devlin, F. J.; Chabalowski C. F.; Frisch, M. J. *J. Phys.Chem.* **1994**, *98*, 11623; (c) Adamo C.; Barone, V. *J. Chem. Phys.* **1999**, *110*, 6158; (d) Ernzerhof M.; Scuseria, G. E. *J. Chem. Phys.* **1999**, *110*, 5029; (e) Jacquemin, D.; Perpète, E. A.; Ciofini I.; Adamo, C. *Chem. Phys. Lett.* **2005**, *405*, 376.
40. (a) Chevrau, H.; de Moreira, I. P. R.; Silvi B.; Illas, F. *J. Phys.Chem. A* **2001**, *105*, 3570; (b) Ruiz, E.; Alemany, P.; Alvarez S.; Cano, S.; *J. Am. Chem. Soc.* **1997**, *119*, 1297.
41. (a) Martin R. L.; Illas, F. *Phys. Rev. Lett.* **1997**, *79*, 1539;(b) Illas F.; Martin, R. L. *J. Chem. Phys.* **1998**, *108*, 2519.
42. Onishi, T.; Takano, Y.; Kitagawa, Y.; Kawakami, T.; Yoshioka Y.; Yamaguchi, K. *Polyhedron* **2001**, *20*, 1177.
43. Becke, A. D. *J. Chem. Phys.* **1993**, *98*, 1372.
44. Caballol, R.; Castell, O.; Illas, F.; Malrieu J. P.; Moreira, I. deP. R. *J. Phys. Chem. A* **1997**, *101*, 7860.

45. Paier, J.; Marsman M.; Kreese, G. *J. Chem. Phys.* **2007**, *127*, 024103.
46. Atanasov, M.; Delley, B.; Neese, F.; Tregenna-Piggott P. L.; Sigrist, M. *Inorg. Chem.* **2011**, *50*, 2112.
47. Pantazis, D. A.; Orio, M.; Petrenko, T.; Zein, S.; Bill, E.; Lubitz, W.; Messinger J. Neese, F. *Chem. Eur. J.* **2009**, *15*, 5108.
48. (a) Orio, M.; Pantazis, D. A.; Petrenko T.; Neese, F. *Inorg.Chem.* **2009**, *48*, 7251; (b) Pantazis, D. A.; Krewald, V.; Orio M.; Neese, F. *Dalton Trans.* **2010**, *39*, 4959.
49. (a) Pantazis, D. A.; Orio, M.; Petrenko, T.; Zein, S.; Lubitz, W.; Messinger J.; Neese, F. *Phys. Chem. Chem. Phys.* **2009**, *11*, 6788; (b) Tao, J.; Perdew, J. P.; Staroverov V. N.; Scuseria, G. E. *Phys. Rev. Lett.* **2003**, *91*, 146401; (c) Staroverov, V. N.; Scuseria, G. E.; Tao J.; Perdew, J. P. *J. Chem. Phys.* **2003**, *119*, 12129.
50. Mödl, M.; Dolg, M.; Fulde P.; Stoll, H. *J. Chem. Phys.* **1997**, *106*, 1836.
51. (a) Mouesca, J. M.; Noodleman L.; Case, D. A. *Int.J. Quantum Chem., Quantum Biol. Symp.* **1995**, *22*, 95; (b) Daudey, J. P.; de Loth P.; Malrieu, J. P. In *Magnetic Structural Correlation in Exchange Coupled Systems*, NATO Symposium, D. Gatteschi, O. Kahn and R. D. Willett (Eds.), Reidel, Dordrecht, **1984**.
52. (a) Andersson, K.; Malmqvist, P. A.; Roos, B. O.; Sadlej A. J.; Wolinski, K. *J. Phys. Chem.* **1990**, *94*, 5483; (b) Andersson, K.; Malmqvist P. A.; Roos, B. O. *J. Chem. Phys.* **1992**, *96*, 1218; (c) de Graaf, C.; Sousa, C.; de Moreira I. P. R.; Illas, F. *J. Phys. Chem. A* **2001**, *105*, 11371.
53. Calzado, C. J.; Celestino, A.; Caballol R.; Malrieu, J. P. *Theor. Chem. Acc.* **2010**, *126*, 185.
54. (a) Miralles, J.; Daudey J. P.; Caballol, R. *Chem. Phys. Lett.* **1992**, *198*, 555; (b) Miralles, J.; Castell, O.; Caballol R.; Malrieu, J. P. *Chem. Phys.* **1993**, *172*, 33.
55. de Graaf, C.; Broe R.; Nieuwpoort, W. C. *Chem. Phys. Lett.* **1997**, *271*, 372.
56. Frisch, M. J.; Trucks, G. W.; Schlegel, H. B.; Scuseria, G. E.; Robb, M. A.; Cheesman, J. R.; Zakrzewski, V. G.; Montgomery, J. A.; Strtmann, R. E.; Burant, J. C.; Dapprich, S.; Milliam, J. M.; Daniels, A. D.; Kudin, K. N.; Strain, M. C.; Farkas, O.; Tomasi, J.; Barone, V.; Cossi, M.; Camme, R.; Mennucci, B.; Pomelli, C.; Adamo, C.; Clifford, S.; Ochterski, J.; Petersson, G. A.; Ayala, P. Y.; Cui, Q.; Morokuma, K.; Rega, N.; Salvador, P.; Dannenberg, J. J.; Malich, D. K.; Rabuck, A. D.; Raghavachari, K.; Foresman, J. B.; Cioslowski, J.; Ortiz, J. V.; Baboul, A. G.; Stetanov, B. B.; Liu, G.; Liashenko, A.; Piskorz, P.; Komaromi, I.; Gomperts, R.; Martin, R. L.; Fox, D. J.; Keith, T.; Al-Laham, M. A.; Peng, C. Y.; Nsnsyskkara, A.; Challacombe, M.; Gill, P. M. W.; Johnson, B.; Chen, W.; Wong, M. W.; Andres, J. L.; Gonzalez, C.; Head-Gordon, M.; Replogle E. S.; Pople, J. A. GAUSSIAN09, Revision A.02, Gaussian Inc., Pittsburgh (2009).
57. O'Boyle, N. M.; Tenderholt A. L.; Langner, K. M. *J. Comput. Chem.* **2008**, *29*, 839.

58. (a) Castellani, M. P.; Geib, S. J.; Rheingold A. L.; Trogler, W. C. *Organometallics* **1987**, *6*, 1703; (b) Stroppa, A.; Barone, P.; Jain, P.; Perez-Mato J. M.; Picozzi, S. *Adv. Mater.* **2013**, *25*, 2284.
59. Gruschus J. M.; Kuki, A. *J. Phys. Chem.* **1993**, *97*, 5581.
60. (a) Staemmler V.; Fink, K. *Chem. Phys.* **2002**, *278*, 79; (b) Stoll H.; Doll, K. *J. Chem. Phys.* **2012**, *136*, 074106.
61. Noga, J.; Baňacký, P.; Biskupič, S.; Boča, R.; Pelikán, P.; Svrček M.; Zajac, A. *J. Comput. Chem.* **1999**, *20*, 253.
62. (a) Yoshizawa K.; Hoffmann, R. *J. Chem. Phys.* **1995**, *103*, 2126; (b) Wang, W. J.; Yao K. L.; Lin, H. Q.; *J. Chem. Phys.* **1998**, *108*, 2867.
63. Bicout D. J.; Kats, E. *Phys. Lett. A* **2002**, *300*, 479.
64. de Moreira, I. P. R.; Illas F.; Martin, R. L. *Phys. Rev. B: Condens. Matter Mater. Phys.* **2002**, *65*, 155102.
65. Improta, R.; Kudin, K. N.; Scuseria G. E.; Barone, V. *J. Am. Chem. Soc.* **2002**, *124*, 113.
66. Miller, J. S.; Epstein A. J.; Reiff, W. M. *Chem. Rev.* **1988**, *201*.
67. (a) Cramer C. J.; Truhlar, D. G. *Phys. Chem. Chem. Phys.* **2009**, *11*, 10757; (b) Marsman, M.; Paier, J.; Stroppa A.; Kresse, G.; *J. Phys.: Condens. Matter* **2008**, *20*, 064201; (c) Stroppa A.; Picozzi, S. *Phys. Chem. Chem. Phys.* **2010**, *12*, 5405.
68. Gangopadhyay, S.; Masunov, A. E.; Poalelungi E.; Leuenberger, M. N. *J. Chem. Phys.* **2010**, *132*, 244104.
69. Ederer C.; Komelj, M. *Phys. Rev. B: Condens. Matter Mater. Phys.* **2007**, *76*, 064409.
70. Wynn, C. M.; Girtu, M. A.; Brinckerhoff, W. B.; Suguira, K. I.; Miller J. S.; Epstein A. J. *Chem. Mater.* **1997**, *9*, 2156.
71. Miller, J. S. *J. Mater. Chem.* **2010**, *20*, 1846.
72. Stryjewski E.; Giordano, N. *Adv. Phys.* **1977**, *26*, 487.

Chapter 5.

1. Kahn, O. *Molecular Magnetism*; VCH: New York, 1993.
2. Oshio, H.; Nakano, M. *Chem. -Eur. J.* **2005**, *11*, 5178.
3. Gatteschi, D.; Sessoli, R. *J. Magn. Magn. Mater.* **2004**, *272*, 1030.
4. Krzystek, J.; Ozarowski, A.; Telser, J. *Coord. Chem. Rev.* **2006**, *250*, 2308.
5. (a) Sessoli, R.; Tsai, H. L.; Schake, A. R.; Wang, S.; Vincent, J. B.; Folting, K.; Gatteschi, D.; Christou, G.; Hendricson, D. N. *J. Am. Chem. Soc.* **1993**, *115*, 1804; (b) Sessoli, R.; Gatteschi, D.; Caneschi, A.; Novak, M. A. *Nature* **1993**, *365*, 141.

6. (a) Gatteschi, D.; Sessoli, R.; Villain, J. *Molecular Nanomagnets*; Oxford University Press: New York, 2006; (b) Milios, C. J.; Vinslava, A.; Wernsdorfer, W.; Moggach, S.; Parsons, S.; Perlepes, S. P.; Christou, G.; Brechin, E. K. *J. Am. Chem. Soc.* **2007**, *129*, 2754; (c) Freedman, D. E.; Jenkins, D. M.; Ivarone, A. T.; Long, J. R. *J. Am. Chem. Soc.* **2008**, *130*, 2884; (d) Yoshihara, D.; Karasawa, S.; Koga, N. *J. Am. Chem. Soc.* **2008**, *130*, 10460.
7. Gatteschi, D.; Caneschi, A.; Pardi, L.; Sessoli, R. *Science* **1994**, *265*, 1054.
8. Aubin, S. M. J.; Wemple, M. W.; Adams, D. M.; Tsai, H. L.; Christou, G.; Hendrickson, D. N. *J. Am. Chem. Soc.* **1996**, *118*, 7746.
9. Ritter, S. K. *Chem. Eng. News* **2004**, *82*, 29.
10. (a) Garanin, D. A.; Chudnovsky, E. M. *Phys. Rev. B* **1997**, *56*, 11102; (b) Leuenberger, M. N.; Loss, D. *Nature* **2001**, *410*, 789; (c) Jo, M. H.; Grose, J. E.; Baheti, K.; Deshmukh, M. M.; Sokol, J. J.; Rumberger, E. M.; Hendrickson, D. N.; Long, J. R.; Park, H.; Ralph, D. C. *Nano Lett.* **2006**, *6*, 2014; (d) Ardavan, A.; Rival, O.; Morton, J. J. L.; Blundell, S. J.; Tyryshkin, A. M.; Timco, G. A.; Winpenny, R. E. P. *Phys. Rev. Lett.* **2007**, *98*, 572011; (e) Bogani, L.; Wernsdorfer, W. *Nat. Mater.* **2008**, *7*, 179; (f) Stamp, P. C. E.; Gaita-Arino, A. *J. Mater. Chem.* **2009**, *19*, 1718.
11. (a) Affronte, M.; Troiani, F.; Ghirri, A.; Candini, A.; Evangelisti, M.; Corradini, V.; Carretta, S.; Santini, P.; Amoretti, G.; Tuna, F.; Timco, G.; Winpenny, R. E. P. *J. Phys. D Appl. Phys.* **2007**, *40*, 2999; (b) Manoli, M.; Johnstone, R. D. L.; Parsons, S.; Murrie, M.; Affronte, M.; Evangelisti, M.; Brechin, E. K. *Angew. Chem., Int. Ed.* **2007**, *46*, 4456; (c) Mannini, M.; Pineider, F.; Sainctavit, P.; Danieli, C.; Otero, E.; Sciancalepore, C.; Talarico, A. M.; Arrio, M. A.; Cornia, A.; Gatteschi, D.; Sessoli, R. *Nat. Mater.* **2009**, *8*, 194; (d) Loth, S.; von Bergmann, K.; Ternes, M.; Otte, A. F.; Lutz, C. P.; Heinrich, A. J. *Nat. Phys.* **2010**, *6*, 340.
12. (a) Collison, D.; Murrie, M.; Oganessian, V. S.; Piligkos, S.; Poolton, N. R. J.; Rajaraman, G.; Smith, G. M.; Thomson, A. J.; Timco, G. A.; Wernsdorfer, W.; Winpenny, R. E. P.; McInnes, E. J. L. *Inorg. Chem.*, **2003**, *42*, 5293; (b) Vallejo, J.; Castro, I.; Cañadillas-Delgado, L.; Ruiz-Pérez, C.; Ferrando-Soria, J.; Ruiz-García, R.; Cano, J.; Lloret, F.; Julve, M. *Dalton Trans.* **2010**, *39*, 2350.
13. (a) AlDamen, M. A.; Clemente-Juan, J. M.; Coronado, E.; Marti-Gastaldo, C.; Gaita-Arino, A. *J. Am. Chem. Soc.* **2008**, *130*, 8874; (b) AlDamen, M. A.; Cardona-Serra, S.; Clemente-Juan, J. M.; Coronado, E.; Gaita-Arino, A.; Marti-Gastaldo, C.; Luis, F.; Montero, O. *Inorg. Chem.* **2009**, *48*, 3467–3479.
14. (a) Branzoli, F.; Carretta, P.; Filibian, M.; Zoppellaro, G.; Graf, M. J.; Galan-Mascaros, J. R.; Fuhr, O.; Brink, S.; Ruben, M. *J. Am. Chem. Soc.* **2009**, *131*, 4387; (b) Kyatskaya, S.; Galan-Mascaros, J. R.; Bogani, L.; Hennrich, F.; Kappes, M.; Wernsdorfer, W.; Ruben, M. *J. Am. Chem. Soc.* **2009**, *131*, 15143.
15. Jiang, S. D.; Wang, B. W.; Su, G.; Wang, Z. M.; Gao, S. *Angew. Chem., Int. Ed.* **2010**, *49*, 7448.
16. (a) Rinehart, J. D.; Long, J. R. *J. Am. Chem. Soc.* **2009**, *131*, 12558; (b) Rinehart, J. D.; Meihaus, K. R.; Long, J. R. *J. Am. Chem. Soc.* **2010**, *132*, 7572.

17. Freedman, D. E.; Harman, W. H.; Harris, T. D.; Long, G. J.; Chang, C. J.; Long, J. R. *J. Am. Chem. Soc.* **2010**, *132*, 1224.
18. Clerac, R.; Miyasaka, H.; Yamashita, M.; Coulon, C. *J. Am. Chem. Soc.* **2002**, *124*, 12837.
19. Ferbinteanu, M.; Miyasaka, H.; Wernsdorfer, W.; Nakata, K.; Sugiura, K.; Yamashita, M.; Coulon, C.; Clerac, R. *J. Am. Chem. Soc.* **2005**, *127*, 3090.
20. Miyasaka, H.; Nezu, T.; Sugimoto, K.; Sugiura, K.; Yamashita, M.; Clerac, R. *Chem.–Eur. J.* **2005**, *11*, 1592.
21. Kajiwara, T.; Nakano, M.; Kaneko, Y.; Takaishi, S.; Ito, T.; Yamashita, M.; Kamiyama, A. I.; Nojiri, H.; Ono, Y.; Kojima, N. *J. Am. Chem. Soc.* **2005**, *127*, 10150.
22. Miyasaka, H.; Madanbashi, T.; Sugimoto, K.; Nakazawa, Y.; Wernsdorfer, W.; Sugiura, K.; Yamashita, M.; Coulon, C.; Clerac, R. *Chem.–Eur. J.* **2006**, *12*, 7028.
23. Caneschi, A.; Gatteschi, D.; Lalioti, N.; Sangregorio, C.; Sessoli, R.; Venturi, G.; Vindigni, A.; Rettori, A.; Pini, M. G.; Novak, M. A. *Angew. Chem., Int. Ed.* **2001**, *40*, 1760.
24. Harris, T. D.; Bennett, M. V.; Clerac, R.; Long, J. R. *J. Am. Chem. Soc.* **2010**, *132*, 3980.
25. Nakano, M.; Oshio, H. *Chem. Soc. Rev.* **2011**, *40*, 3239.
26. (a) Busey, R. H.; Sonder, E. *J. Chem. Phys.* **1962**, *36*, 93; (b) Desrochers, P. J.; Telser, J.; Zvyagin, S. A.; Ozarowski, A.; Krzystek, J.; Vicic, D. A. *Inorg. Chem.* **2006**, *45*, 8930; (c) Duboc, C.; Phoeung, T.; Zein, S.; Pecaut, J.; Collomb, M.-N.; Neese, F. *Inorg. Chem.* **2007**, *46*, 4905.
27. Karunadasa, H. I.; Arquero, K. D.; Berben, L. A.; Long, J. R. *Inorg. Chem.* **2010**, *49*, 4738.
28. Kanis, D. R.; Lacroix, P. G.; Ratner, M. A.; Marks, T. J. *J. Am. Chem. Soc.* **1994**, *116*, 10089.
29. Zyss, J. *Molecular Nonlinear Optics: Materials, Physics and Devices*; Academic: Boston, MA, 1994; *Nonlinear Optical Properties of Matter: From Molecules to Condensed Phases*; Papadopoulos, M. G., Leszczynski, J., Sadlej, A. J., Eds.; Kluwer: Dordrecht, The Netherlands, 2005.
30. (a) Marder, S. R.; Gorman, C. B.; Meyers, F.; Perry, J. W.; Bourhill, G.; Bré das, J. L.; Pierce, B. M. *Science* **1994**, *265*, 632; (b) Marder, S. R. *Chem. Commun.* **2006**, 131; (c) Kang, H.; Evmenenko, G.; Dutta, P.; Clays, K.; Song, K.; Marks, T. J. *J. Am. Chem. Soc.* **2006**, *128*, 6194; (d) Yang, M.; Champagne, B. *J. Phys. Chem. A* **2003**, *107*, 3942; (e) Liao, Y.; Bhattacharjee, S.; Firestone, K. A.; Eichinger, B. E.; Paranj, R.; Anderson, C. A.; Robinson, B. H.; Reid, P. J.; Dalton, L. R. *J. Am. Chem. Soc.* **2006**, *128*, 6847; (f) Kang, H.; Facchetti, A.; Jiang, H.; Cariati, E.; Righetto, S.; Ugo, R.; Zuccaccia, C.; Macchioni, A.; Stern, C. L.; Liu, Z.; Ho, S.-T.; Brown, E. C.; Ratner, M. A.; Marks, T. J. *J. Am. Chem. Soc.* **2007**, *129*, 3267.
31. Paul, S.; Misra, A. *Inorg. Chem.* **2011**, *50*, 3234.

- 32.** (a) Cariati, E.; Ugo, R.; Santoro, G.; Tordin, E.; Sorace, L.; Caneschi, A.; Sironi, A.; Macchi, P.; Casati, N. *Inorg. Chem.* **2010**, *49*, 10894; (b) Lacroix, P. G.; Malfant, I.; Bé nard, S.; Yu, P.; Riviè re, E.; Nakatani, K. *Chem. Mater.* **2001**, *13*, 441; (c) Dragonetti, C.; Righetto, S.; Roberto, D.; Ugo, R.; Valore, A.; Fantacci, S.; Sgamellotti, A.; Angelis, F. D. *Chem. Commun.* **2007**, 4116; (d) Janjua, M. R. S. A.; Guan, W.; Yan, L.; Su, Z. -M.; Ali, M.; Bukhari, I. H. *J. Mol. Graph. Model.* **2010**, *28*, 735.
- 33.** Zein, S.; Duboc, C.; Lubitz, W.; Neese, F. *Inorg. Chem.* **2008**, *47*, 134.
- 34.** Pederson, M. R.; Khanna, S. N. *Phys. Rev. B* **1999**, *60*, 9566.
- 35.** Neese, F.; Pantazis, D. A. *Faraday Discuss.* **2011**, *148*, 229.
- 36.** Neese, F.; Neese, F. ORCA 2.8.0; University of Bonn: Bonn, Germany, 2010.
- 37.** (a) van Wüllen, C. *J. Chem. Phys.* **2009**, *130*, 194109; (b) Aquino, F.; Rodriguez, J. H. *J. Phys. Chem. A* **2009**, *113*, 9150; (c) Aquino, F.; Rodriguez, J. H. *J. Chem. Phys.* **2005**, *123*, 204902.
- 38.** (a) Schäfer, A.; Horn, H.; Ahlrichs, R. *J. Chem. Phys.* **1992**, *97*, 2571; (b) Schäfer, A.; Huber, C.; Ahlrichs, R. *J. Chem. Phys.* **1994**, *100*, 5829.
- 39.** Weigend, F. *Phys. Chem. Chem. Phys.* **2006**, *8*, 1057.
- 40.** (a) Takeda, R.; Mitsuo, S.; Yamanaka, S.; Yamaguchi, K. *Polyhedron* **2005**, *24*, 2238; (b) Kortus, J.; Pederson, M. R.; Baruah, T.; Bernstein, N.; Hellberg, C. S. *Polyhedron* **2003**, *22*, 1871; (c) Park, K.; Pederson, M. R.; Richardson, S. L.; Aliaga-Alcalde, N.; Christou, G. *Phys. Rev. B* **2003**, *68*, 020405; (d) Baruah, T.; Pederson, M. R. *Int. J. Quantum Chem.* **2003**, *93*, 324; (e) Ribas-Ariño, J.; Baruah, T.; Pederson, M. R. *J. Am. Chem. Soc.* **2006**, *128*, 9497.
- 41.** Neese, F. *J. Am. Chem. Soc.* **2006**, *128*, 10213.
- 42.** Neese, F. *J. Chem. Phys.* **2007**, *127*, 164112.
- 43.** Maurice, R.; Sivalingam, K.; Ganyushin, D.; Guihé ry, N.; de Graaf, C.; Neese, F. *Inorg. Chem.* **2011**, *50*, 6229.
- 44.** Reviakine, R.; Arbuznikov, A. V.; Tremblay, J. C.; Remenyi, C.; Malkina, O. L.; Malkin, V. G.; Kaupp, M. *J. Chem. Phys.* **2006**, *125*, 054110.
- 45.** Misochko, E. Y.; Korchagin, D. V.; Bozhenko, K. V.; Chapyshev, S. V.; Aldoshin, S. M. *J. Chem. Phys.* **2010**, *133*, 064101.
- 46.** Frisch, M. J.; Trucks, G. W.; Schlegel, H. B.; Scuseria, G. E.; Robb, M. A.; Cheesman, J. R.; Zakrzewski, V. G.; Montgomery, J. A.; Strtmann, R. E.; Burant, J. C.; Dapprich, S.; Milliam, J. M.; Daniels, A. D.; Kudin, K. N.; Strain, M. C.; Farkas, O.; Tomasi, J.; Barone, V.; Cossi, M.; Camme, R.; Mennucci, B.; Pomelli, C.; Adamo, C.; Clifford, S.; Ochterski, J.; Petersson, G. A.; Ayala, P. Y.; Cui, Q.; Morokuma, K.; Rega, N.; Salvador, P.; Dannenberg, J. J.; Malich, D. K.; Rabuck, A. D.; Raghavachari, K.; Foresman, J. B.; Cioslowski, J.; Ortiz, J. V.; Baboul, A. G.; Stetanov, B. B.; Liu, G.; Liashenko, A.; Piskorz, P.; Komaromi, I.; Gomperts, R.; Martin, R. L.; Fox, D. J.; Keith, T.; Al-Laham, M. A.; Peng, C. Y.; Nnsyskkara, A.; Challacombe, M.; Gill, P. M. W.; Johnson, B.; Chen, W.; Wong, M. W.;

Andres, J. L.; Gonzalez, C.; Head-Gordon, M.; Replogle E. S.; Pople, J. A. GAUSSIAN09, Revision A.02, Gaussian Inc., Pittsburgh (2009).

47. (a) Easton, R. E.; Giesen, D. J.; Welch, A.; Cramer, C. J.; Truhlar, D. G. *Theor. Chim. Acta* **1996**, *93*, 281; (b) Li, J.; Cramer, C. J.; Truhlar, D. G. *Theor. Chem. Acc.* **1998**, *99*, 192.

48. Neese, F.; Solomon, E. I. *Inorg. Chem.* **1998**, *37*, 6568.

49. Solomon, E. I. *Inorg. Chem.* **2006**, *45*, 8012.

50. Stevens, K. W. H. *Proc. R. Soc. A (London)* **1953**, *219*, 542.

51. Nyholm, R. S. *Pure Appl. Chem.* **1968**, *17*, 1.

52. Tofield, B. C. *J. Phys. Colloq.* **1976**, *37*, C6–539.

53. Atanasov, M.; Baerends, E. J.; Baettig, P.; Bruyndonckx, R.; Daul, C.; Rauzy, C.; Zbiri, M. *Chem. Phys. Lett.* **2004**, *399*, 433.

54. O'Reilly, T. J.; Offenbacher, E. L. *J. Chem. Phys.* **1971**, *54*, 3065.

55. Pellow, R.; Vala, M. *J. Chem. Phys.* **1989**, *90*, 5612.

56. (a) Debrunner, P. G.; Dexter, A. F.; Schulz, C. E.; Xia, Y.-M.; Hager, L. P. *Proc. Natl. Acad. Sci. U.S.A.* **1996**, *93*, 12791; (b) Griffith, J. S. *Mol. Phys.* **1971**, *21*, 135.

57. Neese, F.; Solomon, E. I., Magnetism: Molecules to Materials IV; Miller, J. S., Drillon, M., Eds; Wiley-VCH: Weinheim, 2002; Chapter 9, p 406.

58. Schöneboom, J. C.; Neese, F.; Thiel, W. *J. Am. Chem. Soc.* **2005**, *127*, 5840.

59. Maganas, D.; Sottini, S; Kyritsis, P.; Groenen, E. J. J.; Neese, F. *Inorg. Chem.* **2011**, *50*, 8741.

60. Kanis, D. R.; Ratner, M. A.; Marks, T. J. *Chem. Rev.* **1994**, *94*, 195.

61. Boguslawski, K.; Jacob, C. R.; Reiher, M. *J. Chem. Theory. Comput.* **2011**, *7*, 2740.

62. de Andrade, A. V. M; da Costa, N. B., Jr.; Longo, R. L.; Malta, O. L.; Simas, A. M.; de Sá, G.F. *Mol. Eng.* **1997**, *7*, 293.

63. (a) Meissler, G. L.; Tarr, D. A. Inorganic Chemistry; Pearson Education and Pearson Prentice Hall: Upper Saddle River, NJ, 2004. (b) Caughey, W. S.; Eberspaecher, H.; Fuchsman, W. H.; McCoy, S.; Alben, J. O. *Ann. N.Y. Acad. Sci.* **1969**, *153*, 722.

64. Kittilstved, K. R.; Sorgho, L. A.; Amstutz, N.; Tregenna-Piggott, P. L. W.; Hauser, A. *Inorg. Chem.* **2009**, *48*, 7750.

65. Solomon, E. I.; Brunold, T. C.; Davis, M. I.; Kemsley, J. N.; Lee, S.-K.; Lehnert, N.; Neese, F.; Skulan, A. J.; Yang, Y.-S.; Zhou, J. *Chem. Rev.* **2000**, *100*, 235.

66. Solomon, E. I.; Pavel, E. G.; Loeb, K. E.; Campochiaro, C. *Coord. Chem. Rev.* **1995**, *144*, 369.

Chapter 6.

1. (a) Boussac, A.; Girerd, J. J.; Rutherford, A. W. *Biochemistry* **1996**, *35*, 6984; (b) Horner, O.; Rivire, E.; Blondin, G.; Un, S.; Rutherford, A. W.; Girerd, J. J.; Boussac, A. *J. Am. Chem. Soc.* **1998**, *120*, 7924 – 7928; (c) Dub, C. E.; Sessoli, R.; Hendrich, M. P.; Gatteschi, D.; Armstrong, W. H. *J. Am. Chem. Soc.* **1999**, *121*, 3537 – 3538; (d) Wernsdorfer, W.; Sessoli, R. *Science* **1999**, *284*, 133.
2. (a) Sessoli, R.; Tsai, H. L.; Schake, A. R.; Wang, S. Y.; Vincent, J. B.; Folting, K.; Gatteschi, D.; Christou, G.; Hendrickson, D. N. *J. Am. Chem. Soc.* **1993**, *115*, 1804 – 1816; (b) Gatteschi, D.; Sessoli, R.; Villain, J. In *Molecular Nanomagnets*, Oxford University Press, New York, **2006**; (c) Milios, C. J.; Vinslava, A.; Wernsdorfer, W.; Moggach, S.; Parsons, S.; Perlepes, S. P.; Christou, G.; Brechin, E. K. *J. Am. Chem. Soc.* **2007**, *129*, 2754 – 2755; (d) Yoshihara, D.; Karasawa, S.; Koga, N. *J. Am. Chem. Soc.* **2008**, *130*, 10460 – 10461.
3. Mannini, M.; Pineider, F.; Sainctavit, P.; Danieli, C.; Otero, E.; Sciancalepore, C.; Talarico, M.; Arrio, M. A.; Cornia, A.; Gatteschi, D.; Sessoli, R. *Nat. Mater.* **2009**, *8*, 194 – 197.
4. (a) Leuenberger, M. N.; Loss, D.; *Nature* **2001**, *410*, 789 – 793; (b) Ardavan, A.; Rival, O.; Morton, J. J. L.; Blundell, S. J.; Tyryshkin, A. M.; Timco, G. A.; Winpenny, R. E. P.; *Phys. Rev. Lett.* **2007**, *98*, 057201; (c) Stamp, P. C. E.; Gaita-Arino, A. *J. Mater. Chem.* **2009**, *19*, 1718 – 1730.
5. Sessoli, R., Gatteschi, D.; Caneschi, A.; Novak, M. A. *Nature* **1993**, *365*, 141 – 143.
6. Lis, T. *Acta Cryst. B* **1980**, *36*, 2042 – 2046.
7. Caneschi, A.; Gatteschi, D.; Sessoli, R.; Barra, A. L.; Brunel, L. C.; Guillot, M. *J. Am. Chem. Soc.* **1991**, *113*, 5873 – 5874.
8. Lawrence, J.; Lee, S. C.; Kim, S.; Anderson, N.; Hill, S.; Murugesu, M.; Christou, G. *AIP Conf. Proc.* **2006**, *850*, 1133 – 1134.
9. (a) Waldmann, O. *Inorg. Chem.* **2007**, *46*, 10035 – 10037; (b) Kirchner, N.; van Slageren, J.; Dressel, M. *Inorg. Chim. Acta.* **2007**, *360*, 3813 – 3819.
10. Arom, G.; Brechin, E. K. *Struct. Bonding (Berlin)* **2006**, *122*, 1 – 67.
11. (a) Bogani, L.; Wernsdorfer, W. *Nat. Mater.* **2008**, *7*, 179 – 186; (b) Urdampilleta, M.; Klyatskaya, S.; Cleuziou, J.P.; Ruben, M.; Wernsdorfer, W.; *Nat. Mater.* **2011**, *10*, 502 – 506; (c) Ritter, S. K. *Chem. Eng. News* **2004**, *82*, 29–32.
12. Liu, J.; Datta, S.; Bolin, E.; Lawrence, J.; Beedle, C. C.; Yang, E. C.; Goy, P.; Hendrickson, D. N.; Hill, S.; *Polyhedron* **2009**, *28*, 1922 – 1926.
13. (a) Lloret, F.; Julve, M.; Cano, J.; Ruiz-García, R.; Pardo, E. *Inorg. Chim. Acta* **2008**, *361*, 3432 – 3445; (b) Pali, A.; Tsukerblat, B.; Clemente-Juan, J. M.; Coronado, E.; *Int. Rev. Phys. Chem.* **2010**, *29*, 135 – 230.
14. Goswami, T.; Misra, A. *J. Phys. Chem. A* **2012**, *116*, 5207 – 5215.
15. Shil, S.; Misra, A.; *RSC Adv.* **2013**, *3*, 14352 – 14362.

16. (a) Chiba, D.; Sawicki, M.; Nishitani, Y.; Nakatani, Y.; Matsukura, F.; Ohno, H. *Nature* **2008**, *455*, 515 – 518; (b) Lebeugle, D.; Mougín, A.; Viret, M.; Colson, D.; Ranno, L. *Phys. Rev. Lett.* **2009**, *103*, 257601.
17. (a) Accorsi, S.; Barra, A. L.; Caneschi, A.; Chastanet, G.; Cornia, A.; Fabretti, A. C.; Gatteschi, D.; Mortalo, C.; Olivieri, E.; Parenti, F.; Rosa, P.; Sessoli, R.; Sorace, L.; Wernsdorfer, W.; Zoppi, L. *J. Am. Chem. Soc.* **2006**, *128*, 4742 – 4755; (b) Gregoli, L.; Danieli, C.; Barra, A. L.; Neugebauer, P.; Pellegrino, G.; Poneti, G.; Sessoli, R.; Cornia, A.; *Chem. Eur. J.* **2009**, *15*, 6456 – 6467.
18. Zyazin, A. S.; van den Berg, J. W. G.; Osorio, E. A.; van der Zant, H. S. J.; Konstantinidis, N. P.; Leijnse, M.; Wegewijs, M. R.; May, F.; Hofstetter, W.; Danieli, C.; Cornia, A. *Nano Lett.* **2010**, *10*, 3307 – 3311.
19. Zein, S.; Duboc, C.; Lubitz, W.; Neese, F. *Inorg. Chem.* **2008**, *47*, 134.
20. Pederson, M. R.; Khanna, S. N. *Phys. Rev. B* **1999**, *60*, 9566 – 9572.
21. Neese, F. *ORCA 2.8.0; University of Bonn, Bonn, Germany*, **2010**.
22. (a) van Wllen, C. *J. Chem. Phys.* **2009**, *130*, 194109; (b) Aquino, F.; Rodriguez, J. H. *J. Phys. Chem. A* **2009**, *113*, 9150 – 9156.
23. (a) Schfer, A.; Horn, H.; Ahlrichs, R. *J. Chem. Phys.* **1992**, *97*, 2571 – 2577; (b) Schfer, A.; Huber, C.; Ahlrichs, R. *J. Chem. Phys.* **1994**, *100*, 5829 – 5835.
24. Weigend, F. *Phys. Chem. Chem. Phys.* **2006**, *8*, 1057 – 1065.
25. (a) Park, K.; Pederson, M. R.; Richardson, S. L.; Aliaga-Alcalde, N.; Christou, G. *Phys. Rev. B* **2003**, *68*, 020405; (b) Ribas-Ariço, J.; Baruah, T.; Pederson, M. R. *J. Am. Chem. Soc.* **2006**, *128*, 9497 – 9505.
26. Aquino, F.; Rodriguez, J. H. *J. Chem. Phys.* **2005**, *123*, 204902.
27. (a) Davari, N.; P.-O. strand, Ingebrigtsen, S.; Unge, M. *J. Appl. Phys.* **2013**, *113*, 143707; (b) Davari, N.; P.-O. strand, Van Voorhis, T.; *Mol. Phys.* **2013**, *111*, 1456 – 1461; (c) Smirnov, M. B.; Krainov, V. P. *J. Exp. Theor. Phys.* **1997**, *85*, 447 – 450.
28. Vallejo, J.; Castro, I.; Ruiz-Garca, R.; Cano, J.; Julve, M.; Lloret, F.; Munno, G. D.; Wernsdorfer, W.; Pardo, E. *J. Am. Chem. Soc.* **2012**, *134*, 15704 – 15707.
29. Singh, S. K.; Rajaraman, G. *Chem. Eur. J.* **2013**, *19*, 1 – 12.
30. Frisch, M. J.; Trucks, G. W.; Schlegel, H. B.; Scuseria, G. E.; Robb, M. A.; Cheesman, J. R.; Zakrzewski, V. G.; Montgomery, J. A.; Strtmann, R. E.; Burant, J. C.; Dapprich, S.; Milliam, J. M.; Daniels, A. D.; Kudin, K. N.; Strain, M. C.; Farkas, O.; Tomasi, J.; Barone, V.; Cossi, M.; Camme, R.; Mennucci, B.; Pomelli, C.; Adamo, C.; Clifford, S.; Ochterski, J.; Petersson, G. A.; Ayala, P. Y.; Cui, Q.; Morokuma, K.; Rega, N.; Salvador, P.; Dannenberg, J. J.; Malich, D. K.; Rabuck, A. D.; Raghavachari, K.; Foresman, J. B.; Cioslowski, J.; Ortiz, J. V.; Baboul, A. G.; Stetanov, B. B.; Liu, G.; Liashenko, A.; Piskorz, P.; Komaromi, I.; Gomperts, R.; Martin, R. L.; Fox, D. J.; Keith, T.; Al-Laham, M. A.; Peng, C. Y.; Nsnsyskkara, A.; Challacombe, M.; Gill, P. M. W.; Johnson, B.; Chen, W.; Wong, M. W.;

Andres, J. L.; Gonzalez, C.; Head-Gordon, M.; Replogle E. S.; Pople, J. A. GAUSSIAN09, Revision A.02, Gaussian Inc., Pittsburgh (2009).

31. Beeler, M. C.; Williams, R. A.; Jimenez-Garcia, K.; LeBlanc, L. J.; Perry, A. R.; Spielman, I. B. *Nature* **2013**, *498*, 201 – 204.

32. Nitta, J.; Akazaki, T.; Takayanagi, H.; Enoki, T.; *Phys. Rev. Lett.* **1997**, *78*, 1335.

33. Dresselhaus, G. *Phys. Rev.* **1955**, *100*, 580 – 586.

INDEX

<u>A</u>	
all-metal aromatic systems (AMAS)	6
antiaromatic	2
antiferromagnetic	20
aromatic	1
axial ZFS parameter	25
<u>B</u>	
bonding energy decomposition	36
broken Symmetry Approach	21
<u>C</u>	
charge transfer	48
coupled-perturbed spin orbit coupling (CP-SOC)	27
<u>D</u>	
delocalization index	19
density of states	54
diatropic ring current	18
<u>E</u>	
easy-axis anisotropy	68
easy-plane anisotropy	68
electric field	90
electron Localization Function	18
<u>F</u>	
ferrimagnetic	9
ferromagnetic	9
first hyperpolarizability	74
<u>H</u>	
Hall effect	96
HDvV Hamiltonian	20
hopping integral	58
<u>K</u>	
<i>k</i> point	53
<u>L</u>	
ligand effects	79
<u>M</u>	
magnetism	6
magnetic anisotropy	24
magnetic anisotropy energy (MAE)	93
magnetic exchange coupling constant (<i>J</i>)	20
metalloaromaticity	2
metallocene based donor-acceptor complexes (MBCTC)	48
multi-centre electron delocalization index	19
<u>N</u>	
Neese technique	26
NICS scan	18
non-Aufbau	55
nucleus independent chemical shifts (NICS)	17
<u>O</u>	
orbital reduction factor	71
orbital splitting	76
<u>P</u>	
parallel-plate capacitor	90
paratropic ring current	18
Pauli repulsion	36
Pederson-Khanna (PK) method	24
periodic boundary condition	59
<u>Q</u>	
quantum theory of atoms in molecules (QTAIM)	31
<u>R</u>	
rhombic ZFS parameter	25
<u>S</u>	
second-order NLO response	82
single molecule magnet	10
south pointer	7
spherical aromaticity	3
spin-flip DFT	23
spin-orbit coupling (SOC)	24
superexchange	61

<u>T</u>	
three-dimensional aromaticity	3
two-state approximation	56

Y	
Yamaguchi equation	56

Z	
zero-field splitting (ZFS)	67

REPRINTS OF PUBLISHED PAPERS
IN CONNECTION TO THIS THESIS

1. Concurrent loss of aromaticity and onset of superexchange in Mg_3Na_2 with an increasing Na – Mg_3 distance (2013) Paul, S.; **Goswami, T.**; Misra, A. and Chattaraj, P. K. *Theor. Chem. Acc.* 132, 1391-10. (**Chapter 3**)
2. Effect of Charge Transfer and Periodicity on the Magnetism of $[Cr(Cp^*)_2][ETCE]$ (2014) **Goswami, T.**; Paul, S. and Misra, A. *RSC Adv.* 4, 14847-14857. (**Chapter 4**)
3. Ligand Effects toward the Modulation of Magnetic Anisotropy and Design of Magnetic Systems with Desired Anisotropy Characteristics (2012) **Goswami, T.** and Misra, A. *J. Phys. Chem. A.* 116, 5207-5215. (**Chapter 5**)
4. On the Control of Magnetic Anisotropy through External Electric Field (2014) **Goswami, T.** and Misra, A. *Chem. Eur. J.* 20 13951-13956. (**Chapter 6**)

Concurrent loss of aromaticity and onset of superexchange in Mg_3Na_2 with an increasing Na–Mg₃ distance

Satadal Paul · Tamal Goswami · Anirban Misra ·
Pratim K. Chattaraj

Received: 6 May 2013 / Accepted: 8 August 2013
© Springer-Verlag Berlin Heidelberg 2013

Abstract Gradual migration of Na^+ from Mg_3^{2-} brings about fascinating change in aromatic and magnetic behavior of inorganic Mg_3Na_2 cluster, which is addressed at the B3LYP and QCISD levels. During this process, Na^+ takes away the electron density from Mg_3^{2-} causing a net decrease in aromaticity. A tug-of-war between the Pauli repulsion and the aromaticity is shown to be responsible for the observed stability and aromaticity trends in singlet and triplet states. Implications of a spin crossover vis-à-vis a possible superexchange are also explored.

Keywords Aromaticity · Magnetic exchange coupling · Mg_3^{2-} · Bond energy decomposition · Pauli repulsion · Superexchange

1 Introduction

Triggered by the pioneering concept of “all metal aromaticity” by Boldyrev et al. [1, 2], all-metal annular systems have received a keen attention in past decade. The exceptional nature of aromaticity in this class of molecules has led the researchers to go through several experimental and

theoretical studies of such all-metal aromatic systems [3–30]. These systems include XAl_3^- ($\text{X} = \text{Si}, \text{Ge}, \text{Sn}, \text{Pb}$) [3, 4], M_4^{2-} ($\text{M} = \text{Ga}, \text{In}, \text{Tl}, \text{Sb}, \text{Bi}$) [5–8], T_5^{6-} ($\text{T} = \text{Ge}, \text{Sn}, \text{Pb}$) [9, 10], M_4^{2+} ($\text{M} = \text{Se}, \text{Te}$) [11–15], M^{3-} ($\text{M} = \text{Al}, \text{Ga}$) [16–19], Al_6^{2-} [20], Hg_4 [5, 8], M_5^- ($\text{M} = \text{Sb}, \text{Bi}$) [24–26], Au_5Zn^+ [27], Cu_3^{3+} [28], Cu_4^{2-} [29], $[\text{Fe}(\text{X}_5)]^+$ ($\text{X} = \text{Sb}, \text{Bi}$) [30], and so on. *Ab initio* and density functional theory (DFT)-based methods have been exercised to explain the stability and reactivity of a wide range of all-metal aromatic and antiaromatic systems [31]. The dianionic annular systems containing main group metals have been perceived as stable building blocks for multi-decker sandwich complexes [32–36]. The feasibility of using anionic annular systems to sandwich the cationic metal was first theoretically examined by Mercero and Ugalde, who found the proposed molecule $[\text{Al}_4\text{TiAl}_4]^{2-}$ to have large binding energy comparable to conventional metallocenes [37]. Apart from the metal, the annular system N_4^{2-} is found to fulfill all the aromaticity criteria [38] and is also able to form stable sandwich complexes with transition metals [39]. Among the anionic annular systems, Be_3^{2-} , Mg_3^{2-} , and Ca_3^{2-} have been paid a special attention for their interesting nature of stability, reactivity, and aromaticity [40–43]. Such electron-surplus anions are unstable due to large inter-electronic repulsion [44–46] and hence require suitable counterions to attain necessary stability [47, 48]. In a recent work, Chakrabarty et al. [49] addressed the effect of Na^+ counterions on the bonding, stability, and aromaticity of Mg_3^{2-} in a neutral Mg_3Na_2 complex of D_{3h} symmetry, which can also be seen as an “inverted” sandwich compound with reference to the sandwich type clusters [37, 39]. Chakrabarty et al. [49] have shown that with the increasing separation of Na^+ ion from the Mg_3^{2-} triangular plane, the counterion is found to take away considerable amount of electron density from

Electronic supplementary material The online version of this article (doi:10.1007/s00214-013-1391-3) contains supplementary material, which is available to authorized users.

S. Paul · T. Goswami · A. Misra (✉)
Department of Chemistry, University of North Bengal,
Siliguri 734013, West Bengal, India
e-mail: anirbanmisra@yahoo.com

P. K. Chattaraj (✉)
Department of Chemistry and Center for Theoretical Studies,
Indian Institute of Technology, Kharagpur 721302, India
e-mail: pkc@chem.iitkgp.ernet.in

the planar dianion. Thus, the complex does not follow the common trend of ionic dissociation of inorganic salt and produces neutral Na and Mg₃ at large separation. Further, with an increase in separation of Na⁺ from Mg₃²⁻ plane, the trigonal dianion cluster Mg₃²⁻ also experiences a gradual loss in its well-known π -aromaticity [40–43, 47, 48]. All these interesting observations [49], arising from gradual separation of Na from Mg₃, prompted us to opt for the present theoretical investigation where the genesis of such observations in Mg₃Na₂ is thoroughly explored.

The molecule Mg₃Na₂ shows an interesting convergence in its singlet and triplet state at a 5 Å separation between the counterion Na⁺ and triangular anion Mg₃²⁻. This observation alludes toward the stabilization of the high-spin state at some particular distance between the Mg₃ plane and Na. Moreover, during migration, Na⁺ ion tends to pull away the loosely bound π -cloud of the trigonal Mg₃²⁻ ring [49], and they accumulate unpaired spin in neutral Na atoms at fairly large distance. Hence, at this critical Na–Mg₃ distance, spins on two doublet sodium atoms can interact through planar Mg₃ ring and superexchange mechanism is switched on. Through the superexchange of spins on doublet sodium atoms, the molecule can turn magnetic and gain significant stability even with wide-stretched axis joining Na and Mg₃. This possibility of magnetic phase transition in Mg₃Na₂ is the crux of present investigation. The extent of magnetic interaction is intimately related to the relative stability of the singlet and triplet states which may also vary with Mg₃–Na separation in the Mg₃Na₂ molecule. Thus, the change in the aromaticity may have some role in tuning the magnetic status of the molecule. In fact, an antagonistic relationship between aromaticity and magnetism has already been established in similar type of all-metal aromatic systems [50]. Hence, in the present work with continuous migration of Na⁺ ion from the Mg₃²⁻ plane, the possibility of appearance of magnetism due to onset of superexchange and its relation with the loss of aromaticity is put in focus. A part of the present results echoes and thus validates the fact in Ref. [49], and another segment of this work describes the interplay between magnetism and aromaticity in Mg₃Na₂.

2 Theoretical background and computational details

The aromaticity of the present system is measured in terms of the magnetic criterion of aromaticity. The hypothesis that magnetic shielding tensor on a test dipole at the center of a ring can be used to quantify its magnetic property was first proposed by Elser and Haddon [51], which eventually became popular as nucleus-independent chemical shift (NICS). Negative (Positive) shielding tensor values are taken to indicate the presence of a diatropic (paratropic)

ring current, and accordingly, the system is defined as aromatic (antiaromatic) [52]. However, the poor correlation between different measures has led the scientific community to debate about the proper characterization of aromaticity [53–57]. At this circumstance, the use of more than one aromaticity indices to describe the aromaticity in molecules occurs to be a logical suggestion [66]. Although NICS is the most widely used descriptor of aromaticity in inorganic systems, nowadays delocalization-based indices are found to perform well in describing the aromaticity of materials [58–62]. One of such indices is the delocalization index (DI), $\delta(A, B)$, based on quantum theory of atoms in molecules (QTAIM) methodology. This is estimated as the double integration of the exchange–correlation density over the atomic basins as defined by the QTAIM theory. This index gives a quantitative idea of the number of electrons delocalized between atoms A and B [60]. A larger DI value indicates more aromatic nature and corresponds to a more negative NICS [60]. Being based directly on electron delocalization, which is the essence of aromaticity, NICS and the DI can be regarded as the absolute measure of aromaticity in the sense of not requiring reference standards for its quantification. Another such DI is the multicenter index (MCI) based on the extended delocalized bonding which is considered to be a typical characteristic of aromaticity [63]. Following the suggestions of Giambiagi et al. [64], Bultinck et al. [63] formulated the MCI as

$$\begin{aligned} \text{MCI}_{\text{ABC...K}} &= \eta \sum_{\mu \in A} \sum_{\nu \in B} \cdots \sum_{\kappa \in K} \sum_i \Gamma_i \left[(\text{PS})_{\mu\nu} (\text{PS})_{\nu\rho} \cdots (\text{PS})_{\kappa\mu} \right] \end{aligned} \quad (1)$$

where P and S represent charge density bond order and overlap matrices, respectively, and η is a normalization constant. Γ_i is the permutation operator which runs over the μ, ν, \dots, κ basis to take into account all the terms of generalized population analysis.

In the preceding section, a link between aromaticity and magnetism is outlined, at a fairly large separation between Na and Mg₃. According to Ref. [40–43], the counterion Na⁺ moves away with the electron and eventually at a large distance becomes neutral. Na in the neutral state is expected to be in the doublet state which can undergo magnetic interaction with another doublet Na through diamagnetic Mg₃ ring. Hence, at some optimum distance, superexchange mechanism may be operative due to charge transfer from Mg₃ to Na. The second-order perturbation energy for such a charge transfer has been formulated by Anderson [65–67] as follows,

$$\Delta E = \frac{t_{ij}^2}{U} \left(\frac{1}{2} + 2\hat{S}_i \cdot \hat{S}_j \right). \quad (2)$$

here, t_{ij} is the hopping integral which carries an electron from site i to site j , U is the single ion repulsion energy, and \hat{S}_i and \hat{S}_j are the spin angular momentum operators on magnetic sites i and j . However, this t^2/U term is well-known in the Hubbard model and related to the coupling constant (J) of a spin exchange process [68, 69]. However, in a recent formalism, instead of direct estimation of this t^2/U term, the above expression is modified to estimate the coupling constant in terms of the second-order perturbation energy (ΔE) for charge transfer between sites and spin density on those centers (ρ_i and ρ_j) [70]. This model suits in the present context, since here the magnetic interaction sets in due to charge migration from Mg_3 to Na,

$$J_{\text{CT}} = \frac{2\Delta E}{1 + \rho_i \cdot \rho_j}. \quad (3)$$

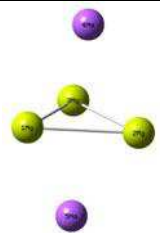
To study the system under investigation DFT as well as post Hartree–Fock level methods are used. In DFT, hybrid functional B3LYP, coupled with 6-311+g(d) basis set, is used in the unrestricted framework to optimize the structure. Besides, quadratic configuration interaction method QCISD is also employed with Dunning's correlation consistent basis set aug-cc-pVDZ for geometry optimization. The shielding tensors on the dummy atoms are reported as the NICS value. While computing NICS, the sign convention coined by Schleyer et al. [71] is followed. According to this convention, the signs of the computed values are reversed and negative (positive) sign is assigned for diamagnetic (paramagnetic) shielding. The choice of the gauge for the vector potential of the magnetic field is an important factor in the computation of shielding tensors. This well-known gauge problem had been resolved by adopting the gauge-independent atomic orbitals (GIAO) method [72–75], and the same method is followed in the present work to compute the shielding tensors. To find out the contributions of σ and π electrons to aromaticity, NICS has been calculated both at the center of the ring [NICS(0)] [71], and 1 Å above the plane [NICS(1)] [76, 77]. The second-order perturbation energies [ΔE in Eq. (3)] due to the charge transfer from Mg_3^{2-} to Na^+ are obtained from the natural bond orbital (NBO) output, carried out in the Gaussian NBO version 3.1 [78–81]. Bond energy decomposition is performed using *Amsterdam Density Functional* (ADF) software [82–84]. The DI, $\delta(\text{A}, \text{B})$ terms are computed by the Proaim and Promega first-order algorithms as implemented in the AIMAll suite of programs [85]. To validate the DFT result, the NICS values of the singlet Mg_3Na_2 is also computed in CCSD method using DALTON [86]. The MCI index is calculated by ESI-3D suit of program [87], which is popularly used for the calculation of electron sharing indices [88, 89]. Other calculations are performed using *Gaussian 09W* suite of quantum chemical package [90].

3 Results and discussion

The energy and geometry comparison of the system is reported in Table 1. It is interesting to observe that irrespective of the computational level, the system reserves its D_{3h} symmetry at its energy minima. It is also apparent from the Table 1 that the geometries in the singlet and triplet states only differ in the distance of Na^+ ion from the equatorial plane of Mg_3^{2-} , whereas the sides of Mg_3^{2-} triangle remains almost constant in both the spin states, irrespective of the methodology. Moreover, in both the methodologies, the triplet state of the molecule is found to have a longer separation between Na and Mg_3 compared to the singlet state. This dependence of spin state energies on the Na– Mg_3 separation is in agreement with the results in Refs. [40–43]. To further investigate the dependence of spin state energies on Na– Mg_3 separation, two Na^+ ions are allowed to move away by 0.25 Å from their ground state position along the axis lying perpendicular to the Mg_3^{2-} triangular plane till they reach a distance as large as ~14 Å (distance of Na is measured perpendicularly from the center of the Mg_3 ring).

It is interesting to note that in the DFT framework, the singlet state wave function with $\langle \hat{S}^2 \rangle = 0$ shows an internal instability at longer separation between Na and Mg_3 . For this reason, the wave function corresponding to all the singlet states is optimized which results in the nonzero value of $\langle \hat{S}^2 \rangle$ onward 3.7 Å distance between Na and Mg_3 [Table S1 in the supplementary information]. Moreover, the spin square value approaches toward unity with gradual stretching of Na– Mg_3 distance, indicating the attainment of open-shell singlet state [Table S1 in the supplementary information]. This observation is quite similar to that in the Ref. [91], which says that for a two-electron two-radical system, if the bonding orbitals are beyond the range of any kind of interaction, the unrestricted solution is produced with an equal mixture of singlet state ($S = 0$) and triplet state ($S = 1$). Noodleman et al. [92, 93] described such a spin state to be a broken symmetry (BS) state which is obtained by polarizing spins with antiparallel alignment at different magnetic sites within unrestricted formalism. The BS state, being a weighted average of high-spin and low-spin states [92, 93], is characterized by $\langle \hat{S}^2 \rangle = 1$. Hence, in the present case, the gradual separation of Na from Mg_3 plane causes the appearance of BS situation in Mg_3Na_2 . Next, the potential energy scan is executed on the optimized geometry of singlet state (with optimized wave function) with spin multiplicities one and three, which provides the information of vertical excitation energy. In another scan, optimized geometries of both the spin states are used at their respective spin multiplicities, and thus, the adiabatic excitation energy can be figured out.

Table 1 Energy and geometry comparison of the singlet and triplet states of Mg_3Na_2 , optimized at (a) UB3LYP/6-311+g(d) and (b) QCISD/aug-cc-pVDZ level of theories

System	Singlet		Triplet	
	Bond Length (Å)	Energy (a.u)	Bond Length (Å)	Energy (a.u)
	(a) Mg – Mg = 3.13 Mg 3 – Na = 2.75	(a) – 924.918	(a) Mg – Mg = 3.1 6 Mg 3 – Na = 3.19	(a) – 924. 877
	(b) Mg – Mg = 3.15 Mg 3 – Na = 2.84	(b) – 922.694	(b) Mg – Mg = 3.17 Mg 3 – Na = 3.16	(b) – 922.654

Interestingly, all the plots delineate that the singlet state is gradually destabilized with the increase in Na– Mg_3 distance and ultimately overlaps with the triplet energy profile (Fig. 1). However, the geometries and energies of the molecules in different spin states, the nature of the potential energy surface in Fig. 1, obtained in the computational levels UB3LYP/6-311+g(d) and QCISD/aug-cc-pVDZ, are all found to be similar and concordant to each other. Hence, following computations on Mg_3Na_2 (with optimized wave function) are carried out only at UB3LYP/6-311+g(d) level with its geometry optimized at QCISD/aug-cc-pVDZ level (if not specified otherwise).

The explanation of the above schematics can be attributed to the gradual charge neutralization of Na^+ and Mg_3^{2-} with their increasing separation as evident from Ref. [49] as well as from the change in the pattern of highest occupied molecular orbital (HOMO) of singlet ground state (Fig. 2). This is characterized by the delocalized electron density above and below the trigonal Mg_3 plane, which itself defines the nodal plane (Fig. 2a). The electron density gradually migrates toward Na from Mg_3 and ultimately resorts solely on Na.

Since the HOMO of the singlet state retains two excess π -bonding electrons, they experience a repulsion which significantly reduces at large Na– Mg_3 distance owing to the charge accumulation on the Na atoms above and below the plane. The repulsion between the bonding electrons is computed in terms of Pauli repulsion using ADF quantum chemical package [82–84]. In ADF, the interaction energy between different fragments is split into

$$\Delta E_{\text{bnd}} = \Delta E_{\text{Stat}} + \Delta E_{\text{Pauli}} + \Delta E_{\text{oi}} \quad (4)$$

The first term usually corresponds to the attractive potential [94, 95], whereas ΔE_{Pauli} is usually repulsive in nature. In ADF, ΔE_{Pauli} is equated as the energy change associated with going from superposition of fragment densities ($\rho_A + \rho_B$) to the wave function $\text{NA}|\psi_A\psi_B|$ that properly obeys the Pauli principle through explicit antisymmetrization (A) and renormalization (N) of the product of fragment wave functions [82]. ΔE_{oi} accounts for electron pair bonding, charge transfer, and polarization.

However, due to charge migration, the Mg_3 plane becomes completely devoid of any electron, and the system loses the bonding energy. This fact is apparent from the following plot (Fig. 3), where both the attractive potential and Pauli repulsion are found to decrease with an increase in the Na– Mg_3 distance. However, the stability gain by the system due to the decrease in Pauli repulsion energy cannot overcome the loss of attractive potential, resulting in a net decrease in binding energy.

Next, to investigate the variation of aromaticity with increasing separation of Na from Mg_3 plane, NICS(0) and NICS(1) are scanned by varying the distance, at both the spin states of the system with its optimized geometry at the singlet state (Fig. 4a). At the singlet ground state, large negative values of both NICS(0) and NICS(1) refer to the coexistence of σ - and π -aromaticity, rendering Mg_3Na_2 to be multiply aromatic. Existence of π -electron cloud above and below the Mg_3 plane in the HOMO can well explain π -aromaticity, whereas the maximum diamagnetic contribution toward the total NICS(0) value comes from the 26th MO (Fig. 4b) of the system. As graphically represented in Fig. 4b, this MO can evidently be narrated to be composed solely of Mg 's' atomic orbitals. The contribution of individual MOs toward the total NICS(0) value is computed in the ADF computational package. Contrary to the singlet state, low negative values of NICS(0) and NICS(1) are obtained near the ground state geometry of Mg_3Na_2 in its triplet state indicating lower degree of aromaticity than in the singlet state. This reduced aromaticity in the triplet state is due to the presence of unpaired spin in Na atoms which exalts the paratropic shielding tensor compared to its diatropic analog resulting in low aromaticity [50]. To further verify the variation of aromaticity, the average of DI among Mg atoms and the MCI values in the singlet state are also plotted against the increasing Na– Mg_3 separation (Fig. 4c). A decaying nature of the average DI and MCI confirms the trend in the change of NICS. In addition to the DFT, ab initio method such as CCSD is also adopted to compute NICS. The plot shows the same trend of decreasing negativity of NICS particularly after spin density grows on Na atoms (Fig. S1 in supplementary

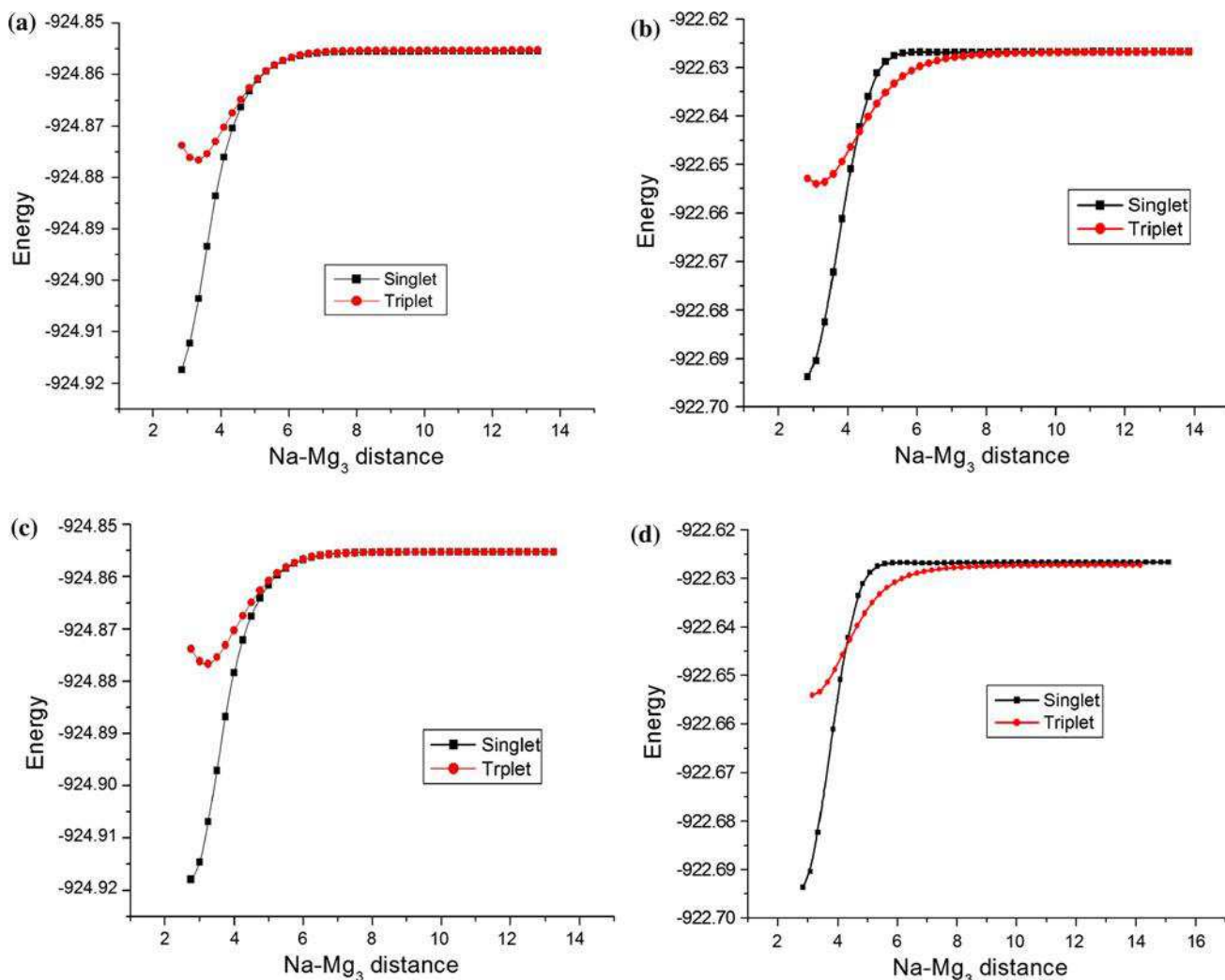


Fig. 1 Energy (a.u.) profile of Mg_3Na_2 with increasing Na– Mg_3 distance (Å) on the **a** geometry of singlet state optimized at UB3LYP/6-311+g(d) level, **b** geometry of singlet state optimized at QCISD/aug-cc-pvdz level, **c** geometry of singlet and triplet states, both

optimized at UB3LYP/6-311+g(d) level, and **d** geometry of singlet and triplet states, both optimized at QCISD/aug-cc-pvdz level of theory

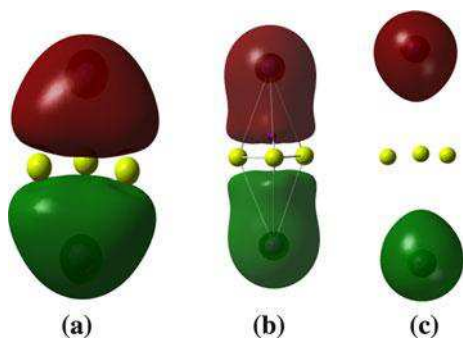


Fig. 2 Schematics of the HOMO generated at **a** optimized geometry, **b** Na– Mg_3 distance of 4.08 Å where the singlet energy approaches close to the triplet energy, and **c** Na– Mg_3 distance of 5.58 Å

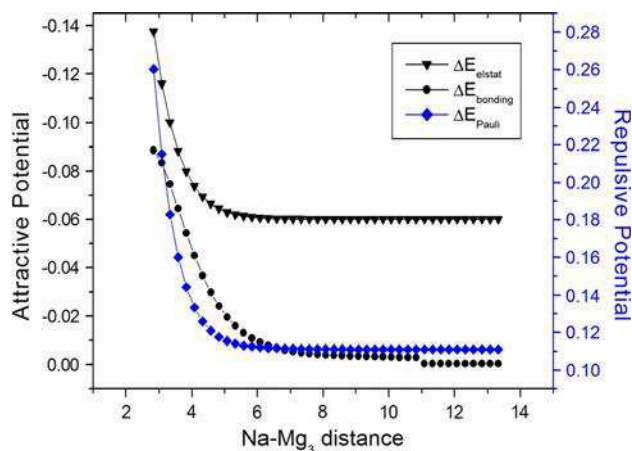


Fig. 3 Bonding energy decomposition analysis in the singlet state of the molecule

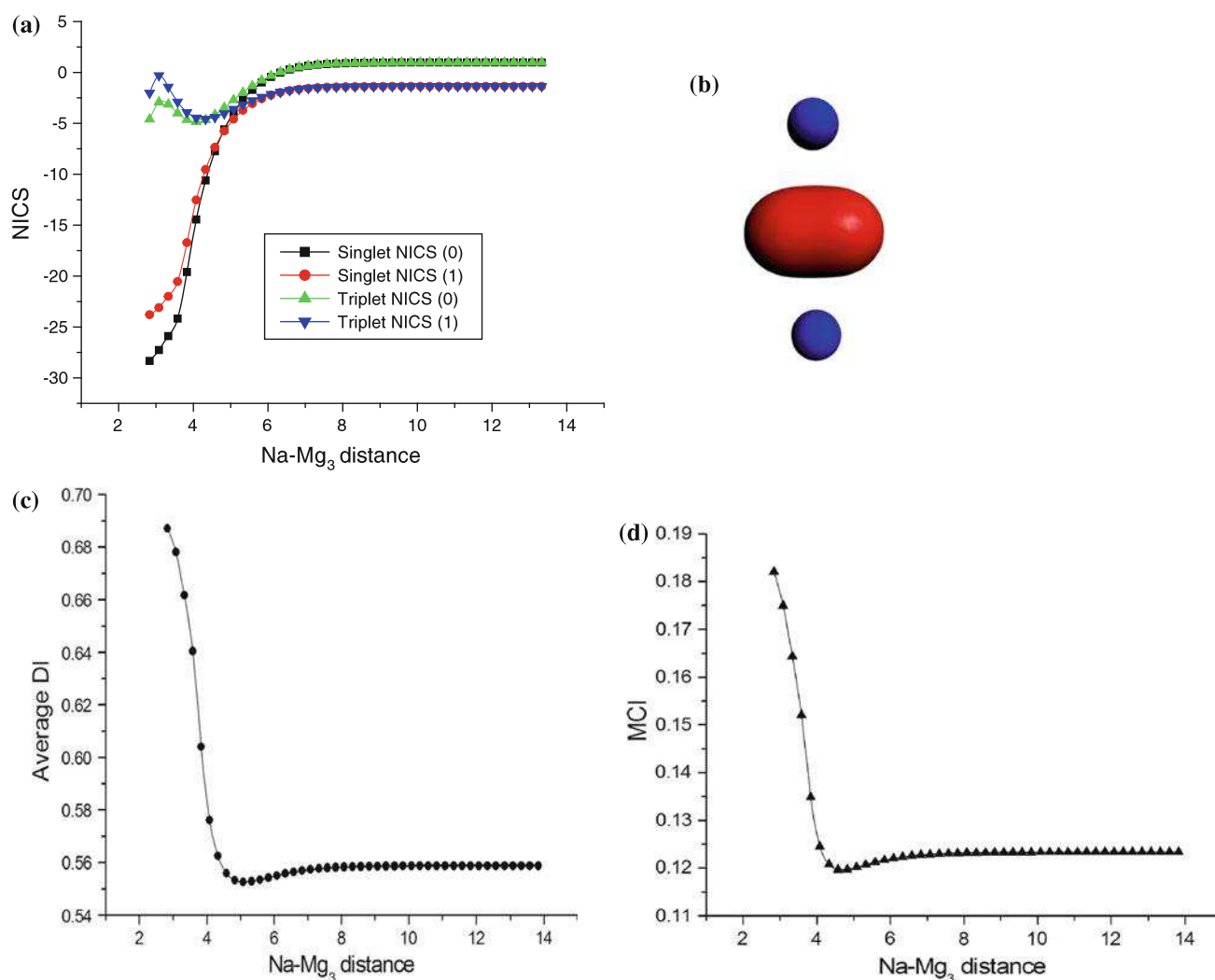


Fig. 4 Plot of **a** NICS(0) and NICS(1) in the singlet and triplet state of Na₂Mg₃ at DFT level. **b** The 26th MO contributing maximum toward the diamagnetic NICS(0). **c** The average DI and **d** MCI index of aromaticity for the singlet state as a function of increasing Na–Mg₃ distance (Å)

information) and hence once again solicits gradual loss of aromaticity with increasing Na–Mg₃ separation. However, with an increase in vertical distance of Na from the center of Mg₃ plane, the aromaticity in both the spin states decays almost to a null value, which is quite obvious, since Na atoms take away all the charge density which has been maintaining the ring current. Since two apical Na atoms are pulled apart which leave behind the Mg₃ moiety in the neutral state, the effect of dispersion can be argued to play a significant role in such scenario [96]. Hence, a verification of the effect of dispersion interaction in aromaticity of the singlet Mg₃Na₂ is performed at the DFT level with dispersion correction due to Grimme [97, 98]. From Figure S2 in supplementary information, it is apparent that the effect of dispersion on the NICS values is negligible which is also obvious from the literature [99–101]. However, the dispersion may have effects on the energy of the molecule, and hence, the energy profiles of the system are compared

with and without dispersion correction. The variation in energy with increase in Na–Mg₃ distance appears similar with and without the dispersion correction (Figure S3 in supplementary information).

Since, with an increase in Na–Mg₃ distance, Na move away with the pair of electrons responsible for maintaining the aromaticity, the system loses the aromatic stabilization energy though gains stability due to reduction in the Pauli repulsion, particularly in the singlet state. The loss of aromaticity with increasing Na–Mg₃ distance is formulated as

$$\delta_{\text{NICS}}(r) = \text{NICS}(r - \Delta r) - \text{NICS}(r) \quad (5)$$

where Δr is fixed at 0.25 Å in the present work. The plot of Pauli repulsion energy (ΔE_{Pauli}) and the loss of aromaticity with increasing separation between Na and Mg₃ are depicted in Fig. 5, which clarifies that as in one hand, a minimization of Pauli repulsion energy tends to stabilize

the system and on the other hand, loss of aromaticity acts as an instability factor. It is further interesting to note that the maximum loss of aromaticity occurs near to the critical value of Na–Mg₃ distance (4.33 Å) where the singlet and triplet state energies are converged (Figs. 1b, d, 5). It is also noted here that the spin-crossover region corresponds to the zone of maximum change in the MCI and DI indices, which can be found from the derivative plots of the average DI and the MCI indices (Figure S4 of the supplementary information). This observation advocates the fact that such spin-crossover occurs at the cost of the loss of delocalization which corroborates to aromaticity. This suggests that the appearance of BS state and consequent spin accumulation on the Na atoms at that point plays a definite role in reducing the aromaticity of the system. The localization of those two extra charges, which maintain the aromaticity, on the Na⁺ ions causes cessation in circulation of those electrons and explains the maximum loss of aromaticity as well the minimal ΔE_{Pauli} continuum after that point.

Since, with the gradual increase in the Na–Mg₃ separation, a charge transfer is occurred from Mg₃ to apical Na atoms, decrease in charge density in the Mg₃ plane causes weak bonding interaction (Fig. 3). In this situation, the stability of the molecule can partly be compensated through the energy minimization due to charge migration from Mg₃ moiety to Na. The stability gained by such charge migration was given by Anderson in the framework of second-order perturbation theory and was equated with the energy of superexchange [65–67]. In the present case also, the superexchange becomes possible between the spins accumulated on Na atoms as a consequence of charge transfer and gradual neutralization of Na⁺. The fact of gradual spin accumulation on Na with increase in Na–Mg₃ separation can be ascertained from the spin density plot in the Fig. 6.

The value of coupling constant associated with the superexchange process can now be estimated through Eq. (3). From the variation in MO with increase in Na–Mg₃ (Fig. 2), it becomes evident that the charge migration involves the out-of-plane *p* orbitals of all the three Mg atoms and *s* orbitals of the Na atoms particularly for low Na–Mg₃ distance. Thus, during NBO analysis, the out-of-plane *p* orbitals in Mg₃ plane and *s* orbitals in Na are only considered as the donor and acceptor orbitals for obtaining the appropriate value of second-order perturbation energy (ΔE) due to charge migration. To clarify this choice of relevant orbitals, a truncated part of the NBO output corresponding to the Na–Mg₃ distance of 5.08 Å, showing the donor and acceptor orbitals, and their composition are given in Table S2 in the supplementary information as an example. From the plots in Fig. 1 and the Table S1 in supplementary, it appears that significant amount of spin

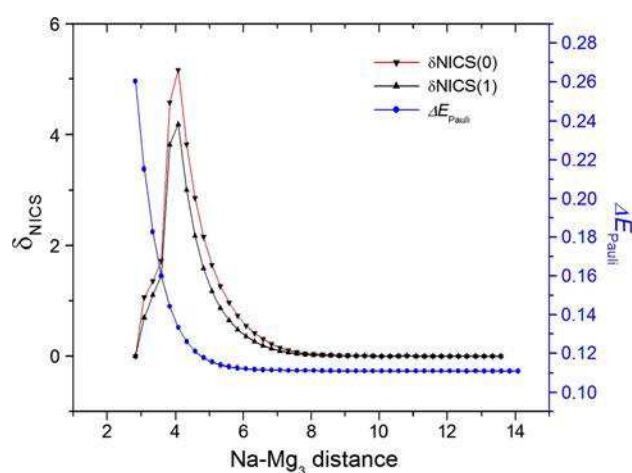


Fig. 5 Plot of Pauli repulsion energy (ΔE_{Pauli}) and $\delta_{\text{NICS}(0)}(r)$ and $\delta_{\text{NICS}(1)}(r)$ with increasing Na–Mg₃ distance (Å) in the singlet state of Na₂Mg₃

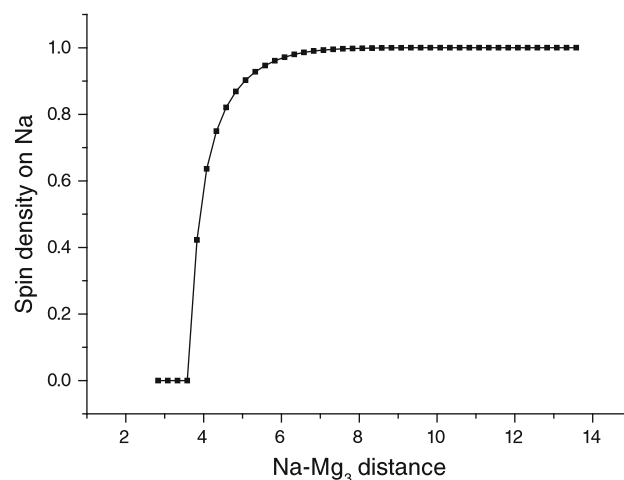
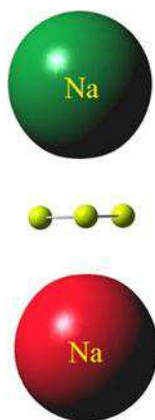


Fig. 6 Plot of spin density on Na and Mg₃ in the ground state with increasing Na–Mg₃ distance (Å)

density starts to grow on the Na atoms from the Na–Mg₃ distance of 4.08 Å. This open-shell singlet state is found to be more stable than the corresponding triplet state by a considerable amount up to ~6 Å distance between Na and Mg₃, beyond which the singlet–triplet energy gap almost vanishes. Thus, the superexchange energies (ΔE) are obtained from the NBO analysis of singlet state of Mg₃Na₂ with Na–Mg₃ separation in the range of 4.08–6.08 Å. While using this ΔE value in the estimation of coupling constant, the right-hand side of Eq. (3) is multiplied by 2 since there are two such transitions from Mg₃ to first and second Na atoms. Moreover, these transitions leave almost zero spin density in Mg₃ plane, and thus, the denominator in the right-hand side of Eq. (3) takes the value of one with which Eq. (3) transforms into,

Table 2 ΔE and calculated J value on the basis of Eq. (6)

Na–Mg ₃ distance (Å)	ΔE (kcal/mol)	J (cm ⁻¹)
4.08	-0.69	-966
4.58	-0.51	-714
5.08	-0.12	-168
5.58	-0.07	-98
6.08	-0.04	-56

Fig. 7 Spin density plot at a Na–Mg₃ separation onward 3.83 Å (green and red color denote up-spin and down-spin density)

$$J = 4\Delta E \quad (6)$$

which is ultimately used in this work to estimate the exchange coupling constant associated with superexchange. Moreover, no contribution from the Na–Na direct exchange is taken into account due to their large separation. The interaction between two spins on Na atoms expectedly decreases with an increase in separation between Mg₃ and Na, and can be understood from Table 2. The negative value of coupling constant indicates the antiferromagnetic interaction which is also attested by the spin density plot showing up-spin and down-spin on different Na atoms (Fig. 7).

4 Conclusions

Present study explains the change in the aromaticity and energy profile of the singlet state of Mg₃Na₂ molecule and gradual attainment of the BS state with an increase in Na–Mg₃ distance. Near the ground state, Mg atoms are held together by a pair of π -bonding electrons onto which Na⁺ ions are impregnated. The circulation of π -electron cloud above and below the Mg₃ plane also contributes to the σ - and π -aromaticity of the molecule. However, in this situation, the stability due to aromaticity has to compete with the Pauli repulsion. When the Na ions move away from Mg₃ plane with all the charge density, the aromaticity

is also gradually lost, though the system gets stability due to decrease in Pauli repulsion. At a critical value (~4.33 Å) of Na–Mg₃ distance, the Pauli repulsion approaches a minimum due to localization of charge density on Na atoms above and below the plane. This charge accumulation on Na atoms makes these neutral doublet species with up-spin polarization at one Na and down-spin at another. The spins on Na atoms undergo superexchange which is quantified through Eq. (6). The stabilization due to superexchange and lowering of Pauli repulsion partly compensates the loss in bonding energy in the molecule for the charge migration to Na atoms. The Na spins are found to be engaged in antiferromagnetic interaction which gradually decreases with an increase in Na–Mg₃ separation.

Acknowledgments We sincerely thank the Department of Science and Technology, India, for financial support. TG thanks CSIR for Senior Research Fellowship. PKC would like to thank DST, New Delhi, for the J. C. Bose National Fellowship. Tamal Sarkar of University Science and Instrumentation Center, University of North Bengal, is gratefully acknowledged for technical support. The authors also thank Eduard Matito, Institute of Computational Chemistry, University of Girona, for his generous help regarding the calculation of MCI index.

References

- Li X, Kuznetsov AE, Zhang H-F, Boldyrev AI, Wang L-S (2001) *Science* 291:859
- Kuznetsov AE, Birch KA, Boldyrev AI, Li X, Zhai H-J, Wang L-S (2003) *Science* 300:622
- Li X, Zhang HF, Wang LS, Kuznetsov AE, Cannon NA, Boldyrev AI (1867) *Angew Chem Int Ed* 40:1867
- Kuznetsov AE, Boldyrev AI, Li X, Wang LS (2001) *J Am Chem Soc* 123:8825
- Twamley B, Power PP (2000) *Angew Chem Int Ed* 39:3500
- Cisar A, Corbett JD (1977) *Inorg Chem* 16:2482
- Critchlow SC, Corbett JD (1984) *Inorg Chem* 23:770
- Tuononen HM, Suontamo R, Valkonen J, Laitinen RS (2004) *J Phys Chem A* 108:5670
- Todorov I, Sevov SC (2004) *Inorg Chem* 43:6490
- Todorov I, Sevov SC (2005) *Inorg Chem* 44:5361
- Gillespie RJ, Barr J, Kapoor R, Malhotra KC (1968) *Can J Chem* 46:149
- Gillespie RJ, Barr J, Crump DB, Kapoor R, Ummat PK (1968) *Can J Chem* 46:3607
- Barr J, Gillespie RJ, Kapoor R, Pez GP (6855) *J Am Chem Soc* 90:6855
- Couch TW, Lokken DA, Corbett JD (1972) *Inorg Chem* 11:357
- Burford N, Passmore J, Sanders JCP (1989) In: Liebman JF, Greenburg A (eds) *From atoms to polymers. Isoelectronic analogies*. VCH, New York, p 53
- Li X, Wang XB, Wang LS (1998) *Phys Rev Lett* 81:1909
- Wu H, Li X, Wang XB, Ding CF, Wang LS (1998) *J Chem Phys* 109:449
- Baeck KK, Bartlett RJ (1998) *J Chem Phys* 109:1334
- Kuznetsov AE, Boldyrev AI (2002) *Struct Chem* 13:141
- Kuznetsov AE, Boldyrev AI, Zhai HJ, Li X, Wang LS (2002) *J Am Chem Soc* 124:11791

21. Nielsen JW, Baenziger NC (1954) *Acta Crystallogr* 7:277
22. Corbett JD (1969) *Inorg Nucl Chem Lett* 5:81
23. Kuznetsov AE, Corbett JD, Wang LS, Boldyrev AI (2001) *Angew Chem Int Ed* 40:3369
24. Gausa M, Kaschner R, Lutz HO, Seifert G, Meiwes-Broer K-H (1994) *Chem Phys Lett* 230:99
25. Gausa M, Kaschner R, Seifert G, Faehrmann JH, Lutz HO, Meiwes KHB (1996) *J Chem Phys* 104:9719
26. Zhai HJ, Wang LS, Kuznetsov AE, Boldyrev AI (2002) *J Phys Chem A* 106:5600
27. Tanaka H, Neukermans S, Janssens E, Silverans RE, Lievens P (2003) *J Am Chem Soc* 125:2862
28. Alexandrova AN, Boldyrev AI, Zhai HI, Wang LS (2005) *J Phys Chem A* 109:562
29. Wannere CS, Corminboeuf C, Wang ZX, Wodrich MD, King RB, Schleyer PvR (2005) *J Am Chem Soc* 127:5701
30. Lein M, Frunzke J, Frenking G (2003) *Angew Chem Int Ed* 42:1303
31. Chattaraj PK, Roy DR, Elango M, Subramanian V (2005) *J Phys Chem A* 109:9590
32. Chattaraj PK, Giri S (2008) *J Mol Struct (Theochem)* 865:53
33. Chattaraj PK, Roy DR, Duley S (2008) *Chem Phys Lett* 460:382
34. Roy DR, Duley S, Chattaraj PK (2008) *Proc Indian Natl Sci Acad Part-A* 74:11
35. Chattaraj PK, Giri S (2009) *Int J Quantum Chem* 109:2373
36. Chakrabarty A, Giri S, Chattaraj PK (2009) *J Mol Struct (Theochem)* 913:70
37. Mercero JM, Ugalde JM (2004) *J Am Chem Soc* 126:3380
38. Van Zandwijk G, Janssen RAJ, Buck HM (1990) *J Am Chem Soc* 112:4155
39. Mercero JM, Matxain JM, Ugalde JM (2004) *Angew Chem Int Ed* 43:5485
40. Giri S, Roy DR, Duley S, Chakrabarty A, Parathasarathi R, Elango M, Vijayraj R, Subramanian V, Islas R, Merino G, Chattaraj PK (2010) *J Comput Chem* 31:1815
41. Kuznetsov AE, Boldyrev AI (2004) *Chem Phys Lett* 388:452
42. Roy DR, Chattaraj PK (2008) *J Phys Chem A* 112:1612
43. Oscar J, Jimenez-Halla C, Matito E, Blancafort L, Robles J, Sola M (2009) *J Comput Chem* 30:2764
44. Boldyrev AI, Gutowski M, Simons J (1996) *Acc Chem Res* 29:497
45. Boldyrev AI, Simons J (1994) *J Phys Chem* 98:2298
46. Janoschek RZ (1992) *Z Anorg Allg Chem* 616:101
47. Wang XB, Ding CF, Nicholas JB, Dixon DA, Wang LS (1999) *J Phys Chem A* 103:3423
48. Wang XB, Nicholas JB, Wang LS (2000) *J Chem Phys* 113:10837
49. Chakrabarty A, Giri S, Duley S, Anoop A, Bultinck P, Chattaraj PK (2011) *Phys Chem Chem Phys* 13:14865
50. Paul S, Misra A (2011) *Inorg Chem* 50:3234
51. Elser V, Haddon RC (1987) *Nature (London)* 325:792
52. Lazzeretti P (2004) *Phys Chem Chem Phys* 6:217
53. Cyrański M, Krygowski TM, Katritzky AR, Schleyer PvR (2002) *J Org Chem* 67:1333
54. Poater J, GarcFa-Cruz I, Illas F, SolV M (2004) *Phys Chem Chem Phys* 6:314
55. Katritzky AR, Jug K, Oniciu DC (2001) *Chem Rev* 101:1421
56. Krygowski TM, Cyranfski MK (2001) *Chem Rev* 101:1385
57. Katritzky AR, Karelson M, Sild S, Krygowski TM, Jug KJ (1998) *Org Chem* 63:5228
58. Fias S, Fowler PW, Delgado JL, Hahn U, Bultinck P (2008) *Chem Eur J* 14:3093
59. Ghiasi R, Pasdar H (2012) *J Mex Chem Soc* 56:426
60. Poater J, Fradera X, Duran M, Sola M (2003) *Chem Eur J* 9:400
61. Mandado M, González-Moa MJ, Mosquera RA (2007) *J Comput Chem* 28:127
62. Foroutan-Nejad C (2012) *Phys Chem Chem Phys* 14:9738
63. Bultinck P, Rafat M, Ponere R, Gheluwe BV, Carbo-Dorca R, Popelier P (2006) *J Phys Chem A* 110:7642
64. Giambiagi M, de Giambiagi MS, dos Santos Silva CD, Paivade Figueiredo A (2000) *Phys Chem Chem Phys* 2:3381
65. Anderson PW (1950) *Phys Rev* 79:350
66. Anderson PW (1959) *Phys Rev* 115:2
67. Anderson PW (1963) In: Seitz F, Turnbull D (eds) *Solid state physics*, vol 14. Academic Press Inc., New York, p 99
68. Munoz D, Illas F, de Moreira IPR (2000) *Phys Rev Lett* 84:1579
69. Caballol R, Castell O, Illas F, de Moreira IPR, Malrieu JP (1997) *J Phys Chem A* 101:7860
70. Paul S, Misra A (2012) *J Chem Theory Comput* 8:843
71. Schleyer PvR, Maerker C, Dransfeld A, Jiao H, Hommes NJRVE (1996) *J Am Chem Soc* 118:6317
72. Ditchfield R (1974) *Mol Phys* 27:789
73. Fukui H (1987) *Magn Res Rev* 11:205
74. Freidrich K, Seifert G, Grossmann G (1990) *Z Phys D* 17:45
75. Malkin VG, Malkina OL, Erikson LA, Salahub DR (1995) In: Politzer P, Seminario JM (eds) *Modern density functional theory: a tool for chemistry*, vol 2. Elsevier, Amsterdam
76. Schleyer PvR, Jiao H, Hommes NJRVE, Malkin VG, Malkina O (1997) *J Am Chem Soc* 119:12669
77. Schleyer PvR, Manoharan M, Wang ZX, Kiran B, Jiao H, Pachta R, Hommes NJRVE (2001) *Org Lett* 3:2465
78. Foster JP, Weinhold F (1980) *J Am Chem Soc* 102:7211
79. Carpenter JE (1987) *Extension of Lewis structure concepts to open shell and excited state molecular species*. Ph. D. Thesis, University of Wisconsin, Madison
80. Reed AE, Curtiss LA, Weinhold F (1988) *Chem Rev* 88:899
81. Weinhold F, Carpenter JE (1988) In: Naaman R, Vager Z (eds) *The structure of small molecules and ions*. Plenum, New York, p 227
82. te Velde G, Bickelhaupt FM, van Gisbergen SJA, Guerra CF, Baerends EJ, Snijders JG, Ziegler T (2001) *J Comput Chem* 22:931
83. Guerra CF, Snijders JG, te Velde G, Baerends EJ (1998) *Theor Chem Acc* 99:391
84. ADF (2012) *SCM, theoretical chemistry*. Vrije Universiteit, Amsterdam, The Netherlands, <http://www.scm.com>
85. AIMAll (version 13.05.06), Keith TA (2011) <http://aim.tkgristmill.com>
86. Angeli C, Bak KL, Bakken V, Christiansen O, Cimiraglia R, Coriani S, Dahle P, Dalskov EK, Enevoldsen T, Fernandez B, Ferrighi L, Frediani L, Hattig C, Hald K, Halkier A, Heiberg H, Helgaker T, Hettema H, Jansik B, Jensen HJA, Jonsson D, Jørgensen P, Kirpekar S, Klopper W, Knecht S, Kobayashi R, Kongsted J, Koch H, Ligabue A, Lutnaes OB, Mikkelsen KV, Nielsen CB, Norman P, Olsen J, Osted A, Packer MJ, Pedersen TB, Rinkevicius Z, Rudberg E, Ruden TA, Ruud K, Salek P, Samson CCM, Sanchez de Meras A, Saue T, Sauer SPA, Schimmelpfennig B, Steindal AH, Sylvester-Hvid KO, Taylor PR, Vahtras O, Wilson DJ, Ågren H, Dalton et al. (2011) a molecular electronic structure program, Release Dalton 2011 see <http://daltonprogram.org>
87. Matito E (2006) *ESI-3D: electron sharing indices program for 3D molecular space partitioning*. Institute of Computational chemistry and Catalysis (IQCC), University of Girona, Catalonia, Spain, <http://iqc.udg.es/~eduard/ESI>
88. Matito E, Duran M, Solà M (2005) *J Chem Phys* 122:014109
89. Matito E, Solà M, Salvador P, Duran M (2007) *Faraday Discuss* 135:325
90. Frisch MJ, Trucks GW, Schlegel HB, Scuseria GE, Robb MA, Cheeseman JR, Scalmani G, Barone V, Mennucci B, Petersson GA, Nakatsuji H, Caricato M, Li X, Hratchian HP, Izmaylov AF, Bloino J, Zheng G, Sonnenberg JL, Hada M, Ehara M,

- Toyota K, Fukuda R, Hasegawa R, Ishida M, Nakajima T, Honda Y, Kitao O, Nakai H, Vreven T, Jr. Montgomery JA, Peralta JE, Ogliaro F, Bearpark M, Heyd JJ, Brothers E, Kudin KN, Staroverov VN, Kobayashi R, Normand J, Raghavachari K, Rendell A, Burant JC, Iyengar SS, Tomasi J, Cossi M, Rega N, Millam NJ, Klene M, Knox JE, Cross JB, Bakken V, Adamo C, Jaramillo J, Gomperts R, Stratmann RE, Yazyev O, Austin AJ, Cammi R, Pomelli C, Ochterski JW, Martin RL, Morokuma K, Zakrzewski VG, Voth GA, Salvador P, Dannenberg JJ, Dapprich S, Daniels AD, Farkas Ö, Foresman JB, Ortiz JV, Cioslowski J, Fox DJ et al. (2009) Gaussian 09, Revision A.1, Gaussian Inc., Wallingford CT
91. Chen W, Schelgel HB (1994) *J Chem Phys* 101:5957
92. Noodleman L (1981) *J Chem Phys* 74:5737
93. Noodleman L, Case DA (1992) *Adv Inorg Chem* 38:423
94. Bickelhaupt FM, Baerends EJ (2000) In: Lipkowitz KB, Boyd DB (eds) *Reviews of computational chemistry*, vol 15. Wiley-VCH, New York, p 1
95. Baerends EJ (1992) In: Pacchioni G, Bagus PS (eds) *Cluster models for surface and bulk phenomena*, Nato ASI series B, vol 283. Plenum Press, New York, p 189
96. Chattaraj PK (ed) (2011) In: *Aromaticity and metal clusters*. CRC, New York
97. Grimme S (2004) *J Comput Chem* 25:1463
98. Grimme S (2006) *J Comput Chem* 27:1787
99. Ochsenfeld C, Koziol F, Brown SP, Schaller T, Seelbach UP, Klärner F-G (2002) *Solid State Nucl Magn Reson* 22:128
100. Ochsenfeld C (2000) *Phys Chem Chem Phys* 2:2153
101. Ochsenfeld C, Brown SP, Schnell I, Gauss J, Spiess HW (2001) *J Am Chem Soc* 123:2597

Effect of charge transfer and periodicity on the magnetism of $[\text{Cr}(\text{Cp}^*)_2][\text{ETCE}]^\dagger$

 Cite this: *RSC Adv.*, 2014, 4, 14847

Tamal Goswami, Satadal Paul and Anirban Misra*

Magnetism in metallocene based donor–acceptor complexes stems from the donor to acceptor charge transfer. Thus, to correlate the exchange coupling constant J and the charge transfer integral, a formalism is developed which enables one to obtain the coupling constant from the value of the charge transfer integral and the spin topology of the system. The variance in the magnetic interaction between donor and acceptor is also investigated along two perpendicular directions in the three dimensional crystal structure of the reference system, decamethylchromocenium ethyl tricyanoethylenecarboxylate $[\text{Cr}(\text{Cp}^*)_2][\text{ETCE}]$. These donor–acceptor pairs (V-pair and H-pair), oriented along vertical and horizontal directions respectively, are found to have different extents of J , which is attributed to the difference in exchange coupling mechanisms, viz., direct exchange and superexchange. Next, V-pair and H-pair are taken together to treat both the intrachain and interchain magnetic interactions, since this competition is necessary to decipher the overall magnetic ordering in the bulk phase. In fact, this truncated model produces a small positive value of J supporting the weak ferromagnetic nature of the complex. Lastly, a periodic condition is imposed on the system to comprehend the nature of magnetism in the extended system. Interestingly, the ferromagnetism, prevailing in the aperiodic system, turns into weak antiferromagnetism in the periodic environment. This is explained through the comparison of density of states (DOS) plots in aperiodic and periodic systems. This DOS analysis reveals proximity of the donor and acceptor orbitals, facilitating their mixing in periodic conditions. This mixing causes the antiferromagnetic interaction to prevail over the ferromagnetic one, and imparts an overall antiferromagnetic nature in periodic conditions. This change over in magnetic nature with the imposition of periodicity may be useful to understand the dependence of magnetic behavior with dimensionality in extended systems.

 Received 6th December 2013
Accepted 10th March 2014

DOI: 10.1039/c3ra47360k

www.rsc.org/advances

1. Introduction

The synthesis and characterization of charge transfer (CT) ferromagnetic compound $[\text{Fe}(\text{Cp}^*)_2][\text{TCNE}]$ ($\text{Cp}^* = \eta^5\text{-C}_5\text{Me}_5$ and TCNE = tetracyanoethylene) by Miller *et al.* in 1985 was a breakthrough in the field of metallocene-based magnets.¹ This was the first reported complex where the unpaired electron of a p-orbital also participates in the exchange interaction along with metal d-electrons. Nanoscale charge transfer is also known to have widespread application in sensors, photonics, electrocatalysis, solar photoconversion, molecular electronics and so on.² The occurrence of charge transfer in organoligand–metal fragments is found to induce a high dielectric polarization and concomitant intense nonlinear optical (NLO) response.³ Long spin coherence time in such materials renders them as potential candidates for high-density information storage and also for

quantum computing.⁴ Their applicability can further be proliferated by simply tuning their magnetic interaction through simple adjustment of organic fragments therein. All these facts tantalize the scientific community to explore a plethora of such metallocene based charge transfer complexes (MBCTCs).^{5–7} In these compounds such as $[\text{M}(\text{Cp}^*)_2][\text{TCNE}]$ ($\text{M} = \text{Cr}, \text{Mn}$ or Fe); $[\text{M}(\text{Cp}^*)_2]$ fragment donates one electron from the magnetic orbital of the metal to the initially diamagnetic $[\text{TCNE}]$ part. This leads to ferromagnetic interaction among the localized spins on the donor part (D^+) and the acceptor part (A^-).⁷ Divergent mechanisms have been proposed for the spin exchange in these CT salts. One such proposition is the McConnell-II mechanism where the stability of a particular spin state is attributed to the interaction of ground spin state and lowest excited state of same spin multiplicity.⁸ Miller *et al.* supported this mechanism assuming a forward charge transfer from the donor to the acceptor leading to the triplet excited state.^{7b} In $[\text{Fe}(\text{Cp}^*)_2]^+[\text{TCNE}]^-$, the triplet ground state becomes stabilized through its interaction with the lowest lying triplet excited state.^{8c} However, in case of $[\text{Mn}(\text{Cp}^*)_2]^+[\text{TCNE}]^-$ and $[\text{Cr}(\text{Cp}^*)_2]^+[\text{TCNE}]^-$, the interaction between the ground and

Department of Chemistry, University of North Bengal, Siliguri 734013, West Bengal, India. E-mail: anirbanmisra@yahoo.com

† Electronic supplementary information (ESI) available. See DOI: 10.1039/c3ra47360k

excited states leads to the stabilization of the antiferromagnetic situation which is in opposition to the experimentally reported high spin state of the molecules. Hence, the McConnell-II mechanism based explanation appears insufficient to justify this observation.^{7b,c,9} To explain this anomaly, Kollmar and Kahn coined a new mechanism of back charge transfer from A^- to D^+ , which is justified by the presence of positive spin density on Cp^* ring.^{9b} Another proposition is McConnell-I mechanism,¹⁰ where a large positive spin density on the transition metal induces a negative spin density on Cp^* ring, which again induces a positive spin density on the acceptor. These conflicting mechanisms about the origin of magnetic nature in MBCTCs urge for the development of a complete theoretical model.^{7b}

To investigate the charge transfer induced magnetic interaction in the MBCTCs, the compound decamethylchromocenium ethyl tricyanoethylenecarboxylate $[Cr(Cp^*)_2][ETCE]$ is taken as the representative system in the present work. This complex is recently synthesized by Wang *et al.* and found to have a ferrimagnetic ordering.¹¹ This ferrimagnetism may arise from the competition of ferro- and antiferromagnetic interactions in three different lattice dimensions as interestingly probed by Datta and Misra.¹² The $[Cr(Cp^*)_2][ETCE]$ is known to crystallize in orthorhombic geometry with parallel arrangement of vertical one dimensional D^+A^- chains. These one dimensional chains in a crystal can have two possible parallel orientations. In one type, the D^+ segments are oriented side by side and termed as in registry chains (Fig. 1a). On the other hand, in the out of registry chains, D^+ finds A^- in the neighboring chain in its nearest position (Fig. 1).^{11,13} The D^+A^- pair of a vertical chain is defined as the V-pair in this work (Fig. 1b). As the nearest neighbor spin interaction is known to govern the magnetic nature of any system,¹³ a nearest D^+A^- pair from the horizontally stacked out of registry chains is selected for this investigation. This D^+A^- pair, where the D^+ and A^- belong to two different vertical columns arranged in an out of registry manner which is termed as H-pair in this work (Fig. 1b). Although, the origin of ferromagnetism in the V-pair has been well explained by McConnell-I mechanism,¹⁰ the weak ferromagnetic ordering of H-pair is not yet addressed properly.¹¹

This study makes an attempt to address the charge transfer induced magnetism in a particular MBCTC, $[Cr(Cp^*)_2][ETCE]$, keeping three different goals in its focus. Primarily, the charge

transfer in between donor and acceptor is explored and the donor–acceptor magnetic coupling is quantified in terms of this charge transfer energy. Secondly, the architecture of this complex hints towards a different degree of magnetic interaction between the donor and the acceptor in V-pair and H-pair. In the V-pair, the d-electrons on Cr can be transferred to the acceptor *via* Cp^* bridge;¹⁴ whereas, absence of any such mediator in case of H-pair obstacles the CT process. The difference in horizontal and vertical direction definitely has an important role in governing the overall magnetic nature of this crystal. This stimulates us to investigate the nature of magnetic interaction in the V-pair and H-pair individually and in presence of each other. Lastly, we cultivate the role of periodicity in governing charge transfer and concomitant magnetic interaction. Dealing with such extended system also enables one to explore the effect of dimension on magnetic characteristics. The systems in reduced dimension are found to depart from their usual bulk behavior which inspires the study of electronic properties in nano scale.¹⁵ Intensified magnetism in the reduced dimension has recently been the subject of several theoretical and experimental investigations.¹⁶ This fact has already been realized in cases of Au-nanoparticle, alkali metal clusters, Mn nanosheet and many other systems.^{16e,h,17} All these facts spur the study of the effect of periodicity on the magnetic behavior of $[Cr(Cp^*)_2][ETCE]$.

2. Theoretical framework

The magnetic sites in a system are characterized by a non-vanishing spin angular momentum quantum number, S_i . Interaction among these localized spin moments govern the overall magnetic nature of the system. The magnetic interaction, often termed as exchange coupling is described by the well-known phenomenological Heisenberg–Dirac–van Vleck (HDVV) Hamiltonian, which describes the isotropic interaction between localized magnetic moments S_i and S_j as

$$\hat{H} = - \sum_{i < j} J_{ij} \hat{S}_i \hat{S}_j, \quad (1)$$

where, J_{ij} is the exchange coupling constant between the localized spin moments, and the i, j symbols indicate that the sum extends to the nearest neighbor interactions only. According to the spin Hamiltonian in eqn (1), a positive (negative) value of J_{ij} corresponds to a ferromagnetic (antiferromagnetic) interaction, thus favoring a situation with parallel (antiparallel) spins. Symmetrically equivalent magnetic sites must necessarily have equal amplitude of spin density which imposes a delocalized solution for the system. Thus, such “full-symmetry” calculations are unable to consider the weakly coupled limit, where the electrons are fully localized.¹⁸ Therefore, the removal of all symmetry elements connecting the magnetic centers is necessary to account for weak coupling limit. Noodleman and co-workers worked out a “broken-symmetry” (BS) approach, where the space and spin symmetry can be removed by polarizing the up-spin and down-spin onto different magnetic centers.¹⁹ Later on, Bencini and Ruiz modified this expression for the limit of strongly interacting magnetic sites.²⁰ On the other hand,

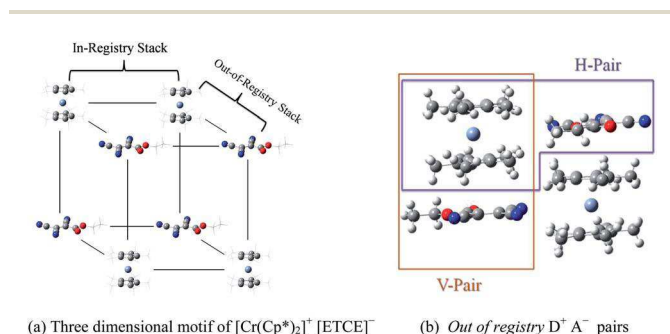


Fig. 1 (a) Representation of the in registry and out of registry chains (b) blue and brown rectangles in the out of registry chains designate the H-pair and V-pair respectively.

Yamaguchi's expression encompasses the appropriate limit, depending on the interaction strength and thus fulfills the criterion of general applicability,²¹

$$J_{ij} = \frac{E_{\text{BS}}^{\text{HS}} - E_{\text{HS}}^{\text{BS}}}{\langle \hat{S}^2 \rangle_{\text{BS}} - \langle \hat{S}^2 \rangle_{\text{HS}}}. \quad (2)$$

The general applicability of the eqn (2) can be understood through the following dependence of $\langle \hat{S}^2 \rangle$ on the overlap of magnetic orbitals²²

$$\langle S^2 \rangle = M_S(M_S + 1) + N_\beta - \sum_{ij}^{N_\alpha, N_\beta} (O_{ij}^{\alpha, \beta})^2. \quad (3)$$

Here, $O_{ij}^{\alpha, \beta}$ is an integral describing the overlap between the spatial parts of α and β spin orbitals.^{22,23} In the strong coupling limit, all pairs of α and β orbitals overlap and the double sum in eqn (3) is reduced to N_β . Therefore, the total spin expectation value indicates a pure spin state with $\langle S^2 \rangle_{\text{BS}} = 0$ for a diradical with equal number of α and β electrons. Hence, the denominator in eqn (2) transforms to $S_{\text{HS}}(S_{\text{HS}} + 1)$ which resembles the Noodleman–Bencini–Ruiz formula.²⁰ On the other hand, if magnetic orbitals do not overlap (BS determinant), the sum in eqn (3) becomes $N_\beta - 2S_A$, where S_A is the sum of α and β magnetic orbitals. In this weakly coupled limit, $\langle S^2 \rangle_{\text{BS}} = 2S_A = S_{\text{HS}}$ and resembles Noodleman's original expression.²³ The BS state is usually constructed by mixing two magnetic orbitals which usually belongs to different irreducible representations.^{19,20b} So, the magnetic orbitals should be close enough in order to interact with each other. Hence, for the remote magnetic sites, the construction of BS state becomes difficult. However, the BS state is usually achieved by performing HF or DFT in spin-unrestricted formalism where up-spin and down-spin densities are allowed to localize on different centers.^{20b} Though an open shell singlet state can best be represented through multi-configuration techniques;²⁴ DFT uses a single Slater determinant to describe the BS state and thus becomes more advantageous than post-HF methods in handling larger systems.^{20b}

As discussed in the introduction, the donor–acceptor magnetic coupling is induced by electron transfer from donor to acceptor. Among the various models of charge transfer in electronic systems, a perturbative treatment has widely been adopted to account for the electron tunneling process.²⁵ Anderson in his pioneering work, derived the second order perturbation energy (ΔE) for such an intersite charge transfer and correlated this energy with magnetic interaction as,²⁶

$$\Delta E = \frac{t_{ij}^2}{U} \left(\frac{1}{2} + 2\hat{S}_i \hat{S}_j \right). \quad (4)$$

Here, t_{ij} is the hopping integral which carries an electron from site i to site j and U is the single ion repulsion energy. However, this t^2/U term is well-known in the Hubbard model and related to the exchange coupling constant (J).²⁷ In their seminal works Calzado *et al.* applied *ab initio* CI techniques to compute these individual contributions to the magnetic coupling constant using effective Hamiltonian theory.²⁸ However, in a recent

formalism, instead of direct estimation of this t^2/U term; the above expression is modified to estimate the coupling constant (J_{SX}) in a superexchange process in terms of the second order perturbation energy (ΔE) for charge transfer between sites and spin population on those centers (ρ_i and ρ_j),²⁹

$$J_{\text{SX}} = \frac{2\Delta E}{1 + \rho_i \rho_j}. \quad (5)$$

The charge transfer matrix element between the donor and acceptor can be expressed as^{30–33}

$$H_{\text{DA}} = \frac{E_{\text{D}} - E_{\text{A}}}{2}. \quad (6)$$

where, H_{DA} is a pure one electron matrix element, coupling the effective donor and acceptor orbitals as

$$H_{\text{DA}} = \langle \phi_{\text{D}} | \hat{H} | \phi_{\text{A}} \rangle \quad (7)$$

and, E_{D} and E_{A} are the energies of the LUMO in cationic donor and neutral acceptor. Again, the second order perturbation energy (ΔE) for the charge transfer process is related to the transfer matrix element H_{DA} for the donor–acceptor pair in the following manner,³⁴

$$\Delta E = \frac{|H_{\text{DA}}|^2}{E_{\text{D}} - E_{\text{A}}}. \quad (8)$$

Now, substituting $2\Delta E$ term in eqn (5), using eqn (8) and (6), the following modified form is obtained,

$$J_{\text{T}} = \frac{H_{\text{DA}}}{1 + \rho_{\text{D}} \rho_{\text{A}}}. \quad (9)$$

This can be conveniently used to calculate the exchange coupling constant value (J_{T}) in electron transfer systems.

3. Computational details

In the present work, the effective exchange integral J is estimated in two approaches, one of which is the state-of-the-art spin projection technique of Yamaguchi (eqn (2)). In the second approach, the electron transfer matrix element for charge transfer from donor to acceptor and the spin populations on the donor and acceptor sites are used to estimate J through presently derived eqn (9). The eqn (2) is generally implemented through an unrestricted or spin polarized formalism, where the up-spin and down-spin densities are allowed to localize on magnetic sites.^{21,22} Thus, in the present work unrestricted DFT (U-DFT) is applied to compute the coupling constant. The same U-DFT method is adopted to derive the parameters in eqn (9). The U-DFT method is reported to produce a reliable estimate of such transfer integrals, at least in cases of metal-based systems.³⁵ To evaluate J through eqn (9), standard DFT calculation on the isolated donor and acceptor molecules is first carried out to extract the energies of the LUMO of the cationic fragment $[\text{Cr}(\text{Cp}^*)_2]^+$ and that of the neutral acceptor $[\text{ETCE}]$. These energy values along with the spin populations on the

donor and acceptor in the ground state of dimer $[\text{Cr}(\text{Cp}^*)_2]^+[\text{ETCE}]^-$ are utilized to compute the J_T in eqn (9).

To understand the magnetic effect of V-pair on H-pair and *vice versa* in the crystal motif of $[\text{Cr}(\text{Cp}^*)_2][\text{ETCE}]$, it becomes necessary to estimate the exchange-coupling constant between every D^+A^- pair in vertical and horizontal directions in presence of each other. A recently adopted technique to determine J in a system with multiple magnetic sites (SMMS) becomes useful in this regard.³¹ In this particular strategy, which is mentioned as the “dummy approach” in the present work; first the effect of all the magnetic sites on each other is realized in the form of ground state spin population. Then the exchange coupling constant between any two magnetic sites is calculated on the basis of their ground state spin population while regarding other magnetic sites inert. However, in the present context the computational scheme of ref. 31 is applied on a 2D crystal motif displayed in Fig. 1b so as to consider both the direct exchange and superexchange in the H-pair and V-pair respectively. The spin density distribution of this system is first obtained. Next, the exchange coupling for one V-pair is computed while its neighboring V-pair is made dummy. Although, other than a specific magnetic pair all other magnetic sites are made dummy, their effect is imposed on the specific pair in terms of pre-calculated spin population which can be understood from the spin density parameterization of the Heisenberg Hamiltonian.³¹

In order to investigate the effect of periodicity on the magnetic interaction, the periodic boundary condition is imposed on the system. To deal with the extended solid, different level of theoretical platforms are used which ranges from the simple tight-binding model to the *ab initio* periodic Hartree–Fock and modern DFT based methods.³³ The eigenstates of such periodic system can be labelled by the reciprocal-lattice vectors, \mathbf{k} , in the first Brillouin zone (BZ).³³ Since the system is infinite, the quantum numbers \mathbf{k} are continuous. Calculation of the total energy requires a self-consistent calculation of the eigenvalues, which are performed at a finite number of points in the Brillouin zone.³⁴ A recent work expresses the charge transfer integral as the function of \mathbf{k} point³⁶ and thus stimulates us to investigate the influence of increasing \mathbf{k} point (within the first BZ) on the charge transfer induced magnetism.

The structure of the complex is available in crystallographic file format,¹¹ this geometry of the complex is taken as its ground state structure. While doing the periodic boundary calculation with different \mathbf{k} points, the Perdew–Burke–Ernzerhof exchange and correlation functional (PBE) is employed.³⁷ This exchange correlation functional is found to produce superior accuracy for a broad variety of systems under periodic boundary conditions.³⁸ This advanced GGA functional includes some electron correlation effects at larger distances. The LANL2DZ basis set is chosen selectively for Cr atoms and 6-311++g(d,p) for all other atoms and this has been maintained throughout for DFT calculations. The success of exchange correlation functionals in accurate estimation of J is believed to be intrinsically linked to the introduction of an amount of Hartree–Fock (HF) exchange.³⁹ In this regard, the B(X)LYP functional is prescribed as the optimum performer, where X is

related to the percentage of Fock exchange.⁴⁰ However, Martin and Illas have shown that the coupling constant vary with X and the result becomes satisfactory with $X = 50$.⁴¹ Hence, in this work we use BHandHLYP functional with $X = 50$, which has already been found efficient to reproduce the experimental value of coupling constant.⁴² This particular functional is characterized to be a 1 : 1 mixture of DFT and exact exchange energies which can be represented as $E_{XC} = 0.5E_X^{\text{HF}} + 0.5E_X^{\text{LSDA}} + 0.5\Delta E_X^{\text{Becke88}} + E_C^{\text{LYP}}$.⁴³ This is also supported by Caballol *et al.*⁴⁴ who have concluded that functionals assuming fully delocalized open shell magnetic orbitals, such as B3LYP, produce a poor description of local moments.⁴¹ Particularly, the B3LYP functional is reported to produce inaccurate structural and thermochemical parameters in the extended systems due to its failure to attain homogeneous electron gas limit.⁴⁵ On the contrary, another school of thought advocate the use of B3LYP with less amount of HF exchange to get a reliable estimate of J .⁴⁶ Nevertheless, the hybrid functionals are questioned for their tendency to overstabilize the higher spin multiplet, whereas the GGA functionals overestimate the stability of the ground state.⁴⁷ On the other hand, the hybrid meta GGA functional TPSSh with 10% HF exchange shows a minimum deviation (10–15%) in the J value compared to experiment.⁴⁸ Thus, among several other functionals, the TPSSh functional is chosen by several groups for evaluating the exchange coupling constant.⁴⁹ In order to get a self-consistent result, here also a set of exchange correlational functionals is applied to compute the exchange coupling constant. The results obtained with DFT are also validated with the multireference Complete Active Space Self-Consistent Field (CASSCF) technique, based on the active electron approximation. This technique incorporates several important physical effects in both direct exchange and superexchange cases for the calculation of magnetic interaction.⁵⁰ However, the CAS method disregards important physical mechanisms like ligand-spin polarization, dynamic spin polarization, double spin polarization *etc.* and underestimates the coupling constant in effect.⁵¹ These effects can be included through the second order perturbation theory based upon the UHF wave function. The complete active space second-order perturbation theory (CASPT2) is a method which imposes second order correction to the CAS wave functions, and found useful in producing J close to experimental values.⁵² This method can further be refined by considering “external correlation” through multireference configuration interaction (MRCI) tools,⁵³ among which the difference dedicated CI (DDCI) approach by Miralles *et al.* has been particularly successful to produce the desired degree of accuracy.⁵⁴ However, to avoid computational rigor associated with such sophisticated methods, in the present work the CASSCF is used with a large active space which includes different configurations connected to charge transfer excitation,⁵⁵ and thus partially overrule the limitations of CASSCF. An active space of ten electrons in nine orbitals [CASSCF (10, 9)] is used to calculate the exchange coupling constant of the V-pair in this work. All calculations are performed using Gaussian 09W suite of quantum chemical package.⁵⁶ The density of states (DOS) plots are generated with GaussSum 2.2.⁵⁷

4. Results and discussion

Before dealing with the present dimeric system $[\text{Cr}(\text{Cp}^*)_2][\text{ETCE}]$, first the ground states of monomers (D and A) are taken for pursuit. Since, there exists a probability for the neutral $[\text{Cr}^{\text{II}}(\text{Cp}^*)_2]$ to remain in the low-spin triplet or high-spin quintet state, it requires a theoretical confirmation. The ground state of the monomers is thus checked with different DFT functional. These results are also compared with multireference CASSCF to verify the reliability of DFT methods in properly describing the ground state of the monomers. Everywhere, the ground state is recognized as the low-spin triplet (Table S1 in the ESI[†]), which is also reported experimentally.⁴² Concerning to an orbitally degenerate ground state of $[\text{Cr}^{\text{II}}(\text{Cp}^*)_2]$, Cr^{2+} ion is supposed to experience a quenching of the orbital angular momentum due to static Jahn–Teller (JT) effect.⁵⁸ Moreover, the Cr ion in the D^+A^- species is also reported to be reluctant to magnetic hysteresis and exhibit no magnetic anisotropy.¹¹ The neutral acceptor unit, which initially exists in singlet ground state, turns into an anionic doublet after accepting an electron from neutral donor, leaving the donor in cationic quartet state. The overall quintet spin state in $[\text{Cr}(\text{Cp}^*)_2][\text{ETCE}]$ dimer, with three d-electrons on the Cr atom and one in the acceptor unit finds validation in its spin density plot and references of similar

systems.^{11,5b} From the molecular orbital (MO) analysis of V-pair and H-pair, 131 to 134 MOs appear as singly occupied molecular orbitals (SOMO), of which 133 α MO is found to be composed of the acceptor orbitals solely in both the pairs (Fig. 2). Since, the computations are performed at U-DFT level, all the occupied orbitals are in fact possessed by single electrons. Thus, here the SOMOs are referred to as the α -occupied MOs which do not have any β -counterpart of comparable energy.

Existence of this MO advocates for the single electron transfer to the acceptor moiety. Rest of the SOMOs shows an equitable contribution of Cp^* and ETCE orbitals. Although in such complexes metal d orbitals are reported as magnetic orbitals,¹³ in the present case any contribution from Cr d-orbitals is found surprisingly missing in the construction of the highest occupied α -MOs. This contradiction probably stems from the non-Aufbau kind of behavior, where the singly occupied metal orbitals are buried below doubly occupied orbitals.⁴⁴ The density of states (DOS) plot which shows the highest occupied β -spin orbitals at higher energy levels than the highest occupied α -MOs (Fig. 3) also supports this observation. This problem is often encountered in systems having bonds with prevalently ionic character. Due to this rearrangement of the electrons in shuffled MOs, the contribution of d-orbitals is found in 126, 127 and 128 α -MOs which are below the so called SOMOs. However, applying spin projection technique (eqn (2)), the coupling is found to be very weak ($J = 0.004 \text{ cm}^{-1}$) in the H-pair, compared to V-pair ($J = 511 \text{ cm}^{-1}$). Though weakly coupled, the H-pair takes a decisive role in setting up the gross magnetic behavior in such crystals.^{6b}

Now, to understand the charge transfer phenomenon, the electronic configuration of D^+ and A^- in the V-pair is compared with its neutral analogues (D^0 and A^0). From the comparison of the molecular orbitals of the individual D^0 and A^0 units, it appears that the electron transits from the 86th β -orbital of D^0 to the 46th α MO of A^0 . In the receptor part, the antibonding nature of the olefinic C–C orbitals further clarifies that this is the π^* MO (Fig. 4). This analysis, performed in the background of monomer approach, also provides necessary information for the appropriate selection of donor and acceptor orbitals,

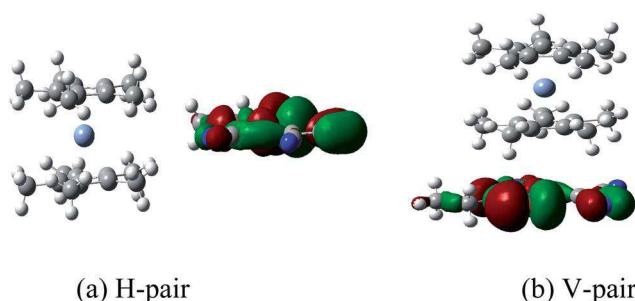


Fig. 2 The 133rd α -SOMO in (a) H-pair, and (b) V-pair, solely centered on the acceptor.

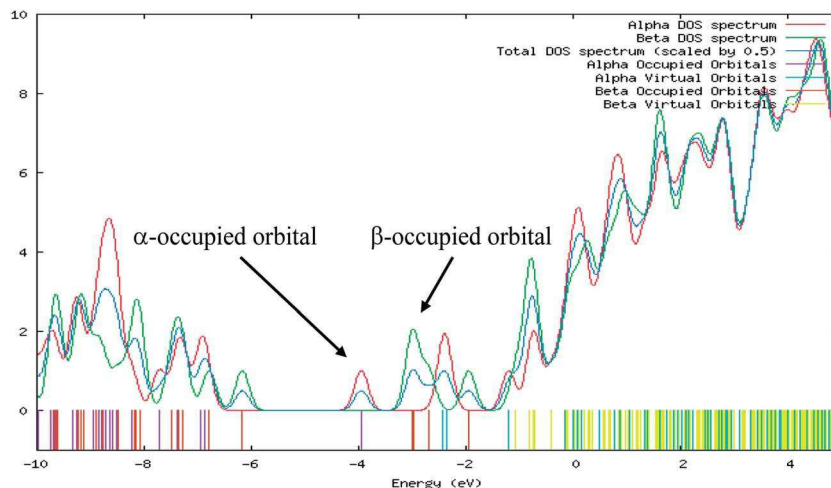


Fig. 3 The DOS plot of the V-pair.

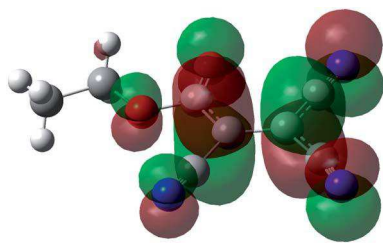


Fig. 4 The 46th α -MO of acceptor unit in both of the V-pair and H-pair.

participating in the charge transfer process. To trace the charge transfer process, the system is analyzed at the transition state, when one electron is being transferred from the donor β -orbital to the π^* MO of the acceptor. It has been shown previously that the superexchange electronic charge resonance energy, which we have denoted here as $2\Delta E$ in eqn (5), can be substituted by the charge transfer integral (H_{DA}) or the direct vacuum electronic coupling term.⁵⁹ The initial and final states of electron transfer has been crucial in the determination of the two-state approximation. In determining the initial and final states of the electron transfer, the β -LUMO of the isolated donor D^+ is taken as the donor orbital since the electron was initially localized on that particular orbital. Whereas, in the acceptor part A, the α -LUMO is taken as the recipient orbital since the hopping electron is going to be localized on that orbital.⁴⁶ Using the energies of the concerned orbitals, the magnetic exchange coupling constant is estimated as 514 cm^{-1} through eqn (9) (at UBH and HLYP/6-311++g(d,p) with LANL2DZ extrabasis on Cr) which is in reasonable agreement with the J , estimated at same level of theory through the famous spin projection technique (eqn (2)) of Yamaguchi (Table 1). To compare these values obtained through DFT, a more accurate CASSCF technique is adopted as well, which is capable to describe the multireference character of involved radicals. The CASSCF wave function is constructed allowing all possible combination of ten electrons in nine orbitals resulting in a CASSCF (10,9) active space. The active space includes SOMOs, *i.e.*, Cr d_z^2 , $d_x^2 - y^2$ and d_{xy} -orbitals on the donor fragment and also the singly occupied π^* -orbital on the acceptor fragment. The orbitals, which on a test calculation using a larger active space (namely a 14 electrons and 11 orbitals space), shows an occupancy of 1.99 electrons, are moved to core orbitals. The chosen active orbitals are shown in Fig. 5. From Table 1, the chosen functional BHandHLYP and CASSCF are found to produce similar value of exchange coupling constant. Moreover, in all the methodologies, same kind of spin density alternation (up–down–up) in Cr–Cp*–ETCE is observed, which is indicative of the superexchange mechanism (see Table S2 in the ESI[†]).

Table 1 Comparison of coupling constant values (J) for the V-pair, obtained through different methodology

Level of theory	J in cm^{-1}
BHandHLYP/6-311++g(d,p) with LANL2DZ extrabasis on Cr	511
CASSCF(10,9)/LANL2DZ	439

Competition between exchange mechanisms

So far the spin topology of the V-pair is concerned, it is interesting to note significant spin density on Cp* moiety which intervenes the magnetic sites Cr and the acceptor ETCE. This observation suggests that bridging Cp* ligand is playing a role to couple the spins on Cr and ETCE through superexchange process. The spin density alternation further affirms the possibility of superexchange.⁴⁷ The spin density alternation in the V-pair also justifies the McConnell-I mechanism, according to which, the majority spin on the metal atom induces a negative spin density on the Cp* motif, which in its turn spawns positive spin density on the acceptor part. On the other hand; absence of any such bridging ligand in between the magnetic sites of H-pair makes direct exchange the only mechanism for the interaction of spins. Earlier studies pointed out two such contributions to the magnetic coupling;

$$J \equiv J_F \text{ (for FM interaction)} + J_{AF} \text{ (for AFM interaction)} \\ = 2K_{ij} - 4t_{ij}^2/U, \quad (10)$$

where K_{ij} describes direct exchange between magnetic orbitals and generally considered as ferromagnetic contribution.⁴⁸ The second part, including the hopping integral t_{ij} and the on-site Coulomb repulsion U , is usually termed as kinetic exchange in Anderson's interpretation and antiferromagnetically contributes to the total coupling constant.⁴⁹ In a model proposed by Heitler and London, J is similarly split into ferro- and antiferromagnetic parts

$$J = K + 2\beta S. \quad (11)$$

The first part, being the two-electron exchange integral is necessarily positive; whereas the second part contains resonance integral (β) and an overlap integral (S), which are of opposite sign and thus their product becomes negative. Hence, the value of overlap integral plays a crucial role in controlling the overall nature of magnetic interaction.^{9b} However, the value of direct exchange coupling constant, estimated through spin projection technique, in case of H-pair is found to be very weak (0.004 cm^{-1}) compared to that (511 cm^{-1}) in case of V-pair, where the superexchange is operative. This observation is in agreement with Anderson's explanation where the superexchange is argued to be more intense than direct exchange on the basis of metal–ligand overlap.^{48b} The direct exchange interaction is considered to be comparatively weaker because it operates between spatially orthogonal wave functions.⁵⁰ Further, the degree of exchange is found to be largely affected from the distance between the magnetic sites.⁵¹ Hence, the large distance of 7.248 \AA between the donor and acceptor in H-pair is another reason for the weaker direct exchange compared to superexchange. This observation is in agreement with the result of theoretical and experimental works, executed on similar systems,⁵⁷ where the intrachain (V-pair) magnetic interaction is found to be much stronger than interchain (H-pair) interaction.

Though weak, the interchain coupling takes a significant role in deciding the overall magnetic ordering of the system.^{6b,11,57} Hence, both of these V-pair superexchange and H-pair direct

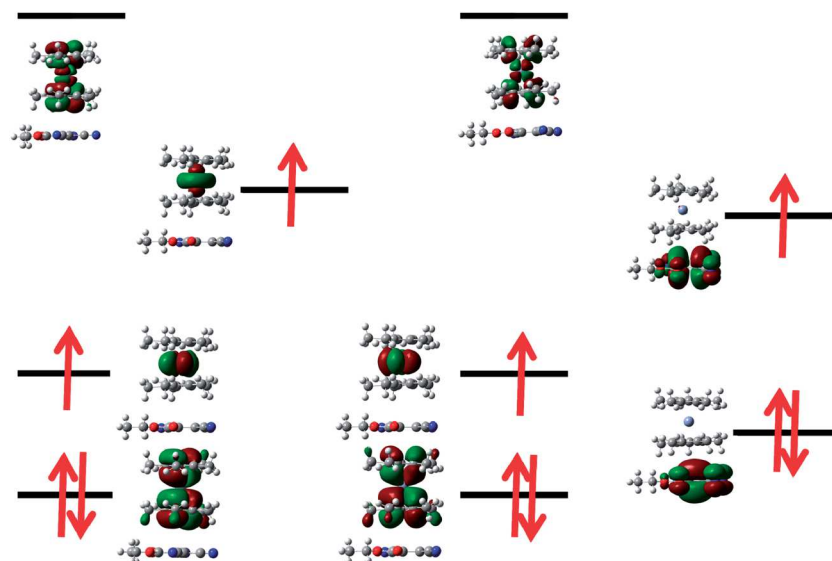


Fig. 5 A qualitative MO diagram of the chosen active space for the CASSCF calculation, containing 10 electrons in 9 orbitals.

exchange are to be simultaneously taken into account to explain the bulk magnetic behavior. As a replica of the bulk system, a two-dimensional (2D) motif of the crystal (Fig. 1b) is scooped out where both H-pair and V-pair are present. Next, following the computational strategy stated in ref. 31, the second vertical column is made dummy in order to compute the coupling constant in the 1st V-pair. The exchange interaction between the donor-acceptor pair in horizontal direction is quantified through similar approach. A comparable approach requires embedding the central unit in a field of point charges.⁶⁰ Inclusion of neighboring units is found to be a good approximation to the bulk property.⁶¹ The value of coupling constant (J_D), obtained in this way for the V-pair considerably decreased to 13 cm^{-1} compared to the earlier computed J value of 511 cm^{-1} (Table 1). On the other hand, in the H-pair there is a slight increase (0.007 cm^{-1}). This indicates some kind of antagonism between direct exchange and superexchange. Since this truncated model reproduces the bulk-behavior, the coupling constant of this system is ideal to compare with that obtained from experimental data.

The value of J drastically decreases in a two-dimensional system, compared to that in the single V-pair. A close comparison of the parameters, required to get coupling constant from eqn (2), reveals that except the energy of BS state all other factors are nearly same in single pair and 2D model. This clearly indicates that in the 2D model the BS state gets more stability compared to single D^+A^- pair, which can be attributed to the interchain interaction. In the extended model, one single D^+A^- pair finds another such A^-D^+ pair in its neighbor, which causes a distortion in its equilibrium configuration.⁵⁷ Following the second order perturbation it can be shown that there is an orbital interaction between neighboring chains, which eventually stabilizes the broken-symmetry state.⁶² Moreover, the difference of spin density in these two situations, also contributes to such steep change in the value of coupling constant (see Fig. S1 in the ESI†). A decrease of spin density is noticed in the

two dimensional array due to dispersion of spin densities from magnetic sites, which affect the coupling constants. This fact finds its support from the recent works which advocate for an intimate relationship between the spin population and coupling constant.^{29,31}

Effect of periodicity

For a proper understanding of the magnetic interaction in the extended system, one must concentrate on studying the magnetic interaction as a periodic function. To gain an insight to the magnetic property in the periodic lattice system, periodic boundary condition is imposed on the system with the translational vectors 10.796 \AA in the vertical direction and 16.161 \AA in the horizontal direction. An attempt to compute the J value in the periodic boundary is failed in case of the horizontal pair because of the non-convergence of BS solution. This can be attributed to the large distance between donor and acceptor which does not allow mixing of the orbitals on magnetic centers and the BS state cannot be constructed in consequence. This fact is also ensured from a very weak value of coupling constant for H-pair. The electron tunneling rate is also found to decay exponentially with distance.^{59,63} For this, the vertical pair is only chosen to investigate the effect of periodicity on its magnetism.

It has been previously anticipated that the prediction of a local property, *e.g.*, spin density for a system in cluster or in PBC are similar for a particular functional.⁶⁴ The comparison of spin density in PBE functional can be found in Tables S2 and S3 of the ESI.† A close inspection of Tables S2 and S3† reveals a change in the spin density under PBC (see Table S3 in the ESI†). This is expected to bring about the variation in magnetic interaction. However, a variation in the choice of the k -point grid shows that after the 3rd k -point, the change in spin density becomes insignificant which implies the attainment of the bulk limit. Computation of magnetic exchange coupling constant with the constraint of periodic boundary reveals an antiferromagnetic

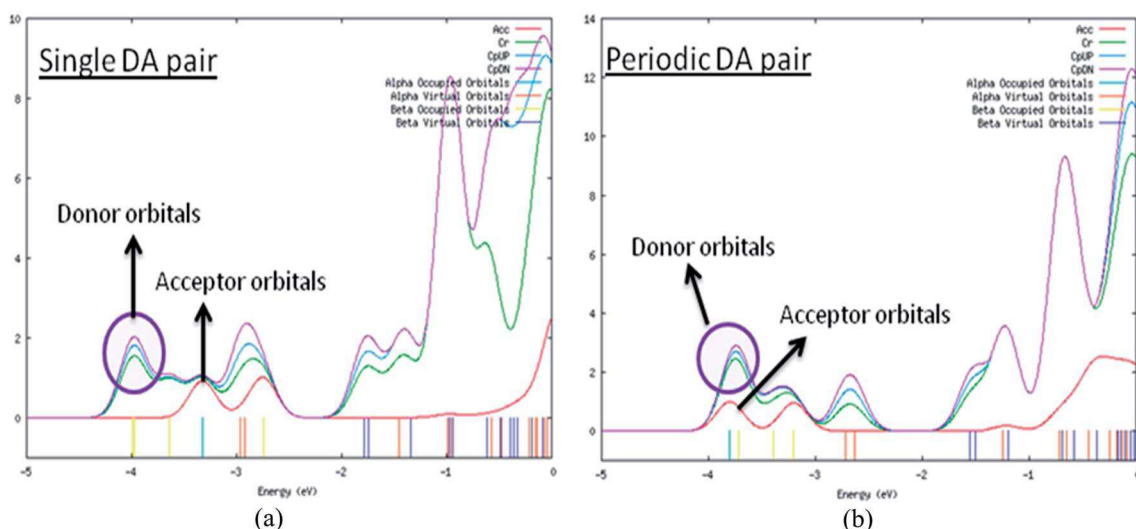


Fig. 6 The density of states plots of the V-pair in (a) gas phase and (b) under periodic boundary condition.

(AFM) interaction in vertical direction. The AFM interaction in the V-pair under periodic boundary condition (PBC) is in stark contrast to the positive value of coupling constant in absence of PBC. The change over from FM to AFM exchange within the periodic boundary condition may be argued to be arising out of this difference in functionals. To verify this, in absence of PBC the exchange coupling constant for the V-pair is also estimated using PBE functional in unrestricted framework which results in the J value of 133 cm^{-1} . This result shows that from the methodological point of concern, though the functional may alter the extent of coupling,⁶⁵ it cannot overturn the magnetic nature at least in the present case. Thus imposition of periodicity only can be attributed to such change in the magnetic behavior. This spin crossover can be understood in terms of charge transfer integral t_{ij} in eqn (4).⁶⁶ In this extended model, a particular donor (D^+) finds two acceptor units (A^-) below and above it unlike in the single V-pair. This increases the possibility of charge transfer, leading to the stabilization of AFM state. The exchange coupling constant under PBC is also calculated in the hybrid PBE0 functional for convenience,⁶⁷ which also predicts antiferromagnetic exchange in the periodic lattice. The results are given in Table S4 of the ESI.† The larger estimate of J produced by the hybrid PBE0 functional, in comparison to the pure PBE functional, can be explained due to the presence of a fraction of exact exchange which has a much larger extent than the DFT exchange considered in the pure functional. The AFM exchange coupling within the periodic boundary approach can further be envisaged as the effect induced by increasing the degrees of freedom of an electron. Thus the system gains stabilization in presence of PBC which can be confirmed from the energy comparison of V-pair, computed at same theoretical level [UPBEPBE/6-311++g(d,p) level with LANL2DZ as extrabasis on Cr atom]. The energy of the system without periodic boundary is -2445.135 a.u. and with the periodic boundary the energy is -2445.142 a.u. The periodic electron density can thus be assumed to be more delocalized which in turn induces a decreasing shift in Hubbard U parameter.⁶⁸ Now, there is a

report of the lowering of energy of the d-states with increase in U parameter.⁶⁹ So, a decreasing shift in U should uplift the energy levels of d-states, which is apparent from the DOS plots in aperiodic and periodic conditions (Fig. 6). Hence, a small value of U is expected in a periodic boundary formulation.⁶⁸ From the comparison of DOS plots in aperiodic and periodic systems, not only the upliftment of Cr d-states, but also the destabilization of Cp* ligands can be noticed. In addition, the up-spin orbital of acceptor lowers down in energy in the periodic condition. This situation brings the down-spin orbital of lower Cp* ring and the up-spin orbital of acceptor unit within the same energy range and thus facilitate their overlap in the periodic condition of the system. Hence, a small value of U together with non-zero value of S result in a stronger AFM interaction, which eventually supersedes the FM interaction and turns the system into a weak antiferromagnet in the periodic condition. However, the overall ferromagnetism in the bulk is manifested through an ensemble of different mechanisms.^{65,66,70,71}

5. Conclusion

The phenomenon of charge transfer (CT) is of paramount impact in guiding the courses of several biological and chemical processes. In the present study, the charge transfer process is also found effective in governing the magnetic behavior of metallocene based charge transfer complexes. A recently synthesized system, $[\text{Cr}(\text{Cp}^*)_2][\text{ETCE}]$ is taken as the representative MBCTC to explore the influence of charge transfer on the magnetic behavior of such donor–acceptor complexes. Anderson in his pioneering work ascribed charge transfer as the origin of kinetic exchange and correlated this exchange with the second order perturbation energy for such charge transfer. In a recent work, using this approach of Anderson, the coupling constant is parameterized with spin population (eqn (5)). However, eqn (5) is employed to account for through bond charge transfer in a superexchange process. On the contrary, NBO analysis for the present system clarifies a zero overlap

status in between the donor and acceptor, which necessitates the tunneling of electron in its journey from the donor to the acceptor. Hence, in the present work, eqn (5) is modified to take the electron tunneling matrix element (H_{DA}) into account to determine the coupling constant. This integral, is evaluated from the zeroth order eigenvalues of pure donor and acceptor at the transition state of the electron transfer process. The exchange coupling constant (J_T), obtained in this way (eqn (9)) is well in agreement with J , the coupling constant derived through well-known spin projection technique of Yamaguchi (eqn (2)). The charge transfer interaction happens to be the central in such type of complexes where the magnetic interaction begins after the charge dislocates from the donor to the acceptor creating one magnetic site at the acceptor.

The topological difference of V-pair and H-pair leads to the possibility of concurrent and competitive exchange interactions at different directions. In V-pair, the intervening Cp* ring assists the transfer of electron from metal to acceptor unit and hence there operates the superexchange process in this direction. In the other direction, the donor and acceptor are far separated and there is no such aid for the spins to be transferred from the donor to the acceptor. Hence the direct exchange process becomes only viable in H-pair. From the comparison of the coupling constant values, the superexchange interaction is found dominant in between two exchange processes in $[\text{Cr}(\text{Cp}^*)_2][\text{ETCE}]$. Since, the weak interaction in the horizontal direction takes a decisive role to render overall magnetic ordering; the V- and H-pairs are simultaneously taken into account. This situation opens up the possibility of several exchange interactions among multiple magnetic sites, which is estimated through one of our earlier developed computational scheme, referred to as dummy approach within the text. The coupling constant value for the V-pair, obtained through this approach is found to be very low compared to the previous value, where only the V-pair is considered. The drastic decrease in the J value through dummy approach is attributed to the interchain interaction. The coexistence of competitive superexchange and direct exchange in this truncated model replicates the bulk behavior. The small positive value of J supports the weak ferromagnetic nature of this MBCTC by Wang *et al.*¹¹

It has been of optimal challenge to investigate the nature of magnetism in a crystal system. The best way to mimic the real network of spins of a cluster demands the application of periodic boundary condition. The PBC can treat systems in bulk condition with much less computational effort without taking the finite size-effect and border-effect. Our calculation clearly shows that the magnetic interaction in one dimensional periodic lattice of such kind of system in the vertical direction is antiferromagnetic and the extent of magnetism is too low. Moreover, it is interesting to note that the FM system turns into an AFM one with imposition of periodic boundary condition. This change over in the magnetic status of the system is explained with the rearrangement of the density of states in $[\text{Cr}(\text{Cp}^*)_2][\text{ETCE}]$. In this condition, there occurs a simultaneous higher and lower energy shifts in the donor and acceptor orbitals respectively and the donor-acceptor overlap integral gains a non-zero value, which is otherwise zero in the system.

This lift in energy of the d-states is also supported from the easy dispersion of alpha spin to the Cp* ligand orbital. Hence, this situation facilitates electron delocalization and results a lower Hubbard U value. As a consequence of all these facts the $[\text{Cr}(\text{Cp}^*)_2][\text{ETCE}]$ which exhibits ferromagnetic coupling in the single D^+A^- pair, turns into an antiferromagnetic system in the periodic condition along vertical direction. However, the convolution of different exchanges pervading the crystal makes it a weak ferromagnet. An extended review on MBCTC divulges that there is a delicate balance in the sign of coupling constant in horizontal direction.⁶⁵ This weak, still competing magnetic interaction is regarded as the principle criterion for metamagnetism.⁷² However, this work suggests a delicate poise of magnetic interaction in the vertical direction as well.

Acknowledgements

We sincerely thank the Department of Science and Technology, India, for financial support. Authors also thank Prof. Carl Trindle, University of Virginia, for fruitful discussions.

References

- (a) J. S. Miller, A. J. Epstein and W. M. Reiff, *Mol. Cryst. Liq. Cryst.*, 1985, **120**, 27; (b) J. S. Miller, J. C. Calabrese, H. Rommelmann, S. R. Chittipeddi, J. H. Zang, W. M. Reiff and A. J. Epstein, *J. Am. Chem. Soc.*, 1987, **109**, 769.
- (a) J. Jortner and M. Ratner, *Molecular Electronics*, Blackwell Science, Cambridge, MA, 1997; (b) A. Aviram and M. Ratner, *Molecular Electronics: Science and Technology (Annals of the New York Academy of Sciences)*, The New York Academy of Sciences, New York, NY, 1998, vol. 852.
- (a) E. Goovaerts, W. E. Wenseleers, M. H. Garcia and G. H. Cross, *Nonlinear Optical Materials*, in *Handbook of Advanced Electronic and Photonic Materials and Devices*, Academic Press, New York, 2001; (b) J. P. Morall, G. T. Dalton, M. G. Humphrey and M. Samoc, *Adv. Organomet. Chem.*, 2008, **55**, 61; (c) C. E. Powell and M. G. Humphrey, *Coord. Chem. Rev.*, 2004, **248**, 725; (d) N. J. Long, *Angew. Chem., Int. Ed. Engl.*, 1995, **34**, 21; (e) S. Di Bella, C. Dragonetti, M. Pizzotti, D. Roberto, F. Tessore and R. Ugo, *Top. Organomet. Chem.*, 2010, **28**, 1; (f) D. Astruc, *Organometallic Chemistry and Catalysis*, Springer, Heidelberg, 2007; (g) M. Fuentealba, L. Toupet, C. Manzur, D. Carrillo, I. Ledoux-Rak and J.-R. Hamon, *J. Organomet. Chem.*, 2007, **692**, 1099; (h) C. Lambert, W. Gaschler, M. Zabel, R. Matschiner and R. Wortmann, *J. Organomet. Chem.*, 1999, **592**, 109.
- (a) S. Carretta, P. Santini, G. Amoretti, T. Guidi, J. R. D. Copley, Y. Qiu, R. Caciuffo, G. Timco and R. E. P. Winpenny, *Phys. Rev. Lett.*, 2007, **98**, 167401; (b) A. Ardavan, O. Rival, J. J. L. Morton, S. J. Blundell, A. M. Tyryshkin, G. Timco and R. E. P. Winpenny, *Phys. Rev. Lett.*, 2007, **98**, 057201; (c) M. N. Leuenberger and D. Loss, *Nature*, 2001, **410**, 789; (d) F. Troiani, A. Ghirri, M. Affronte, S. Carretta, P. Santini, G. Amoretti, S. Piligkos, G. Timco and R. E. P. Winpenny, *Phys. Rev. Lett.*, 2005, **94**,

- 207208; (e) J. Lehmann, A. Gaita-Arino, E. Coronado and D. Loss, *Nat. Nanotechnol.*, 2007, **2**, 312.
- 5 G. T. Yee, M. J. Whitton, R. D. Sommet, C. M. Frommen and W. M. Reiff, *Inorg. Chem.*, 2000, **39**, 1874.
- 6 (a) B. B. Kaul, W. S. Durfee and G. T. Yee, *J. Am. Chem. Soc.*, 1999, **121**, 6862; (b) B. B. Kaul, R. D. Sommer, B. C. Noll and G. T. Yee, *Inorg. Chem.*, 2000, **39**, 865.
- 7 (a) W. E. Boderick, X. Liu and B. M. Hoffman, *J. Am. Chem. Soc.*, 1991, **113**, 6334; (b) J. S. Miller, R. S. McLean, C. Vazquez, J. C. Calabrese, F. Zuo and A. J. Epstein, *J. Mater. Chem.*, 1993, **3**, 215; (c) G. T. Yee, J. M. Manriquez, D. A. Dixon, R. S. McLean, D. M. Groski, R. B. Flippen, K. S. Narayan, A. J. Epstein and J. S. Miller, *Adv. Mater.*, 1991, **3**, 309.
- 8 (a) H. M. McConnell, *Proc. Robert A. Welch Found. Conf. Chem. Res.*, 1967, **11**, 144; (b) R. Breslow, *Pure Appl. Chem.*, 1982, **54**, 927; (c) O. Kahn, *Molecular Magnetism*, VCH, New York, 1993.
- 9 (a) J. Schweizer, S. Golhen, E. Lelièvre-Berna, L. Ouahab, Y. Pontillon and E. Ressouche, *Phys. B*, 2001, **297**, 213; (b) C. Kollmar and O. Kahn, *Acc. Chem. Res.*, 1993, **26**, 259.
- 10 H. D. McConnell, *J. Chem. Phys.*, 1963, **39**, 1910.
- 11 G. Wang, C. Slebodnick, R. J. Butcher and G. T. Yee, *Inorg. Chim. Acta*, 2009, **362**, 2423.
- 12 S. N. Datta and A. Misra, *J. Chem. Phys.*, 1999, **111**, 9009.
- 13 W. S. Tyree, Thesis submitted to the faculty of the Virginia Polytechnic Institute and State University for the degree of Master of Science in Chemistry, 2005.
- 14 T. Okamura, Y. Takano, Y. Yoshioka, N. Ueyama, A. Nakamura and K. Yamaguchi, *J. Organomet. Chem.*, 1998, **569**, 177.
- 15 H. Brune, H. Röder, H. Boragno and K. Kern, *Phys. Rev. Lett.*, 1994, **73**, 1955.
- 16 (a) M. R. Pederson, F. Reuse and S. N. Khanna, *Phys. Rev. B: Condens. Matter Mater. Phys.*, 1998, **58**, 5632; (b) S. K. Nayak, B. K. Rao and P. Jena, *J. Phys.: Condens. Matter*, 1998, **10**, 10863; (c) S. K. Nayak and P. Jena, *Chem. Phys. Lett.*, 1998, **289**, 473; (d) M. B. Nickelbein, *Phys. Rev. Lett.*, 2001, **86**, 5255; (e) F. Michael, C. Gonzalez, V. Mujica, M. Marquez and M. A. Ratner, *Phys. Rev. B: Condens. Matter Mater. Phys.*, 2007, **76**, 224409; (f) E. M. Sosa-Hernandez, P. G. Alvarado-Leyva, J. M. Montezano-Carrizales and F. Aguilera-Granja, *Rev. Mex. Fis.*, 2004, **50**, 30; (g) F. Liu, S. N. Khanna and P. Jena, *Phys. Rev. B: Condens. Matter Mater. Phys.*, 1991, **43**, 8179; (h) S. Mitra, A. Mandal, A. Datta, S. Banerjee and D. Chakravorty, *J. Phys. Chem. C*, 2011, **115**, 14673.
- 17 (a) B. V. Reddy, S. N. Khanna and B. I. Dunlap, *Phys. Rev. Lett.*, 1993, **70**, 3323; (b) Y. Nozue, T. Kodaira and T. Goto, *Phys. Rev. Lett.*, 1992, **68**, 3789; (c) A. J. Cox, J. G. Louderback and L. A. Bloomfield, *Phys. Rev. Lett.*, 1993, **71**, 923; (d) P. Villaseñor-González, J. Dorantes-Dávila, H. Dreyssé and G. M. Pastor, *Phys. Rev. B: Condens. Matter Mater. Phys.*, 1997, **55**, 15084; (e) R. Guirado-López, D. Spanjaard and M. C. Desjonqueres, *Phys. Rev. B: Condens. Matter Mater. Phys.*, 1998, **57**, 6305.
- 18 J. E. McGrady, R. Stranger and T. Lovell, *J. Phys. Chem. A*, 1997, **101**, 6265.
- 19 L. Noodleman, *J. Chem. Phys.*, 1981, **74**, 5737.
- 20 (a) A. Bencini, F. Totti, C. A. Daul, K. Doclo, P. Fantucci and V. Barone, *Inorg. Chem.*, 1997, **36**, 5022; (b) E. Ruiz, J. Cano, S. Alvarez and P. Alemany, *J. Comput. Chem.*, 1999, **20**, 1391.
- 21 T. Soda, Y. Kitagawa, T. Onishi, Y. Takano, Y. Shigeta, H. Nagao, Y. Yoshioka and K. Yamaguchi, *Chem. Phys. Lett.*, 2000, **319**, 223.
- 22 A. Szabo and N. S. Ostlund, *Modern Quantum Chemistry: Introduction to Advanced Electronic Structure Theory*, Dover Publications, New York, 1996.
- 23 C. Herrmann, L. Yu and M. Reiher, *J. Comput. Chem.*, 2006, **27**, 1223.
- 24 R. C. Binning Jr and D. E. Babelo, *J. Comput. Chem.*, 2008, **29**, 716.
- 25 M. Galperin, D. Segal and A. Nitzam, *J. Chem. Phys.*, 1999, **111**, 1569.
- 26 (a) P. W. Anderson, *Phys. Rev.*, 1950, **79**, 350; (b) P. W. Anderson, *Phys. Rev.*, 1959, **115**, 2; (c) P. W. Anderson, in *Theory of the Magnetic Interaction: Exchange in Insulators and Superconductors*, Solid State Physics, Academic, New York, 1963, vol. 14, p. 99.
- 27 D. Munoz, F. Illas and I. P. R. de Moreira, *Phys. Rev. Lett.*, 2000, **84**, 1579.
- 28 (a) C. J. Calzado, J. Cabrero, J. P. Malrieu and R. Caballol, *J. Chem. Phys.*, 2002, **116**, 2728; (b) C. J. Calzado, J. Cabrero, J. P. Malrieu and R. Caballol, *J. Chem. Phys.*, 2002, **116**, 3985; (c) C. J. Calzado, C. Angeli, D. Taratiel, R. Caballol and J. P. Malrieu, *J. Chem. Phys.*, 2009, **131**, 044327.
- 29 (a) S. Paul and A. Misra, *J. Chem. Theory Comput.*, 2012, **8**, 843; (b) S. Shil, S. Paul and A. Misra, *J. Phys. Chem. C*, 2013, **117**, 2016.
- 30 E. G. Petrov, Y. V. Shevchenko, V. I. Teslenko and V. May, *J. Chem. Phys.*, 2001, **115**, 7107.
- 31 S. Paul and A. Misra, *J. Phys. Chem. A*, 2010, **114**, 6641.
- 32 (a) I. Daizadeh, D. M. Medvedev and A. A. Stuchebrukhov, *Mol. Biol. Evol.*, 2002, **19**, 406; (b) M. M. Mikolajczyk, R. Zalesny, Z. Czyżnikowska, P. Toman, J. Leszczynski and W. Bartkowiak, *J. Mol. Model.*, 2011, **17**, 2143.
- 33 G. Makov, R. Shah and M. C. Payne, *Phys. Rev. B: Condens. Matter Mater. Phys.*, 1996, **53**, 15513.
- 34 (a) J. P. Foster and F. Weinhold, *J. Am. Chem. Soc.*, 1980, **102**, 7211; (b) A. E. Reed, L. A. Curtiss and F. Weinhold, *Chem. Rev.*, 1988, **88**, 899.
- 35 B. Baumeier, J. Kirkpatrick and D. Andrienko, *Phys. Chem. Chem. Phys.*, 2010, **12**, 11103.
- 36 J. Huang and M. Kertesz, *J. Chem. Phys.*, 2005, **122**, 234707.
- 37 J. P. Perdew, K. Burke and M. Ernzerhof, *Phys. Rev. Lett.*, 1996, **77**, 3865.
- 38 (a) R. Improta, V. Barone, K. N. Kudin and G. E. Scuseria, *J. Chem. Phys.*, 2001, **114**, 254; (b) G. Zhao, L. Jiang, Y. He, J. Li, H. Dong, X. Wang and W. Hu, *Adv. Mater.*, 2011, **23**, 3959; (c) R. Improta, V. Barone, K. N. Kudin and G. E. Scuseria, *J. Am. Chem. Soc.*, 2001, **123**, 3311.
- 39 (a) A. D. Becke, *J. Chem. Phys.*, 1993, **98**, 5648; (b) J. Stephens, F. J. Devlin, C. F. Chabalowski and M. J. Frisch, *J. Phys.*

- Chem.*, 1994, **98**, 11623; (c) C. Adamo and V. Barone, *J. Chem. Phys.*, 1999, **110**, 6158; (d) M. Ernzerhof and G. E. Scuseria, *J. Chem. Phys.*, 1999, **110**, 5029; (e) D. Jacquemin, E. A. Perpète, I. Ciofini and C. Adamo, *Chem. Phys. Lett.*, 2005, **405**, 376.
- 40 (a) H. Chevrau, I. P. R. de Moreira, B. Silvi and F. Illas, *J. Phys. Chem. A*, 2001, **105**, 3570; (b) E. Ruiz, P. Alemany, S. Alvarez and S. Cano, *J. Am. Chem. Soc.*, 1997, **119**, 1297.
- 41 (a) R. L. Martin and F. Illas, *Phys. Rev. Lett.*, 1997, **79**, 1539; (b) F. Illas and R. L. Martin, *J. Chem. Phys.*, 1998, **108**, 2519.
- 42 T. Onishi, Y. Takano, Y. Kitagawa, T. Kawakami, Y. Yoshioka and K. Yamaguchi, *Polyhedron*, 2001, **20**, 1177.
- 43 A. D. Becke, *J. Chem. Phys.*, 1993, **98**, 1372.
- 44 R. Caballol, O. Castell, F. Illas, J. P. Malrieu and I. P. R. de Moreira, *J. Phys. Chem. A*, 1997, **101**, 7860.
- 45 J. Paier, M. Marsman and G. Kreese, *J. Chem. Phys.*, 2007, **127**, 024103.
- 46 M. Atanasov, B. Delley, F. Neese, P. L. Tregenna-Piggott and M. Sgrist, *Inorg. Chem.*, 2011, **50**, 2112.
- 47 D. A. Pantazis, M. Orío, T. Petrenko, S. Zein, E. Bill, W. Lubitz, J. Messinger and F. Neese, *Chem.–Eur. J.*, 2009, **15**, 5108.
- 48 (a) M. Orío, D. A. Pantazis, T. Petrenko and F. Neese, *Inorg. Chem.*, 2009, **48**, 7251; (b) D. A. Pantazis, V. Krewald, M. Orío and F. Neese, *Dalton Trans.*, 2010, **39**, 4959.
- 49 (a) D. A. Pantazis, M. Orío, T. Petrenko, S. Zein, W. Lubitz, J. Messinger and F. Neese, *Phys. Chem. Chem. Phys.*, 2009, **11**, 6788; (b) J. Tao, J. P. Perdew, V. N. Staroverov and G. E. Scuseria, *Phys. Rev. Lett.*, 2003, **91**, 146401; (c) V. N. Staroverov, G. E. Scuseria, J. Tao and J. P. Perdew, *J. Chem. Phys.*, 2003, **119**, 12129.
- 50 M. Mödl, M. Dolg, P. Fulde and H. Stoll, *J. Chem. Phys.*, 1997, **106**, 1836.
- 51 (a) J. M. Mouesca, L. Noodleman and D. A. Case, *Int. J. Quantum Chem., Quantum Biol. Symp.*, 1995, **22**, 95; (b) J. P. Daudey, P. de Loth and J. P. Malrieu, in *Magnetic Structural Correlation in Exchange Coupled Systems*, NATO Symposium, ed. D. Gatteschi, O. Kahn and R. D. Willett, Reidel, Dordrecht, 1984.
- 52 (a) K. Andersson, P.-A. Malmqvist, B. O. Roos, A. J. Sadlej and K. Wolinski, *J. Phys. Chem.*, 1990, **94**, 5483; (b) K. Andersson, P.-A. Malmqvist and B. O. Roos, *J. Chem. Phys.*, 1992, **96**, 1218; (c) C. de Graaf, C. Sousa, I. P. R. de Moreira and F. Illas, *J. Phys. Chem. A*, 2001, **105**, 11371.
- 53 C. J. Calzado, A. Celestino, R. Caballol and J. P. Malrieu, *Theor. Chem. Acc.*, 2010, **126**, 185.
- 54 (a) J. Miralles, J. P. Daudey and R. Caballol, *Chem. Phys. Lett.*, 1992, **198**, 555; (b) J. Miralles, O. Castell, R. Caballol and J. P. Malrieu, *Chem. Phys.*, 1993, **172**, 33.
- 55 C. de Graaf, R. Broe and W. C. Nieuwpoort, *Chem. Phys. Lett.*, 1997, **271**, 372.
- 56 M. J. Frisch, G. W. Trucks, H. B. Schlegel, G. E. Scuseria, M. A. Robb, J. R. Cheeseman, G. Scalmani, V. Barone, B. Mennucci, G. A. Petersson, H. Nakatsuji, M. Caricato, X. Li, H. P. Hratchian, A. F. Izmaylov, J. Bloino, G. Zheng, J. L. Sonnenberg, M. Hada, M. Ehara, K. Toyota, R. Fukuda, J. Hasegawa, M. Ishida, T. Nakajima, Y. Honda, O. Kitao, H. Nakai, T. Vreven, J. A. Montgomery Jr, J. E. Peralta, F. Ogliaro, M. Bearpark, J. J. Heyd, E. Brothers, K. N. Kudin, V. N. Staroverov, R. Kobayashi, J. Normand, K. Raghavachari, A. Rendell, J. C. Burant, S. S. Iyengar, J. Tomasi, M. Cossi, N. Rega, N. J. Millam, M. Klene, J. E. Knox, J. B. Cross, V. Bakken, C. Adamo, J. Jaramillo, R. Gomperts, R. E. Stratmann, O. Yazyev, A. J. Austin, R. Cammi, C. Pomelli, J. W. Ochterski, R. L. Martin, K. Morokuma, V. G. Zakrzewski, G. A. Voth, P. Salvador, J. J. Dannenberg, S. Dapprich, A. D. Daniels, Ö. Farkas, J. B. Foresman, J. V. Ortiz, J. Cioslowski and D. J. Fox, *Gaussian 09, Revision A.1*, Gaussian, Inc., Wallingford CT, 2009.
- 57 N. M. O'Boyle, A. L. Tenderholt and K. M. Langner, *J. Comput. Chem.*, 2008, **29**, 839.
- 58 (a) M. P. Castellani, S. J. Geib, A. L. Rheingold and W. C. Trogler, *Organometallics*, 1987, **6**, 1703; (b) A. Stroppa, P. Barone, P. Jain, J. M. Perez-Mato and S. Picozzi, *Adv. Mater.*, 2013, **25**, 2284.
- 59 J. M. Gruschus and A. Kuki, *J. Phys. Chem.*, 1993, **97**, 5581.
- 60 (a) V. Staemmler and K. Fink, *Chem. Phys.*, 2002, **278**, 79; (b) H. Stoll and K. Doll, *J. Chem. Phys.*, 2012, **136**, 074106.
- 61 J. Noga, P. Baňacký, S. Biskupič, R. Boča, P. Pelikán, M. Svrček and A. Zajac, *J. Comput. Chem.*, 1999, **20**, 253.
- 62 (a) K. Yoshizawa and R. Hoffmann, *J. Chem. Phys.*, 1995, **103**, 1216; (b) W. J. Wang, K. L. Yao and H. Q. Lin, *J. Chem. Phys.*, 1998, **108**, 2867.
- 63 D. J. Bicout and E. Kats, *Phys. Lett. A*, 2002, **300**, 479.
- 64 I. P. R. de Moreira, F. Illas and R. L. Martin, *Phys. Rev. B: Condens. Matter Mater. Phys.*, 2002, **65**, 155102.
- 65 R. Impropa, K. N. Kudin, G. E. Scuseria and V. Barone, *J. Am. Chem. Soc.*, 2002, **124**, 113.
- 66 J. S. Miller, A. J. Epstein and W. M. Reiff, *Chem. Rev.*, 1988, 201.
- 67 (a) C. J. Cramer and D. G. Truhlar, *Phys. Chem. Chem. Phys.*, 2009, **11**, 10757; (b) M. Marsman, J. Paier, A. Stroppa and G. Kresse, *J. Phys.: Condens. Matter*, 2008, **20**, 064201; (c) A. Stroppa and S. Picozzi, *Phys. Chem. Chem. Phys.*, 2010, **12**, 5405.
- 68 S. Gangopadhyay, A. E. Masunov, E. Poalelungi and M. N. Leuenberger, *J. Chem. Phys.*, 2010, **132**, 244104.
- 69 C. Ederer and M. Komelj, *Phys. Rev. B: Condens. Matter Mater. Phys.*, 2007, **76**, 064409.
- 70 C. M. Wynn, M. A. Girtu, W. B. Brinckerhoff, K.-I. Suguira, J. S. Miller and A. J. Epstein, *Chem. Mater.*, 1997, **9**, 2156.
- 71 J. S. Miller, *J. Mater. Chem.*, 2010, **20**, 1846.
- 72 E. Stryjewski and N. Giordano, *Adv. Phys.*, 1977, **26**, 487.

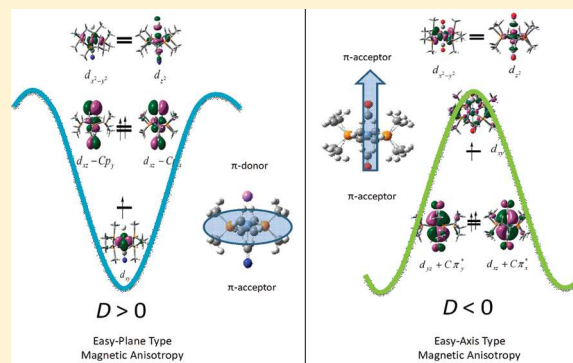
Ligand Effects toward the Modulation of Magnetic Anisotropy and Design of Magnetic Systems with Desired Anisotropy Characteristics

Tamal Goswami and Anirban Misra*

Department of Chemistry, University of North Bengal, Siliguri, Darjeeling 734013, West Bengal, India

S Supporting Information

ABSTRACT: Magnetic anisotropy of a set of octahedral Cr(III) complexes is studied theoretically. The magnetic anisotropy is quantified in terms of zero-field splitting (ZFS) parameter D , which appeared sensitive toward ligand substitution. The increased π -donation capacity of the ligand enhances the magnetic anisotropy of the complexes. The axial π -donor ligand of a complex is found to produce an easy-plane type ($D > 0$) magnetic anisotropy, while the replacement of the axial ligands with π -acceptors entails the inversion of magnetic anisotropy into the easy-axis type ($D < 0$). This observation enables one to fabricate a single molecule magnet for which easy-axis type magnetic anisotropy is an indispensable criterion. The equatorial ligands are also found to play a role in tuning the magnetic anisotropy. The magnetic anisotropy property is also correlated with the nonlinear optical (NLO) response. The value of the first hyperpolarizability varies proportionately with the magnitude of the ZFS parameter. Finally, it has also been shown that a rational design of simple octahedral complexes with desired anisotropy characteristics is possible through the proper ligand selection.

**■ INTRODUCTION**

Magnetically interacting open-shell transition metal ion clusters have been a topic of thorough investigation in the past few decades, which has caused the divergent areas of chemistry and physics to meet.¹ Interesting catalytic, biochemical, and physical properties of paramagnetic metal complexes have drawn the attention of many researchers and material scientists.² Magnetic materials based on molecular lattices, rather than continuous lattices of classical magnets, have been designed and synthesized.³ Recently, polynuclear clusters assembled from mononuclear coordination complexes have become a subject of increased interest since it is relevant for the study of “single-molecule magnets” (SMMs).⁴ A phenomenon hindering spin inversion causes certain molecules to exhibit slow relaxation of the magnetization after removal of an applied magnetic field, thus showing SMM behavior.^{5,6} The discovery that some metal coordination clusters may behave as SMMs^{5,7,8} has provoked plentiful research in the direction of their potential applications in high-density information storage and quantum computing.^{9–11}

The genesis of SMM behavior is a large easy-axis magnetic anisotropy and concomitant high energy barrier that needs to be overcome for the reversal of the magnetic moment. The barrier to reorient spin in magnetic molecules can be given by $|D|S^2$ for molecules with integer spins and $|D|(S^2 - 1/4)$ for molecules with half integer spins, where D is the zero-field splitting (ZFS) parameter and S is the ground state spin.¹² Molecular systems containing a large number of paramagnetic centers with significant negative D are the most suitable

candidates to be used as SMMs.⁵ However, most of these species show either low negative or positive D value in spite of having high ground state spin. Recently, a few lanthanide complexes have been reported to show slow magnetic relaxation behavior. For example, phthalocyanine double-decker complexes with Tb(IV) and Er(III) encapsulated in a polyoxometalate framework exhibit an extremely high negative anisotropy barrier.^{13,14} Several complexes of Fe(II), U(III) and Dy(III) also show similar characteristics.^{15–17} Another novel class of nanomagnets called the single-chain magnets (SCMs), can be formed by combination of the SMMs.^{18–23} A series of one-dimensional cyano-bridged coordination solids $(DMF)_4MReCl_4(CN)_2$, with $M = Mn, Fe, Co, Ni$, have been reported to show a slow relaxation of magnetization.²⁴ Moreover, in the combination of SMMs in which the easy-axes of anisotropies are linked in a parallel manner, can lead to a large easy-axis type ($D < 0$) anisotropy in the long-chain range, and manifestation of a slow relaxation of magnetization can occur.²⁵

The dependence of the ZFS parameter (D) on the nature of ligands has long been a subject of enormous interest.²⁶ For example, the synthesis and characterization of a series of high-spin hexa-coordinated dihalide Mn(II) complexes $[Mn(tpa)X_2]$ ($tpa = \text{tris-2-picolyamine}$; $X = I, Br, \text{ and } Cl$) advocate for the presence of such ligand effects showing an increase in the D

Received: January 19, 2012

Revised: May 6, 2012

Published: May 8, 2012

value with I relative to that with Br and Cl ($D_I > D_{Br} > D_{Cl}$).^{26b} Recently Karunadasa et al. have shown the variation in magnetic anisotropy in a few pseudo-octahedral first-row transition metal complexes by varying ligands.²⁷ A series of octahedral complexes $[\text{Cr}(\text{dmpe})_2(\text{CN})\text{X}]^+$ (dmpe = 1,2-bis-(dimethylphosphino)ethane, X = Cl, Br, I) and $\text{Cr}(\text{dmpe})_2(\text{CN})\text{X}$ (X = Cl, I) has been studied, and a similar trend as that discussed above has been observed. Logically, the observed trends can be attributed to factors such as changes in *d*-orbital splitting with the nature of the halide, the influence of ligand spin-orbit coupling, and so on. A simple computational model may be useful for a clear analysis of the observed changes in *D* as a function of the nature of the ligands. One of the interesting properties that such types of organometallic complexes manifest is the nonlinear optical (NLO) property.²⁸ Molecular NLO materials are of considerable scientific interest due to their potential application in the field of optoelectronics and all-optical data processing technologies.^{29,30} In a number of works, the magnetic property of materials has been related to the NLO response.^{31,32} Therefore, it can be intuited that there exists a correlation between NLO response and ZFS parameter.

In order to understand the effect of the ligands to tune the magnetic anisotropy in transition metal complexes, a systematic DFT study was carried out on a few chosen systems (Figure 1).

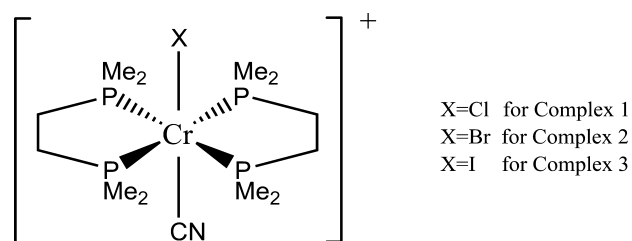


Figure 1. Structures of the octahedral complexes $[\text{Cr}(\text{dmpe})_2(\text{CN})\text{X}]^+$, (X = Cl, Br, I for complexes 1, 2, and 3, respectively).

The observed trends in the *D* values of the octahedral complexes $[\text{Cr}(\text{dmpe})_2(\text{CN})\text{X}]^+$ (dmpe = 1,2-bis-(dimethylphosphino)ethane, X = Cl, Br, I) enable one to estimate the contribution of the halides toward the ZFS of the whole molecule. Such contributions of the ligands are correlated with the energy difference between the highest occupied molecular orbital (HOMO) and lowest unoccupied molecular orbital (LUMO), and second-order NLO response. A positive value of *D* would correspond to an easy-plane type (i.e., $D > 0$) magnetic anisotropy. On the other hand, a negative value relating to the easy-axis type (i.e., $D < 0$) magnetic anisotropy would make the systems more interesting for various applications. As a logical consequence, the second part of our work involves the study of the magnetic nature of the complexes in which both the axial positions of the complex are replaced either by π -donor or π -acceptor ligands to inspect the magnetic nature of the complexes as a function of ligand substitution.

THEORETICAL BACKGROUND

Magnetic anisotropy leads to the splitting of $2S+1$ magnetic sublevels even in the absence of an external magnetic field, and this phenomenon is called ZFS. The degeneracy of the M_s states is lifted due to ZFS in molecules having $S > 1/2$. Prediction of the ZFS in transition-metal complexes using density functional theory (DFT)-based methods has been a

subject of scientific interest.^{26b} The uncoupled perturbation theoretical approach in the framework of unrestricted Kohn-Sham formalism is adopted to determine the spin-orbit coupling contribution to ZFS.³³ The second-order correction to the total energy of a system due to spin-orbit coupling can be expressed as³⁴

$$\Delta_2 = \sum_{\sigma\sigma'} \sum_{ij} M_{ij}^{\sigma\sigma'} S_i^{\sigma\sigma'} S_j^{\sigma'\sigma} \quad (1)$$

where σ is used to denote different spin degrees of freedom and *i* and *j* denote coordinate labels, *x*, *y*, and *z*. Here $S_i^{\sigma\sigma'}$ is defined as

$$S_i^{\sigma\sigma'} = \langle \chi^\sigma | S_i | \chi^{\sigma'} \rangle \quad (2)$$

χ^σ and $\chi^{\sigma'}$ are a set of spinors that are constructed from a unitary transformation on the S_z eigenstates. The matrix elements $M_{ij}^{\sigma\sigma'}$ are described as

$$M_{ij}^{\sigma\sigma'} = - \sum_{kl} \frac{\langle \varphi_{l\sigma} | V_i | \varphi_{k\sigma'} \rangle \langle \varphi_{k\sigma'} | V_j | \varphi_{l\sigma} \rangle}{\epsilon_{l\sigma} - \epsilon_{k\sigma'}} \quad (3)$$

In this equation, $\varphi_{l\sigma}$ and $\varphi_{k\sigma'}$ are occupied and unoccupied states with energies $\epsilon_{l\sigma}$ and $\epsilon_{k\sigma'}$, respectively. The operator V_x is related to the derivative of coulomb potential. In the absence of magnetic field, the change in energy of the system in the second-order can be written as

$$\Delta_2 = \sum_{ij} \gamma_{ij} \langle S_i \rangle \langle S_j \rangle \quad (4)$$

Diagonalizing the anisotropy tensor γ , one can obtain the eigenvalues γ_{xx} , γ_{yy} , and γ_{zz} and, consequently, the second-order perturbation energy can be written as

$$\begin{aligned} \Delta_2 = & \frac{1}{3}(\gamma_{xx} + \gamma_{yy} + \gamma_{zz})S(S+1) \\ & + \frac{1}{3} \left[\gamma_{zz} - \frac{1}{2}(\gamma_{xx} + \gamma_{yy}) \right] [3S_z^2 - S(S+1)] \\ & + \frac{1}{2}(\gamma_{xx} - \gamma_{yy})(S_x^2 - S_y^2) \end{aligned} \quad (5)$$

Parameterization of the anisotropy tensor components (γ_{xx} , γ_{yy} , γ_{zz}) with *D* and *E*, which are the axial and the rhombic ZFS parameters, respectively, gives rise to the following simplified expression:

$$H_{\text{ZFS}} = D \left[S_z^2 - \frac{1}{3}S(S+1) \right] + E[S_x^2 - S_y^2] \quad (6)$$

The sign of the axial ZFS parameter *D* is important in determining the nature of the magnetic property associated with the system. For a positive value of *D*, the system cannot show magnetic phenomena, and the magnetic anisotropy is termed easy-plane anisotropy. On the other hand, the negative value of *D* is the basic requirement for a material to become SMM.³⁵

COMPUTATIONAL DETAILS

Single-point calculations on the chosen octahedral Cr(III)-complexes (Figure 1) are carried out on the crystallographic geometries obtained from ref 27. Following the methodology proposed by Pederson and Khanna,³⁴ the ORCA³⁶ code is used to calculate the ZFS tensor in DFT formalism. We have calculated the ZFS parameters using the BPW91 functional,³⁷

and TZV basis set,³⁸ and taking advantage of the resolution of the identity (RI) approximation with the auxiliary TZV/J Coulomb fitting basis set,³⁹ under unrestricted Kohn–Sham formalism. This methodology, as adopted in this work, is being widely used to compute the ZFS parameter.^{37b,c,40} Although there are several methods available for the computation of the ZFS parameter, the Pederson and Khanna (PK) method is known to produce the correct sign of the ZFS parameter.^{37b,c} Moreover, it has also been observed that the ZFS contributions predicted by this method show fair agreement with accurate *ab initio* and experimental results. With regard to the computation of the ZFS parameter, other DFT methods that are being used are Neese’s quasi-restricted (QR) approach,⁴¹ and the coupled-perturbed spin orbit coupling (CP-SOC) method.⁴² Recently, some more sophisticated *ab initio* techniques have proven to produce excellent results.⁴³ Nevertheless, the justification of using the PK method in the case of Mn(II) systems by Neese and co-workers solicits for the selection of this method in the present work.³³ Earlier studies have concluded that magnetic anisotropy values have strong dependence on the functionals; however, the same is less dependent on basis sets.^{37a,44} It has also been previously explained that the performance of the nonhybrid functionals toward the prediction of the *D* parameter is excellent.⁴⁵ Thus it can be expected that the BPW91 functional will be a good choice for the calculation of the ZFS parameter, which has also been shown by Rodriguez et al.^{37b,c} The second-order NLO response β has been calculated using the Gaussian 09W⁴⁶ suite of software, using the same methodology as the ZFS parameter. As the Gaussian suit of software does not allow the use of TZV basis set for the element iodine, we supply the midi-x basis set as an extrabasis for the element iodine. The midi-x basis set is a heteroatom-polarized valence-double- ζ basis set that is known to be good at predicting partial atomic charges accurately.⁴⁷

RESULTS AND DISCUSSION

A. Role of π -Donation from Ligand. The ZFS parameters are computed for complexes 1, 2, and 3 (Figure 1). The agreement between the calculated and the experimental values can be followed from Table 1. The ZFS is known to arise from

Table 1. Experimental (D_{exp}) and Calculated (D_{calc}) ZFS Parameters for the Complexes 1, 2, and 3

complex	formula	$ D_{\text{exp}} $ (cm ⁻¹)	D_{calc} (cm ⁻¹)
1	[Cr(dmpe) ₂ (CN)Cl] ⁺	0.11	0.27
2	[Cr(dmpe) ₂ (CN)Br] ⁺	1.28	1.45
3	[Cr(dmpe) ₂ (CN)I] ⁺	2.30	5.66

small differences of various contributions; thus, a better agreement with the experimental results can rarely be expected.⁴⁸ However, the order of magnitude of the ZFS parameters are in parity with experimental observations. Moreover, similar to the experimental trend, the magnitude of *D* increases gradually from complex 1 to 3 in the present study. Although it is difficult to relate the electron pulling capacity of a ligand with the help of electronegativity of the ligand in the complex, the effect of covalency cannot be ignored. A covalent interaction of the central metal with the ligand aids in the delocalization of unpaired spins away from the metal.⁴⁹ This phenomenon is often explained through the orbital reduction factor *k*, which is defined by Stevens as the decrease in the orbital angular momentum of an unpaired

electron in the *d*-orbital.⁵⁰ Previously, it has been shown that the orbital reduction factor is associated with the time spent by the unpaired electron in the adjacent ligands.⁵¹ The orbital reduction factor is expressed as follows:

$$k = \frac{\langle \Psi_l | l | \Psi_l \rangle}{\langle d_i | l | d_i \rangle} \quad (7)$$

where *l* is the orbital angular momentum operator, and $|d\rangle$ and $|\Psi\rangle$ are free ion *d*-orbitals and molecular orbitals, respectively.⁵² However, *k* can be reduced to the following working equation for computational realization:

$$k = \frac{\sum_{i=1}^{2l+1} \sum_{\mu=1}^{2l+1} c(i, \mu)^2}{2l + 1} \quad (8)$$

for *l* = 2, *i* runs over *d* atomic orbitals (AOs) and μ runs over molecular orbitals (MOs) with dominant *d*-contributions, with $c(i, \mu)$ being the contribution of *i*th AO to the μ th MO.⁵³ The orbital reduction factor value obtained for complexes 1, 2, and 3 are 1.16, 0.95, and 0.85, respectively. A reduction in the orbital angular momentum from the free ion value can be taken as evidence of covalency between the central ion and the ligand ion.⁵⁴ Following Pellow and Vala,⁵⁵ it clearly appears that the value of orbital reduction factor is dependent on the ratio of the metal and the ligand spin–orbit coupling. Hence, a smaller value of the orbital reduction factor depicts a larger spin–orbit coupling contribution from the ligand to the overall magnetic anisotropy characteristics of the complex. Although the conventional orbital reduction factor has values within 0 and 1, a *k* value larger than 1 can arise due to the admixture of states with different multiplicity.⁵⁶ A value of *k* greater than 1 signifies that the spin–orbit coupling of the complex is greater than the free ion value.⁵⁵ This point has been explained thoroughly by Griffith on the basis of the delocalization of the *d*-orbitals.^{56b} The halogen ligands are also known for their π -donation ability, which increases down the halogen group. Hence gradual increase in the magnitude of *D* parameter can primarily be attributed to the π -donation strength or the basicity of the halide ligands.

The ZFS parameters are usually understood in the framework of ligand-field (LF) theory as many other properties of transition metal complexes.³³ In an octahedral field, the degenerate *d*-orbitals of the metal ion is split into two levels, namely, t_{2g} and e_g . The ground state of Cr(III) in an octahedral environment has the electronic configuration t_{2g}^3 which gives rise to the $^4A_{2g}$ state. The three unpaired electrons in this d^3 system remain in the nonbonding d_{xy} , d_{yz} , and d_{zx} orbitals of the t_{2g} group. There are six one-electron promotions that give rise to $^4T_{1g}$ and $^4T_{2g}$ excited states. These two states are different in energy, but only the $^4T_{2g}$ state can couple to the ground state.⁵⁷ However $t_{2g}^2 e_g^1$ configuration corresponds to a 4T state, and, particularly, these excitations within the metal *d*-shell make the most important contributions to the ZFS.⁵⁸ Four types of excitations that are found to contribute to the *D* tensor are SOMO–VMO ($\alpha \rightarrow \alpha$), SOMO–SOMO ($\alpha \rightarrow \beta$), DOMO–VMO ($\beta \rightarrow \alpha$), and DOMO–SOMO ($\beta \rightarrow \beta$), where SOMO, VMO, and DOMO refer to singly occupied, virtual, and doubly occupied MOs, respectively. In the unrestricted formalism, all the orbitals are singly occupied by up-spin or down-spin. Thus, the SOMOs are referred to as those occupied up-spin MOs that do not have any population in their down-spin counter parts. Similarly, those orbitals having population in both the up and their corresponding down spin MOs are considered here as

DOMOs. In Table 2, these individual excitation contributions to the D are listed. It can be seen from Table 2 that all the

Table 2. Individual Excitation Contribution to the Total ZFS Parameter D

complexes	SOMO→SOMO ($\alpha \rightarrow \beta$)	DOMO→VMO ($\beta \rightarrow \alpha$)	SOMO→VMO ($\alpha \rightarrow \alpha$)	DOMO→SOMO ($\beta \rightarrow \beta$)
complex 1	0.02	-0.35	0.29	0.31
complex 2	1.53	-4.78	3.64	1.06
complex 3	11.87	-25.22	17.99	1.02

individual contributions are more or less in accordance with the experimentally observed trend in the values of ZFS parameters, i.e., these contributions also increase from Cl to I in almost all cases. The crucial dependence of the ZFS parameter on various important $d \rightarrow d$ excited states, involving spin-allowed and forbidden intra-SOMO spin flip excitations can be observed from Table 2.⁵⁹ Among the four excitations, two important contributions stem from $\alpha \rightarrow \alpha$ and $\beta \rightarrow \alpha$ excitations, which correspond to the SOMO→VMO and DOMO→VMO transitions, respectively. The first one has maximum positive contribution toward the overall D of the molecule, while the DOMO → VMO has the highest negative contribution for the same. The magnetic response of the electronic ground state is largely determined by the $d-d$ excited states of the same multiplicity as that of the ground state.⁵⁸ The HOMO → LUMO transition is so spin conserving that the $d-d$ transition can exclusively be made responsible for the ZFS.⁴¹ This observation draws our attention to the HOMO–LUMO gap of the molecules, where HOMO is the highest energy SOMO. TDDFT calculations for the study of the $d-d$ vertical excitations are carried out with the same basis set and functional to see which of these excitations are most important for the ZFS. The TDDFT results (see Supporting Information) for all three complexes reveal that, among the $d-d$ transitions, those transitions that correspond to the highest oscillator strength are HOMO–LUMO transitions.

The HOMOs in all three cases are $p\pi-d\pi$ antibonding orbitals (Figure 2), while the LUMOs are mainly concentrated



Figure 2. The HOMOs and the LUMOs of the octahedral Cr(III) complexes. The equatorial ligands are in tube form for clarity.

on the metal d -orbitals with no contribution from the ligands. Since the LUMOs, mainly composed of metal $d_{x^2-y^2}$ orbitals, are not in a desired orientation to interact with halides, they are found to be almost constant in energy with the variation in halides (Figure 3). Interaction of halide p -orbitals with the metal d -orbitals leads to destabilization of those orbitals by mixing with them in an antibonding fashion. The extent of destabilization increases with the donation property of the halide π -donor. Hence, the HOMO–LUMO gap eventually

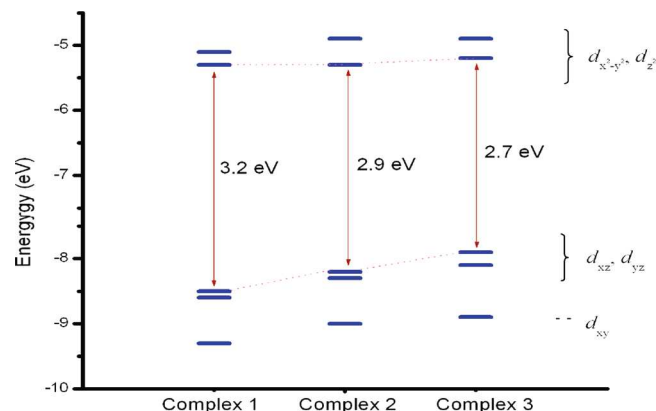


Figure 3. Decrease in the HOMO–LUMO gap on going from complex 1 to complex 3, with the increase in π -donation strength from Cl to I.

reduces from the chloride complex to the iodide complex (Figure 3). Thus, it is expected that in case of the chloride complex, the D value will be lowest in magnitude as the denominator in eq 3 is largest. Hence the increase in the D value from complex 1 to 3 is justifiable from the standpoint of the reducing HOMO–LUMO gap.

Moreover, a reduction in the HOMO–LUMO gap has its manifestation in the NLO properties of materials.³¹ This single parameter, the HOMO–LUMO gap, is established as a key factor to tune both the magnetic behavior and the NLO response simultaneously.³¹ Electronic charge-transfer transition is responsible for NLO response in materials. Analysis of the results obtained from the calculation of the second-order NLO response reveals that there is a unidirectional charge-transfer transition, as one particular tensorial component of β , namely β_{zzz} is the dominating term, with z -axis being parallel to the metal halogen bond.⁶⁰ A good π -donation from the ligand increases the diffusibility of the electronic cloud in between the metal and the ligand, which in turn is responsible for the hyperpolarizability of the molecule. Hence, the physical origin of the high β_{zzz} for complex 3 can be correlated with the strong π -donation ability of iodine. On the other hand, it is clear from eq 3 that the denominator of the tensorial component of magnetic anisotropy corresponds to the energy difference between the occupied and unoccupied energy levels. In that case, an increase in first hyperpolarizability value can be envisaged as a tool toward the prediction of increasing magnetic anisotropy. Keeping this view in mind, we have also computed the first hyperpolarizability that is the second-order NLO response of the complexes. The first hyperpolarizability values are given in Table 3 along with the HOMO–LUMO energy gap. Scrutiny of Table 3 shows that as we go from complex 1 to complex 3 with increased π -donation of one axial ligand, the value of β_{zzz} is increased, showing the validity of the idea of

Table 3. The First Hyperpolarizability Values of Complexes 1, 2, and 3 and Corresponding HOMO–LUMO Gaps (ΔE_{HL})

complexes	HOMO–LUMO energy gap (ΔE_{HL}) (in eV)	hyperpolarizability (β_{zzz}) (in a.u.)
1	3.2	-146.61
2	2.9	-393.90
3	2.7	-546.01

getting a prediction over the magnitude of ZFS from the NLO response.

B. Effect of Individual Ligands toward the ZFS of a Molecule. The interaction of the π -donor ligand with the d -orbitals in the t_{2g} group is shown in Figure 4. The π -interaction

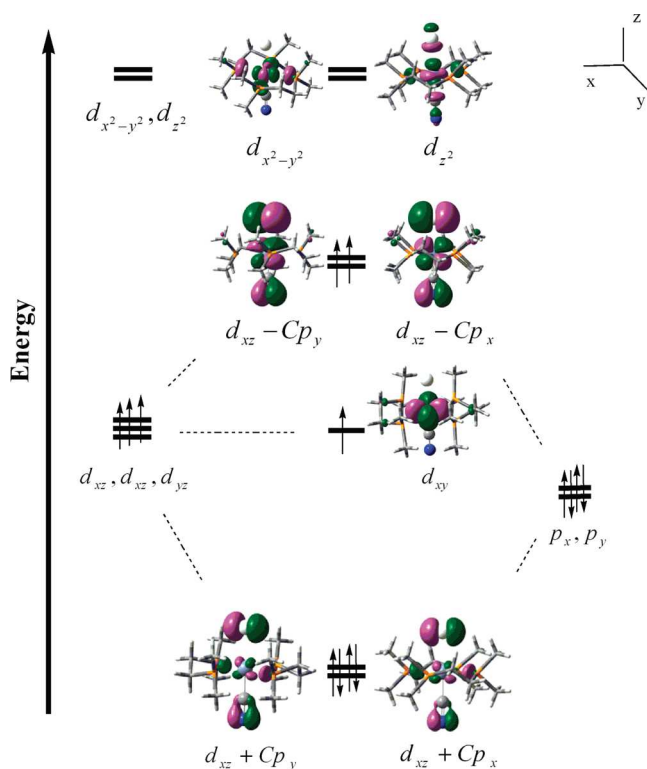


Figure 4. A qualitative MO diagram of $[\text{Cr}(\text{dmpe})_2(\text{CN})\text{X}]^+$ showing interaction of the metal d -orbitals with π -donor ligands.

lifts the SOMOs containing d_{xz} and d_{yz} orbitals upward by forming $p\pi-d\pi$ antibonding orbitals. In order to study the effect imparted by the ligands, a DFT calculation is performed by replacing the ligands of focus by point charges of same magnitude as that on the ligand. The purpose of this model is to nullify the π -interaction between the ligand orbitals and the metal d -orbitals. The charge in place of the ligand is retained to model the same crystal field environment as in the original complex and enforces a similar occupation of the orbitals.⁶¹ When the ligand is replaced by a point charge, the D value, which is denoted here as D_X , corresponds to the ZFS of the complex, excluding that specific ligand. The idea as coined by Neese and Solomon⁴⁷ is that the ligand contribution to the total D can be estimated from the difference of the D_X from the molecular D values. The use of point charges in the calculation of the electronic spectra of complexes is known as the “Sparkle” model.⁶² Hence, the method employing the point charge, described above, can be used as a scheme for getting a fingerprint of the ligand contribution toward the total SOC of the complex in the DFT framework. The results given in Table 4 depict that there is a considerable contribution from the halide ligands to the magnetic anisotropy of the complexes, i.e., the participation of the halide ligands in the spin–orbit coupling is very pronounced. The contribution from ligand is also increased from chloride to iodide. This result is quite consistent with the fact that, as iodine has a very heavy nucleus, the spin–orbit coupling imparted by this ligand will be higher

Table 4. The Values of the Total ZFS Parameter (D) and after Replacement of the Halide Ligands with Point Charges of the Same Magnitude (D_X with $X = \text{Cl}, \text{Br}, \text{and I}$)

complex	D (cm^{-1})	D_X (cm^{-1})
1	0.27	0.23
2	1.45	−0.14
3	5.66	−0.14

than bromide, which will in turn be greater than chloride. The comparison of the D values with and without π -donor explores that, in the cases of complexes 2 and 3, the halide ligands play a significant role to make the value of D positive and the replacement of ligand with point charge brings forth a negative D_X value. The π -acceptor ligand on the other side, which has been kept intact, may be responsible for the switch in the D value. However, for complex 1, the D_X value is not altered much and is of positive sign. This apparent anomaly in D_X values can be attributed to the altering electron availability at the Cr(III) atom, which in its turn increases the π -acceptor capacity of the CN^- ligand.⁶³ In the presence of a weak donor Cl^- ligand in complex 1, the π -accepting tendency of the CN^- is less efficient. Hence, in the case of complex 1, the cyanide ligand can not act as an effective π -acceptor, and, consequently, the effect is less prominent. As bromide or iodide effectively donates electrons to the metal ion, the electron density on the metal in complex 2 and 3 is much higher than that in complex 1. The availability of electrons in the metal ion in bromide and iodide complexes is much higher, and the π -accepting tendencies of the CN^- ligands are very similar. So, the replacement of these groups with point charge produces D values that differ so little that rounding off leads to the same value of D_X , and both are of negative sign. This reversal in D in the case of complexes 2 and 3 is explained below from the arrangement of the MOs and d -orbital splitting of the Cr(III) ion in the octahedral ligand field. At zero applied magnetic field, the ligand field Hamiltonian is written as

$$\hat{H}_{\text{LF}} = \Delta_{\text{ax}} \left[\hat{L}_z^2 - \frac{1}{3}L(L+1) \right] + \Delta_{\text{rh}} [\hat{L}_x^2 - \hat{L}_y^2] - A\lambda L \cdot S \quad (9)$$

where Δ_{ax} and Δ_{rh} are the axial and rhombic splitting parameters, respectively, λ is the spin–orbit coupling constant, and A is a constant having a value between 1.0 (strong ligand field) and 1.5 (weak ligand field).⁶⁴ The Δ_{ax} is the splitting of the d_{xy} -orbital relative to the d_{xz} and d_{yz} -orbitals ($\Delta_{\text{ax}} = E_{xz,yz} - E_{xy}$).⁶⁵ The sign of Δ_{ax} determines the sign of the D parameter. The positive sign of D requires Δ_{ax} to be positive, which indicates that the d_{xz} and d_{yz} -orbitals are at higher energy than the d_{xy} -orbital. A negative Δ_{ax} would certainly give rise to a state where the d_{xy} -orbital lies higher in the energy level diagram than the d_{xz} and d_{yz} -orbitals.⁶⁶ Figure 4 clearly explains the positive sign of the ZFS parameter in the cases of complexes 1, 2, and 3. Thus, the MO analysis of the complexes with different ligands can serve as a good indicator to forecast the sign of the ZFS parameter.

C. Effect of Axial Ligand Substitution. To examine the effect of π -donation and π -acceptance from the axial positions on the magnetic anisotropy of a complexes, two sets of test calculations were performed. The first set of calculations were carried out with complexes where both the axial positions occupied by π -donor ligands and the other set of calculations

are performed with the complexes containing π -acceptor ligands in axial positions.

SET-I. Set-I includes complexes of formula $[\text{Cr}(\text{dmpe})_2\text{L}_2]^+$, with $\text{L} = \text{Cl}, \text{Br}, \text{and I}$ (Figure 5). These structures are also

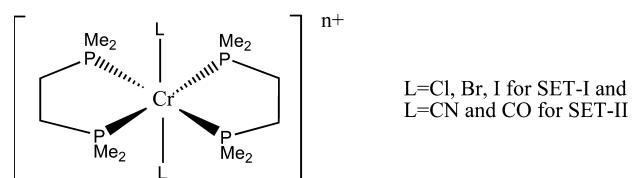


Figure 5. Schematic representation of the complexes used in SET-I and SET-II.

available in crystallographic information file format in ref 27. The intention to carry out the first set of calculations arose from the observation of Table 4, as there we can see that the presence of a π -donor is found to increase the value of D . Hence further replacement of the other axial ligand with the same π -donor is made, and the results are tabulated in Table 5.

Table 5. Calculated ZFS Parameters for Complex Series $[\text{Cr}(\text{dmpe})_2\text{X}_2]^+$, with $\text{X} = \text{Cl}, \text{Br}, \text{and I}$

$[\text{Cr}(\text{dmpe})_2\text{X}_2]^+$	calculated ZFS parameter D in cm^{-1}
$\text{L}=\text{Cl}$	0.38
$\text{L}=\text{Br}$	3.80
$\text{L}=\text{I}$	16.98

From the results it is clear that when both the axial ligands are halides, the magnitude of D is much higher than those complexes with only one halide ligand in an axial position. The d -orbital splitting in such complexes are such that the d_{xy} -orbital lies at a lower energy than the d_{xz} or d_{yz} -orbital, i.e., in these cases, Δ_{ax} is positive. The positive sign of the axial splitting parameter Δ_{ax} explains the positive ZFS value. It is also obvious from Tables 1 and 5 that this ligand effect is additive in nature.

SET-II. While the effect of the π -donor ligands can be understood as a controlling factor of the sign and magnitude of D , it is obvious that with a π -acceptor ligand, the sign of D would be negative. A negative D value is desired for making SMMs. So, this set of numerical experiment is carried out with the π -acceptor ligands in the axial positions, and ZFS parameters are calculated. The calculated values of D are kept in Table 6. A qualitative MO diagram for such set of complexes

Table 6. Calculated ZFS Parameters for Complex Series $[\text{Cr}(\text{dmpe})_2\text{L}_2]^{n+}$, with $\text{L} = \text{CN}$ and CO

$[\text{Cr}(\text{dmpe})_2\text{L}_2]^{n+}$	calculated ZFS parameter D in cm^{-1}
$[\text{Cr}(\text{dmpe})_2(\text{CN})_2]^+$	-0.09
$[\text{Cr}(\text{dmpe})_2(\text{CO})_2]^{3+}$	-0.14

is given in Figure 6. An alteration in the position of the singly occupied d_{xy} orbital in the energy spectrum of these complexes compared to that in Set-I complexes is observed. Hence, from the discussions given in the previous section, the change in the sign of the D values for this set of complexes can be explained. Moreover, a higher negative D is obtained with a stronger π -accepting carbonyl (CO) ligand. It has been reported previously that if easy-axis anisotropies are linked in tandem, they can lead to a large easy-axis type anisotropy in the long-chain range, and exhibition of a slow relaxation of magnet-

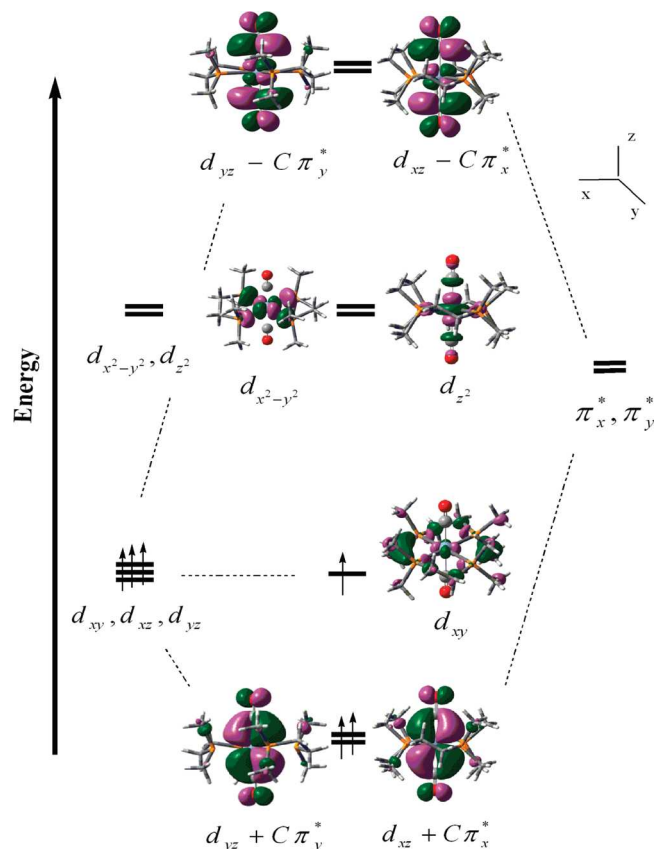


Figure 6. A qualitative MO diagram of $[\text{Cr}(\text{dmpe})_2(\text{CN})\text{X}/\text{CN}]^+$ showing interaction of the metal d -orbitals with π -acceptor ligands.

ization can be realized.²⁵ Hence it seems to be quite a general effect that, while a π -donor ligand causes an easy-plane anisotropy, a π -acid ligand on the other hand makes the nature of the anisotropy of the complexes to be of easy-axis type.

D. Effect of Equatorial Ligand Substitution. On the basis of the results of the numerical experiment employing point charge given in Table 4, the effect of the axial ligand substitution is carried out as described in the above sections. It seems from the discussion in Table 4 that the electron density on the metal ion is vital when π -acceptor ligands are employed from both axial positions. The greater the electron density on the metal, the more effective the π -acceptor ligands will be. The equatorial ligands here can aid in the increment of electron density on the central metal, which in turn can lead to greater π -acceptance of the axial ligands. Hence, for the verification of the above speculation, a few complexes are designed with two π -acceptor ligands in the axial positions, and the equatorial ligands are changed through the halides (Figure 7). The designed octahedral complexes contain chloride, bromide, and iodide ligands, respectively, in their equatorial positions. First

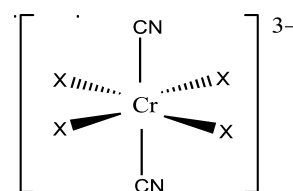


Figure 7. Schematic representation of the designed complexes where equatorial positions are replaced with halides ($\text{X} = \text{Cl}, \text{Br}, \text{and I}$).

we have tried out three octahedral Cr(III) complexes with CN^- as two axial ligands. Here we see that, as the donation from the equatorial ligands increase, the magnitude of the negative D is increased (Table 7). Thus following the interplay between the

Table 7. Calculated ZFS Parameters for Complex Series $[\text{CrX}_4(\text{CN})_2]^{3-}$, with $X = \text{Cl}, \text{Br},$ and I

$X =$	calculated ZFS parameter D in cm^{-1} for complex $[\text{CrX}_4(\text{CN})_2]^{3-}$
Cl	-0.13
Br	-0.69
I	-5.18

nature of the ligand and the axial crystal field splitting (Δ_{ax}), one can systematically change the magnetic anisotropy of a complex. To sum up, we can say that a negative D value can be achieved if there is sufficient donation of electrons from the equatorial ligands to the metal, so that a larger availability of electrons on the metal occurs and the designing of single molecule magnets with a high degree of magnetic anisotropy is possible by suitable placement of the π -acid ligands in the axial positions of octahedral metal complexes.

CONCLUSIONS

In the present work, the magnetic anisotropy property of a series of octahedral Cr(III) complexes is studied. It has been shown that π -donor and π -acceptor ligands, in the axial position of the octahedral complexes, have different effects on the magnetic anisotropy of the complexes. The interaction of the ligands with the metal d -orbitals gives rise to two different situations responsible for this kind of switch in the ZFS parameter. The π -donor ligands play a role in making the magnitude of ZFS larger with an increased π -donation from the halide ligands, while a π -acceptor ligand causes the anisotropy property to be of easy-axis type ($D < 0$). Moreover, a π -acceptor ligand in both the axial positions imparts single molecular magnetic nature to the system having an easy-axis of the magnetic anisotropy. An increased donation from the equatorial positions is seen to enhance the magnitude of easy-axis type magnetic anisotropy. This can be attributed to the increased π -accepting efficiency of the axial ligands due to an enhanced metallic electron density, pushed by the equatorial ligands. On the basis of the above observations regarding the ligand replacement, octahedral Cr(III) complexes can be designed in such a way that it can meet our desired anisotropy characteristics. The NLO response is found to vary with π -donation similarly as the magnetic anisotropy. The second-order NLO response, β , has been related to the magnetic anisotropy in the case of the noncentrosymmetric octahedral complexes, where we can see that the NLO response can lead us to good anticipation of magnetic anisotropy.

From the systematic DFT study with these octahedral complexes, a clear understanding about the influence of the ligands on modulating the magnetic anisotropy of the Cr(III) complexes is possible. For convenience, we perform a few numerical experimentations. The D value for $[\text{CrBr}_4(\text{CN})_2]^{3-}$, as we recollect from Table 7, is -0.69 cm^{-1} . We calculate the ZFS parameter for $[\text{CrBr}_4(\text{CO})_2]^-$, which comes out to be -2.51 cm^{-1} . Now relying on the above method of prediction, we design a complex of formula $[\text{CrBr}_4(\text{CN})(\text{CO})]^{2-}$ and expect the D value to be in between -0.69 cm^{-1} and -2.51 cm^{-1} and get a value of -0.94 cm^{-1} . Thus, from this observation, a general conclusion can be drawn that the

anisotropy of such metal complexes is greatly controlled by the ligands. To summarize, this work explicates a simple application of DFT to calculate anisotropy parameters in metal complexes to devise a rule of thumb for the occurrence of SMM behavior in such complexes.

ASSOCIATED CONTENT

Supporting Information

Calculated TDDFT results for the excitations of complexes 1, 2, and 3 are available in Tables S1, S2, and S3, respectively. The xyz coordinates of the complexes taken for numerical experiments and also the complexes with dicyano and dicarbonyl complexes are available. Complete reference of refs 11a, 11c, 12a, 30f, and 46 are also provided. This information is available free of charge via the Internet at <http://pubs.acs.org>.

AUTHOR INFORMATION

Corresponding Author

*E-mail: anirbanmisra@yahoo.com.

Notes

The authors declare no competing financial interest.

ACKNOWLEDGMENTS

The authors thank the Department of Science and Technology, India, for financial support.

REFERENCES

- (1) Kahn, O. *Molecular Magnetism*; VCH: New York, 1993.
- (2) Oshio, H.; Nakano, M. *Chem.—Eur. J.* **2005**, *11*, 5178–5185.
- (3) Gatteschi, D.; Sessoli, R. *J. Magn. Magn. Mater.* **2004**, *272–276*, 1030–1036.
- (4) Krzystek, J.; Ozarowski, A.; Telser, J. *Coord. Chem. Rev.* **2006**, *250*, 2308–2324.
- (5) (a) Sessoli, R.; Tsai, H. L.; Schake, A. R.; Wang, S.; Vincent, J. B.; Folting, K.; Gatteschi, D.; Christou, G.; Hendricson, D. N. *J. Am. Chem. Soc.* **1993**, *115*, 1804–1816. (b) Sessoli, R.; Gatteschi, D.; Caneschi, A.; Novak, M. A. *Nature* **1993**, *365*, 141–143.
- (6) (a) Gatteschi, D.; Sessoli, R.; Villain, J. *Molecular Nanomagnets*; Oxford University Press: New York, 2006. (b) Milios, C. J.; Vinslava, A.; Wernsdorfer, W.; Moggach, S.; Parsons, S.; Perlepes, S. P.; Christou, G.; Brechin, E. K. *J. Am. Chem. Soc.* **2007**, *129*, 2754–2755. (c) Freedman, D. E.; Jenkins, D. M.; Ivarone, A. T.; Long, J. R. *J. Am. Chem. Soc.* **2008**, *130*, 2884–2885. (d) Yoshihara, D.; Karasawa, S.; Koga, N. *J. Am. Chem. Soc.* **2008**, *130*, 10460–10461.
- (7) Gatteschi, D.; Caneschi, A.; Pardi, L.; Sessoli, R. *Science* **1994**, *265*, 1054–1058.
- (8) Aubin, S. M. J.; Wemple, M. W.; Adams, D. M.; Tsai, H. L.; Christou, G.; Hendricson, D. N. *J. Am. Chem. Soc.* **1996**, *118*, 7746–7754.
- (9) Ritter, S. K. *Chem. Eng. News* **2004**, *82*, 29–32.
- (10) (a) Garanin, D. A.; Chudnovsky, E. M. *Phys. Rev. B* **1997**, *56*, 11102–11118. (b) Leuenberger, M. N.; Loss, D. *Nature* **2001**, *410*, 789–793. (c) Jo, M. H.; Grose, J. E.; Baheti, K.; Deshmukh, M. M.; Sokol, J. J.; Rumberger, E. M.; Hendrickson, D. N.; Long, J. R.; Park, H.; Ralph, D. C. *Nano Lett.* **2006**, *6*, 2014–2020. (d) Ardavan, A.; Rival, O.; Morton, J. J. L.; Blundell, S. J.; Tyryshkin, A. M.; Timco, G. A.; Winpenny, R. E. P. *Phys. Rev. Lett.* **2007**, *98*, 572011–572014. (e) Bogani, L.; Wernsdorfer, W. *Nat. Mater.* **2008**, *7*, 179–186. (f) Stamp, P. C. E.; Gaita-Arino, A. *J. Mater. Chem.* **2009**, *19*, 1718–1730.
- (11) (a) Affronte, M.; Troiani, F.; Ghirri, A.; Candini, A.; Evangelisti, M.; Corradini, V.; Carretta, S.; Santini, P.; Amoretti, G.; Tuna, F.; et al. *J. Phys. D: Appl. Phys.* **2007**, *40*, 2999–3004. (b) Manoli, M.; Johnstone, R. D. L.; Parsons, S.; Murrie, M.; Affronte, M.; Evangelisti, M.; Brechin, E. K. *Angew. Chem., Int. Ed.* **2007**, *46*, 4456–4460.

- (c) Mannini, M.; Pineider, F.; Sainctavit, P.; Danieli, C.; Otero, E.; Sciancalepore, C.; Talarico, A. M.; Arrio, M. A.; Cornia, A.; Gatteschi, D.; et al. *Nat. Mater.* **2009**, *8*, 194–197. (d) Loth, S.; von Bergmann, K.; Ternes, M.; Otte, A. F.; Lutz, C. P.; Heinrich, A. J. *Nat. Phys.* **2010**, *6*, 340–344.
- (12) (a) Collison, D.; Murrie, M.; Oganessian, V. S.; Piligkos, S.; Poulton, N. R. J.; Rajaraman, G.; Smith, G. M.; Thomson, A. J.; Timko, G. A.; Wernsdorfer, W.; et al. *Inorg. Chem.* **2003**, *42*, 5293–5303. (b) Vallejo, J.; Castro, I.; Cañadillas-Delgado, L.; Ruiz-Pérez, C.; Ferrando-Soria, J.; Ruiz-García, R.; Cano, J.; Lloret, F.; Julve, M. *Dalton Trans.* **2010**, *39*, 2350–2358.
- (13) (a) AlDamen, M. A.; Clemente-Juan, J. M.; Coronado, E.; Marti-Gastaldo, C.; Gaita-Arino, A. J. *Am. Chem. Soc.* **2008**, *130*, 8874–8875. (b) AlDamen, M. A.; Cardona-Serra, S.; Clemente-Juan, J. M.; Coronado, E.; Gaita-Arino, A.; Marti-Gastaldo, C.; Luis, F.; Montero, O. *Inorg. Chem.* **2009**, *48*, 3467–3479.
- (14) (a) Branzoli, F.; Carretta, P.; Filibian, M.; Zoppellaro, G.; Graf, M. J.; Galan-Mascaros, J. R.; Fuhr, O.; Brink, S.; Ruben, M. J. *Am. Chem. Soc.* **2009**, *131*, 4387–4396. (b) Kyatskaya, S.; Galan-Mascaros, J. R.; Bogani, L.; Hennrich, F.; Kappes, M.; Wernsdorfer, W.; Ruben, M. J. *Am. Chem. Soc.* **2009**, *131*, 15143–15151.
- (15) Jiang, S. D.; Wang, B. W.; Su, G.; Wang, Z. M.; Gao, S. *Angew. Chem., Int. Ed.* **2010**, *49*, 7448–7451.
- (16) (a) Rinehart, J. D.; Long, J. R. *J. Am. Chem. Soc.* **2009**, *131*, 12558–12559. (b) Rinehart, J. D.; Meihaus, K. R.; Long, J. R. *J. Am. Chem. Soc.* **2010**, *132*, 7572–7573.
- (17) Freedman, D. E.; Harman, W. H.; Harris, T. D.; Long, G. J.; Chang, C. J.; Long, J. R. *J. Am. Chem. Soc.* **2010**, *132*, 1224–1225.
- (18) Clerac, R.; Miyasaka, H.; Yamashita, M.; Coulon, C. *J. Am. Chem. Soc.* **2002**, *124*, 12837–12844.
- (19) Ferbinteanu, M.; Miyasaka, H.; Wernsdorfer, W.; Nakata, K.; Sugiura, K.; Yamashita, M.; Coulon, C.; Clerac, R. *J. Am. Chem. Soc.* **2005**, *127*, 3090–3099.
- (20) Miyasaka, H.; Nezu, T.; Sugimoto, K.; Sugiura, K.; Yamashita, M.; Clerac, R. *Chem.–Eur. J.* **2005**, *11*, 1592–1602.
- (21) Kajiwara, T.; Nakano, M.; Kaneko, Y.; Takaishi, S.; Ito, T.; Yamashita, M.; Kamiyama, A. I.; Nojiri, H.; Ono, Y.; Kojima, N. *J. Am. Chem. Soc.* **2005**, *127*, 10150–10151.
- (22) Miyasaka, H.; Madanbashi, T.; Sugimoto, K.; Nakazawa, Y.; Wernsdorfer, W.; Sugiura, K.; Yamashita, M.; Coulon, C.; Clerac, R. *Chem.–Eur. J.* **2006**, *12*, 7028–7040.
- (23) Caneschi, A.; Gatteschi, D.; Lalioti, N.; Sangregorio, C.; Sessoli, R.; Venturi, G.; Vindigni, A.; Rettori, A.; Pini, M. G.; Novak, M. A. *Angew. Chem., Int. Ed.* **2001**, *40*, 1760–1763.
- (24) Harris, T. D.; Bennett, M. V.; Clerac, R.; Long, J. R. *J. Am. Chem. Soc.* **2010**, *132*, 3980–3988.
- (25) Nakano, M.; Oshio, H. *Chem. Soc. Rev.* **2011**, *40*, 3239–3248.
- (26) (a) Busey, R. H.; Sonder, E. *J. Chem. Phys.* **1962**, *36*, 93–97. (b) Desrochers, P. J.; Telsler, J.; Zvyagin, S. A.; Ozarowski, A.; Krzystek, J.; Vivic, D. A. *Inorg. Chem.* **2006**, *45*, 8930–8941. (c) Duboc, C.; Phoeung, T.; Zein, S.; Pecaut, J.; Collomb, M.-N.; Neese, F. *Inorg. Chem.* **2007**, *46*, 4905–4916.
- (27) Karunadasa, H. I.; Arquero, K. D.; Berben, L. A.; Long, J. R. *Inorg. Chem.* **2010**, *49*, 4738–4740.
- (28) Kanis, D. R.; Lacroix, P. G.; Ratner, M. A.; Marks, T. J. *J. Am. Chem. Soc.* **1994**, *116*, 10089–10102.
- (29) Zyss, J. *Molecular Nonlinear Optics: Materials, Physics and Devices*; Academic: Boston, MA, 1994; *Nonlinear Optical Properties of Matter: From Molecules to Condensed Phases*; Papadopoulos, M. G., Leszczynski, J., Sadlej, A. J., Eds.; Kluwer: Dordrecht, The Netherlands, 2005.
- (30) (a) Marder, S. R.; Gorman, C. B.; Meyers, F.; Perry, J. W.; Bourhill, G.; Brédas, J. L.; Pierce, B. M. *Science* **1994**, *265*, 632–635. (b) Marder, S. R. *Chem. Commun.* **2006**, 131–134. (c) Kang, H.; Evmenenko, G.; Dutta, P.; Clays, K.; Song, K.; Marks, T. J. *J. Am. Chem. Soc.* **2006**, *128*, 6194–6205. (d) Yang, M.; Champagne, B. J. *Phys. Chem. A* **2003**, *107*, 3942–3951. (e) Liao, Y.; Bhattacharjee, S.; Firestone, K. A.; Eichinger, B. E.; Paranj, R.; Anderson, C. A.; Robinson, B. H.; Reid, P. J.; Dalton, L. R. *J. Am. Chem. Soc.* **2006**, *128*, 6847–6853. (f) Kang, H.; Facchetti, A.; Jiang, H.; Cariati, E.; Righetto, S.; Ugo, R.; Zuccaccia, C.; Macchioni, A.; Stern, C. L.; Liu, Z.; et al. *J. Am. Chem. Soc.* **2007**, *129*, 3267–3286.
- (31) Paul, S.; Misra, A. *Inorg. Chem.* **2011**, *50*, 3234–3246.
- (32) (a) Cariati, E.; Ugo, R.; Santoro, G.; Tordin, E.; Sorace, L.; Caneschi, A.; Sironi, A.; Macchi, P.; Casati, N. *Inorg. Chem.* **2010**, *49*, 10894–10901. (b) Lacroix, P. G.; Malfant, I.; Bénard, S.; Yu, P.; Rivière, E.; Nakatani, K. *Chem. Mater.* **2001**, *13*, 441–449. (c) Dragonetti, C.; Righetto, S.; Roberto, D.; Ugo, R.; Valore, A.; Fantacci, S.; Sgamellotti, A.; Angelis, F. D. *Chem. Commun.* **2007**, 4116–4118. (d) Janjua, M. R. S. A.; Guan, W.; Yan, L.; Su, Z. -M.; Ali, M.; Bukhari, I. H. *J. Mol. Graph. Model.* **2010**, *28*, 735–745.
- (33) Zein, S.; Duboc, C.; Lubitz, W.; Neese, F. *Inorg. Chem.* **2008**, *47*, 134–142.
- (34) Pederson, M. R.; Khanna, S. N. *Phys. Rev. B* **1999**, *60*, 9566–9572.
- (35) Neese, F.; Pantazis, D. A. *Faraday Discuss.* **2011**, *148*, 229–238.
- (36) Neese, F.; Neese, F. *ORCA 2.8.0*; University of Bonn: Bonn, Germany, 2010.
- (37) (a) van Wüllen, C. *J. Chem. Phys.* **2009**, *130*, 194109. (b) Aquino, F.; Rodriguez, J. H. *J. Phys. Chem. A* **2009**, *113*, 9150–9156. (c) Aquino, F.; Rodriguez, J. H. *J. Chem. Phys.* **2005**, *123*, 204902.
- (38) (a) Schäfer, A.; Horn, H.; Ahlrichs, R. *J. Chem. Phys.* **1992**, *97*, 2571–2577. (b) Schäfer, A.; Huber, C.; Ahlrichs, R. *J. Chem. Phys.* **1994**, *100*, 5829–5835.
- (39) Weigend, F. *Phys. Chem. Chem. Phys.* **2006**, *8*, 1057–1065.
- (40) (a) Takeda, R.; Mitsuo, S.; Yamanaka, S.; Yamaguchi, K. *Polyhedron* **2005**, *24*, 2238–2241. (b) Kortus, J.; Pederson, M. R.; Baruah, T.; Bernstein, N.; Hellberg, C. S. *Polyhedron* **2003**, *22*, 1871–1876. (c) Park, K.; Pederson, M. R.; Richardson, S. L.; Aliaga-Alcalde, N.; Christou, G. *Phys. Rev. B* **2003**, *68*, 020405–1–020405–4. (d) Baruah, T.; Pederson, M. R. *Int. J. Quantum Chem.* **2003**, *93*, 324–331. (e) Ribas-Ariño, J.; Baruah, T.; Pederson, M. R. *J. Am. Chem. Soc.* **2006**, *128*, 9497–9505.
- (41) Neese, F. *J. Am. Chem. Soc.* **2006**, *128*, 10213–10222.
- (42) Neese, F. *J. Chem. Phys.* **2007**, *127*, 164112.
- (43) Maurice, R.; Sivalingam, K.; Ganyushin, D.; Guihéry, N.; de Graaf, C.; Neese, F. *Inorg. Chem.* **2011**, *50*, 6229–6236.
- (44) Reviakine, R.; Arbuznikov, A. V.; Tremblay, J. C.; Remenyi, C.; Malkina, O. L.; Malkin, V. G.; Kaupp, M. *J. Chem. Phys.* **2006**, *125*, 054110.
- (45) Misochko, E. Y.; Korchagin, D. V.; Bozhenko, K. V.; Chapyshev, S. V.; Aldoshin, S. M. *J. Chem. Phys.* **2010**, *133*, 064101.
- (46) Frisch, M. J.; Trucks, G. W.; Schlegel, H. B.; Scuseria, G. E.; Robb, M. A.; Cheesman, J. R.; Zakrzewski, V. G.; Montgomery, J. A.; Strtmann, R. E.; Burant, J. C. et al. *Gaussian 09*, revision A.02; Gaussian Inc.: Pittsburgh, PA, 2009.
- (47) (a) Easton, R. E.; Giesen, D. J.; Welch, A.; Cramer, C. J.; Truhlar, D. G. *Theor. Chim. Acta* **1996**, *93*, 281–301. (b) Li, J.; Cramer, C. J.; Truhlar, D. G. *Theor. Chem. Acc.* **1998**, *99*, 192–196. (48) Neese, F.; Solomon, E. I. *Inorg. Chem.* **1998**, *37*, 6568–6582. (49) Solomon, E. I. *Inorg. Chem.* **2006**, *45*, 8012–8025. (50) Stevens, K. W. H. *Proc. R. Soc. A (London)* **1953**, *219*, 542–555. (51) Nyholm, R. S. *Pure Appl. Chem.* **1968**, *17*, 1–19. (52) Tofield, B. C. *J. Phys. Colloq.* **1976**, *37*, C6–539–C6–570. (53) Atanasov, M.; Baerends, E. J.; Baettig, P.; Bruyndonckx, R.; Daul, C.; Rauzy, C.; Zbiri, M. *Chem. Phys. Lett.* **2004**, *399*, 433–439. (54) O'Reilly, T. J.; Offenbacher, E. L. *J. Chem. Phys.* **1971**, *54*, 3065–3076. (55) Pellow, R.; Vala, M. *J. Chem. Phys.* **1989**, *90*, 5612–5621. (56) (a) Debrunner, P. G.; Dexter, A. F.; Schulz, C. E.; Xia, Y. -M.; Hager, L. P. *Proc. Natl. Acad. Sci. U.S.A.* **1996**, *93*, 12791–12798. (b) Griffith, J. S. *Mol. Phys.* **1971**, *21*, 135–139. (57) Neese, F.; Solomon, E. I., *Magnetism: Molecules to Materials IV*; Miller, J. S., Drillon, M., Eds; Wiley-VCH: Weinheim, 2002; Chapter 9, p 406. (58) Schöneboom, J. C.; Neese, F.; Thiel, W. *J. Am. Chem. Soc.* **2005**, *127*, 5840–5853.

- (59) Maganas, D.; Sottini, S.; Kyritsis, P.; Groenen, E. J. J.; Neese, F. *Inorg. Chem.* **2011**, *50*, 8741–8754.
- (60) Kanis, D. R.; Ratner, M. A.; Marks, T. J. *Chem. Rev.* **1994**, *94*, 195–242.
- (61) Boguslawski, K.; Jacob, C. R.; Reiher, M. J. *Chem. Theory Comput.* **2011**, *7*, 2740–2752.
- (62) de Andrade, A. V. M.; da Costa, N. B., Jr.; Longo, R. L.; Malta, O. L.; Simas, A. M.; de Sá, G. F. *Mol. Eng.* **1997**, *7*, 293–308.
- (63) (a) Meissler, G. L.; Tarr, D. A. *Inorganic Chemistry*; Pearson Education and Pearson Prentice Hall: Upper Saddle River, NJ, 2004. (b) Caughey, W. S.; Eberspaecher, H.; Fuchsman, W. H.; McCoy, S.; Alben, J. O. *Ann. N.Y. Acad. Sci.* **1969**, *153*, 722–737.
- (64) Kittilstved, K. R.; Sorgho, L. A.; Amstutz, N.; Tregenna-Piggott, P. L. W.; Hauser, A. *Inorg. Chem.* **2009**, *48*, 7750–7764.
- (65) Solomon, E. I.; Brunold, T. C.; Davis, M. I.; Kemsley, J. N.; Lee, S.-K.; Lehnert, N.; Neese, F.; Skulan, A. J.; Yang, Y.-S.; Zhou, J. *Chem. Rev.* **2000**, *100*, 235–350.
- (66) Solomon, E. I.; Pavel, E. G.; Loeb, K. E.; Campochiaro, C. *Coord. Chem. Rev.* **1995**, *144*, 369–460.

CHEMISTRY

A European Journal

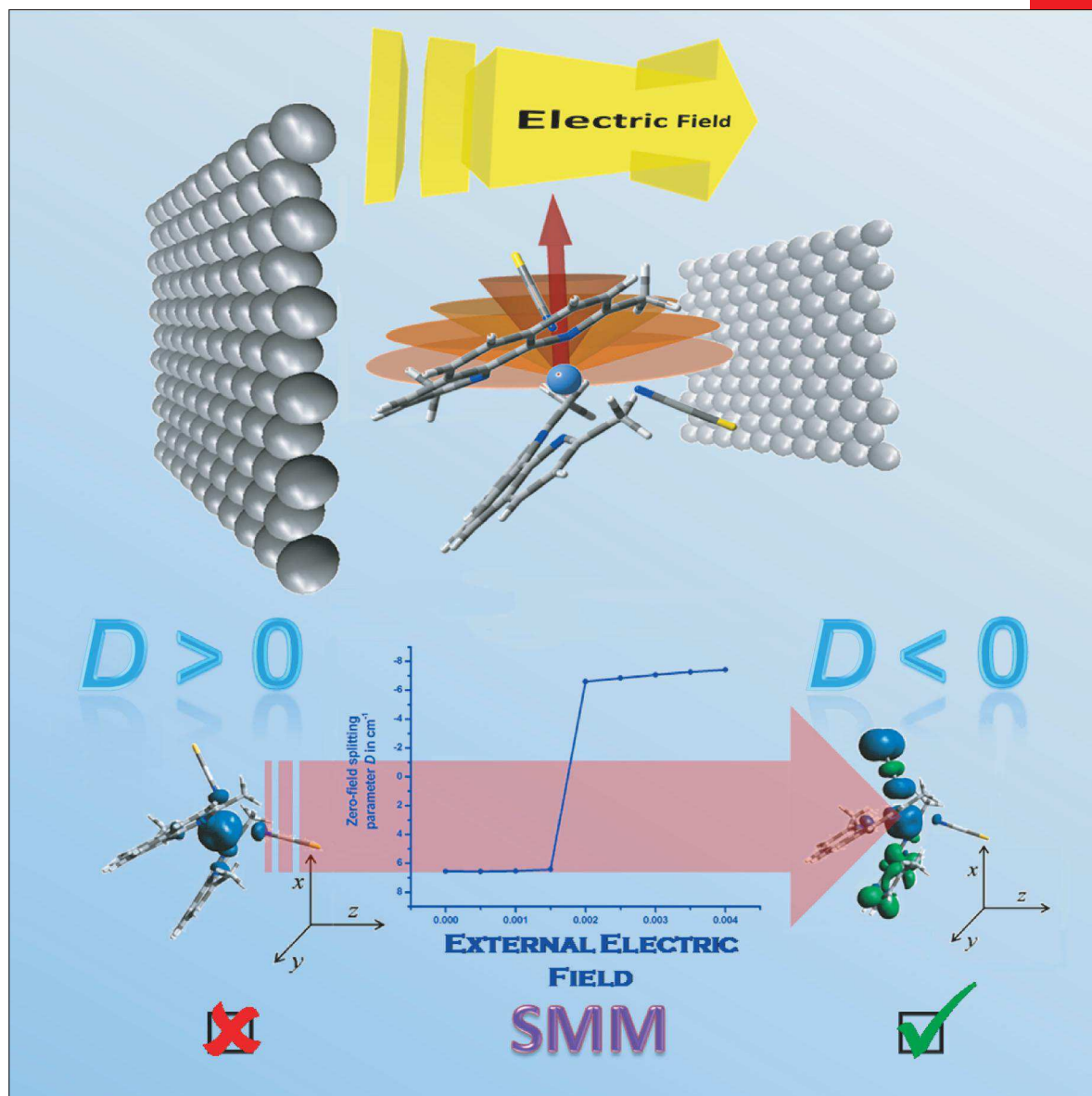
www.chemeurj.org

A Journal of



ChemPubSoc
Europe

2014-20/43



The tuning of spin-orbit coupling ...

... with external electric field and concomitant change in the magnetic anisotropy of a single-molecule magnet was observed. It has been shown by DFT calculations that the application of electric field can alter the magnetic anisotropy from "easy-plane" ($D > 0$) to "easy-axis" ($D < 0$) type. This phenomenon is also found to bring about "Spin-Hall" type of spin separation in single molecule. For more information, see the Full Paper by T. Goswami and A. Misra on page 13951 ff.

Supported by
ACES

WILEY-VCH

Density Functional Calculations | Very Important Paper |

VIP On the Control of Magnetic Anisotropy through an External Electric Field

Tamal Goswami and Anirban Misra*^[a]

Abstract: The effect of an external electric field on the magnetic anisotropy of a single-molecule magnet has been investigated, for the first time, with the help of DFT. The application of an electric field can alter the magnetic anisotropy from "easy-plane" to "easy-axis" type. Excitation analysis per-

formed through time-dependent DFT predicts that the external electric field facilitates metal to π -acceptor ligand charge transfer, leading to uniaxial magnetic anisotropy and concomitant spin Hall effect in a single molecule.

Introduction

Magnetic anisotropy is of central importance in the understanding of single-molecule magnets (SMM).^[1] Molecules that exhibit slow relaxation of their magnetization, leading to a magnetic hysteresis at low temperatures, are termed as SMMs.^[2] The genesis of this interesting magnetic property in a molecule is the existence of two ground states of magnetization $+M_s$ and $-M_s$ separated by an energy barrier. This bistability of the SMMs makes them indispensable in the domain of data storage^[3] and quantum computing.^[4] SMMs are often characterized by a large easy-axis-type magnetic anisotropy and concomitant high energy barrier (U), which restricts the reversal of the magnetization from $+M_s$ to $-M_s$. To reorient spin in the magnetic molecules, the barrier U can be given by $|D|S^2$ for molecules with integer spins and $|D|(S^2 - 1/4)$ for molecules with half integer spins. D is the zero-field splitting (ZFS) parameter and S is the ground-state spin. The large negative ZFS parameter (D) causes the spin (S) of the molecule to point along a preferred easy-axis and makes it a nanomagnet. The requirement of proper SMMs for apposite needs prompted researchers to study the tuning of magnetic anisotropy.

The most investigated molecule of this type is $[\text{Mn}_{12}\text{O}_{12}(\text{CH}_3\text{COO})_{16}(\text{H}_2\text{O})_4]$, which is popularly known as $\text{Mn}_{12}\text{-ac}$.^[5] A central tetrahedron of four Mn^{4+} ions ($S=3/2$) and eight surrounding Mn^{3+} ($S=2$) ions construct the magnetic core of $\text{Mn}_{12}\text{-ac}$. This compound, which was first synthesized by Lis,^[6] has drawn the attention of the scientific community because it has a strikingly large molecular magnetic moment,^[7] and magnetic bistability with a high magnetization reversal barrier.^[8] It is evident from the above discussion that the spin-reversal barrier is dependent on the total spin, S , and the ZFS parameter,

D . The most convenient way to increase the energy barrier within a SMM is through the ground-state spin S . However, increasing S leads to an effective reduction in the ZFS parameter, D ,^[9] which results in a net decrease in the spin-reorientation barrier, U . Thus, the only way to control U is through modulation of the ZFS parameter, D . Although a plethora of compounds with properties that resemble those of $\text{Mn}_{12}\text{-ac}$ have been synthesized to date,^[10] the rational design of SMMs with tunable S and D is far from being achieved. Thus, modulation of the ZFS parameter is now a promising field of research for its wide-ranging applications in high-density information storage, quantum computing, and spintronic devices.^[11]

Cobalt(II) complexes are known to exhibit strong spin-orbit coupling in comparison to manganese(II–IV), iron(III), or nickel(II), to which the distinguished members of the SMM family belong.^[12] This is because such octahedral or pseudo-octahedral cobalt(II) ions are known to exert strong first-order orbital magnetism. The ground-state spin configuration for Co^{II} in an octahedral coordination environment is $t_{2g}^5e_g^2$, which designates a 4F ground state.^[13] The 4F ground state is split into two triplet states ($^4T_{1g}$, $^4T_{2g}$) and one singlet state ($^4A_{2g}$). The triplet nature of the $^4T_{1g}$ ground state is responsible for first-order orbital momentum.^[13] The large unquenched orbital angular momentum in Co^{II} makes it an important candidate for the study of magnetic anisotropy. Current literature in the domain of SMM research suggests a drift towards the tuning of the magnetic anisotropy through various means.

The modulation of the ZFS parameter by ligand substitution has recently been studied in the framework of DFT.^[14] Structural modification in an octahedral Cr^{III} system can switch the magnetization behavior of a molecule from easy-plane to easy-axis type. Herein, we investigate the effect of an external electric field on the ZFS parameter of a pseudo-octahedral $[\text{Co}^{\text{II}}(\text{dmphen})_2(\text{NCS})_2]$ complex (dmphen = 2,9-dimethyl-1,10-phenanthroline; Figure 1) to control magnetization through external stimuli. The use of an electric field in tuning magnetic and transport properties has also been demonstrated recently.^[15] To control magnetization, the use of an electric field is highly ad-

[a] T. Goswami, Dr. A. Misra

Department of Chemistry, University of North Bengal
Darjeeling 734013, West Bengal (India)
E-mail: anirbanmisra@yahoo.com

Supporting information for this article is available on the WWW under <http://dx.doi.org/10.1002/chem.201403370>.

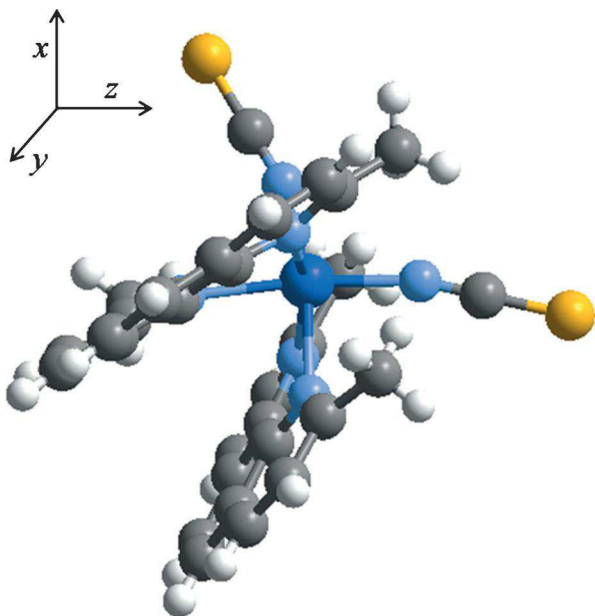


Figure 1. Structure of the pseudo-octahedral Co^{II}-complex, [Co^{II}(dmphen)₂(NCS)₂].

vantageous.^[16] Although the bulk properties of SMMs are well documented in their unperturbed state,^[17] the study of the effect of an external electric field on the magnetization of SMMs is relatively recent.^[18]

Methods

The formation of a static electric field between two oppositely charged parallel plates is well known from the laws of classical electrophysics. It is also common practice to create a uniform static field between the central area of large parallel plates because in that area the electric lines of force become parallel. This simple concept from elementary physics encouraged us to construct a device to calculate ZFS under the influence of an external electric field. Thus, to realize the magnetization behavior of the molecule under an electric pulse, we placed the molecule between two oppositely charged parallel plates with an area of about 600 Å². We chose the atomic arrangements of the Pt (111) surface, and subsequently, replaced the atoms with point charges uniformly to create the charged plates. The plates were 40 Å apart, which maintained a distance of at least 18 Å from the molecule and would avoid any structural deformation due to point charges. The whole arrangement is pictorially represented in Figure 2. This is typically the same arrangement as a parallel-plate capacitor. The left plate is charged as positive, while the right plate contains negative point charges of the same magnitude in the platinum atomic positions. In this way, we create an electric field along the positive z axis. Calculations of the ZFS parameters were performed by following the methodology discussed in the following paragraphs.

ZFS lifts the degeneracy of the M_s states in a molecule with $S > 1/2$, in the absence of an external magnetic field. It is customary to treat the spin-orbit coupling contribution to ZFS

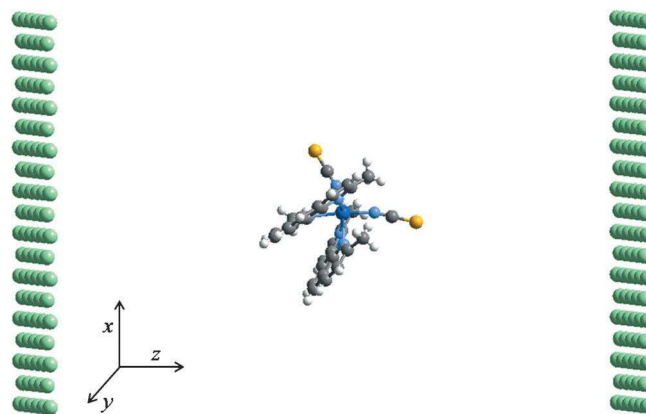


Figure 2. The arrangement of the [Co^{II}(dmphen)₂(NCS)₂] complex between two oppositely charged parallel plates.

through an uncoupled perturbation theoretical approach in unrestricted Kohn–Sham formalism.^[19] The corresponding correction to the total energy can be expressed as Equation (1):^[20]

$$\Delta_2 = \sum_{\sigma\sigma'} \sum_{ij} M_{ij}^{\sigma\sigma'} S_i^{\sigma\sigma'} S_j^{\sigma'\sigma} \quad (1)$$

in which $S_i^{\sigma\sigma'} = \langle \chi^\sigma | S_i | \chi^{\sigma'} \rangle$; χ^σ and $\chi^{\sigma'}$ are different spinors; σ denotes different spin degrees of freedom and the coordinate labels, x , y , and z are represented by i , j , and so forth. The matrix elements $M_{ij}^{\sigma\sigma'}$ in Equation (1) are described by Equation (2):

$$M_{ij}^{\sigma\sigma'} = \sum_{kl} \frac{\langle \phi_{l\sigma} | V_i | \phi_{k\sigma'} \rangle \langle \phi_{k\sigma} | V_j | \phi_{l\sigma} \rangle}{\epsilon_{l\sigma} - \epsilon_{k\sigma'}} \quad (2)$$

In this equation $\epsilon_{l\sigma}$ and $\epsilon_{k\sigma'}$ are energies of the occupied, $\phi_{l\sigma}$, and unoccupied, $\phi_{k\sigma'}$, states, respectively. In the absence of a magnetic field, the change in energy of the system in the second-order is written as Equation (3):

$$\Delta_2 = \sum_{ij} \gamma_{ij} \langle S_i \rangle \langle S_j \rangle \quad (3)$$

Upon diagonalization of the anisotropy tensor, γ , the eigenvalues γ_{xx} , γ_{yy} , and γ_{zz} are obtained and the second-order perturbation energy can now be written as Equation (4):

$$\begin{aligned} \Delta_2 = & \frac{1}{3} (\gamma_{xx} + \gamma_{yy} + \gamma_{zz}) S(S+1) \\ & + \frac{1}{3} \left[\gamma_{zz} - \frac{1}{2} (\gamma_{xx} + \gamma_{yy}) \right] [3S_z^2 - S(S+1)] \\ & + \frac{1}{2} (\gamma_{xx} - \gamma_{yy}) (S_x^2 - S_y^2) \end{aligned} \quad (4)$$

These anisotropy tensor components (γ_{xx} , γ_{yy} , γ_{zz}) are parameterized to obtain Equation (5) as a simplified expression:

$$H_{ZFS} = D[S_z^2 - \frac{1}{3}S(S+1)] + E[S_x^2 - S_y^2] \quad (5)$$

in which D and E are axial and rhombic ZFS parameters, respectively. Calculation of parameters D and E was performed in the ORCA suit of a density functional package.^[21] The methodology adopted herein was the BPW91 functional,^[22] TZV basis set,^[23] with the auxiliary TZV/J Coulomb-fitting basis set.^[24] This methodology, under unrestricted Kohn–Sham formalism, as adopted herein, is being widely used to compute ZFS parameters.^[22a,25] Although there are several methods available for the computation of the ZFS parameter, the Pederson and Khanna (PK) method is known to produce the correct sign of the ZFS parameter;^[22a,26] therefore, we use this methodology^[20] to calculate the ZFS parameters. The ZFS contributions predicted by this method show fair agreement with accurate ab initio and experimental results.

Results and Discussion

Single-point calculations on the crystallographic structure, which are available in ref. [28], were performed and used for further calculations. It is known from the EPR spectra of complex $[\text{Co}^{\text{II}}(\text{dmphen})_2(\text{NCS})_2]$ that it has ground-state spin $S = 3/2$. The value of D is calculated for the complex in its unperturbed ground state and also under the application of bias voltage in the range of -4×10^{-3} to 4×10^{-3} a.u. Herein, the positive and negative values of the external electric field are designated with the application of the field along the positive direction of the z axis, that is, along one axial direction of the Co–NCS bond. The complex is put under a static electric field of different strengths, according to the arrangement discussed in the previous section. It was shown previously that typically a critical electric field in the order of 0.01 a.u. was required to bring about ionization in a molecule.^[27] Hence, application of an electric field in the order of 0.004 a.u., as in the present case, is not expected to bring about any undesired polarization or ionization of the molecule.

In the ground state, the ZFS parameter of the complex is positive, which signifies easy-plane type magnetic anisotropy. The computed value of D is given in Table 1, along with individual excitation contributions. The MAE barrier, U , was also computed and compared with experimental values.^[28] We found reasonable agreement of the calculated value of U with the experimentally obtained MAE barrier. However, from experimental results reported previously,^[28] we also find an ab initio CASSCF result of $D = +196 \text{ cm}^{-1}$ with a clear dictation

Table 1. A comparison of the experimental magnetic anisotropy energy (MAE) barrier with that computed at the BPW91/TZV level and the individual excitation contributions towards the ZFS parameter in the ground state.

Computed D and U at BPW91/TZV level		Calculated MAE barrier U [cm^{-1}]	Experimental MAE barrier [cm^{-1}] ^[27]
Individual excitation contributions to ZFS	Calculated D [cm^{-1}]		
$\alpha \rightarrow \alpha$	0.178	13.122	≈ 17
$\alpha \rightarrow \beta$	1.385		
$\beta \rightarrow \alpha$	-0.266		
$\beta \rightarrow \beta$	5.265		

of the disagreement between the calculated and experimental values of U . There has been a debate about whether DFT is better than ab initio methods in the logical prediction of ZFS parameters. Nevertheless, in a recent study, it was categorically shown that DFT provided efficient estimates of the ZFS parameters compared with popular ab initio methods.^[29]

Computation of the ZFS parameters is also executed under different external electric fields. The values of D , along with the individual excitation contributions towards ZFS, are given in Table 2. A plot of the variation in D with applied electric field in Figure 3 suggests that after a certain critical field strength the easy-plane magnetization of the Co^{II} complex changes to easy-axis type. Thus, it can be interpreted that, after a threshold field, the molecule starts to behave as an SMM. Moreover, the switch in the D value in both field directions is also clear from Figure 3. This flip in D is in the range of 1.6×10^{-3} and 1.7×10^{-3} a.u. of electric field strength when the field is applied along the positive z axis.

It can be seen from Tables 1 and 2 that the major excitation contribution towards D comes from the $\beta \rightarrow \beta$ excitation. To further investigate the effect of electric field on the excitation

Table 2. The ZFS parameters computed at the BPW91/TZV level and the individual excitation contributions towards ZFS under the influence of a finite electric field.

External electric field [a.u.]	D [cm^{-1}]	Different excitation contributions to D			
		$\alpha \rightarrow \alpha$	$\alpha \rightarrow \beta$	$\beta \rightarrow \alpha$	$\beta \rightarrow \beta$
under negative applied field					
-0.0040	-5.828	-0.132	-1.288	0.211	-4.619
-0.0035	-5.762	-0.131	-1.267	0.216	-4.580
-0.0030	-5.700	-0.130	-1.236	0.222	-4.557
-0.0025	5.668	0.168	1.429	-0.230	4.301
-0.0020	5.909	0.172	1.451	-0.238	4.524
-0.0015	6.133	0.175	1.463	-0.247	4.742
-0.0010	6.325	0.177	1.460	-0.255	4.943
-0.0005	6.470	0.178	1.436	-0.261	5.117
under positive applied field					
0.0005	6.578	0.177	1.323	-0.268	5.347
0.0010	6.537	0.177	1.231	-0.270	5.399
0.0015	6.428	0.179	1.105	-0.273	5.418
0.0020	-6.593	-0.107	-0.646	0.258	-6.096
0.0025	-6.835	-0.107	-0.602	0.255	-6.380
0.0030	-7.059	-0.104	-0.560	0.249	-6.644
0.0035	-7.254	-0.107	-0.516	0.248	-6.879
0.0040	-7.406	-0.110	-0.477	0.246	-7.066

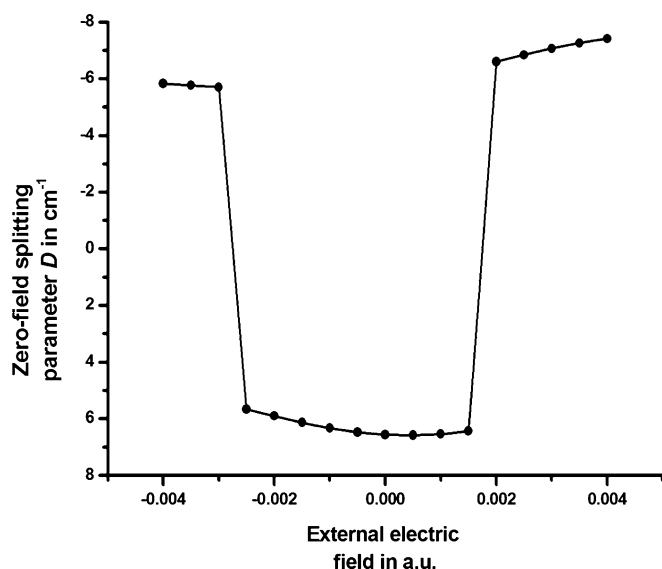


Figure 3. A plot of the variation in D with external electric field.

pattern of the molecule, we performed time-dependent (TD) DFT calculations at the same computational level by using the Gaussian 09W^[30] suite of programs. Excitations with maximum oscillator strengths are characterized to involve β electrons only. The molecular orbitals (MOs) from and to which excitation occurs are summarized in Table 3. In the ground state, the

source MO involves the metal d orbitals and the thiocyanate ligands. The destination MOs in the unperturbed state corroborate the interaction of the dmphen ligand with the central metal ion. No significant change in the picture is observed for a field strength lower than that of the critical value at which D is still positive. On the other hand, above the critical field strength, the excitation spectrum reverses. At a field strength of 0.004 a.u., the source MO is essentially centered on the dmphen ligand, whereas the destination is the MO based on

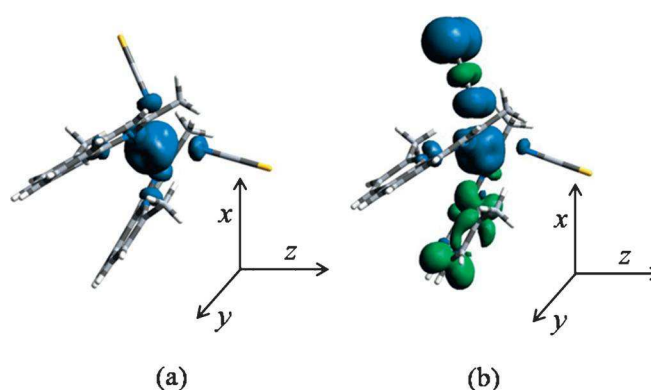


Figure 4. The spin-density plots (at an isosurface value of 0.004) of the Co^{II} complex in a) the ground state and b) under the applied electric field with a magnitude of 4.0×10^{-3} a.u. The blue color specifies α -spin density and the green color indicates β -spin density.

Table 3. The excitation behavior of [Co^{II}(dmphen)₂(NCS)₂] in the ground state and under application of a finite electric field computed at the BPW91/TZV level.

Applied electric field strength [a.u.]	Source MO	Destination MO
0.000		
0.004		

the NCS ligands. Hence, from the above discussion, it is evident that the natural tendency of the electrons to flow towards the π -acceptor NCS ligands is developed at a field strength higher than that of the critical field. It follows from our previous work that the π -accepting tendency of the ligands exerts easy-axis-type magnetic anisotropy ($D < 0$) in a molecule.^[14] Thus, it can be concluded that the switch in the D value arises from metal-to-ligand back charge transfer in the molecule facilitated by exposure to the external electric field.

A similar and more interesting portrayal of the phenomenon is found in the spin density plots depicted in Figure 4. We compared the spin densities of the complex at zero-external field and finite external electric fields above the critical field. Separation of the α and β spins is observed at a higher electric field strength than that of the unperturbed state. This dispersion of the β spin is further confirmed from a comparison of the density of states (DOS) plots at different electric fields given in Figure S1 in the Supporting Information. Close inspection of the DOS plots reveals the shift in the energies of the α and β electrons. Although electrons of both spins show a shift in the energy level, an alteration in the energy of the β spin is specifically observed. This interesting feature of a shift in the energy levels of different spins due to opposite spin accumulation on

two different sides of a molecule is termed as the spin Hall effect.^[31]

The molecular origin of this correlation of the electron spin and applied electric field is steered by spin-orbit coupling. In this context, the Rashba-type spin-orbit interaction draws the attention of the scientific community due to its tunable nature under an applied electric field.^[32] The spin-orbit coupling Hamiltonian in Equation (6) describes the coupling of electron spin σ and momentum p under an external electric field E :

$$\hat{H}_{\text{SO}} = -\mu_{\text{B}}\sigma\left(p\frac{E}{2mc^2}\right) \quad (6)$$

in which σ , μ_{B} , and c are Pauli spin matrices, the Bohr magneton, and the velocity of light, respectively. It is evident from Equation (6) that a momentum-dependent internal magnetic field is generated, as shown in Equation (7):

$$B_{\text{int}} = p\frac{E}{2mc^2} \quad (7)$$

and the resulting spin polarization is crucially dependent on both p and E and their relative directions.^[33] It can be argued that there is a generalized tendency of the electrons to move towards the π -accepting NCS ligands, and hence, the direction of the resultant momentum of the electrons can be along the $+x$ axis (see the Supporting Information). The interaction of the electron momentum with the external electric field generates an internal magnetic field. A magnetic field thus generated, in turn, accelerates the α and β electrons in opposite directions through a spin-dependent force, represented by Equation (8):

$$F_{\uparrow\downarrow} = \pm g\mu_{\text{B}}\frac{dB_{\text{int}}}{dq} \quad (8)$$

in which g is the electronic g factor and μ_{B} is the Bohr magneton. The clear bifurcation of the α and β spin densities in opposite directions in the present complex indicates a modification in the spin-orbit interaction. It is also commonly understood that the ZFS in metal systems originates from spin-orbit coupling. Thus, modification in the spin-orbit coupling is further established through alteration to the ZFS parameter under an external electric field.

Conclusion

Emerging interest in mononuclear complexes, in comparison to polynuclear ones, has meant that the field of quantum magnets has turned to tuning of the ZFS parameter D through structural modification or external aids. This study contemplated the magnetic anisotropy of an octahedral Co^{II} complex, namely, $[\text{Co}^{\text{II}}(\text{dmphen})_2(\text{NCS})_2]$, in connection with the tunability of ZFS parameter D by exploiting an electric field as an external stimuli. Previously, it was shown that the presence of

a π -accepting ligand in the axial position of an octahedral complex could result in magnetization of the molecular magnetic dipole along a specific direction. The external electric field in the present situation assisted such metal-to-ligand charge transfer and led to a switchover in the anisotropic characteristics. A spin-Hall spatial spin separation was also observed due to modulation in the Rashba spin-orbit coupling in a single molecule, for the first time, rather than in mesoscopic systems.

Acknowledgements

We thank the Department of Science and Technology (DST), India, for financial support. T.G. thanks CSIR, India, for a Senior Research Fellowship.

Keywords: charge transfer · density functional calculations · electrochemistry · magnetic properties · spin Hall effects

- [1] a) A. Boussac, J. J. Girerd, A. W. Rutherford, *Biochemistry* **1996**, *35*, 6984–6989; b) O. Horner, E. Rivière, G. Blondin, S. Un, A. W. Rutherford, J. J. Girerd, A. Boussac, *J. Am. Chem. Soc.* **1998**, *120*, 7924–7928; c) C. E. Dubé, R. Sessoli, M. P. Hendrich, D. Gatteschi, W. H. Armstrong, *J. Am. Chem. Soc.* **1999**, *121*, 3537–3538; d) W. Wernsdorfer, R. Sessoli, *Science* **1999**, *284*, 133.
- [2] a) R. Sessoli, H. L. Tsai, A. R. Schake, S. Y. Wang, J. B. Vincent, K. Folting, D. Gatteschi, G. Christou, D. N. Hendrickson, *J. Am. Chem. Soc.* **1993**, *115*, 1804–1816; b) D. Gatteschi, R. Sessoli, J. Villain, *Molecular Nanomagnets*, Oxford University Press, New York, **2006**; c) C. J. Milios, A. Vin-slava, W. Wernsdorfer, S. Moggach, S. Parsons, S. P. Perlepes, G. Christou, E. K. Brechin, *J. Am. Chem. Soc.* **2007**, *129*, 2754–2755; d) D. Yoshihara, S. Karasawa, N. Koga, *J. Am. Chem. Soc.* **2008**, *130*, 10460–10461.
- [3] M. Mannini, F. Pineider, P. Sainctavit, C. Danieli, E. Otero, C. Sciancalepore, M. Talarico, M. A. Arrio, A. Cornia, D. Gatteschi, R. Sessoli, *Nat. Mater.* **2009**, *8*, 194–197.
- [4] a) M. N. Leuenberger, D. Loss, *Nature* **2001**, *410*, 789–793; b) A. Ardavan, O. Rival, J. J. L. Morton, S. J. Blundell, A. M. Tyryshkin, G. A. Timco, R. E. P. Winpenny, *Phys. Rev. Lett.* **2007**, *98*, 057201; c) P. C. E. Stamp, A. J. Gaita-Arino, *Mater. Chem.* **2009**, *19*, 1718–1730.
- [5] R. Sessoli, D. Gatteschi, A. Caneschi, M. A. Novak, *Nature* **1993**, *365*, 141–143.
- [6] T. Lis, *Acta Cryst. B* **1980**, *36*, 2042–2046.
- [7] A. Caneschi, D. Gatteschi, R. Sessoli, A. L. Barra, L. C. Brunel, M. Guillot, *J. Am. Chem. Soc.* **1991**, *113*, 5873–5874.
- [8] J. Lawrence, S. C. Lee, S. Kim, N. Anderson, S. Hill, M. Murugesu, G. Christou, *AIP Conf. Proc.* **2006**, *850*, 1133–1134.
- [9] a) O. Waldmann, *Inorg. Chem.* **2007**, *46*, 10035–10037; b) N. Kirchner, J. van Slageren, M. Dressel, *Inorg. Chim. Acta* **2007**, *360*, 3813–3819.
- [10] G. Aromí, E. K. Brechin, *Struct. Bonding (Berlin)* **2006**, *122*, 1–67.
- [11] a) L. Bogani, W. Wernsdorfer, *Nat. Mater.* **2008**, *7*, 179–186; b) M. Ur-dampilleta, S. Klyatskaya, J.-P. Cleuziou, M. Ruben, W. Wernsdorfer, *Nat. Mater.* **2011**, *10*, 502–506; c) S. K. Ritter, *Chem. Eng. News* **2004**, *82*, 29–32.
- [12] J. Liu, S. Datta, E. Bolin, J. Lawrence, C. C. Beedle, E. C. Yang, P. Goy, D. N. Hendrickson, S. Hill, *Polyhedron* **2009**, *28*, 1922–1926.
- [13] a) F. Lloret, M. Julve, J. Cano, R. Ruiz-García, E. Pardo, *Inorg. Chim. Acta* **2008**, *361*, 3432–3445; b) A. Palií, B. Tsukerblat, J. M. Clemente-Juan, E. Coronado, *Int. Rev. Phys. Chem.* **2010**, *29*, 135–230.
- [14] T. Goswami, A. Misra, *J. Phys. Chem. A* **2012**, *116*, 5207–5215.
- [15] S. Shil, A. Misra, *RSC Adv.* **2013**, *3*, 14352–14362.
- [16] a) D. Chiba, M. Sawicki, Y. Nishitani, Y. Nakatani, F. Matsukura, H. Ohno, *Nature* **2008**, *455*, 515–518; b) D. Lebeugle, A. Mougín, M. Viret, D. Colson, L. Ranno, *Phys. Rev. Lett.* **2009**, *103*, 257601.
- [17] a) S. Accorsi, A. L. Barra, A. Caneschi, G. Chastanet, A. Cornia, A. C. Fabretti, D. Gatteschi, C. Mortalo, E. Olivieri, F. Parenti, P. Rosa, R. Sessoli, L.

- Sorace, W. Wernsdorfer, L. Zobbi, *J. Am. Chem. Soc.* **2006**, *128*, 4742–4755; b) L. Gregoli, C. Danieli, A. L. Barra, P. Neugebauer, G. Pellegrino, G. Poneti, R. Sessoli, A. Cornia, *Chem. Eur. J.* **2009**, *15*, 6456–6467.
- [18] A. S. Zyazin, J. W. G. van den Berg, E. A. Osorio, H. S. J. van der Zant, N. P. Konstantinidis, M. Leijnse, M. R. Wegewijs, F. May, W. Hofstetter, C. Danieli, A. Cornia, *Nano Lett.* **2010**, *10*, 3307–3311.
- [19] S. Zein, C. Duboc, W. Lubitz, F. Neese, *Inorg. Chem.* **2008**, *47*, 134.
- [20] M. R. Pederson, S. N. Khanna, *Phys. Rev. B* **1999**, *60*, 9566–9572.
- [21] F. Neese, ORCA 2.8.0; University of Bonn, Bonn, Germany, **2010**.
- [22] a) C. van Wüllen, *J. Chem. Phys.* **2009**, *130*, 194109; b) F. Aquino, J. H. Rodriguez, *J. Phys. Chem. A* **2009**, *113*, 9150–9156.
- [23] a) A. Schäfer, H. Horn, R. Ahlrichs, *J. Chem. Phys.* **1992**, *97*, 2571–2577; b) A. Schäfer, C. Huber, R. Ahlrichs, *J. Chem. Phys.* **1994**, *100*, 5829–5835.
- [24] F. Weigend, *Phys. Chem. Chem. Phys.* **2006**, *8*, 1057–1065.
- [25] a) K. Park, M. R. Pederson, S. L. Richardson, N. Aliaga-Alcalde, G. Christou, *Phys. Rev. B* **2003**, *68*, 020405; b) J. Ribas-Ariño, T. Baruah, M. R. Pederson, *J. Am. Chem. Soc.* **2006**, *128*, 9497–9505.
- [26] F. Aquino, J. H. Rodriguez, *J. Chem. Phys.* **2005**, *123*, 204902.
- [27] a) N. Davari, P.-O. Åstrand, S. Ingebrigtsen, M. Unge, *J. Appl. Phys.* **2013**, *113*, 143707; b) N. Davari, P.-O. Åstrand, T. Van Voorhis, *Mol. Phys.* **2013**, *111*, 1456–1461; c) M. B. Smirnov, V. P. Krainov, *J. Exp. Theor. Phys.* **1997**, *85*, 447–450.
- [28] J. Vallejo, I. Castro, R. Ruiz-García, J. Cano, M. Julve, F. Lloret, G. D. Munno, W. Wernsdorfer, E. Pardo, *J. Am. Chem. Soc.* **2012**, *134*, 15704–15707.
- [29] S. K. Singh, G. Rajaraman, *Chem. Eur. J.* **2013**, *19*, 1–12.
- [30] Gaussian 09, Revision A.01, M. J. Frisch, G. W. Trucks, H. B. Schlegel, G. E. Scuseria, M. A. Robb, J. R. Cheeseman, G. Scalmani, V. Barone, B. Menucci, G. A. Petersson, H. Nakatsuji, M. Caricato, X. Li, H. P. Hratchian, A. F. Izmaylov, J. Bloino, G. Zheng, J. L. Sonnenberg, M. Hada, M. Ehara, K. Toyota, R. Fukuda, J. Hasegawa, M. Ishida, T. Nakajima, Y. Honda, O. Kitao, H. Nakai, T. Vreven, J. A. Montgomery, Jr., J. E. Peralta, F. Ogliaro, M. Bearpark, J. J. Heyd, E. Brothers, K. N. Kudin, V. N. Staroverov, R. Kobayashi, J. Normand, K. Raghavachari, A. Rendell, J. C. Burant, S. S. Iyengar, J. Tomasi, M. Cossi, N. Rega, J. M. Millam, M. Klene, J. E. Knox, J. B. Cross, V. Bakken, C. Adamo, J. Jaramillo, R. Gomperts, R. E. Stratmann, O. Yazyev, A. J. Austin, R. Cammi, C. Pomelli, J. W. Ochterski, R. L. Martin, K. Morokuma, V. G. Zakrzewski, G. A. Voth, P. Salvador, J. J. Dannenberg, S. Dapprich, A. D. Daniels, Ö. Farkas, J. B. Foresman, J. V. Ortiz, J. Cioslowski, D. J. Fox, Gaussian, Inc., Wallingford CT, **2009**.
- [31] M. C. Beeler, R. A. Williams, K. Jimenez-Garcia, L. J. LeBlanc, A. R. Perry, I. B. Spielman, *Nature* **2013**, *498*, 201–204.
- [32] J. Nitta, T. Akazaki, H. Takayanagi, T. Enoki, *Phys. Rev. Lett.* **1997**, *78*, 1335.
- [33] G. Dresselhaus, *Phys. Rev.* **1955**, *100*, 580–586.

Received: May 3, 2014

Published online on August 25, 2014